

**PROCESS INTENSIFICATION: THIN FILM SPINNING
DISC REACTOR FOR CONTROLLED CONTINUOUS
PHOTO-POLYMERISATION OF ACRYLATES.**

Julie Charlene Johnstone[†]

A thesis submitted for the degree of Doctor of Philosophy in the Faculty of Engineering
of the University of Newcastle-upon-Tyne.

Process Intensification and Innovation Centre,
Department of Chemical and Process Engineering
University of Newcastle-upon-Tyne
UK

June 2000

[†] Née Dagleish

ABSTRACT

In the last three decades the utilisation of UV radiation to initiate the polymerisation of acrylates and methacrylates has centred on UV curing of thin films to produce highly crosslinked networks. Very little attention has been paid to the initiation of bulk polymerisations using this method. In part this is due to the difficulties of ensuring UV penetration of more than several centimetres into reaction vessels and also to the strongly exothermic nature of the bulk polymerisation of liquid acrylates and methacrylates.

This investigation explores the potential for the use of a thin film spinning disc reactor for the continuous photo-polymerisation of acrylates and methacrylates, considering n-butyl acrylate as a test case. The benefits offered by spinning disc reactors are the controlled formation of thin films, good mixing and enhancement of heat and mass transfer rates. The spinning disc reactor used in this investigation has a novel internal cooling/heating system designed to allow close control of the reaction surface temperature and provide a means of removing the heat of reaction from fast exothermic reactions, such as photo-initiated free-radical polymerisations.

The investigation comprises three individual studies; static film polymerisation (as a benchmark), spinning disc polymerisation and preliminary heat transfer measurement. Conversions of up to 23 % and molecular weights (M_w) of up to 296115 kg/kmol were achieved in the static film polymerisation with corresponding polydispersity indices of 1.98 to 4.43. By comparison, conversions of up to 66 % and M_w of up to 604518 kg/kmol were achieved in the spinning disc polymerisation, with corresponding polydispersity indices of 1.36 to 2.74, indicating a tighter control of molecular weight distribution on the spinning disc. Overall heat transfer coefficients of up to 9 kW/m² were achieved for the internally cooled disc system.

Keywords: process intensification, spinning disc reactors, photo-polymerisation, acrylates.

ACKNOWLEDGEMENTS

I would like to take this opportunity to thank my husband, Graeme, for all his encouragement and support, especially throughout the latter stages of my Ph.D. research.

I would like to thank my supervisor, Dr. Roshan Jachuck, for his input and guidance throughout this investigation, and my second supervisor, Prof. Colin Ramshaw, for his continued interest throughout my time as a Ph.D. student in the Process Intensification and Innovation Centre at Newcastle University. I would also like to thank the Head of the Chemical and Process Engineering Department, Dr. John Backhurst, for the use of the laboratory facilities within the department.

There are several people without whose input the test facility would not have been designed, constructed and working, and I would like to thank Mr. Erick Horsley and his team of technicians, especially Mr. Brian Grover and Mr. Stuart Latimer for this. Also, for his patience and help with experimental procedures and construction of ancillary equipment, Mr. Rob Dixon.

I would also like to thank Mr. Mike Whitton, Mr. Bill Dunk and Mr. Dave Arnold of Courtaulds Coatings for some invaluable practical and industrial input to this investigation.

Lastly, I would like to thank the EPSRC for their award of a three year studentship to fund this project.

CONTENTS

Abstract.....	i
Acknowledgements.....	ii
1. Introduction.....	1
1.1 Process Intensification.....	1
1.2 Spinning Disc Reactors	2
1.3 Present Study.....	3
2. Objectives of Present Investigation	5
3. Literature Review.....	6
3.1 Introduction.....	6
3.2 Polymerisation.....	6
3.2.1 Introduction.....	6
3.2.1.1 Bulk Polymerisation.....	8
3.2.1.2 Solution Polymerisation.....	8
3.2.1.3 Suspension Polymerisation	8
3.2.1.4 Emulsion Polymerisation.....	9
3.2.1.5 Polymerisation Reactors	9
3.2.2 The Polymerisation Reaction.....	10
3.2.2.1 Initiation.....	10
3.2.2.2 Propagation	11
3.2.2.3 Termination.....	11
3.2.3 Molecular Weight and Polydispersity.....	12
3.2.3.1 Molecular Weight	12

Contents

3.2.3.2	Number-Average Molecular Weight.....	13
3.2.3.3	Weight-Average Molecular Weight.....	13
3.2.3.4	Polydispersity.....	13
3.3	Photo-Polymerisation	14
3.3.1	Introduction.....	14
3.3.2	General Concepts.....	14
3.3.2.1	Photo-Chemical Reactions.....	14
3.3.2.2	Experimental UV Intensity	15
3.3.2.3	The Gel Effect.....	16
3.3.2.4	The Cage Effect	16
3.3.3	Photo-Initiation.....	17
3.3.3.1	Introduction.....	17
3.3.3.2	Methods of Photo-Initiation.....	18
3.3.3.3	Mechanisms of Photo-Initiation.....	19
3.3.3.4	Photo-Initiator Concentration	24
3.3.3.5	Photo-Initiators for the Surface Coatings Industry	25
3.3.4	Propagation in Photo-Initiated Acrylate Systems	26
3.3.5	Oxygen Inhibition in Photo-Polymerisation	26
3.3.6	Other Possible Reactions.....	27
3.3.7	UV Curing.....	29
3.3.7.1	Introduction.....	29
3.3.7.2	Background.....	29
3.3.7.3	Applications of UV Curing.....	30
3.4	Kinetics.....	31
3.4.1	Introduction.....	31

Contents

3.4.2 Overall Polymerisation Rate.....	31
3.4.3 Assumptions.....	32
3.4.4 Rate of Radical Production.....	33
3.4.5 Rate of Initiation.....	34
3.4.6 Rate of Propagation.....	34
3.4.7 Rate of Termination.....	35
3.4.8 Quantum Yield of Initiator Photolysis, ϕ_i	35
3.4.9 Quantum Yield of Polymerisation, ϕ_p	35
3.4.10 Measurement of Polymerisation Rate and Kinetic Data.....	36
3.5 Acrylates.....	37
3.5.1 Introduction.....	37
3.5.2 Chemistry.....	38
3.5.3 Brief History of Acrylate and Methacrylate Polymerisation.....	40
3.5.4 Polymerisation of Acrylates and Methacrylates.....	42
3.5.4.1 Considerations.....	42
3.5.4.2 Potential Disadvantages.....	42
3.5.4.3 Use of Acrylates and Methacrylates.....	43
3.6 Review of Experimental Details.....	44
3.6.1 Introduction.....	44
3.6.2 Purification of Reagents.....	44
3.6.3 UV Sources.....	45
3.6.4 Analysis Techniques.....	46
3.6.4.1 Bromination Method.....	46
3.6.4.2 Refractive Index Method.....	47
3.6.4.3 GPC Analysis.....	47

Contents

4. Test Facility	48
4.1 Introduction	48
4.2 Experimental Apparatus.....	48
4.2.1 Mechanical Design	48
4.2.2 Explanation of Design	50
4.2.3 Measurement Techniques.....	51
4.2.4 Testing of UV Light Source.....	51
5. Experimental Procedures and Treatment of Results	60
5.1 Introduction	60
5.2 Experimental Procedures.....	60
5.2.1 Preparation of Monomer.....	60
5.2.2 Static Film Polymerisation	61
5.2.3 Spinning Disc Polymerisation	63
5.2.4 Analysis Techniques	64
5.2.4.1 GPC Analysis	64
5.2.4.2 Preparation of Samples	64
5.2.4.3 Calculation of conversion	65
5.2.4.4 Calculation of Molecular Weights.....	65
5.2.5 Preliminary Heat Transfer Study	65
5.3 Treatment of Results	66
5.3.1 Linear Regression Analysis	66
5.3.1.1 Method	66
5.3.1.2 Data Analysis	66
6. Static Film Polymerisation	68
6.1 Introduction	68

Contents

6.2 Static Film Results.....	69
6.2.1 Exposure Time.....	69
6.2.1.1 Results.....	69
6.2.1.2 Theory.....	69
6.2.2 Film Thickness.....	70
6.2.2.1 Results.....	70
6.2.2.2 Theory.....	70
6.2.3 UV Intensity.....	73
6.2.3.1 Results.....	73
6.2.3.2 Theory.....	73
6.3 Linear Regression Analysis	76
6.4 Discussion.....	77
6.4.1 Effect of Exposure Time	77
6.4.2 Effect of Film Thickness	78
6.4.3 Effect of UV Intensity.....	79
6.4.4 General Discussion.....	80
6.4.4.1 Limitations of Theoretical Model.....	80
6.4.4.2 Characterisation of Polymerisation System.....	81
6.5 Summary.....	81
7. Spinning Disc Polymerisation	83
7.1 Introduction	83
7.2 Experimental Results.....	84
7.2.1 Rotational Speed.....	84
7.2.2 Feed Flowrate.....	84
7.2.3 Photoinitiator Concentration	85

Contents

7.2.4 Temperature.....	89
7.2.5 Photoinitiator Type.....	89
7.2.6 UV Intensity.....	90
7.2.7 Purge Time.....	91
7.3 Linear Regression Analysis.....	93
7.4 Discussion.....	94
7.4.1 Rotational Speed.....	95
7.4.2 Feed Flowrate.....	97
7.4.3 Photo-Initiator Concentration.....	98
7.4.4 Temperature.....	99
7.4.5 Photo-Initiator Type.....	100
7.4.6 UV Intensity.....	101
7.4.7 Nitrogen Purge Time.....	102
7.4.8 General Discussion.....	106
7.4.9 Limitations of Experimental Set-Up.....	107
7.5 Summary.....	107
8. Conclusions.....	109
8.1 Introduction.....	109
8.2 Static Film Polymerisation.....	109
8.3 Spinning Disc Polymerisation.....	109
8.4 Spinning Disc Versus Static Film Polymerisation.....	111
8.5 Heat Transfer.....	111
9. Recommendations for Future Work.....	113
9.1 Introduction.....	113
9.2 Further Polymerisation Work.....	113

Contents

9.2.1 Static Film.....	113
9.2.2 Spinning Disc Reactor.....	113
9.3 Other Applications	115
Nomenclature	118
References.....	123
Appendices	133
Appendix A: Preliminary Heat Transfer Study	133
A.1 Introduction	133
A.2 Treatment of Results.....	133
A.2.1 Heat Balance	134
A.2.2 Calculation of Overall Heat Transfer Coefficient (U Value)	135
A.2.3 Calculation of Reynolds Number	137
A.3 Results and Discussion.....	142
A.3.1 Rotational Speed.....	142
A.3.2 Feed Flowrate.....	142
A.3.3 Cooling Water Flowrate.....	143
A.3.4 Channel Width.....	143
A.3.5 Feed Temperature	144
A.4 Conclusions	144
Appendix B: Engineering Drawings	148
Appendix C: Experimental Procedures and Treatment of Results	170
Appendix D: Static Film Polymerisation	187
Appendix E: Spinning Disc Polymerisation.....	192

TABLE OF FIGURES

Chapter 3 - Literature Review:

Figure 3.1. Possible Stereochemical Configurations	12
Figure 3.2. Homolytic Cleavage	20
Figure 3.3. α -Hydrogen Atom Transfer	20
Figure 3.4. β -Hydrogen Atom Transfer	20
Figure 3.5. Homolytic Cleavage of Benzoin.....	21
Figure 3.6. Homolytic Cleavage of Benzoin Alkyl Ethers.....	21
Figure 3.7. Homolytic Cleavage of DMPA.....	22
Figure 3.8. Recombination of Benzoyl Radicals	22
Figure 3.9. Reaction of Benzophenone with UV Light.....	23
Figure 3.10. Propagation of Vinyl Monomers	26
Figure 3.11. General Structure of Acrylates and Methacrylates.....	38
Figure 3.12. Structure of n-Butyl Acrylate.....	38
Figure 3.13. Structure of Poly (n-Butyl Acrylate).....	40
Figure 3.14. The Electromagnetic Spectrum	46

Chapter 4 - Test Facility:

Figure 4.1. Schematic of Hollow Disc Assembly	53
Figure 4.2. Schematic of Reactor Housing	53
Figure 4.3. Output Characteristics of UV Lamp Used.....	54
Figure 4.4. Change in Output Characteristics Over Time	54
Figure 4.5. Effect of the Glass on UV Intensity Measured.....	55
Figure 4.6. Intensity Measured Through Protective Goggles	55
Plate 4.1. Experimental Test Facility.....	56

Contents

Plate 4.2. Reaction Surface Disc.....	57
Plate 4.3. Hollow Disc Assembly	57
Plate 4.4. Internal Plate.....	58
Plate 4.5. Assembled Disc System.....	58
Plate 4.6. Framework and Rig (Without Glass Top).....	59
Chapter 5 - Experimental Procedures and Treatment of Results:	
Figure 5.1. Top View of Static Film Test Cell	63
Figure 5.2. Cross Section of Static Film Test Cell	63
Chapter 6 - Static Film Polymerisation:	
Figure 6.1. Effect of Exposure Time on Conversion at Film Thickness of 830 μm	71
Figure 6.2. Theoretical Conversion with Exposure Time for a Film Thickness of 830 μm	71
Figure 6.3. Effect of Film Thickness on Conversion for an Exposure Time of 20 Seconds	72
Figure 6.4. Theoretical Effect of Film Thickness on Conversion over a 10 Second Exposure Time.....	72
Figure 6.5. Effect of UV Intensity on Conversion at a Film Thickness of 830 μm	74
Figure 6.6. Effect of UV Intensity on M_n	74
Figure 6.7. Effect of UV Intensity on Polydispersity Index.....	75
Figure 6.8. Theoretical Effect of UV Intensity over a 10 Second Exposure Time.....	75
Figure 6.9. Deviation of Model Predictions from Perfect Correlation	77
Chapter 7 - Spinning Disc Polymerisation:	
Figure 7.1. Effect of Rotational Speed on Conversion	86
Figure 7.2. Effect of Rotational Speed on Molecular Weight	86
Figure 7.3. Effect of Feed Flowrate on Conversion.....	87

Contents

Figure 7.4. Effect of Feed Flowrate on Molecular Weight.....	87
Figure 7.5. Effect of Photo-Initiator Concentration on Conversion	88
Figure 7.6. Effect of Photo-Initiator Concentration on Molecular Weight	88
Figure 7.7. Effect of Temperature on Conversion	89
Figure 7.8. Effect of Photo-Initiator Type on Conversion	91
Figure 7.9. Effect of UV Intensity on Conversion.....	92
Figure 7.10. Effect of Nitrogen Purge Time on Conversion.....	92
Figure 7.11. Deviation of Model Predictions from Perfect Correlation.....	94
Figure 7.12. Comparison of Experimental and Predicted Conversions with Rotational Speed.....	103
Figure 7.13. Comparison of Experimental and Predicted Conversions with Feed Flowrate	103
Figure 7.14. Comparison of Experimental and Predicted Conversions with Photo- Initiator Concentration.....	104
Figure 7.15. Comparison of Experimental and Predicted Conversions with Temperature	104
Figure 7.16. Comparison of Experimental and Predicted Conversions with UV Intensity.....	105
Figure 7.17. Theoretical Effect of UV Intensity on Conversion.....	105
Chapter 9 - Recommendations for Future Work:	
Figure 9.1. Predicted Effect of Increasing Disc Size on Conversion with Varying Rotational Speed.....	116
Figure 9.2. Predicted Effect of Increasing Rotational Speed on Conversion (With Disc Radius).....	117
Appendix A - Preliminary Heat Transfer Study:	
Figure A.1. Example Temperature Profile for Heat Transfer Study.....	134

Contents

Figure A.2. Schematic Representation of System for Heat Balance Purposes	135
Figure A.3. Schematic Diagram to Show Flow Inside the Disc (Cross Section).....	139
Figure A.4. Schematic to Show Flow Inside the Disc (Top View with Reaction Disc Removed).....	140
Figure A.5. Variation in External Reynolds Number with Feed Flowrate	140
Figure A.6. Variation in Internal Reynolds Number with Colling Water Flow.....	141
Figure A.7. Effect of Channel Width on Internal Reynolds Number	141
Figure A.8. Effect of Rotational Speed on the U Value	145
Figure A.9. Effect of Feed Flowrate on the U Value	146
Figure A.10. Effect of Cooling Water Flowrate on the U Value	146
Figure A.11. Effect of Channel Width on the U Value	147
Figure A.12. Effect of Temperature on the U Value	147
Appendix B: Engineering Drawings:	
Figure 4.7. Calibration Curve for Intensity with Lamp Distance	169
Appendix D: Static Film Polymerisation:	
Figure 6.10. Effect of Exposure Time on Conversion (400 μm).....	187
Figure 6.11. Effect of Exposure Time on Conversion (1000 μm).....	187
Figure 6.12. Effect of Exposure Time on M_n (400 μm)	188
Figure 6.13. Effect of Exposure Time on M_w (400 μm).....	188
Figure 6.14. Effect of Exposure Time on Polydispersity Index (400 μm).....	189
Figure 6.15. Effect of Film Thickness on Conversion (30s Exposure Time).....	189
Figure 6.16. Effect of Film Thickness on Conversion (40s Exposure Time).....	190
Figure 6.17. Effect of Film Thickness on M_n (30s Exposure Time).....	190
Figure 6.18. Effect of Film Thickness on M_w (30s Exposure Time).....	191
Figure 6.19. Effect of Film Thickness on Polydispersity Index (30s Exposure Time)	191

Appendix E: Spinning Disc Polymerisation:

Figure 7.18. Effect of Rotational Speed on Polydispersity Index.....	192
Figure 7.19. Effect of Feed Flowrate on Polydispersity Index.....	192
Figure 7.20. Effect of Photo-Initiator Concentration on Polydispersity Index.....	193
Figure 7.21. Effect of Temperature on Molecular Weight.....	193
Figure 7.22. Effect of Temperature on Polydispersity Index.....	194
Figure 7.23. Effect of Photo-Initiator Type on Conversion for 0.076 mol/L Conc.	194
Figure 7.24. Effect of Rotational Speed on Film Thickness and Residence Time.....	195
Figure 7.25. Effect of Feed Flowrate on Film Thickness and Residence Time.....	195
Figure 7.26. Operational Limits for Rotational Speed and Feed Flowrate	196
Figure 7.27. Effect of Temperature on Film Thickness and Residence Time.....	196

LIST OF TABLES

Table 3.1. Characteristics of Step and Chain Growth Polymerisations.....	7
Table 3.2. Chemical Structures of Selected Photo-Initiators.....	24
Table 3.3. Published Values of k_p for Butyl Acrylate.....	37
Table 3.4. Physical and Chemical Properties of n-Butyl Acrylate	39
Table 3.5. Early Reported Polymerisation of Acrylates and Methacrylates.....	41
Table 7.1. Summary of Observed Results	95
Table 7.2. Values of k_p for Butyl Acrylate	99

CHAPTER 1

INTRODUCTION

1.1 Process Intensification

In recent years much research has been conducted in the field of process intensification. The concept of process intensification is the reduction in terms of equipment size and inventory of chemical (or process) operations without a loss of product quality or throughput. Ramshaw highlighted the potential of centrifugal fields as a means of intensifying unit operations [1] in a wide range of applications including; separation, heat transfer, electrochemistry and reactors. The early studies undertaken by ICI in these fields include the concept of Hige distillation (patented in 1979 [2]) which resulted in the construction of a full scale Hige distillation unit, and the work conducted on heat pumps, with the introduction of the “Rotex” design [3] (originally patented in 1986 [4]). Further research focusing on the concept of 'Hige' is now based at the University of Beijing, China, in the dedicated 'Higravitech' Institute [5]. Research and development work in the field of process intensification is widespread, both in terms of applications and location, with much interest in the UK and Europe [6]. Much of the research has been part funded by organisations such as the Department of Environment, Transport and the Regions (Energy Efficiency Best Practice Programme), the European Commission (Joule, Joule II programmes) and the Health and Safety Executive.

The area of compact heat exchangers has been widely researched by a number of institutions including UMIST, Heriot-Watt University, AEA Technology and CEA-Grenoble [7] and the equipment and research in this field has been reviewed in the last five years [8]. Other areas of research undertaken at Heriot-Watt University include oscillatory flow baffled reactors, with the potential to intensify inherently slow reactions (reaction times of hours), which originated (and continues) at Cambridge University [9]. The BHR Group are involved in work on high intensity in-line mixing devices (such as static mixers, ejectors, rotor stator mixers and tee mixers) and also in

combined chemical reactor - heat exchangers for continuous processing of exothermic or endothermic reactions [10]. Intensification in the field of gas-liquid mass transfer is also being conducted, with the development of a co-current downflow contactor at Birmingham University.

In the field of reactors the research extends to catalytic plate reactors (chemical reactor - heat exchangers), spinning disc reactors and micro-reactors. The use of new technology with the benefits of enhanced heat and mass transfer characteristics offer the opportunity to apply process intensification to further industrial applications. The field of process intensification with an emphasis on catalytic plate reactors has been reviewed recently as part of a PhD thesis at Newcastle University [11]. Currently the main areas of interest in the Process Intensification and Innovation Centre (PIIC) at Newcastle University include:

- compact heat exchangers [8]
- catalytic plate reactors [11]
- spinning disc reactors [12,13,14,15]

1.2 Spinning Disc Reactors

The area of relevance to this research is that of spinning disc reactors, and the use of a novel internally cooled disc system. Previous studies on spinning disc hydrodynamics [16,17] and heat and mass transfer [18,19] have been conducted at Newcastle University and the enhancement of heat transfer characteristics by use of rotating surfaces has been highlighted [15]. The potential of this type of reactor in polymerisation reactions was highlighted by Ramshaw [1] in 1993 as a benefit of the use of centrifugal fields in process intensification. This has more recently been studied, both for the polymerisation of unsaturated polyester [14] and the manufacture of polystyrene [12,20]. A recent review of the development and advances in spinning disc reactors is included in a PhD thesis at Newcastle University [20]. The opportunities presented by this technology are due to the following advantages:

1. rapid mixing in the liquid film
2. short liquid residence time
3. rapid solid/liquid heat/mass transfer
4. rapid liquid/vapour heat/mass transfer.

The use of intensified spinning disc reactors also presents opportunities in terms of safety due to:

- reduced inventories of hazardous material for handling and transportation
- reduced dangers of thermal runaway and thermal ignition.

These characteristics make the SDR a potential choice for photo-initiated polymerisations, in which a thin film is required to overcome the problem of UV absorbance by the monomer. The problem of UV penetration prevents the efficient use of stirred tank reactors for this application. The polymerisation reaction is exothermic (ΔH of -77.4 kJ/mole [21]) and temperature control is critical in preventing thermal degradation of the polymer. This exploratory research investigates the suitability of the SDR for photo-initiated polymerisation, using the photo-polymerisation of acrylates as an example of potential industrial interest, and part of the study was conducted in conjunction with Courtaulds Coatings.

1.3 Present Study

The investigation is divided into two main subjects, static film polymerisation and spinning disc polymerisation, and also includes a preliminary heat transfer study. Although this is primarily an investigation into the suitability of the technology for this application (i.e. process engineering based) it is necessary to include the chemistry of the system under study for completeness and this can be found in Chapter 3.

A statement of the objectives of the investigation is included in Chapter 2.

Chapter 1

Detailed descriptions of the novel internally cooled SDR are included in Chapter 4, along with further details of the test facility.

Although the investigation can be divided into more than one subject, much of the experimental method, analysis technique and data treatment and analysis is common to two (or more) of these divisions. For the convenience of the reader these are all included in Chapter 5, allowing easy reference to the areas of interest.

The reason for the division of this investigation into the separate subjects is again for ease of reading, allowing each subject to be considered individually if required. Chapter 6 contains the results and discussion relevant to the static film polymerisation and Chapter 7 refers to the spinning disc polymerisation. The results of the heat transfer study are contained in Appendix A together with the relevant heat balance and calculations.

The conclusions drawn and the comparisons that can be made between subject areas are included in Chapter 8. Chapter 9 then details recommendations for future work based on the conclusions drawn and experience gained from this investigation.

CHAPTER 2

OBJECTIVES OF THE PRESENT INVESTIGATION

The purpose of this research is an exploratory investigation of the suitability of a spinning disc reactor for acrylic / photo-initiated polymerisations and to highlight any potential for development of this type of reactor for application in this field. The investigation has two main areas of interest:

1. Static film (400 - 1000 μm thickness) characterisation of the UV initiated polymerisation system.
2. The use of a spinning disc reactor for the photo-initiated polymerisation of acrylates, and the development of an empirical model from the data obtained.

The first objective is to gain an understanding of the photo-initiated polymerisation of n-butyl acrylate in a static film system, and to determine the factors upon which the polymerisation is dependent. From the results of this study it is anticipated that a predictive model based on the experimental results will be obtained.

The second objective is to conduct the polymerisation in the spinning disc reactor and compare the results obtained with those from the first stage of the investigation to give an indication of the potential of the spinning disc reactor for this type of polymerisation. Again it is anticipated that a predictive model based on the experimental results will be obtained.

A further objective of this investigation is to conduct a preliminary study into the heat transfer characteristics of this novel spinning disc reactor. The reactor is novel in the fact that the spinning disc assembly is hollow and permits internal circulation of cooling or heating fluid, which is anticipated to enhance heat transfer and enable close control of reaction temperature.

CHAPTER 3

LITERATURE REVIEW

3.1 Introduction

The concept of process intensification and the role of spinning disc reactors within this field has been discussed in Chapter 1. The aim of this chapter is to review previous work conducted in the fields of relevance to this study of the photo-polymerisation of acrylates. It is also necessary to provide the reader with sufficient information on the concepts involved in the polymerisation system under study without assuming a background in chemistry. This includes not only the polymerisation reaction itself but the kinetics of polymerisation, photo-chemical reactions utilising ultra-violet (UV) light and the chemistry of acrylates and photo-initiators. As this covers a wide and complex area, the author has attempted to provide only information of relevance or interest to this study in such a way as to allow the reader to follow the interpretation of results and importance of experimental variables without the need for previous knowledge in all these areas.

3.2 Polymerisation

3.2.1 Introduction

There are two general reaction classes of polymerisation which progress by different mechanisms, step (or condensation) polymerisation and chain growth (or addition) polymerisation. There are various characteristics that identify a polymerisation as either a step or chain growth polymerisation. Table 3.1 [22] summarises these characteristics and highlights the differences between the two classifications. Typically, chain growth polymerisations involve unsaturated monomers and the reactive centres involved in the reactions are usually free-radicals although they may also be

anions or cations. Chain growth polymerisation involving free-radicals is both the most versatile and most important commercially, and it is this mechanism which is considered for this investigation. Further details of the basic concepts can be found in any standard polymerisation text [23-26]. The general concepts that are directly relevant to this investigation are outlined in this section.

Table 3.1. Characteristics of Step and Chain Growth Polymerisations.

Characteristic	Step Polymerisation	Chain Growth Polymerisation
Monomer Concentration	Drops rapidly to zero in the early stages of reaction	Decreases steadily with time
Molecular Mass	Rises steadily during reaction	High molecular mass polymer is formed at once and hardly changes
Reaction Time	Long reaction times are required to obtain high molecular mass polymer	Long reaction times increase yield but do not affect molecular mass
Reaction Mixture	Contains all possible molecular species from dimers to polymers of large degrees of polymerisation at all reaction stages	Contains only monomer, high molecular mass polymer and a low concentration of growing chains

The polymerisation reaction comprises three main stages; initiation, propagation and termination, which will be discussed more fully in Section 3.2.2. Briefly, the initiation stage involves the origination of a polymer chain by one of various initiation methods; the propagation stage involves the growth of this polymer chain by addition of further monomeric units; and the termination stage involves the final combination of the actively growing polymer chain to produce a polymer chain with final molecular weight and other properties.

The four main types of polymerisation within this class are bulk, solution, suspension and emulsion. Chain growth (addition) polymerisation is exothermic with ΔH generally in the range (-34)-(-160) kJ/mole. This causes problems which must be overcome by

controlling the rate of reaction or by heat removal. In bulk polymerisations heat removal is difficult, especially at high conversions, due to the increased viscosity and many polymerisations are therefore conducted in solution or emulsions and dispersions.

3.2.1.1 Bulk Polymerisation

Bulk polymerisation requires the presence only of monomer and initiator but can also involve other agents such as chain transfer agents. Bulk polymerisation of liquid monomers is not widely practised but the technique is important for gas phase polymerisations such as ethylene and vinyl chloride [27]. This is due to the rapid rates of polymerisation and strongly exothermic characteristics associated with liquid monomers, especially in acrylate and methacrylate systems. Another potential problem with this type of polymerisation is the onset of auto-acceleration (or Trommsdorff-Norrish effect, refer to Section 3.3.2.3).

3.2.1.2 Solution Polymerisation

Solution polymerisation overcomes some of the problems encountered with bulk polymerisation by the presence of a solvent, which provides a method of heat removal for the reaction. This presents its own disadvantages, requiring isolation and purification of the product, although industrially this method is often performed for applications where the solvent remains present in the product. The influence of the solvent on the course of the polymerisation is an important factor in these polymerisations. Cases wherein both the monomer and polymer are soluble in the solvent are termed 'homogeneous solution polymerisations', and where the polymer is insoluble in the solvent they are termed 'solution precipitation polymerisations'.

3.2.1.3 Suspension Polymerisation

Suspension polymerisation is also known as aqueous suspension, pearl or bead polymerisation. Liquid monomer droplets are suspended in an aqueous phase under vigorous stirring. This method can be regarded as bulk polymerisation of monomer droplets where the surrounding water can easily dissipate the reaction heat. The presence of suspension stabilisers or suspending agents (water-soluble polymeric

compounds or powdery inorganic compounds) is necessary to prevent the coalescence of the droplets. A further type of suspension polymerisation is non-aqueous dispersion polymerisation. This is the polymerisation of monomer soluble in an organic solvent to produce insoluble polymer, the precipitation of which is controlled by the addition of a stabiliser or dispersant.

3.2.1.4 Emulsion Polymerisation

Emulsion polymerisation involves three phases: an aqueous phase containing a water-soluble initiator, a micelle-forming surfactant and a small amount of sparingly soluble monomer; monomer droplets; latex particles consisting of polymer and some monomer.

3.2.1.5 Polymerisation Reactors

There are three main types of reactor commonly used in polymerisations [28], batch, tubular and continuous stirred tank reactors (CSTR). Each type of reactor is best suited to different types of polymerisations and different polymerisation conditions.

Batch reactors are the most commonly used polymerisation reactors although bulk polymerisations present some problems. An important factor in polymerisations is the control of temperature, and therefore good mixing is essential to ensure uniform temperatures and to prevent localised inhomogeneities. The most common heat removal methods from batch reactors are; transfer to vessel jacket, use of internal cooling coils, circulation through an external cooling loop and the use of an overhead condenser to remove heat from the vapour phase. Bulk polymerisations have the characteristic of large viscosity increases with conversion, which makes efficient mixing difficult, although this effect is much less pronounced in emulsion and solution polymerisations. A problem encountered with suspension polymerisations is the difficulty of maintaining the suspension. Internal coils can only be used for low viscosity applications in which polymer fouling is not a problem. The inappropriate use of internal coils results in poor mixing around the coils, leading to lower product quality and long clean-up times between batches.

Tubular reactors are essentially unstirred vessels with high length / radius ratios. They are limited in their application to polymerisation reactions, with the polymer tending to form a slow moving layer on the cool walls, reducing the effective heat transfer coefficient and complicating the problem of heat removal.

CSTRs promise narrower molecular weight distribution in free-radical polymerisations than a comparable batch or tubular reactor due to their mixing characteristics (the feed is assumed to blend instantly with the tank contents in a perfect CSTR). Problems are encountered in the handling and pumping of the high conversion polymer mixes due to their increased viscosity. These problems restrict the opportunities for continuous processing, although a continuous method involving a wiped surface reactor has been patented [29].

3.2.2 The Polymerisation Reaction

3.2.2.1 *Initiation*

As mentioned previously, a polymerisation reaction comprises three main stages, the first of these being termed initiation. This initial step involves the initiation of a polymer chain by one of various methods. The main methods of initiation are free-radical, thermal, anionic and cationic. For the purpose of this investigation we will consider free-radical initiation only. Free-radicals are produced by the decomposition of an initiator either thermally or by irradiation. The general conditions required for successful free-radical initiation are; the initiator decomposition rate remains reasonably constant throughout the polymerisation and the cage effect (Section 3.3.2.4) is small, there are reduced side reactions of the free-radicals (e.g. hydrogen abstraction), and addition of accelerators and / or chain transfer agents (which can reduce the reaction temperature and regulate the average molar mass of the polymer) dependent upon the required properties of the final polymer. Each initiator has either a useful temperature range (thermal decomposition) or a useful wavelength range (decomposition by irradiation). Irradiation can be by UV light, γ -radiation, electron beam, x-ray or ion-beam radiation, and the use of microwaves [30] has also been considered. An advantage of the use of radiation is the lack of specific temperature

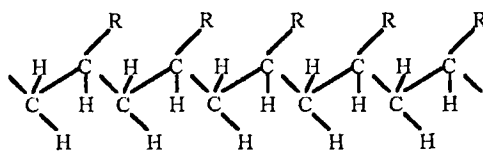
requirement for the initiator, and the lower activation energy required. The activation energy required for an overall free-radical polymerisation, E_{Apol} , is generally in the region of 95 kJ/mole. In a photo-initiated system where no thermal processes are contributing to E_{Apol} then this is reduced to somewhere in the region of 25 kJ/mole [31]. Initiation by UV irradiation is reviewed in more detail in Section 3.3.3.

3.2.2.2 Propagation

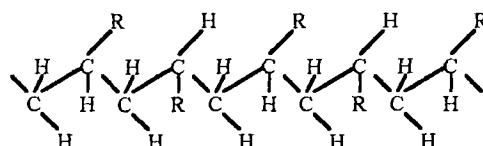
The second of the three main stages in a polymerisation reaction is termed propagation and in the case under investigation (bulk addition polymerisation) involves growth of the polymer chain by the addition of more and more monomer units. Chain growth either occurs head-to-tail (i.e. all monomer units line up the same way) or, where the polymer formed contains asymmetric carbon atoms there are three possible stereochemical arrangements. If all the carbon atoms are configured identically then the polymer is termed isotactic. Polymers in which the carbon atoms are configured in a regular alternating pattern are termed syndiotactic. Finally, if there is no regularity of carbon atoms in the configuration the polymer is termed atactic. Figure 3.1 [22] illustrates these three different configurations. Free-radical polymerisation generally produces atactic polymers with tendency to syndiotacticity at low temperatures, as the activation energy is lowest for head-to-tail chain growth. Linear polymers are usually produced in the free-radical addition polymerisation of bifunctional monomers [32].

3.2.2.3 Termination

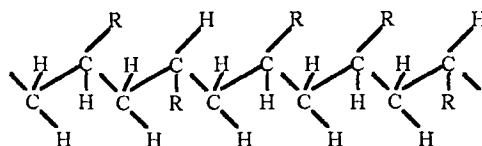
The final of the three main stages in a polymerisation reaction is known as termination and involves the termination of a growing polymer chain. This can occur by reaction with other free-radicals or with impurities in the system, by combination of two growing polymer chains or by disproportionation (hydrogen abstraction from one chain end by the radical end of a second chain).



Isotactic Configuration



Syndiotactic Configuration



Atactic Configuration

Figure 3.1. Possible Stereochemical Configurations.

3.2.3 Molecular Weight and Polydispersity

3.2.3.1 Molecular Weight

The high molecular weight (or more correctly, molecular mass) of polymers results in unique mechanical properties, generally a higher molecular weight exhibits a higher mechanical strength [23]. Many properties of a polymer are dependent upon the molecular mass of the polymer, i.e. polymers which are chemically the same can exhibit very different properties. For this reason it is essential to be able to control the polymerisation closely and fully characterise the resulting polymer in terms of molecular weight and molecular weight distribution to ensure the production of useful polymer (i.e. polymer which has the required properties for the intended application). The molecular weight (and chain length) of a polymer is dependent upon parameters

such as; the type of polymerisation, the chemistry of the system (including the presence of initiators, chain transfer agents and the like), the methods of initiation, propagation and termination, and the presence of impurities within the system, among others.

The definition of molecular weight is dependent upon the method used in its determination, and for this investigation it is sufficient to consider two values, M_w and M_n .

3.2.3.2 Number-Average Molecular Weight

M_n is known as the number-average molecular weight and is defined as “the total weight of all the molecules in a polymer sample divided by the total number of moles present” [23]. M_n is determined experimentally by various methods such as vapour pressure osmometry, cryoscopy or membrane osmometry, all of which involve the counting of polymer molecules in a sample of the polymer.

3.2.3.3 Weight-Average Molecular Weight

M_w is known as the weight-average molecular weight and is defined as the sum of the product of weight fraction and molecular weight for the range of weights in the polymer sample. M_w is determined by measurement of light scattering by the polymer sample, and as such is more accurate for higher molecular weights [23].

3.2.3.4 Polydispersity

The knowledge of one value of molecular weight alone is insufficient to characterise a polymer, as the values of M_n and M_w are equal in one case only - for a monodisperse product. In most instances, a polydisperse product is formed which has $M_w > M_n$ [23]. A useful measure of the polydispersity of a polymer is the ratio of M_w to M_n , and is termed the polydispersity index. The value of this ratio gives an indication of the breadth of the molecular weight distribution, with a value of unity indicating a monodisperse product.

3.3 Photo-Polymerisation

3.3.1 Introduction

This investigation is concerned with the bulk photo-polymerisation of acrylates (namely n-butyl acrylate) and the general concepts, mechanism of reaction and related subjects are reviewed in this section. The kinetics of the reaction and a background of acrylate chemistry are reviewed later in Sections 3.4 and 3.5.

3.3.2 General Concepts

3.3.2.1 Photo-Chemical Reactions.

There are four distinct stages of a photo-chemical reaction [33]:

1. Absorption of one quantum of radiation ($h\nu$) by a molecule M to form an electronically excited state, M^* .
2. The fate of M^* . This includes dissociation, predissociation fluorescence or phosphorescence and collisional deactivation to the ground state.
3. Dark or thermal reaction of dissociation products.
4. Possible molecular rearrangement of the excited state M^* .

The reaction of an excited state molecule (M^*) is termed a 'light reaction', whereas a reaction which proceeds through the ground state molecule (M) is termed a 'dark reaction'.

The first stage of a photo-chemical reaction is governed by two laws, Lambert's and Beer's. Lambert's law is shown as Equation (3.1), and states that the intensity of the absorbed radiation at a given thickness is dependent upon the incident intensity, molar absorption coefficient and film thickness. Beer's law is shown as Equation (3.2), and states that the intensity at a given thickness is dependent upon the incident intensity, a constant (b) and the concentration of initiator. Combining Equations (3.1) and (3.2) gives us the Beer-Lambert Law (Equation (3.3)). This is often expressed in terms of an

extinction coefficient E, optical density D or absorption A and then takes the form of Equation 3.4.

$$I_t = I_0 10^{k_d d_f} \quad (3.1)$$

$$I_t = I_0 10^{-b[PI]} \quad (3.2)$$

$$I_t = I_0 10^{-\epsilon[PI]d_f} \quad (3.3)$$

$$E = D = A = \log \frac{I_t}{I_0} = \epsilon[PI]d_f \quad (3.4)$$

These laws are applicable only to monochromatic light. The Stark-Einstein Law also applies to this first stage in a photo-chemical reaction [27] and considers the energy requirements. It states “initially each molecule which forms an electronically excited state by exposure to radiation absorbs one quantum of the radiation causing the primary process”. The energy available from the radiation to excite the molecules to higher electronic states (E) is related to the wavelength of the radiation (λ) by Equation (3.5), where h is Planck's constant and c is the speed of light.

$$E = h\nu = \frac{hc}{\lambda} \quad (3.5)$$

Organic photo-chemistry is concerned with four types of electronic transition; singlet and triplet $n \rightarrow \pi^*$ and singlet and triplet $\pi \rightarrow \pi^*$. The $n \rightarrow \pi^*$ transitions require longest wavelength UV light and $\pi \rightarrow \pi^*$ transitions require intermediate wavelengths. The promotion of ground state electrons to higher energy states by absorption of energy from light will not be discussed in further detail here, as it is sufficient to be aware that this is the mechanism by which the photo-initiation proceeds. Further details can be readily found in many texts [34-36].

3.3.2.2 Experimental UV Intensity

The range of UV intensities used in previously published work ranges up to 1400 mW/cm² [37] for laser induced polymerisation with conversions of up to 90% being

reached in 2 s using UV intensities in the range 30 - 200 mW/cm² from a laser source [38]. In the application of UV curing it has been reported that a final conversion of 80% was achieved with an intensity of 10 mW/cm² and increasing this to 80 mW/cm² resulted in an increase in final conversion to 95% [39]. For UV curing utilising an unfocused laser beam, it is reported that 85% of the sample was recovered as an insoluble polymer after 5 ms exposure [40].

3.3.2.3 *The Gel Effect*

During the later stages of polymerisation, the gel effect (which is also known as auto-acceleration or the Trommsdorf-Norrish effect) gives rise to a sudden increase in the rate of polymerisation and chain length and is accompanied by a rapid increase in viscosity and temperature [33]. This effect is clearly seen in the polymerisation of methyl methacrylate [41] and has been shown to be due to the diffusion-controlled nature of termination.

The onset of auto-acceleration can be delayed by the use of solvents, higher temperatures and higher initiation rates but these have their disadvantages in terms of downstream processing and product quality. Auto-acceleration occurs at lower conversions with the introduction of pre-polymer and poor polymer-monomer interaction can lead to severe coiling of the polymer chains which triggers the auto-acceleration effect.

3.3.2.4 *The Cage Effect*

The cage effect is the term given to the recombination of original radical partners before they have time to move apart [22]. Primary recombination of two radicals in the solvent cage can occur in two ways; firstly, if the solvent is able to remove the excess kinetic energy by collision between the radicals and the solvent molecules and hence prevent the radicals escaping the solvent cage, and secondly if the radical pair undergo secondary recombination by diffusion. The higher the frequency of the absorbed radiation, the lower the recombination effect. The dissociation particles have a greater excess kinetic energy with higher frequency radiation and are therefore more likely to escape the solvent cage. If the dissociation products are heavier than the solvent

molecules they are also more likely to escape recombination. The mechanisms resulting in the cage effect [20,23] are not confined to photo-initiated polymerisations but are a common occurrence in any free-radical polymerisation.

3.3.3 Photo-Initiation

3.3.3.1 Introduction

The definition of a photo-initiator is “an additive present to facilitate an initiation reaction in photo-polymerisation” [42]. It absorbs radiation and breaks to form the primary reactive species, usually free-radicals. A photo-initiator is consumed during reaction. The main requirement of a photo-initiator is that an emission line from the light source overlaps with an absorption band of the photo-initiator.

The definition of a photo-sensitiser is “a compound having a positive influence on the photo-chemical reaction rate by absorbing energy and transferring that energy to another molecule which then forms the primary reactive species” [42]. A photo-sensitiser is not consumed or structurally altered during the reaction and can be considered a photo-catalyst [43]. Alternatively, the additive is excited to its triplet state (unpaired electrons) which can then accept or donate electrons from another molecule which subsequently acts as reactive species. The additive is either oxidised or reduced during electron transfer. Research conducted on the photo-sensitisation of polymerisation reactions using benzoin and benzil as sensitisers concluded that benzoin is the more efficient of the two [44]. The use of uranyl ions as photo-sensitisers has also been proposed [45].

Photo-initiators can be classified into two types [46-48], PI_1 and PI_2 . PI_1 type photo-initiators undergo intramolecular bond cleavage, which is a unimolecular process, and PI_2 type photo-initiators undergo intermolecular hydrogen abstraction, a bimolecular process.

PI_1 and PI_2 combinations are used to reduce oxygen inhibition in the absence of amines. PI_1 photo-cleavage produces $R\bullet$ radicals that react with oxygen to give peroxy radicals ($RO_2\bullet$). PI_1 photo-cleavage generally competes with oxygen quenching. Although

$\text{RO}_2\bullet$ are poor initiators for acrylates they regenerate radicals by abstracting hydrogen atoms from monomers and oligomers, thus resulting in formation of hydroperoxides (RO_2H) and simultaneous depletion of O_2 . This enhances PI_2^* as an energy transfer agent: $\text{RO}_2\text{H} \rightarrow \text{RO}\bullet + \text{HO}\bullet$ (alkoxy and hydroxy radicals) which are highly effective initiators for acrylates.

PI_1 type photo-initiators are useful due to their good availability and high photo-decomposition quantum efficiencies.

3.3.3.2 Methods of Photo-Initiation

There are various mechanisms by which photo-initiation proceeds and these include fragmentation, hydrogen abstraction, ionic initiation, photo-cross-linking and triplet energy transfer. Photo-initiators can also be classified by their chemistry and the various different types of photo-initiators proceed by different methods. The main types of photo-initiators and their mechanisms are considered briefly here.

The main classes are listed here [43] and the mechanisms by which they produce radicals is detailed later. The main classes are: photo-ionic polymerising compounds (aryldiazonium compounds, diaryliodonium compounds, triarylsulphonium compounds and triarylselenonium compounds); benzoin and derivatives (benzoin, benzoin alkyl ethers, benzil ketals); acetophenone derivatives (dialkoxyacetophenones and chlorinated acetophenone derivatives); aromatic ketone / amine combinations (benzophenone and Michler's ketone); α -acyloxime esters; thioxanthone and derivatives; quinones; dye photo-sensitisers; pigment photo-sensitisers; organic peroxides; organic sulphur compounds; metal compounds and ions; organic phosphorous-containing compounds; chlorosilanes; and azo compounds. As can be seen from this list, there are many different photo-initiators available and the choice of initiator must include careful consideration of the reaction and its requirements.

More recent studies consider the use of new initiator systems in free-radical polymerisation [49] and alternative methods of initiation [48] e.g. via charge transfer processes, via exciplexes of aromatic carbonyl compounds and by the use of photo-chemically active polymers.

3.3.3.3 Mechanisms of Photo-Initiation

i. Aromatic carbonyl compounds.

When excited these compounds undergo one of three types of photo-chemical reaction, the schemes for which are detailed here.

- Norrish type I (Figure 3.2): homolytic cleavage.
- Norrish type II (Figure 3.3): an intramolecular non-radical process resulting in a six-membered cyclic intermediate which decomposes by hydrogen abstraction to olefin and alcohol / aldehyde (α -hydrogen atom transfer).
- Norrish type III (Figure 3.4): an intramolecular non-radical process (β -hydrogen atom transfer).

ii. Benzoin / acetophenone and derivatives.

This group of photo-initiators is the main interest of the surface-coatings industry and as such is discussed in further detail in a later section. Dissociation is thought to occur by Norrish type I cleavage (Figure 3.5).

iii. Benzoin alkyl ethers.

Norrish type I cleavage forms benzoyl radicals (Figure 3.6) which are expected to be reactive and therefore efficient photo-initiators. Photo-initiation is thought to proceed as shown in Figure 3.6. The benzoyl and methoxy benzyl radicals are of different reactivities and it is the benzoyl radical that is main cause of polymer chain initiation. The methoxy benzyl radicals are less reactive and partially dimerise.

iv. Benzil ketals.

Dimethoxy-2-phenyl acetophenone (DMPA or Irgacure 651) is the most important commercially used benzil ketal. It is thought to undergo primarily Norrish type I cleavage (Figure 3.7). The benzoyl radicals can also then undergo recombination to form benzil (Figure 3.8).

v. Aromatic ketone / amine combinations.

An example of this class of photo-initiators is benzophenone, which undergoes hydrogen abstraction and photo-reduces to benzopinacol in the presence of hydrogen donors (Figure 3.9). It undergoes photo-induced excitation (predominantly at 340 nm) to the singlet excited state.

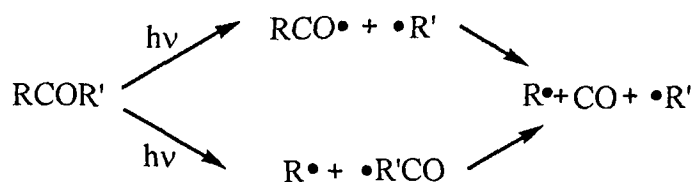
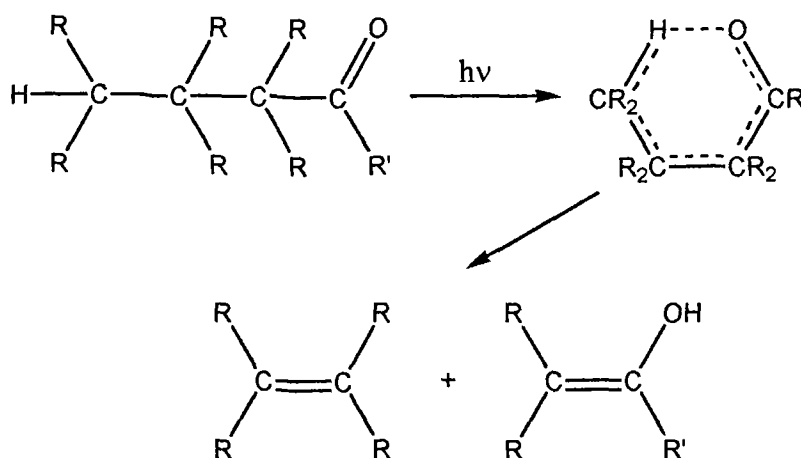
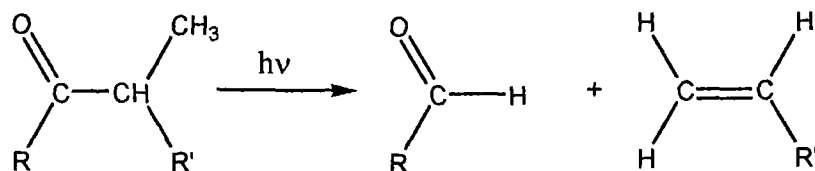


Figure 3.2. Homolytic Cleavage

Figure 3.3. α -Hydrogen Atom TransferFigure 3.4. β -Hydrogen Atom Transfer

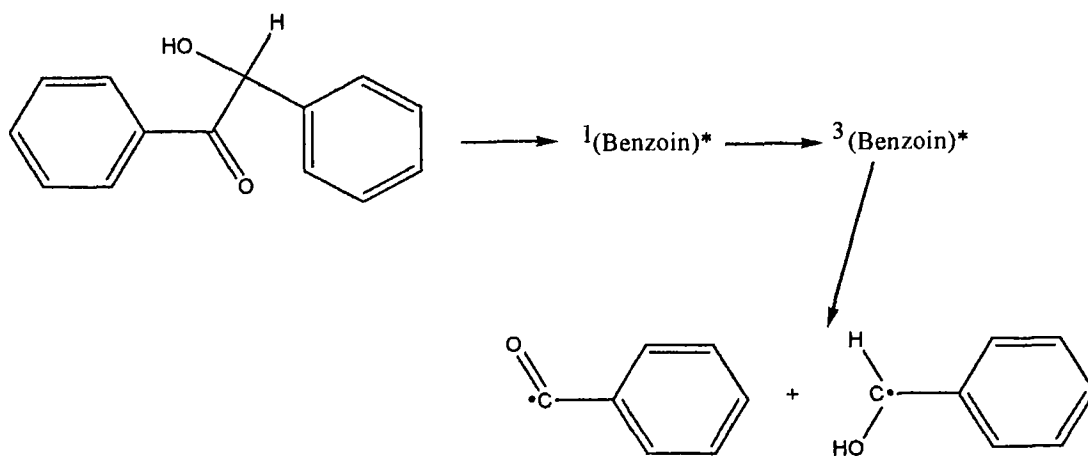


Figure 3.5. Homolytic Cleavage of Benzoin

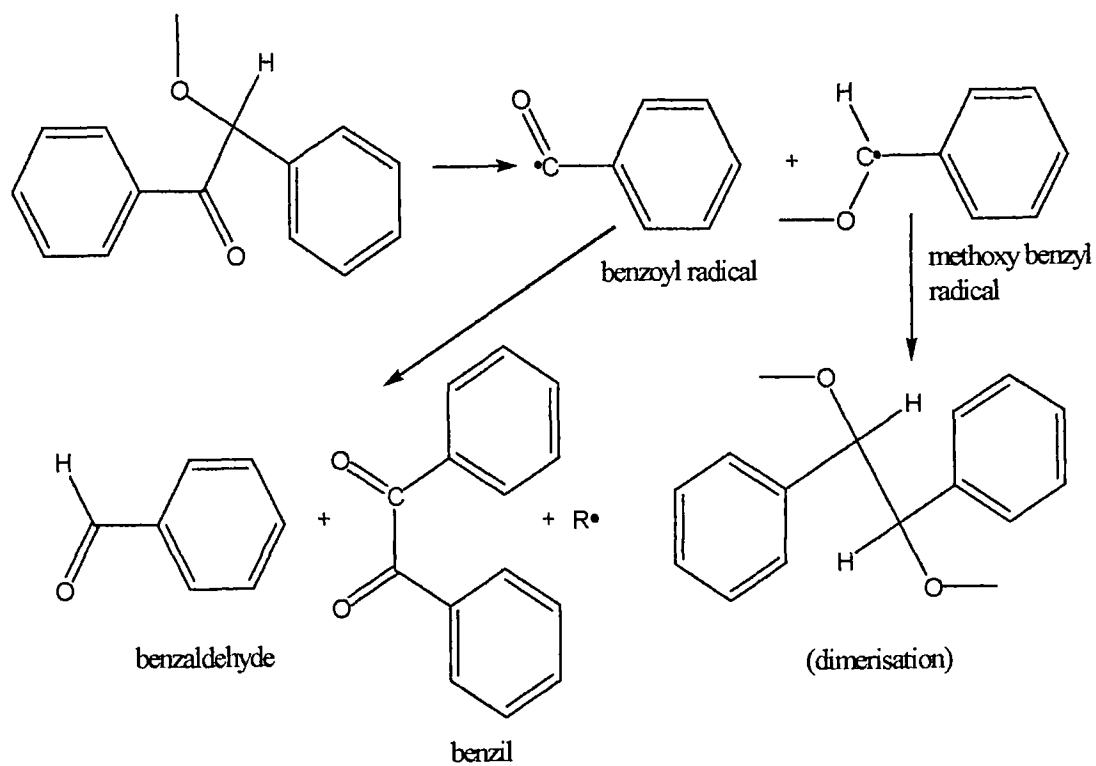


Figure 3.6. Homolytic Cleavage of Benzoin Alkyl Ethers

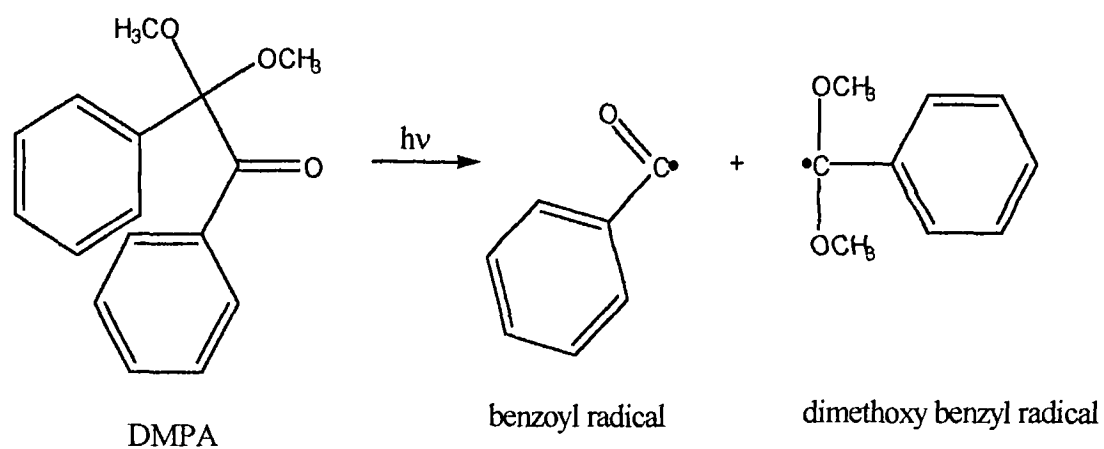


Figure 3.7. Homolytic Cleavage of DMPA

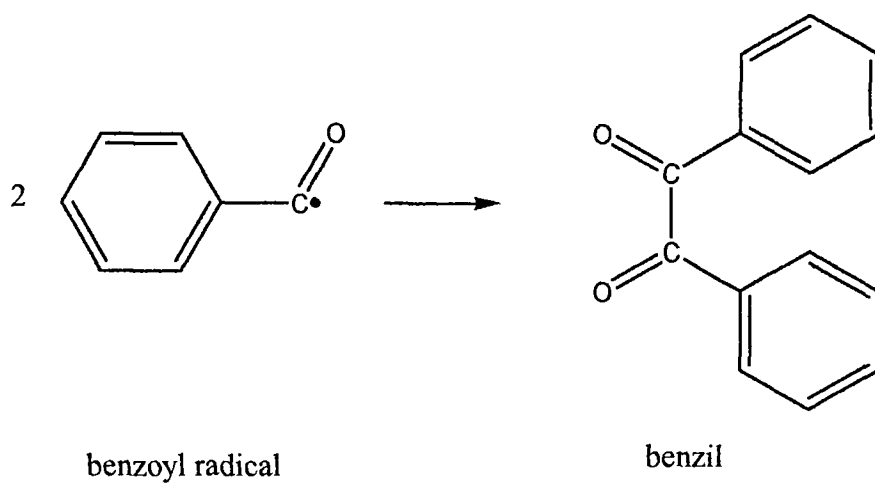


Figure 3.8. Recombination of Benzoyl Radicals

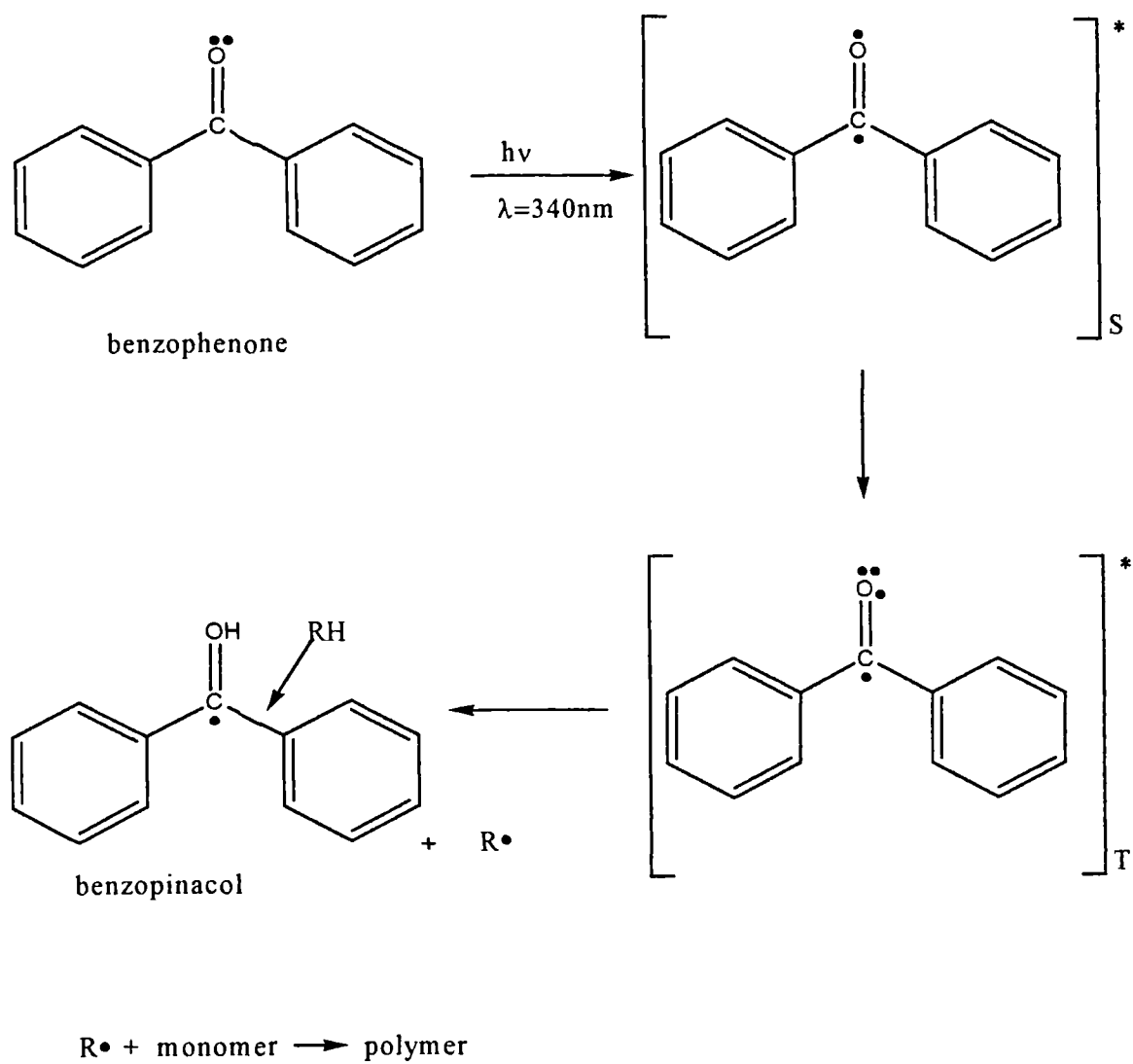
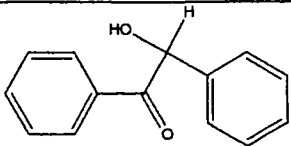
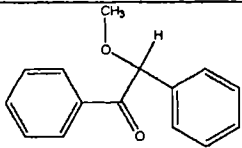
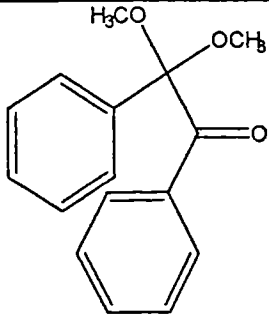
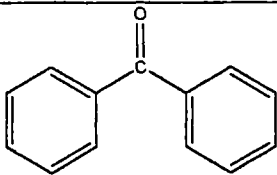


Figure 3.9. Reaction of Benzophenone with UV Light

Table 3.2. Chemical Structures of Selected Photo-Initiators.

Class of Compound	Specific Example	Chemical Structure
Aromatic carbonyl		RCOR'
Benzoin / acetophenone and derivatives	Benzoin	
Benzoin alkyl ethers	Benzoin methyl ether	
Benzil ketals	DMPA (Irgacure 651)	
Aromatic ketone / amine combinations	Benzophenone	

3.3.3.4 Photo-Initiator Concentration

The choice of initiator type is very important in photo-initiated systems and so too is the concentration of initiator used. An optimal photo-initiator concentration exists [46], which is dependent upon light utilisation and screening by the photo-initiator and also on the polymerisation system. The optimal photo-initiator concentration will vary with factors such as film thickness. As film thickness is increased, the significance of the light screening by the initiator increases and the optimal concentration decreases to

prevent the through-cure of the film from being retarded by the light screening of the initiator.

The value of optimal photo-initiator concentration can be estimated from Equation (3.6) [47] but this does not account for variations with light intensity.

$$A = \epsilon d_f [\text{PI}] \quad (3.6)$$

At concentrations below the optimal, full utilisation of the light energy available will not occur and fewer molecules are present to initiate chains. However, increasing concentrations beyond the optimal will result in a decrease in polymerisation rate [50] and will increase the probability of chain termination by the initiator radicals that have not been used in chain initiation.

3.3.3.5 *Photo-Initiators for the Surface Coatings Industry*

As mentioned previously, benzoin and acetophenone derivatives are the photo-initiators of most interest to the surface coatings industry and therefore a brief review is included here. Benzoin derivatives have advantages as photo-initiators; they compete effectively with oxygen quenching due to their relatively high photo-cleavage efficiency and large rate constants ($>10^{10} \text{ s}^{-1}$) [46]; they have short excited lifetimes, large photo-fragmentation yields and large absorption in the near UV range [51]. Experimental work by Lissi and Zanocco [51] concludes that with benzoin ethers there is no dependence in photo-cleavage yield upon excitation wavelength. In the photo-initiation of vinyl monomers using UV light, it is considered that the use of benzoin derivatives, particularly benzoin alkyl ethers, is more efficient than benzoin itself [52]. A study by Carlblom & Pappas [53] indicates that both the radicals produced on photolysis of benzoin methyl ether are equally effective in the photo-initiation of methyl methacrylate and methyl acrylate polymerisation, confirming the suitability of this type of initiator for use in acrylate polymerisation systems.

The use of benzoin derivatives does however have some disadvantages, dependent on the desired applications. Benzoin ethers have a relatively low absorptivity in the 300 – 400 nm wavelength range which will potentially reduce energy utilisation [46]. In the

case of pigmented coatings, where the pigment also competes for light energy, a high absorptivity is required from the initiator. A low absorptivity is desirable in the production of clear coatings however, and this makes these initiators a good choice for such systems. The importance of photo-initiator choice is highlighted in a study of a new initiator for use in clear coatings and printing inks [54]. The study found that a class of aromatic ketones (e.g. Irgacure 907 (2-methyl-1-[4-(methylthiophenyl)]-2-morpholino-propan-1-one)) is very reactive in both pigmented systems and clear coatings, especially in thin film applications.

3.3.4 Propagation in Photo-Initiated Acrylate Systems

The mechanism by which the propagation of vinyl monomers generally occurs [32] is shown in Figure 3.10. For steric and electronic reasons the addition is normally head-to-tail. ΔH for the propagation of vinyl monomers is in the range -62 to -84 kJ/mole and the activation energy associated with this step (E_{Aprop}) is approximately 29 kJ/mole [55].

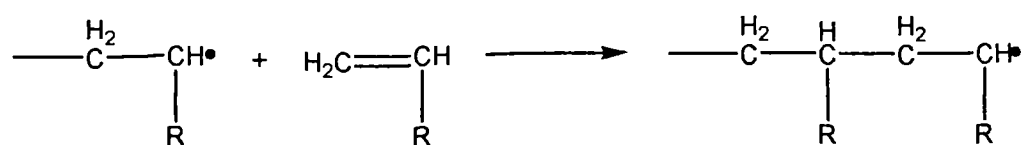


Figure 3.10. Propagation of Vinyl Monomers

3.3.5 Oxygen Inhibition in Photo-Polymerisation

The inhibiting effect of oxygen in free-radical polymerisations is well-documented [56,38,57,58,59,60,61]. Molecular oxygen (dissolved in the monomer or from atmosphere) scavenges free-radicals to form hydroperoxide groups. This is in direct competition with chain initiation and propagation and results in the presence of an 'induction period' during which no polymerisation occurs. This induction period results because the rate of oxygen scavenging is generally much higher than the rate of propagation, $k_p = 5 \times 10^8 \text{ Lmol}^{-1}\text{s}^{-1}$ c.f. $k_p = 10^3 \text{ Lmol}^{-1}\text{s}^{-1}$ for monoacrylate monomers [58]. Once the oxygen present has been combined into the hydroperoxide groups the polymerisation will progress as normal.

In the case of thin films the presence of oxygen strongly inhibits the polymerisation [38] and can also result in a non-polymerised tacky surface in the case of thin film curing [59].

The induction period will vary depending on the conditions of the polymerisation and the UV light source used. Induction periods of 1 ms for a 25 μm film with an argon ion laser have been reported [57]. It is considered that an oxygen concentration of less than 10^{-6} mol L is required to prevent inhibition, and it has been reported that this can be achieved by a few milliseconds of exposure to a high intensity mercury source [60].

Oxygen inhibition can be minimised by performing polymerisations in a nitrogen atmosphere and degassing the monomer before use. In the case of thin film curing, investigations into the use of wax barriers to reduce oxygen inhibition in the place of inert atmospheres have been conducted [59].

3.3.6 Other Possible Reactions

1. During photolysis of the initiator:

- i) Collisional deactivation to the ground state:



- ii) Spontaneous deactivation to the ground state:



- iii) Complex formation:



2. During initiation:

- i) Oxygen scavenging (refer to Section 3.3.5)
- ii) Radical-radical recombination (refer to the Cage effect, Section 3.3.2.4)

ii) Degradative chain transfer

This includes chain transfer to polymer and chain transfer to monomer (rare) and occurs by the abstraction of an atom from another molecule. The effect of this is to stop the polymer chain from growing further without quenching the radical centre.

3. During propagation:

i) Depropagation:



This becomes significant at increased temperatures because the activation energy for depropagation becomes lower than the activation energy required for propagation [62].

ii) Premature termination of growing chains

This can occur by interaction of a growing chain with a free-radical which has not been used in the process of chain initiation.

iii) Crosslinking

Crosslinking can occur due to the presence of certain chemicals or if hydrogen abstraction occurs [32]. A crosslinked polymer is one that contains covalent bonds between macromolecules, the presence of which affects the properties in several ways. Whereas uncrosslinked polymers will melt and flow at suitable temperatures, a crosslinked polymer cannot melt due to the presence of the crosslinks, and they undergo irreversible degradation at high temperatures. Another property worthy of note is that of solubility. Given an appropriate solvent and sufficient time, an uncrosslinked polymer will not dissolve, although some may swell with solvent. The difference is that this solvent can be easily removed and the polymer will return to its original size.

4. During termination:

i) Hydrogen abstraction resulting in disproportionation.

3.3.7 UV Curing

3.3.7.1 Introduction

This study is concerned with the UV initiated polymerisation of bulk monomer but the principles involved in the process of curing thin films by UV irradiation are similar to those involved in UV initiation, the main difference between the two processes being the formulation of monomer, initiator and other additives used. The aim of UV curing is to produce a highly crosslinked insoluble polymer film.

3.3.7.2 Background

The use of radiation in polymer curing for the surface coatings industry has been of growing interest since around 1970 [63]. It was found to be a quick, energy efficient method of producing extensively crosslinked polymer systems whose properties make them ideal for use in surface coatings. On a commercial scale, the first installation of UV curing equipment occurred in the early 1970s [64], and initially UV was the only radiation source used. A process utilising UV irradiation to cure acrylic type pressure sensitive adhesives was patented in 1980 [65] and was capable of preparation of films of up to 1.9 cm thickness using a medium pressure mercury lamp. More recent work on the polymerisation of acrylate monomers by UV irradiation to produce highly crosslinked networks has also reported the curing of films up to 2 cm thick [39].

With developments in laser technology, electron beams and lasers were also introduced as radiation sources. The use of lasers emitting in the near UV region in place of UV lamps has been studied [57,58,66,67] and these present advantages over the traditional UV sources. Such advantages include the ease of tuning the laser to the exact wavelength required, increasing the energy efficiency of the initiation system; the ability to focus the laser beam down to a small spot of high intensity; and also the reduced problem of UV penetration as the light intensity is almost constant along the beam, i.e. there are negligible source - object distance effects, resulting in a more uniform irradiation throughout the sample.

3.3.7.3 *Applications of UV Curing*

The process rapidly found use in many industries including; paper, metal, plastics and wood coatings, adhesives, and inks and printing and the applications are many and varied [63,68]. Some of the applications are mentioned briefly here to illustrate the commercial importance of the process. The main applications can be grouped into four areas [68]:

1. Coatings
2. Inks
3. Adhesives
4. Specialised applications

The first two of these areas are the main applications of UV curing, accounting for the major turnover in terms of both volume and sales. The area of coatings can be further divided into four categories; wood coatings, paper and board coatings, metal coatings and plastic coatings.

UV cured wood coatings include; the use of unsaturated polyesters in fillers, sealers and topcoats, the use of acrylics in fillers, acrylic sealers, acrylic topcoats and wood and cork flooring (the 'no wax' finish), and the use of water based wood finishes.

UV cured paper and board coatings applications include overprint varnishes, metallised foils and papers, silicon release coatings and furniture foil lacquers (for decorative applications).

UV cured plastic coatings applications include PVC furniture lacquers, protective coatings for PVC flooring, abrasion resistant coatings, protective lacquer for snow skis and metallising basecoats and overlacquer.

Specialised applications of UV curing include protective lacquer on laser discs and protective coating systems for optical fibres.

3.4 Kinetics

3.4.1 Introduction

The kinetics of photo-initiated polymerisations are complex and it is sufficient to consider the overall rate of polymerisation, which incorporates radical production, initiation, propagation and termination without detailing full derivations of individual rate equations. In order to present information that is relevant to and of use for this study, simplified reaction schemes only are included for these individual steps. The mechanisms of each polymerisation stage have been detailed previously (Sections 3.2.2 and 3.3.3) and the reaction schemes are included here to provide the reader with a brief background to appreciate their importance in the overall scheme.

Also included in this section are the assumptions made in the kinetic scheme and a review of the methods and advances in the measurement of polymerisation rates and kinetic data by experimental means. The actual measurement of such data is far beyond the scope of this study but accurate modelling of polymerisation systems relies heavily on the accuracy of this data and the author feels that an understanding of these methods is useful when studying polymerisation systems.

3.4.2 Overall Polymerisation Rate

The kinetics of photo-initiated free radical polymerisations are reviewed by Oster & Yang [55]. The kinetics presented are based upon solution polymerisation, however the kinetics of bulk polymerisation are very similar [25] and the use of these equations is justified. Equation (3.11) is the kinetic expression for the overall rate of polymerisation [55] as derived from the rates of initiation, propagation and termination. For the requirements of the present study, the reproduction of this derivation is unnecessary, it being sufficient to consider the overall rate.

$$R_p = -\frac{d[M]}{dt} = k_p[M] \times \sqrt{\left\{ \frac{I_0 \phi_i d_f \varepsilon [PI]}{k_t} \right\}} \times \exp\left(-\frac{1}{2} I_0 \phi_i d_f \varepsilon t\right) \quad (3.11)$$

Integration of Equation (3.11) allows the monomer conversion to be calculated at a given time, t (Equation (3.12)). From this it is possible to predict polymerisation curves for varying conditions.

$$[M]_t = [M]_0 \exp\left\{-\frac{2k_p}{\sqrt{k_t \phi_i \varepsilon d_f}} \sqrt{\frac{[PI]_0}{I_0}} \times \left[1 - \exp\left(-\frac{1}{2} I_0 \phi_i \varepsilon d_f t\right)\right]\right\} \quad (3.12)$$

The fraction of monomer that can be converted to polymer is governed by the initiator concentration and can be calculated from Equation (3.13). This equation is obtained by substitution of the limiting value $t \rightarrow \infty$ and rearranging in terms of monomer fraction.

$$\frac{[M]_0 - [M]_\infty}{[M]_0} = 1 - \exp\left\{-\frac{2k_p}{\sqrt{k_t \phi_i \varepsilon d_f}} \sqrt{\frac{[PI]_0}{I_0}}\right\} \quad (3.13)$$

For the purpose of this investigation a model based on Equation (3.11) is all that is required, the individual rates of initiation, propagation and termination being of no real benefit in predicting conversions. The use of this model in predicting monomer conversion is detailed later in Chapter 5.

3.4.3 Assumptions

In the consideration of the kinetics of photo-polymerisation, various assumptions [56] have to be made:

1. Chain transfer reactions are negligible compared to the rate of propagation. Careful consideration of process conditions and the elimination of impurities within the polymerisation system can control this.
2. Individual rate constants are independent of radical chain length.
3. A stationary state in $[R\bullet]$ exists

4. Good mixing is achieved within the polymerisation as it is known that “the kinetics of photo-initiated polymerisation in a well-stirred system differs significantly from that in an unstirred system” [62].

3.4.4 Rate of Radical Production

The production of free-radicals from an initiator by the action of UV light occurs by two main mechanisms, dependent upon the type of initiator. The first mechanism (PI₁ type) is whereby the initiator undergoes simple self-cleavage to form two radicals as illustrated by (3.14).



The second mechanism (PI₂ type) involves the presence of a sensitizer along with the initiator and can occur in two ways after the excitation of the sensitizer by the absorption of UV light (step (3.15)); by the transfer of energy from the excited sensitizer through a hydrogen transfer mechanism as in steps (3.16) and (3.17), or by direct energy transfer to the initiator in its ground state as in steps (3.18) and (3.19).



The rate of production of these radicals [55,69] is a product of quantum yield of initiator photolysis, ϕ_i (refer to Section 3.4.8) and absorbed intensity, I_a :

$$v_R = \phi_i I_a \quad (3.20)$$

Considering the Beer-Lambert Law (Equation (3.3)) and substituting for I_a gives:

$$v_R = \phi_i I_0 (1 - e^{-\epsilon d_i [PI]}) \quad (3.21)$$

And for low values of the exponent this becomes:

$$v_R = \phi_i I_0 \epsilon d_i [PI] \quad (3.22)$$

3.4.5 Rate of Initiation

The radicals formed by the photolysis of the initiator can be involved in several reactions other than the initiation of polymer chains and these are considered in Section 3.3.6. For the moment we will consider the initiation of a polymer chain only:



The rate of initiation is then given by [55]:

$$v_i = k_i [R \bullet][M] \quad (3.24)$$

3.4.6 Rate of Propagation

In a chain growth polymerisation the propagation of polymer chains can be represented by steps (3.25 - 3.27):



Other reactions of the growing polymer chains are possible and again these are included in Section 3.3.6. The rate of propagation is given by [33,55]:

$$v_p = k_p [P \bullet][M] \quad (3.28)$$

3.4.7 Rate of Termination

In the polymerisation of acrylates the method of termination tends to be by combination of two growing chains [32,61]:



Other reactions can result in premature termination of the polymer chain and these are detailed in Section 3.3.6. The rate of termination is given by [33,55]:

$$v_t = k_t [P\bullet]^2 \quad (3.30)$$

3.4.8 Quantum Yield of Initiator Photolysis, ϕ_i

The quantum yield for initiator photolysis is defined as the number of initiator molecules destroyed per photon (or quantum) absorbed [62]. If there are no competitive processes in the photo-reaction then ϕ_i will equal 2 when each quantum absorbed produces two free-radicals. In reality this is reduced by factors such as light absorption by species other than the photo-initiator, spontaneous deactivation or quenching of the excited state (I^*) and by oxygen radical scavenging.

3.4.9 Quantum Yield of Polymerisation, ϕ_p

The quantum yield of polymerisation is defined as the number of molecules reacting per number of molecules absorbed [69], or as monomer converted per quantum absorbed [55]. The consideration of three possible values of ϕ_p is sufficient for this study, either $\phi_p = 1$, <1 or >1 . If $\phi_p = 1$ then every quantum absorbed produces one photo-chemical reaction. If $\phi_p < 1$ then other chemical reactions are competing with the main photo-chemical reaction and no chain process occurs. If $\phi_p > 1$ then a chain reaction occurs, resulting from the secondary reactions of the primary free-radical species (chain initiation and propagation). Quantum yields of up to 1000000 have been reported [55] and of up to 8000 acrylic double bonds per quantum absorbed for diacrylates utilising high intensity UV [60]. The direct measurement of polymerisation quantum yields can

be achieved through the use of IR spectroscopy, which also measures the residual unsaturation in cured polymers.

3.4.10 Measurement of Polymerisation Rate and Kinetic Data

The accurate modelling of a polymerisation system relies upon the availability of reliable kinetic data such as rate coefficients. This has resulted in difficulties in the modelling of free-radical polymerisations [70], especially in the case of butyl acrylate systems where very little reliable data has been published [71,72]. This is, in part, due to the methods used in determining rate coefficients but also due to the speed of polymerisation in acrylate systems [73], which limits the temperature range for which k_p can be determined.

Recent work on a pulsed laser polymerisation (PLP) method for determining rate coefficients has determined values of k_p for butyl acrylate at temperatures of up to 30°C [71,73]. Previous methods provided very little reliable data for acrylate systems but are briefly detailed here to illustrate some of the problems encountered when modelling free-radical polymerisations.

Early research (1940s) into kinetic analysis was able only to provide data on overall reaction rate and initiation rate, the measurement of individual rate coefficients being unachievable at this time [74]. An early attempt to overcome this proposed the measurement of a further parameter, the stationary concentration of active polymer [74]. Analysis of polymer conversions in this method was by refractive index measurement or by mass of polymer remaining after vacuum evaporation of monomer. Developments in kinetic analysis led to the introduction of the rotating sector and viscometric methods [75]. In 1951, a new method for following non-stationary state polymerisations, known as a dielectric constant method, was published [76,77,78] and was used to determine polymerisation rate and radical lifetimes, although individual rate constants were still not achievable. In 1968 work was published on the use of a differential scanning calorimeter (DSC) to measure R_p directly, even in a gel or solid state [41].

Much later (in the 1980s) the use of infra-red (IR) spectroscopy to follow free-radical polymerisations and determine kinetic coefficients was reported [57,60,37]. The analysis of molecular weight and molecular weight distributions provided a method of determining kinetic data from a polymerisation system [62] and this, combined with the growing use of lasers, led to the development of the PLP method which is currently used in the determination of rate coefficients [70,79,80,81,82,83]. This development in kinetic methods has overcome some of the difficulties previously encountered in acrylate systems and has led to the more recent publication of rate coefficients for the free-radical polymerisation of butyl acrylate [71,73] the values of which are included in Table 3.3.

Table 3.3. Published Values of k_p for Butyl Acrylate.

Temperature (C)	k_p (L mol.s)
10	12500
30	16300
50	20700

3.5 Acrylates

3.5.1 Introduction

The purpose of this section is to introduce the polymerisation of acrylates and to provide some background to the history and chemistry of the monomer to be used in this study. Much of the published work relates to methyl methacrylate rather than n-butyl acrylate but much of the chemistry and many of the issues of polymerisation (e.g. oxygen inhibition) are similar and can be used as guidelines and comparisons.

3.5.2 Chemistry

Acrylates and methacrylates are unsymmetrically substituted ethylenes, the general structure of which is shown in Figure 3.11. The monomer of interest to this study is n-butyl acrylate, the structure of which is shown in Figure 3.12.

Acrylate monomers are also classified as vinyl monomers, the definition of which is the inclusion of a $\text{CH}_2=\text{CH}-$ group [23]. Strictly speaking, methacrylates do not belong to this classification but often the term vinyl is used to include monomers containing a carbon-carbon double bond.

Some physical and chemical properties of n-butyl acrylate are quoted in Table 3.4 and where relevant these are the values used in all calculations. The general structure expected in the polymerisation of n-butyl acrylate is shown in Figure 3.13.

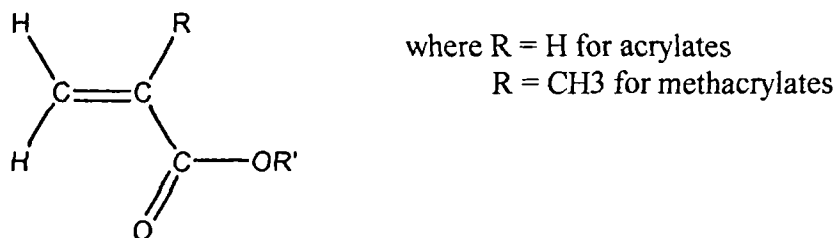


Figure 3.11. General Structure of Acrylates and Methacrylates

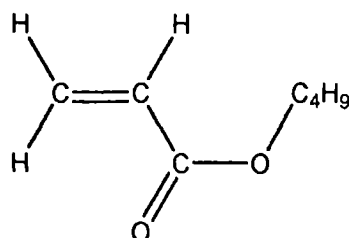


Figure 3.12. Structure of n-Butyl Acrylate

Table 3.4. Physical and Chemical Properties of n-Butyl Acrylate [21,84,85].

Property	Value	Units
ΔH_{pol}	-77.4	kJ/mol
Appearance	n/a	colourless liquid
Boiling Point	145	°C
Chemical Formula	$C_7H_{12}O_2$	(no units)
C_p	1.93	kJ/kgK
Density, ρ @ 20 C	897	kg/m ³
Molecular Mass, M_R	128.19	kg/kmol
Solubility @ 23 C	0.2 0.7	pp100 (in water) pp100 (water in n-ba)
Specific Gravity	0.894	no units
Synonyms	n/a	acrylic acid, butyl ester butyl 2-propenoate
Vapour Pressure @ 0 C @ 20°C @ 40 C	34.5 606.8 1861.7	N/m ²
Viscosity @ 0 C @ 20°C @ 40°C @ 60°C	1.268 0.937 0.713 0.557	cP

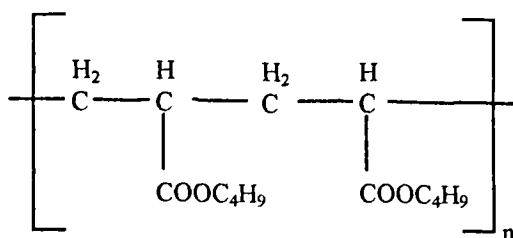


Figure 3.13. Structure of Poly (n-Butyl Acrylate).

3.5.3 Brief History of Acrylate and Methacrylate Polymerisation

Table 3.5 contains a brief history of the early work reported on the polymerisation of acrylates and methacrylates, listed in chronological order, and includes the recognition of the technical potential and consequent production on an industrial scale.

Much of the work on photo-polymerisation and the use of UV irradiation since the 1930s is more correctly classed as UV curing, most cases being concerned with producing highly cross-linked films. This is due to the difficulties encountered in the photo-polymerisation in bulk, the penetration of UV into batch systems. Thus UV irradiation was considered mainly for thin film systems and much research concentrated on the curing of prepolymerised thin films (refer to Section 3.3.7). Some early published work on the bulk photo-polymerisation of an acrylate (methyl acrylate) conducted the reaction in the vapour phase [61] but many of the conclusions drawn hold true for liquid methyl acrylate polymerisation. This study concluded that the rate of polymerisation was proportional to the square root of the UV intensity, and that termination in this system was by combination of two growing polymer chains.

In 1963, Ryan & Gormly [86] presented an experimental method for the photo-polymerisation of an acrylate (isopropyl acrylate) in a small-scale batch system (500 ml stirred vessel). The use of a 500 ml flask for the reaction required the use of four identical UV sources positioned around the flask in order to ensure irradiation of as much of the sample as possible. This polymerisation was conducted at -105°C and

separation of the polymer was a lengthy procedure, reducing the potential for scale-up of this system for industrial processes.

Table 3.5. Early Reported Polymerisation of Acrylates and Methacrylates.

DATE	DESCRIPTION
1877	The first polymeric acrylic ester is reported by Fittig & Paul.
1880	Polymeric methyl acrylate and methacrylates are reported by Fittig & Engelhorn, and Kahlbaum.
1901	The technical potential of polymeric acrylates is recognised by O. Röhm.
1914	A US patent on the "Vulcanisation of Acrylates" is filed by O. Röhm.
1924	The polymerisation of methyl and ethyl acrylates is reported by Barker & Skinner.
1927	Röhm & Haas begin the first industrial production of polymeric acrylic esters in Darmstadt, Germany.
1934+	Röhm & Haas produce organic glass ("plexiglass") by the cast polymerisation process of methyl methacrylate.
1934+	ICI (England), Röhm & Haas (US) and Du Pont de Nemours follow with industrial processes.

In the last three decades although much consideration has been given to the use of UV irradiation very little research into bulk photo-polymerisation utilising UV light has been conducted. A few examples of methods considered for utilising photo-polymerisation on an industrial scale can be found, with Rhone Poulenc having patented the idea of utilising radiation for initiation in a continuous thin film system using a conveyor belt type system [87] and also utilising light in a packed column

system [88]. Neither of these concepts have since been developed for industrial scale use. The development of thin film spinning disc reactors (refer to Chapter 1) now presents a possible solution to the problem of UV penetration into bulk monomer and the removal of heat associated with the exothermic nature of the system.

3.5.4 Polymerisation of Acrylates and Methacrylates

3.5.4.1 Considerations

Acrylates and methacrylates are usually polymerised by either free-radical or anionic initiators, making them a suitable class of monomer for use in photo-polymerisation.

The polymerisation rate and molecular weight distribution are controlled by initiator concentration, monomer concentration and reaction temperature and, in the case of photo-polymerisation, the UV intensity. In this study, the use of photo-initiation reduces the effect of reaction temperature (photo-initiators have no specific temperature requirement, unlike thermal initiators), and the bulk polymerisation of n-butyl acrylate reduces the significance of monomer concentration (initial concentration cannot be varied when no solvent is present).

In order to attain good polymerisation conditions a high purity monomer must be used as impurities affect the polymerisation reaction and can result in chain transfer reactions and premature termination of growing chains. Also, with these acrylic monomers, it is essential to ensure careful degassing of the monomer as the presence of dissolved oxygen will inhibit the polymerisation.

3.5.4.2 Potential Disadvantages

There are three important properties of the bulk polymerisation of acrylates that pose potential difficulties:

i. Strong volume contraction.

The volume contraction of acrylates is relatively high compared with other monomers, e.g. n-butyl acrylate undergoes 14.3% shrinkage [89] during the bulk polymerisation process. This can be overcome by the use of prepolymers.

ii. Considerable reaction heat.

The reaction heat must be removed from the process in order to control the polymerisation rate and the molecular weight distribution, and to prevent the onset of auto-acceleration (gel effect). It is also necessary to remove this heat in order to maintain the product quality, as some systems will undergo degradation or discolouration at too high temperatures. In general, acrylates have higher reaction heats than methacrylates, with n-butyl acrylate having a ΔH of -77.4 kJ mol⁻¹ [21], which corresponds to an adiabatic temperature rise of approximately 300 °C/mol. The spinning disc reactor has an internally cooled/heated disc system to maintain a constant reaction temperature whilst removing the heat of reaction from the reacting film.

iii. Occurrence of branching and cross-linking.

In the bulk polymerisation of acrylates, branching and cross-linking can occur at high conversions. This is the result of chain transfer via the polymer chains and produces an insoluble network. Good mixing of high conversion polymer with unconverted monomer will reduce the amount of cross-linking, and the use of the spinning disc reactor for bulk polymerisation is thought to be a potential solution.

3.5.4.3 Use of Acrylates and Methacrylates

The esters of acrylic acid are very versatile monomers and are widely used for providing performance properties to polymers [90]. The production of many different latex and solution copolymers, ethylene copolymer plastics and crosslinkable polymer systems is dependent on the incorporation of acrylate monomers. The major areas of use include surface coatings, textiles, adhesives and sealants, and plastics. The largest use for acrylic acid is the production of its esters, the largest volume of which is butyl acrylate,

followed by ethyl acrylate. The use of speciality acrylates in radiation curing for radiation curable coatings, inks, electronics manufacturing processes and adhesives is a growing concern.

Poly (acrylates) are generally used in applications requiring flexibility [21], such as surface coatings, textiles and additives for paper and oil, due to their being much softer than the poly (methacrylates). Poly (methyl methacrylate) in particular has a high hardness, making it suitable for rigid applications including glazing materials and optical applications as well as in biomedical appliances.

3.6 Review of Experimental Details

3.6.1 Introduction

The aim of this section is to review the experimental methods required for the polymerisation process and also for the analysis of the polymer produced. It includes physical factors such as UV sources and also chemical factors such as purification of reagents and analysis techniques.

3.6.2 Purification of Reagents

Free-radical polymerisations are especially sensitive to the presence of impurities and therefore the removal of stabilisers from the liquid monomer is essential [91,22]. Various methods are available for the purification of monomers [91] and these include a sequence of washes followed by drying which can be used alone [78] but which is usually followed by distillation under reduced pressure [71,76,80]; the use of fractional distillation alone [73]; the use of inhibitor removing columns [82] such as adsorption chromatography using activated alumina, except in the case of acrylates where the alumina can hydrolyse the ester group [91]; and pre-polymerisation of the monomer by prolonged short wavelength irradiation or thermal means.

3.6.3 UV Sources

The ultra violet spectrum covers the 100-400 nm wavelength range of the electromagnetic spectrum. Within the UV spectrum there are four further classifications [92] dependent on the wavelength of the light; 100-200 nm is classified as 'far' or 'vacuum' UV; 180-280 nm is classified as 'deep' UV; 280-315 is classified as 'mid' UV; 315-400 nm is classified as 'near' UV. The location of these groupings within the electromagnetic spectrum is illustrated in Figure 3.14 [93].

The main sources of UV light used are:

- Mercury vapour lamps (low, medium and high pressure)
- Plasma arcs
- Laser beams
- Electrodeless lamps

The majority of UV sources used are high intensity, medium pressure mercury vapour lamps which operate at 1 bar with intensities of up to 80 W/cm and emit UV light of 265.4 nm, 303 nm, 313 nm or 365nm wavelength (i.e. mid or near UV). An advantage of mercury lamps is the possibility of doping (i.e. additives) to shift both spectral output and power at a given wavelength, meaning they can be tailored to the required application.

With developments in laser technology, the use of laser beams as UV sources has grown, an advantage being the emission of a single wavelength, ensuring efficient energy utilisation. There are many types of laser which can be used as UV sources [92] but it is sufficient to be aware of their use for this study and it is therefore unnecessary to detail them here. A disadvantage of lasers as UV sources is the high cost compared with a typical mercury lamp, which is relatively inexpensive.

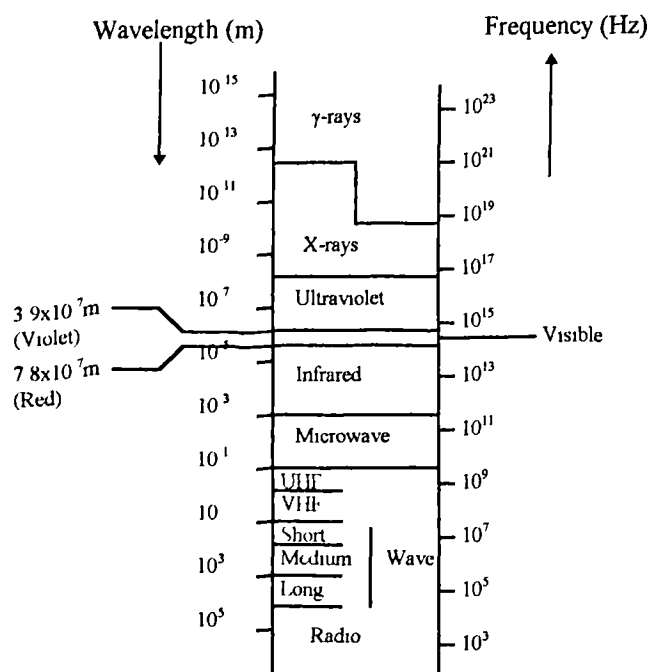


Figure 3.14. The Electromagnetic Spectrum.

3.6.4 Analysis Techniques

An important experimental consideration is the analysis of the polymer produced in the experiments in terms of not only conversion but also molecular weight and molecular weight distribution (for reasons detailed previously). Various techniques exist for measuring conversion, including wet chemistry methods and refractive index although these techniques provide no information on molecular weight. The methods considered are detailed here, and the actual procedures used throughout the experiments are included in Chapter 5.

3.6.4.1 Bromination Method

A standard analysis method involving bromination of the double bond is well-documented [94,95] and this is a relatively quick and simple method of determining conversion of monomer to polymer. This standard method however, is unsuitable for the esters of acrylic acid e.g. butyl acrylate [96], which is a less well documented fact and is due to the slow reaction of bromate-bromide solution with certain acids and

esters under normal conditions. In order to overcome this an additional step is required, involving neutralisation to the sodium salt [96] or alternatively reaction in a carbon dioxide atmosphere [97]. A second drawback of this method is that although it quantifies conversion it provides no information on molecular weight.

3.6.4.2 Refractive Index Method

A possible analysis method is the use of refractive index (measured using an ABBE refractometer) [74,98,99] to determine conversion. Again this gives no indication of molecular weight but is in theory a quick and simple technique. This method requires a reasonable volume of polymer sample to be available for analysis but can be of potential use in first estimating the success of an experiment.

3.6.4.3 GPC Analysis

Gel permeation chromatography (GPC) analysis provides information on both conversion and molecular weights [100] and is a more accurate method for small sample volumes than the previously detailed methods. Molecular weight distribution and molecular weights can be calibrated against appropriate standards and conversion calibrations easily established using samples of polymer and monomer. Polystyrene standards are used in much of the published work involving the polymerisation of acrylates [71] as they are more readily available and more widely used. Consequently, GPC analysis was the method of choice for this investigation and the procedures used are detailed in Chapter 5.

CHAPTER 4

TEST FACILITY

4.1 Introduction

The test facility required was a spinning disc reactor with cooling / heating capacity primarily for the study of exothermic reactions. For this reason a disc was designed with an internal water circulation system. This can be used to circulate cooling water, or alternatively to circulate water at elevated temperatures to maintain a constant disc temperature whilst removing heat formed during the reaction.

The reactor was used for two purposes; firstly the study of the photo-polymerisation of n-butyl acrylate, and secondly a preliminary study of the heat transfer characteristics of the internal circulation system (work has previously been conducted on the heat transfer characteristics from the disc surface as detailed in Chapter 1. The nature of the *initiation is such that* certain modifications were required to enable the study of the polymerisation and as detailed in the following section these modifications are all fully interchangeable to ensure ease of reconfiguration for other applications.

4.2 Experimental Apparatus

4.2.1 Mechanical Design

A full set of engineering drawings can be found in Appendix B.

The test rig can be seen in Plate 4.1 with the corresponding schematics in Figure 4.1 and Figure 4.2. For the purpose of the mechanical design the construction of the test facility can be divided into two main sections, the internally cooled / heated disc (Figure 4.1) and the reactor housing (Figure 4.2). The disc itself is constructed of 5 mm thick stainless steel and is 200 mm in diameter (Plate 4.2). The disc surface is smooth, with a reservoir of 18 mm diameter and 4 mm depth drilled at the centre. The purpose of this

reservoir is to provide a more even distribution of liquid across the disc. The disc is fitted to a stainless steel dish of total depth 65 mm, (Plate 4.3) with a liquid tight seal which provides the hollow disc assembly.

The drive shaft is constructed of stainless steel tubing, external diameter 35 mm and internal diameter 25 mm. This is attached to the hollow disc by means of a collar and o-ring assembly, forming a liquid tight seal. Within the drive shaft is fitted a thin copper tube of approximate diameter 17 mm, to allow for cooling / heating fluid inlet flow. To ensure maximum contact of this fluid with the underside of the disc, a thin circular plate (Plate 4.4) is located at the upper end of this tube, positioned several millimetres below the disc, creating a thin channel for fluid flow. The fluid enters this tube via a rotary union (Deublin 57-000-094) which is fitted at the lower end of the drive shaft. The fluid then circulates through the disc assembly (Plate 4.5) and exits via the annular space remaining inside the drive shaft. A 0.75 kW motor drives the disc assembly, allowing rotational speeds in the vertical axis of up to 2000 rpm.

The disc housing consists of three main parts; a stainless steel base plate, a heat exchanger, and a glass dome. The base plate is constructed of 12 mm thick stainless steel and is 360 mm in diameter. A central hole accommodates the drive shaft of the disc assembly. Three inlet holes allow a nitrogen purge to be maintained from the base. Product collection is facilitated by means of three holes located towards the outer edge of base plate. These are connected to a product collection flask located below the reactor.

The heat exchanger also forms the wall of the reactor housing (Plate 4.6), against which the product is distributed on leaving the disc. This is externally fitted with copper coils to allow for further cooling if required. This is not currently necessary. A standard QVF glass reactor top is fitted above the exchanger and is held in place by means of locating clamps that allow a seal to be formed (3 mm width PTFE tape is used for this purpose). This glass dome has one central flange, which is occupied by an adapter that holds the feed pipe, and three smaller flanges. One of these is connected to a vent line, which contains a water-cooled condenser and collection flask (to collect any condensate). The other two flanges are currently unused, however one has provision for

Chapter 4

a thermocouple to be inserted into the reactor housing. In addition to this dome, a flat glass reactor top is required to allow the use of a UV lamp in the polymerisation reaction. This is constructed of a flat glass plate, 300 mm in diameter with a central hole to allow feed inlet and a second hole to allow connection to the vent line, which fits into a polypropylene adapter to replace the glass dome. This adapter is designed to use the same fittings as the glass dome to enable a straight switch to be made.

In order to study heat transfer characteristics the set-up of the reactor is such that a smooth disc of 3 mm thickness (with no reservoir in the centre) is used. The feed inlet is connected to a temperature controlled water bath via a rotameter to control feed flowrate and the circulating system is connected directly to mains cooling water, again via a rotameter to allow the circulating flowrate to be varied.

In order to study the polymerisation reaction the following set-up is used. The feed system consists of a one litre vessel fitted with a nitrogen sparger, connected via a peristaltic pump to a 6 mm diameter stainless steel pipe located in the central flange. The feed pipe is fitted with a 1 mm diameter capillary at the discharge end, which is positioned 1 mm above the surface of the disc (at the centre of the reservoir in the disc surface). The pipe is also fitted with a small removable stainless steel disc, which allows the reservoir to be shrouded from the UV light. In the case of the flat glass top, the feed reservoir is connected to a small glass pipette that is held in place by a rubber bung in the central hole of the reactor top. The rubber bung also acts as a shroud for the reservoir in the centre of the disc, preventing premature exposure to UV light.

A UV lamp is clamped in position either outside the glass dome, with the beam directed at the centre of the disc or centrally above the flat reactor top with the beam directed downwards at the disc. The cooling / heating system is currently configured to a temperature controlled water bath in order to achieve elevated disc temperatures of up to 60 °C.

4.2.2 Explanation of Design

The circulating water is fed via the rotary union through the central pipe inside the drive shaft into the dish where the circular plate ensures that the cooling water channel runs

full. The water is then circulated inside the dish and out through the annular space inside the drive shaft, through the holes in the shaft and into the specially designed collection vessel. As the disc rotates the liquid feed is introduced onto the centre of the disc where the reaction begins. The product can be further cooled as it leaves the disc and contacts the vessel wall. The product then runs down the wall and is collected from the base plate. The nitrogen purge ensures an inert atmosphere and reduces the effect of oxygen inhibition and a water-cooled condenser condenses out any volatiles escaping in the nitrogen stream.

The design enables the testing of rotational speed, feed flowrates, circulating water flowrates and disc temperature.

4.2.3 Measurement Techniques

Temperature measurement was achieved using six K-type thermocouples and the data collected using “LabTech Notebook” data logging software. The temperatures recorded were circulating water inlet (in two different places), circulating water outlet, feed inlet, feed outlet and internal housing temperature. The water inlet temperature was measured as it enters the shaft and at the closest point to the underside of the disc in order that heat transfer occurring in the shaft between inlet and outlet water can be accounted for.

4.2.4 Testing of UV Light Source

A series of tests were conducted on two different UV sources with the assistance of Dr. Jim White and Mr. Toby Turton in the Department of Materials Science at Newcastle University. These tests allowed the determination of UV intensity at various distances and positions from the UV source by means of a UV sensitive probe.

Firstly, the characteristics of each lamp were determined and Figure 4.3 shows the graph of measured intensity at each wavelength for the lamp used throughout the polymerisation studies.

Tests were also conducted to determine how the characteristics of the lamp change over time and to confirm the warm-up time required for the lamp. The results of these tests are illustrated by Figure 4.4 which shows that after a period of 5 minutes there was no discernible change in output, indicating that a warm-up time of 5 minutes is sufficient.

The effect of the glass surface on the transmission of UV was considered, and Figure 4.5 illustrates the effectiveness of the glass as a filter to all wavelengths except that required, 365 nm. The tests show that 80% of the UV intensity measured without the glass is transmitted through it.

As UV intensity varies with distance from source, a series of measurements were made at various distances from the source in order to produce a calibration curve for UV intensity with lamp position. The resulting calibration curve can be found as Figure 4.7 in Appendix B.

The use of UV light demands the use of suitable eye protection and a test was conducted to determine the effectiveness of the UV goggles. This was achieved by placing the goggles over the measuring probe and directing the UV source at the probe. Figure 4.6 shows the output obtained which clearly confirms the effectiveness of the goggles as UV eye protection.

A potential concern was reflection of UV light from the stainless steel reaction disc and therefore this was measured and found to be small. The results showed a reflection of 10% of the intensity seen at the disc surface, which poses negligible effect on the polymerisation system.

The UV lamp identified by these tests as suitable for the application and used throughout the polymerisation work was a Long Wave UV Lamp, model number B100 AP, available from UV Products.

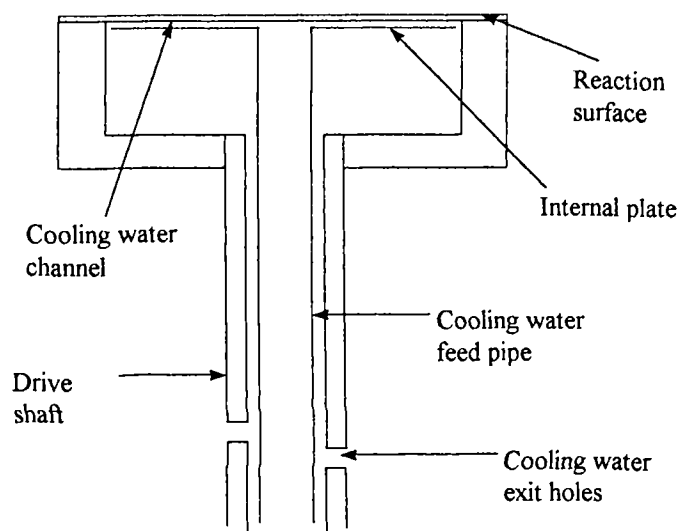


Figure 4.1. Schematic of Hollow Disc Assembly.

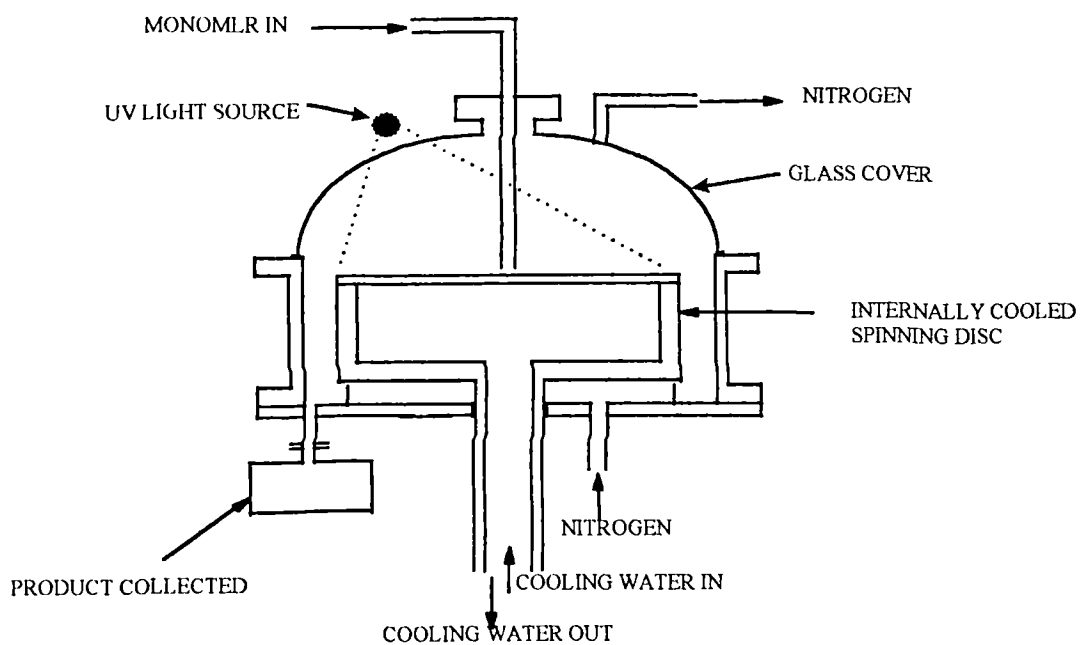


Figure 4.2. Schematic of Reactor Housing.

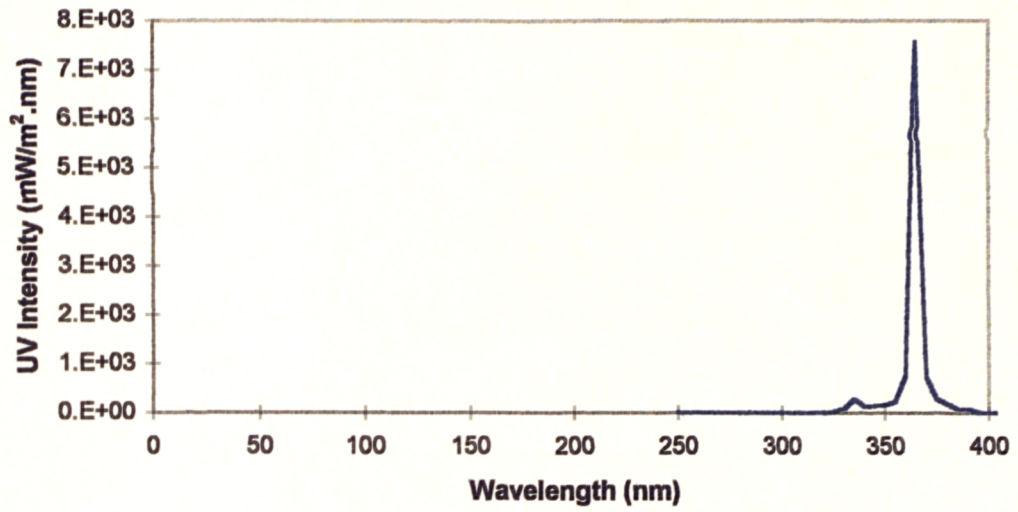


Figure 4.3. Output Characteristics of UV Lamp Used

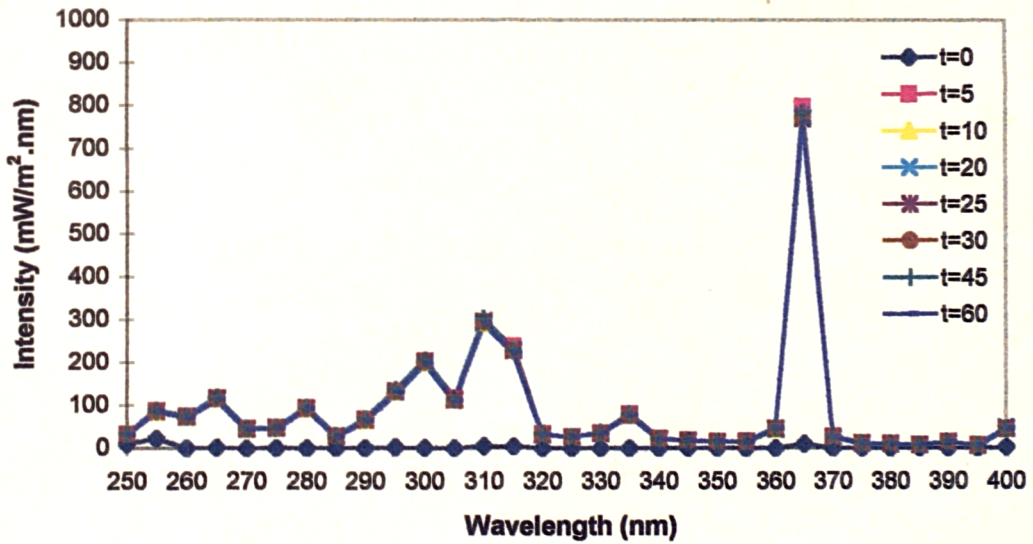


Figure 4.4. Change in Output Characteristics Over Time

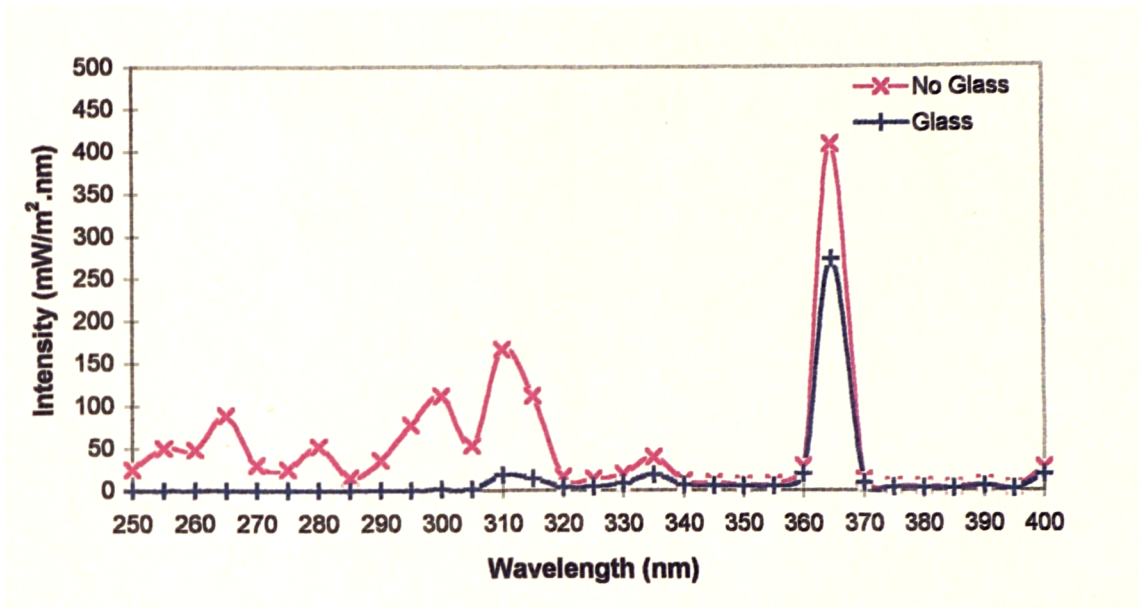


Figure 4.5. Effect of the Glass on UV Intensity Measured

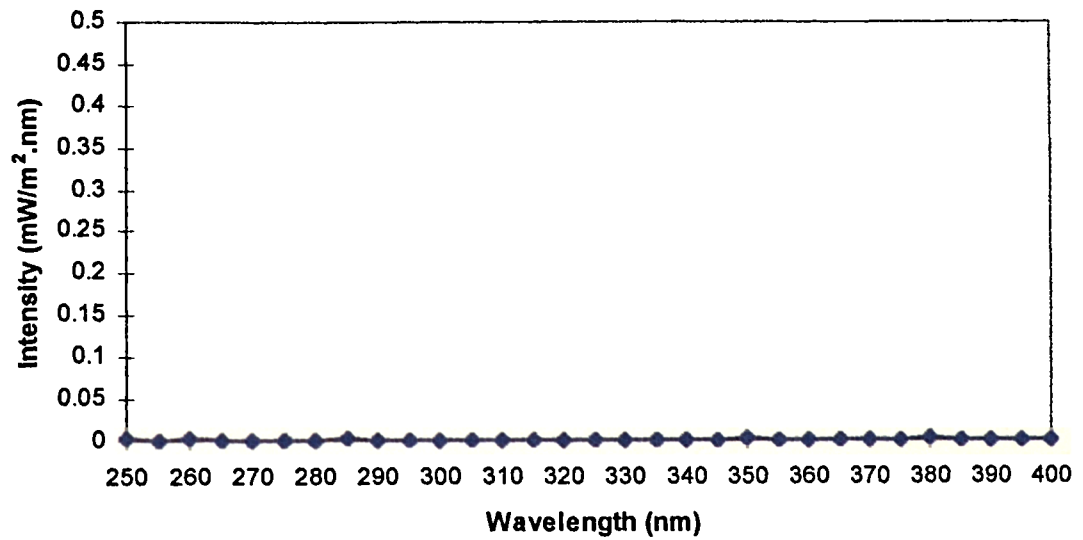


Figure 4.6. Intensity Measured Through Protective Goggles

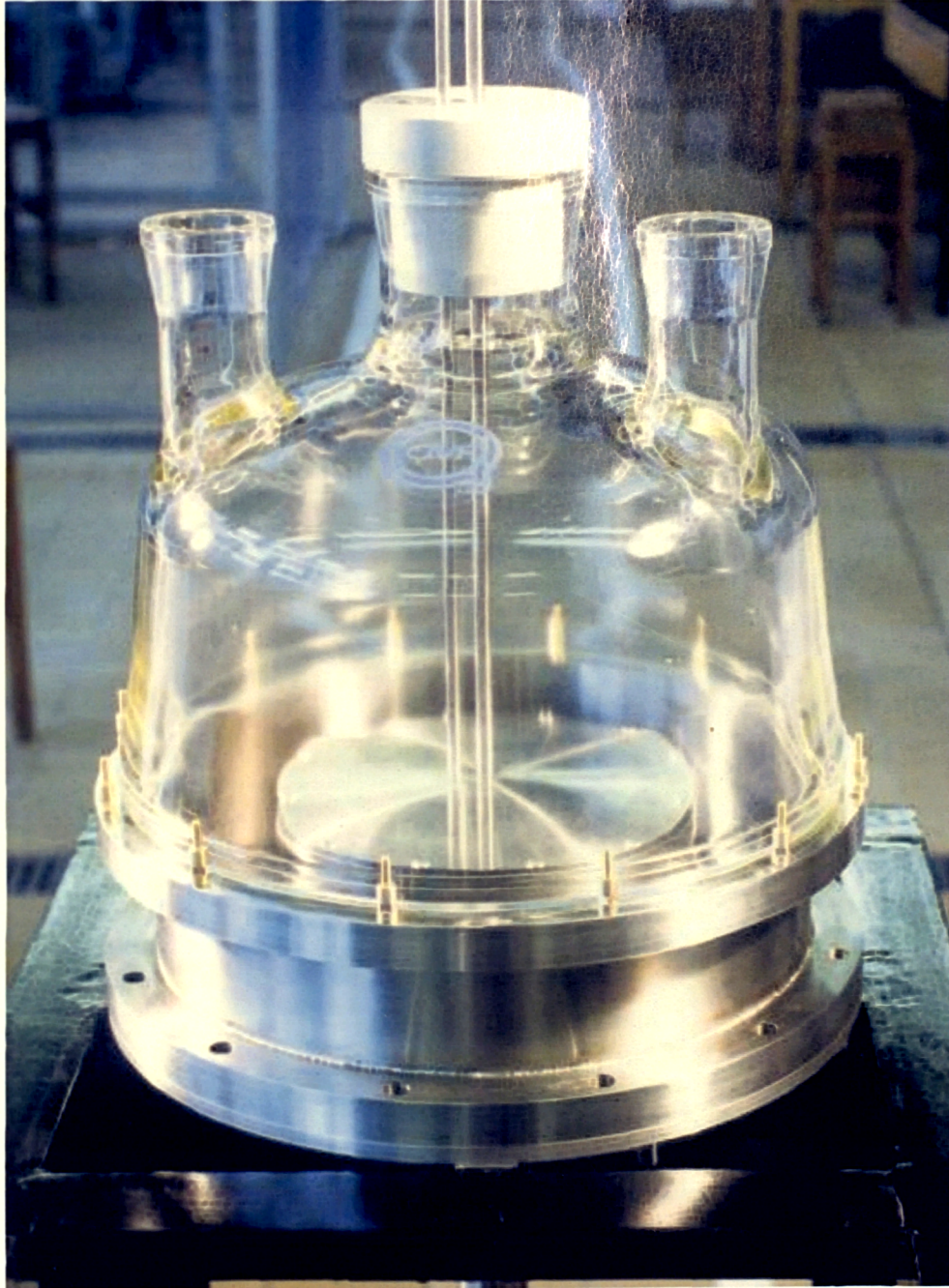


Plate 4.1. Experimental Test Facility

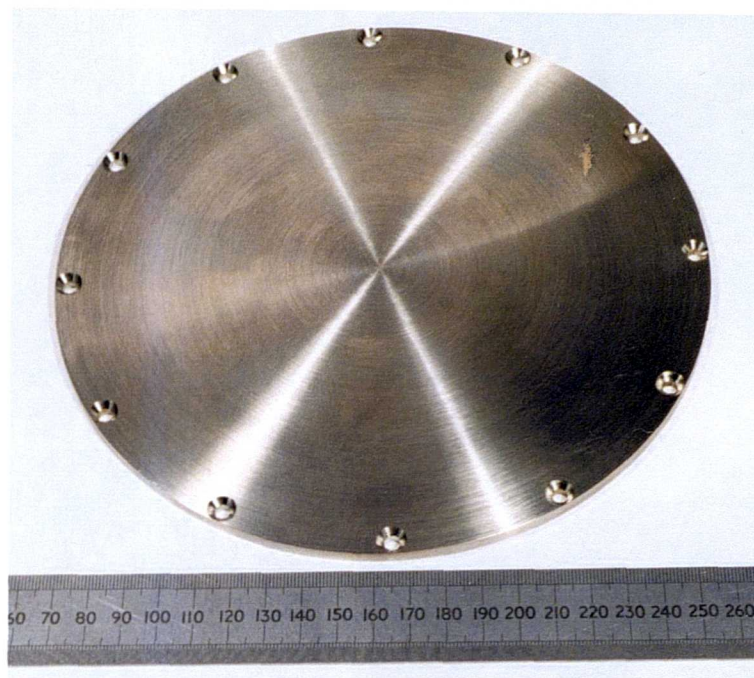


Plate 4.2. Reaction Surface Disc

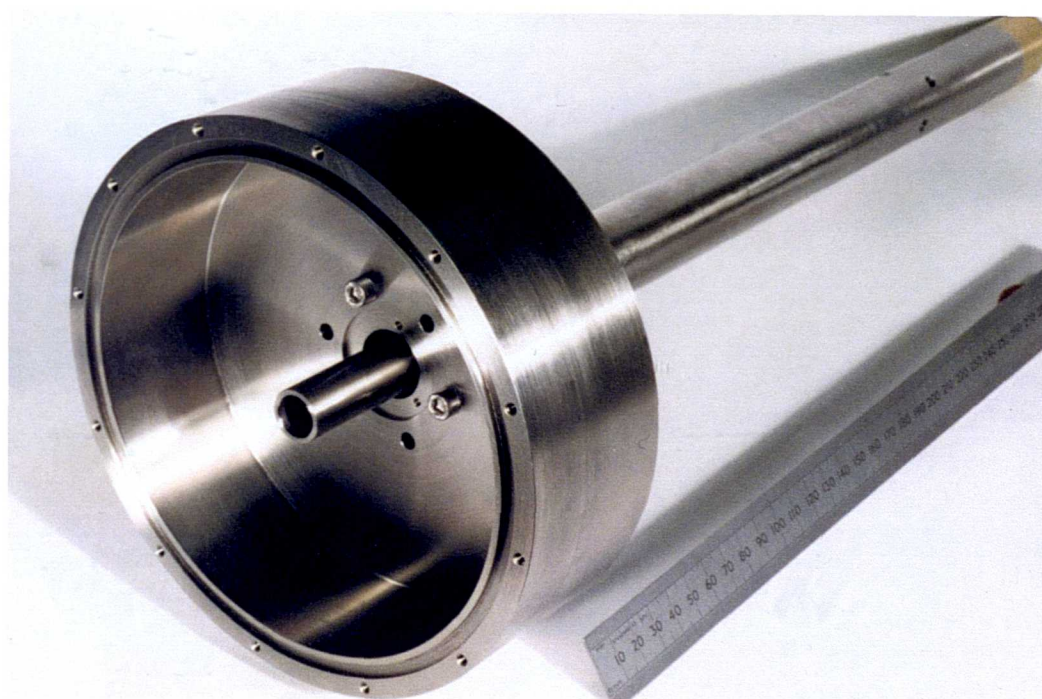


Plate 4.3. Hollow Disc Assembly

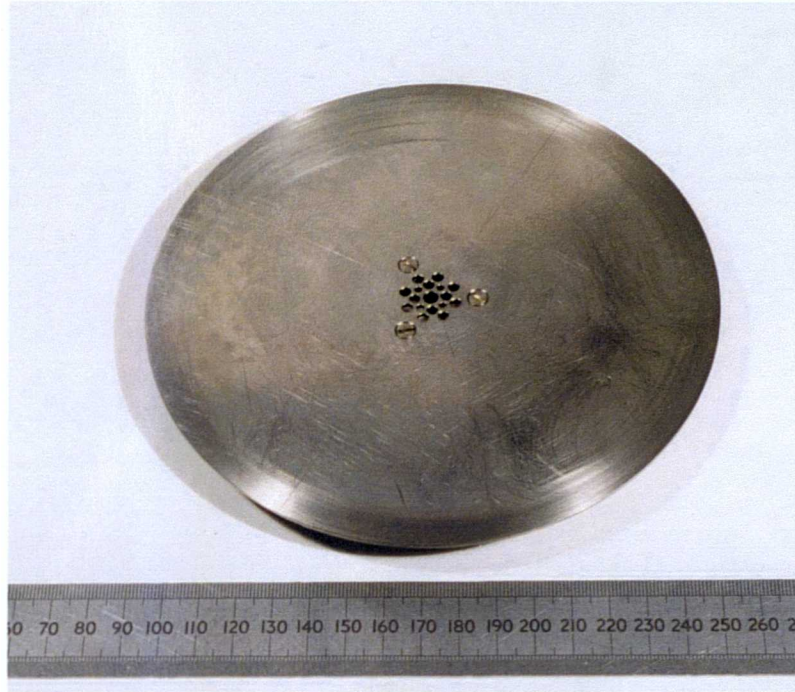


Plate 4.4. Internal Plate

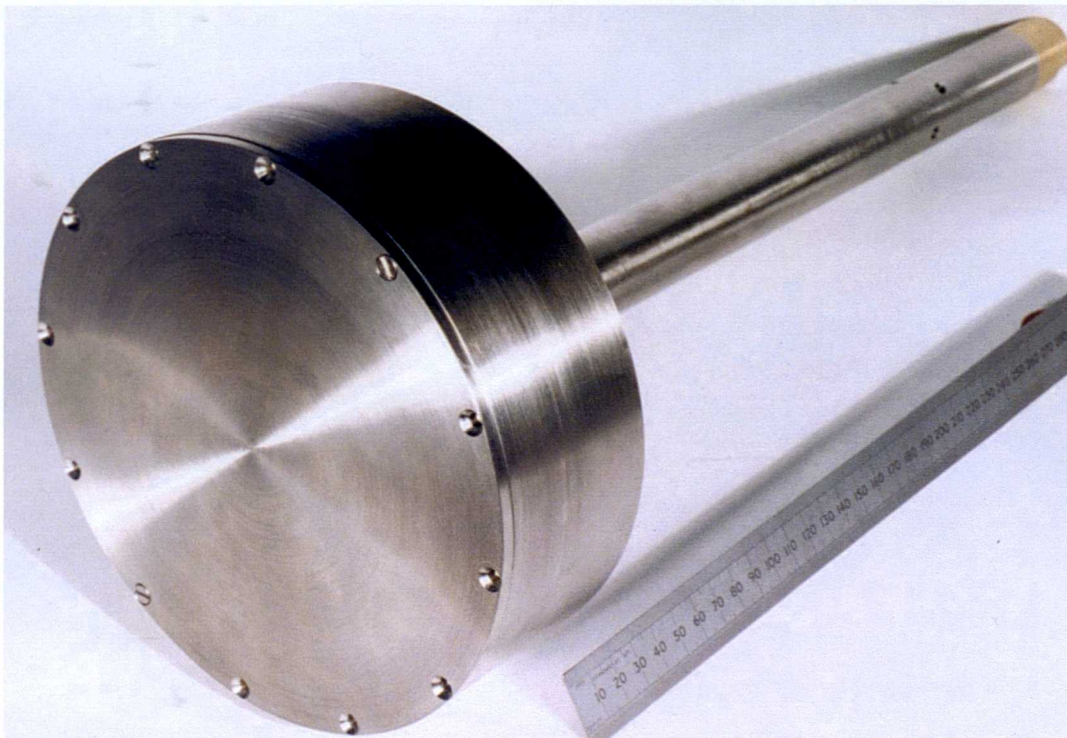


Plate 4.5. Assembled Disc System

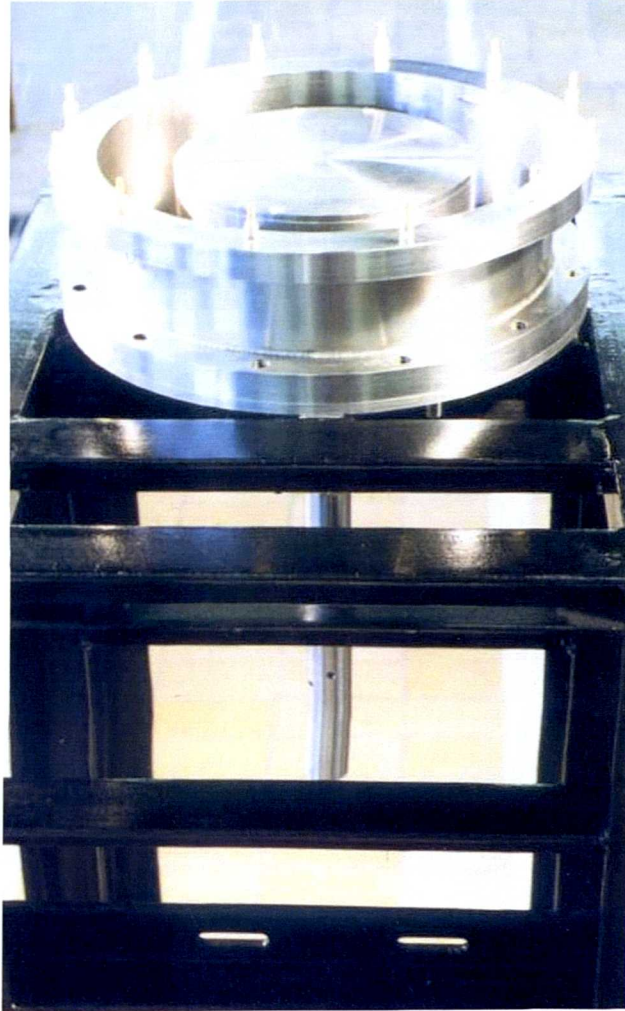


Plate 4.6. Framework and Rig (Without Glass Top)

CHAPTER 5

EXPERIMENTAL PROCEDURES AND TREATMENT OF RESULTS

5.1 Introduction

This chapter details the experimental procedures used for both the polymerisation studies and the preliminary heat transfer study, as well as the analysis procedures used. The treatment of the results obtained from these studies is also detailed here, including the equations used and assumptions made where relevant. The method used in the linear regression and the analysis of the data produced are also explained in detail. These procedures are collected in this chapter, rather than in the results chapters, as many of the procedures are common to more than one of the studies conducted, for example, the analysis procedures and preparation of monomer are common to both the static film and spinning disc polymerisations. The operating and emergency procedures, including a copy of the COSSH assessment and experimental record sheet used can be found in Appendix C.

5.2 Experimental Procedures

5.2.1 Preparation of Monomer

The n-butyl acrylate monomer was washed in order to remove the methyl ether hydroquinone (MEHQ) which was present as an inhibitor for storage purposes. The method used is documented as a standard procedure [78] and is outlined briefly here. The monomer was first washed with the equivalent volume of chilled 0.5% sodium hydroxide solution in three stages (one third of the volume added in each wash). This was followed by a repeat of the procedure using chilled distilled water in place of the sodium hydroxide solution. The solutions were chilled in order to prevent hydrolysis of the monomer occurring. Each wash was shaken, allowed to settle and the water phase run off. On the final water wash the pH of the water phase was compared to that of the

water used. If the pH measurements were not the same then a further water wash was carried out. The washed monomer was then dried by the addition of anhydrous magnesium sulphate. This solution was finally filtered to remove the magnesium sulphate, leaving uninhibited butyl acrylate monomer. Samples of both unwashed and washed butyl acrylate were provided for analysis at Courtaulds Coatings (report number A1/4178/1, author Q. English in Appendix C). This analysis concluded that MEHQ was easily detectable in the unwashed sample but could not be detected in the washed sample, leading us to conclude that this procedure was sufficient to remove the added inhibitor.

The prepared monomer was then chilled until required, and used within several days. The required solution of monomer and initiator was prepared on a % by weight basis. The required mass of initiator was added to the required volume of prepared monomer (50 ml for static polymerisations and 200 ml for spinning disc polymerisations) and the solution was stirred until the initiator had dissolved. In most cases this was easily achieved, however benzoin did not readily dissolve in the monomer and this is noted where relevant (in Chapter 7). The mixture was then placed in the feed flask (protected from light) and purged with nitrogen as detailed in the experimental procedures.

5.2.2 Static Film Polymerisation

A solution of 50 ml washed butyl acrylate and required mass of photo-initiator (2% by weight on monomer) was prepared and placed in the feed flask. The solution was then purged with nitrogen (at ~0.5 bar) for a minimum of 30 minutes to remove dissolved oxygen. The UV lamp was allowed to warm up for a minimum of 10 minutes before use.

Several methods of preparing slides ready for exposure to UV were attempted and are detailed here. A number of tests were carried out by placing a small volume of monomer / initiator solution on a glass slide and immediately placing a second glass slide on top, forming a thin film of monomer which was not exposed to an oxygen atmosphere. The slide was then placed on a UV detector with built in timer and exposed to the UV for the required time. The actual exposure time in milliseconds was

recorded from the detector. By weighing the monomer present on the slides before exposure an approximate film thickness could be calculated. In order to vary the film thickness used the same procedure was carried out using aluminium foil spacers between the glass slides and clamping the slides together. This method proved to have several drawbacks, however. In the case where no spacers were used, it was difficult to separate the plates when higher conversions were achieved; i.e. the polymer held the plates together. Another drawback of this method is the difficulty of ensuring that either all of the monomer / polymer sample or a representative sample is taken for analysis.

In order to produce a consistent film thickness, monomer was applied to a glass slide using a draw down cube (producing a film of 76 μm thickness) within a nitrogen atmosphere. The slide was then exposed to UV whilst remaining in the nitrogen atmosphere. Unfortunately, these samples contained too small a volume of polymer monomer to be detected by GPC analysis. Attempts at NMR analysis also proved unsuccessful for these samples.

The method that proved to be the most successful in terms of sample size for analysis and practical experimentation was the use of aluminium test cells. These cells are illustrated in Figure 5.1 and Figure 5.2 and were constructed with wells of constant diameter and varying depth to provide differing film thickness'. The well in the test cell was carefully filled with the prepared solution, ensuring no air bubbles were present and immediately covered with a glass microscope slide (which was transparent to UV light at the required wavelength as detailed in Chapter 4). This was done immediately to prevent diffusion into the film of atmospheric oxygen. The test cell was then placed under the UV light (which is covered until required i.e. no UV irradiation reaches the test cell until the cover is removed) alongside the UV detector (which measured the exposure time for the sample). The cover was then removed and the test cell exposed to UV irradiation for the required time. A sample was then prepared for analysis using the method detailed in Section 5.2.4.2.

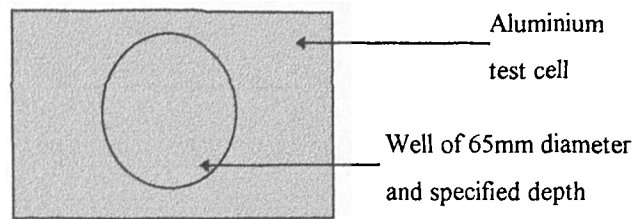


Figure 5.1. Top View of Static Film Test Cell.

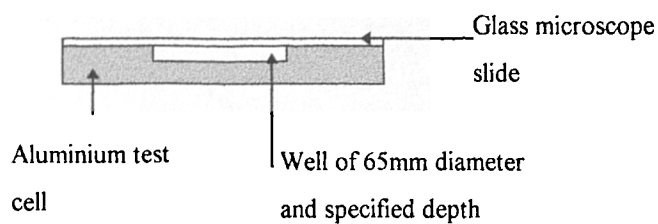


Figure 5.2. Cross-Section of Static Film Test Cell.

5.2.3 Spinning Disc Polymerisation

A solution of 200 ml washed butyl acrylate and the required mass of photo-initiator was prepared as detailed for the static film polymerisation. This solution was then transferred to the feed tank and purged with nitrogen (to remove any dissolved oxygen) for the required time (usually 30 minutes). The reactor housing was simultaneously purged with nitrogen prior to the start of the run and continuously throughout the run. A 30 minute nitrogen purge (with a flow at 0.5 bar pressure) resulted in a concentration reduction from 22% O₂ to less than 0.4%. Equation (5.1) gives the correlation obtained between purge time (seconds) and oxygen concentration. The UV lamp was allowed to warm up for 15 minutes before use. The temperature controlled water bath was set to the correct temperature and allowed to reach this. The water was then circulated through the disc, and the disc set to the required rotational speed. The feed pump was set to the required feed flowrate and allowed to run for the specified time (dependent on flowrate) and then stopped. The lamp was immediately switched off to prevent extra exposure, and the disc stopped. The system was shut down and the reactor top removed

to allow collection of samples. Inhibitor (MEHQ) was added to these samples which were then prepared for as detailed in Section 5.2.4.2.

$$\frac{C_t}{C_0} = 0.47e^{-0.006t} \quad (5.1)$$

5.2.4 Analysis Techniques

Various analysis methods were considered and these are detailed in Chapter 3 (Section 3.6.4). Gel permeation chromatography (GPC) analysis was found to be the most accurate method for this study and provided all required data (molecular weight, molecular weight distribution and conversion).

5.2.4.1 GPC Analysis

GPC analysis was conducted using a double column oven (2PL gel mixed C type column with PL gel 5 μm guard) operating at 30°C in series with a refractive index detector. The solvent in use was tetrahydrofuran (THF) at a flowrate of 1.0 ml/min. Molecular weight distribution and molecular weights were calibrated against polystyrene standards and a conversion calibration was established using samples of poly (butyl acrylate) and n-butyl acrylate monomer.

5.2.4.2 Preparation of Samples

Samples were prepared for analysis by dissolving in 10 ml of THF and a drop of toluene was added as a flow marker. The solution is then filtered using a 0.45 μm syringe filter before use. 0.1 ml of the filtered sample was then injected into the column for analysis and the data generated was collected using GPC software. The output produced shows peaks for monomer, polymer and flow marker, and an example printout can be found in Appendix B. The GPC software generates data that includes the area of each peak, which can then be used to calculate conversions.

5.2.4.3 Calculation of conversion

The required values of polymer and monomer response factors are generated by the calibrations for each of these. The response factor for n-butyl acrylate was found to be 264 and for poly (n-butyl acrylate) was found to be 1254. The conversion is then calculated using Equation (5.2), substituting the peak areas for both the monomer and polymer.

$$\text{Conversion(\%)} = \frac{\frac{\text{polymer peak area}}{\text{polymer response factor}}}{\frac{\text{polymer peak area}}{\text{polymer response factor}} + \frac{\text{monomer peak area}}{\text{monomer response factor}}} * 100 \quad (5.2)$$

5.2.4.4 Calculation of Molecular Weights

Molecular weights and polydispersity indices were calculated by re-running the data generated with the LC-GC software. This software calculates various molecular weights and polydispersity index from the polymer peak. The results required in this case were values of M_w (weight average molecular mass) and M_n (number average molecular mass) for reasons detailed previously in Chapter 3. The polydispersity index gives an indication of the molecular weight distribution, the closer this is to 1, the tighter the distribution.

5.2.5 Preliminary Heat Transfer Study

This study was conducted following the method detailed here, and full results including a heat balance and treatment of experimental data can be found in Appendix A. A temperature controlled water bath was used for the feed flow and the cooling water to the disc was supplied directly from the mains. The cooling water flowrate was set to the required value and rotation of the disc started. The drive speed controller was adjusted until the required rotational speed was reached. The water bath was set to the required temperature and allowed to warm up. The feed flowrate was then started and set to the required value. Once flow across the disc was established the data logger (with connections to all thermocouples) was started. Data was collected over a 30

minute period. At the end of this period, the rig was either shut down, or the variables reset ready for the next trial. 'LabTech' data logging software was used to record the temperatures read by the thermocouples every 30 seconds, and on screen monitoring was continuously running.

5.3 Treatment of Results

5.3.1 Linear Regression Analysis

5.3.1.1 Method

Linear regression was performed on the experimental data using the regression data analysis tool in MSEXcel (version 7.0). All regressions were performed using a 95% confidence interval. Equations of the form $y = ax^b z^c \dots$ were linearised by taking logs of both sides to give equations of the form $\log y = \log a + b \log x + c \log z \dots$. The results produced by the regression software were then analysed with respect to the significance of the individual variables as well as overall significance of the regression model.

5.3.1.2 Data Analysis

Overall Significance of Regression Model

To test the overall significance of the regression, two hypotheses were proposed:

$$H_0: \beta_1 = 0$$

$$H_1: \beta_1 \neq 0$$

If H_0 was not rejected then the implication was that no linear relationship existed. This could be interpreted in two ways, either the variables included in the regression were of little significance in explaining variations in y , or no true linear relationship existed. This would lead to the conclusion that the assumed relationship, i.e. $y = ax^b z^c \dots$, could

not be justified. If however H_0 was rejected in favour of H_1 , the regression could be deemed justified.

The test statistic used was the F-statistic, further details can be found in any text dealing with statistical regression [102]. The criterion for rejection of H_0 was $F_0 > F_{\alpha, k, n-2}$. The value of $F_{\alpha, k, n-2}$ was found from statistical tables [103] and the value of F_0 was generated by the regression software. Table 5.1 in Appendix C summarises the conclusions drawn for each linear regression performed.

Significance of Individual Variables

A similar method was used to test the significance of individual variables within the regression. Again two hypotheses were proposed:

$$H_0: \beta_j = 0$$

$$H_1: \beta_j \neq 0$$

In this case, rejection of H_0 in favour of H_1 indicated that the variable (x_j) was significant within the regression. If H_0 was not rejected then the variable was insignificant within the regression and could be neglected from the regression model.

The test statistic used in this case was the t-statistic [102], and the criteria for rejection of H_0 was $|t_0| > t_{\alpha/2, n-k-1}$. Again, the value of $t_{\alpha/2, n-k-1}$ was found from statistical tables [103] and the value of t_0 was generated by the regression software. Table 5.2 in Appendix C summarises the conclusions drawn for the individual variables for each linear regression performed.

CHAPTER 6

STATIC FILM POLYMERISATION

6.1 Introduction

This chapter presents the results of the static film polymerisation work conducted. Included here are the results of the final experimental procedure developed only, as previous methods proved unsuccessful for various reasons. The methods used, both successful and unsuccessful, are detailed in Chapter 5.

The experimental method used here, and the results presented are the subject of a research project conducted in conjunction with the work for Courtaulds and I would like to acknowledge here the experimental work done by Mr. Majeed Jassim as part of his project for the degree of M.Eng..

A study of the static film polymerisation was required in an attempt to characterise the polymerisation system under study in order to have a benchmark to be used in comparison of results when progressing to the spinning disc reactor, which has unknown mixing characteristics.

Three variables, each independently controllable were studied. The first of these is exposure time to the UV source. In a photo-initiated system this is obviously an important variable to consider, and a profile of the polymerisation can only be generated if exposure time is varied as the facility for real-time analysis is not available to us. Exposure times of up to 40 seconds were studied, beyond this the polymer / monomer mixture became too viscous to allow removal of the glass plate and consequent collection of a representative sample of product for analysis.

Film thickness is another important variable to consider in a photo-initiated polymerisation as absorbance of the UV irradiation is a factor in the polymerisation. Three film thickness' were studied, 400 μm , 830 μm and 1000 μm . These were maintained as constants by the design of the test cells (refer to Chapter 5).

The final variable under study was the intensity of the UV irradiation. The variation of this was achieved by the positioning of the UV lamp, i.e. the closer the lamp the higher the intensity of UV irradiation the sample is exposed to. Studies on the intensity of the UV lamp were conducted and details can be found in Section 4.2.4, Chapter 4. For the purpose of this study, four different lamp positions were used, resulting in four different intensities ranging from 5.49 mW/cm² to 10.85 mW/cm².

6.2 Static Film Results

6.2.1 Exposure Time

6.2.1.1 Results

Figure 6.1 illustrates the effect of exposure time on the conversion achieved. As can be seen from the graph, there is an increasing trend in conversion with exposure time, as would be expected. Figure 6.1 also indicates the presence of an induction period at the beginning of the polymerisation, as the conversion does not increase immediately on exposure to the UV irradiation. This induction period varies with UV intensity, the induction period being higher at lower intensity. The data presented here was collected at a film thickness of 830 µm and Figures 6.10 and 6.11 present the data collected for the remaining two film thickness' studied. Both show very similar trends to those described above.

Molecular weight data is presented in Figures 6.12 - 6.14 in Appendix D. No trends in M_n or M_w are detectable, and consequently no trend in polydispersity index exists. Values of polydispersity index for these data points range from 2 to 3.5.

6.2.1.2 Theory

Figure 6.2 shows the predicted conversions for a film thickness of 830 µm using the theoretical model from the literature (Equation 3.11). As can be seen, the initial rate of polymerisation is high, and this decreases rapidly as we approach the maximum achievable conversion. In ideal conditions, with no inhibition effects, the predicted maximum conversion is achieved within the first few seconds of exposure to UV

irradiation. By comparison, the experimental results show much lower conversions, and this is discussed later in this chapter.

6.2.2 Film Thickness

6.2.2.1 Results

The data presented in Figure 6.3 is based on data points at three film thickness' only and more data is required to prove or disprove the presence of an optimum thickness. Trials at a film thickness of 200 μm were conducted but the samples were unable to be analysed for various reasons (as explained in Chapter 5). Data for film thickness between 400 and 830 μm and also between 830 and 1000 μm is required before any conclusive statement can be made regarding optimum film thickness. Also, the values of conversion are low which could lead to possible misidentification of trends. An exposure time of 20 seconds was used in this example, and data for 30 and 40 second exposure times shows very similar trends (Figures 6.15 and 6.16 in Appendix D).

Molecular weight data is presented in Figures 6.17 - 6.19 in Appendix D. Again no trends in M_n or M_w are detectable, and consequently no trend in polydispersity index exists. Values of polydispersity index for these data points range from 2 to 3.6.

6.2.2.2 Theory

Figure 6.4 shows the predicted conversion (using the theoretical model) at constant intensity for a range of film thickness' from 50 to 2500 μm . Theoretically, the lower film thickness results in a higher conversion, but the time to reach this conversion is longer than for higher film thickness. This difference in the initial rate of polymerisation is highlighted as the graph shows only the first ten seconds of exposure to UV irradiation. The model has its limitations and these are discussed later in this chapter, the most obvious limitation being the lack of accounting for induction periods.

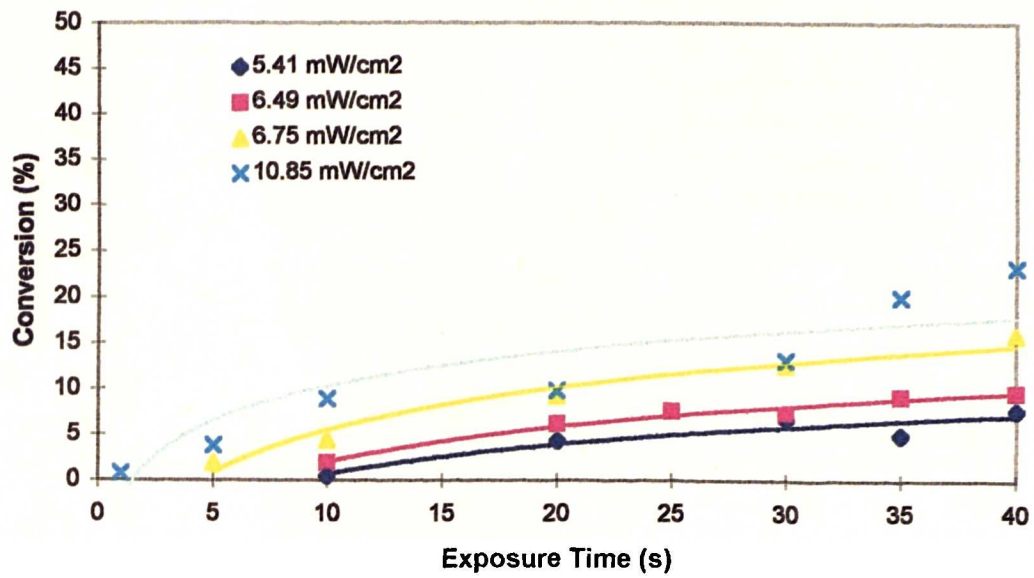


Figure 6.1. Effect of Exposure Time on Conversion at a Film Thickness of 830µm.

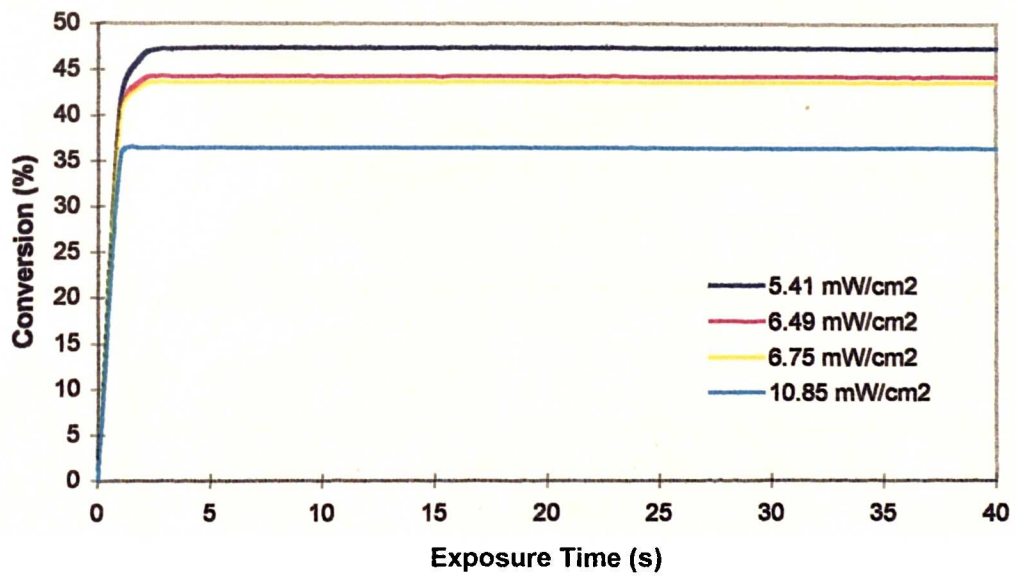


Figure 6.2. Theoretical Conversion with Exposure Time for a Film Thickness of 830µm.

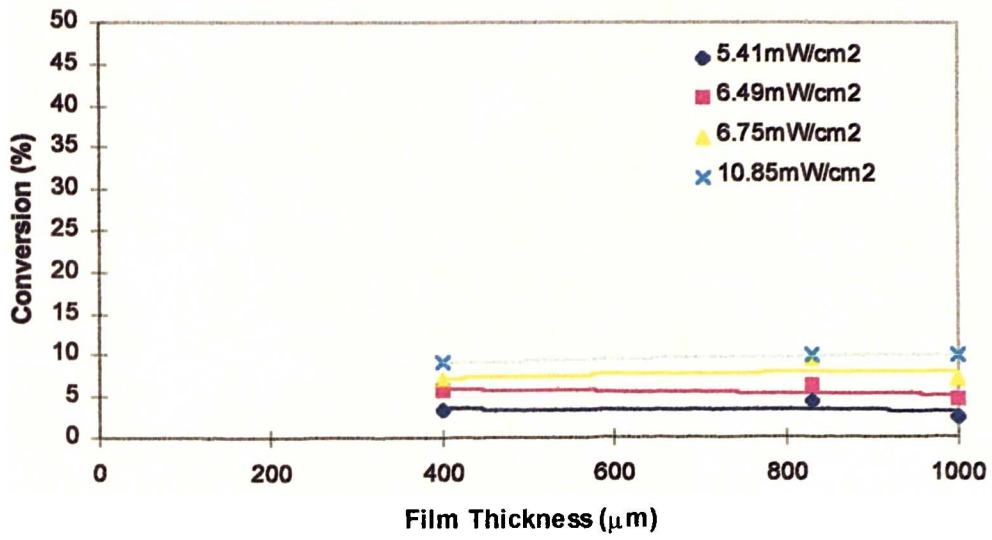


Figure 6.3. Effect of Film Thickness on Conversion for an Exposure Time of 20 Seconds.

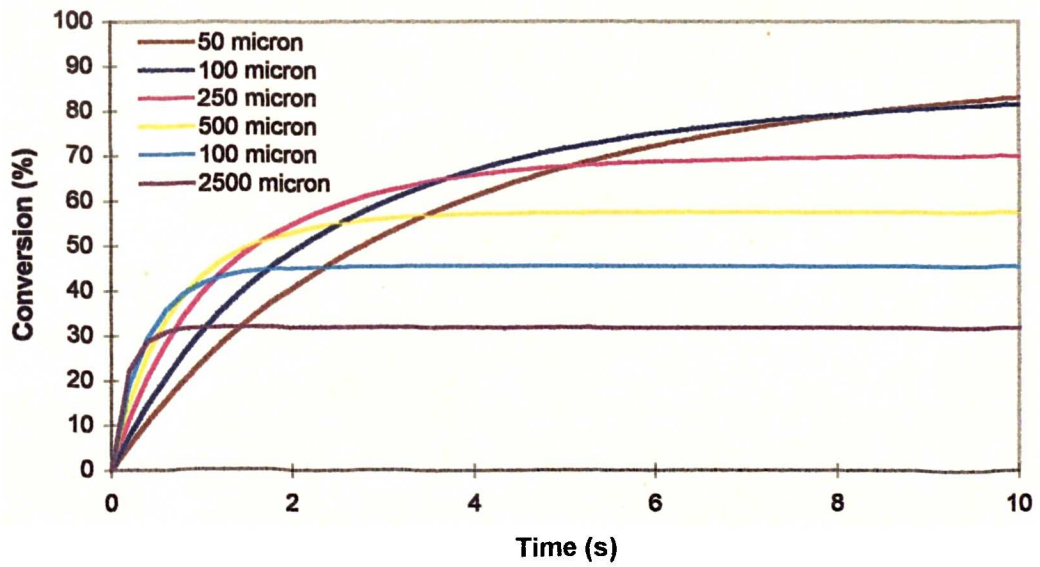


Figure 6.4. Theoretical Effect of Film Thickness on Conversion over a 10 Second Exposure Time.

6.2.3 UV Intensity

6.2.3.1 Results

Figure 6.5 shows an increasing trend in conversion with UV intensity. It can also be seen that for an exposure time of 40 seconds the increase in conversion with UV intensity is much greater than for 20 or 30 second exposure times. This same trend is found at all film thickness' tested.

Figure 6.6 highlights the decreasing trend seen in molecular weight with increasing intensity. A definite decrease in both M_n and M_w can be seen as UV intensity is increased. A 40 second exposure time shows a smaller decrease in molecular weight than exposure times of 20 and 30 seconds.

The trend apparent in polydispersity index with UV intensity is shown in Figure 6.7. In this case there is an increase in polydispersity index with increasing intensity and again this change is smaller at higher exposure times as illustrated by the trendlines in Figure 6.7.

6.2.3.2 Theory

Figure 6.8 is based upon the theoretical model previously used in this chapter. In the initial stages of the graph the higher intensities show the higher rates of polymerisation, however the actual conversion achieved with a higher UV intensity is lower than the eventual conversion reached using lower intensities. This means that the time to reach maximum conversion is lower at higher UV intensities. As well as illustrating the theoretical predictions for the range of UV intensities used experimentally in this study, Figure 6.8 also compares the theoretical predictions for UV intensities of up to 300 mW/cm^2 .

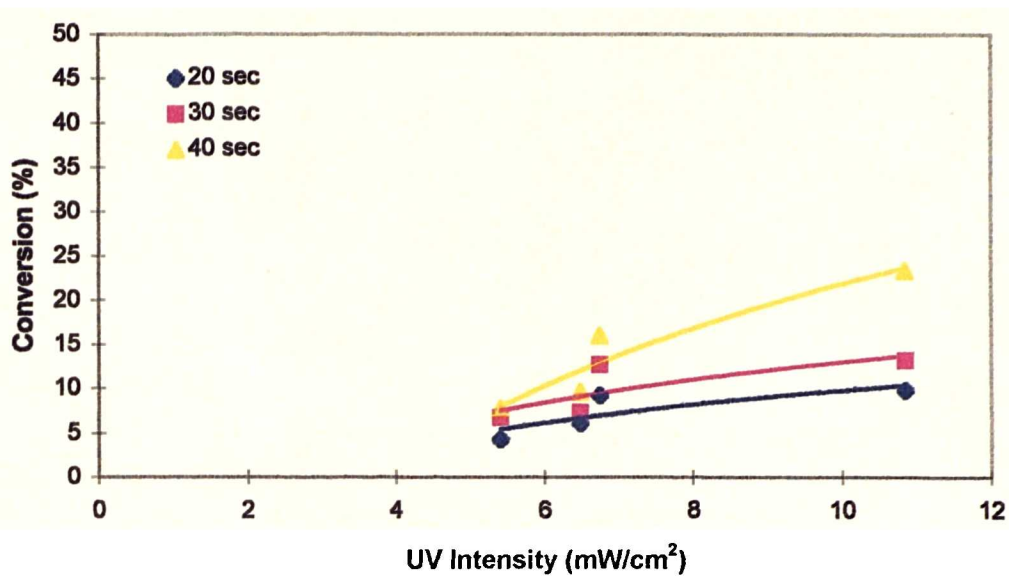


Figure 6.5. Effect of UV Intensity on Conversion at a Film Thickness of 830 μm .

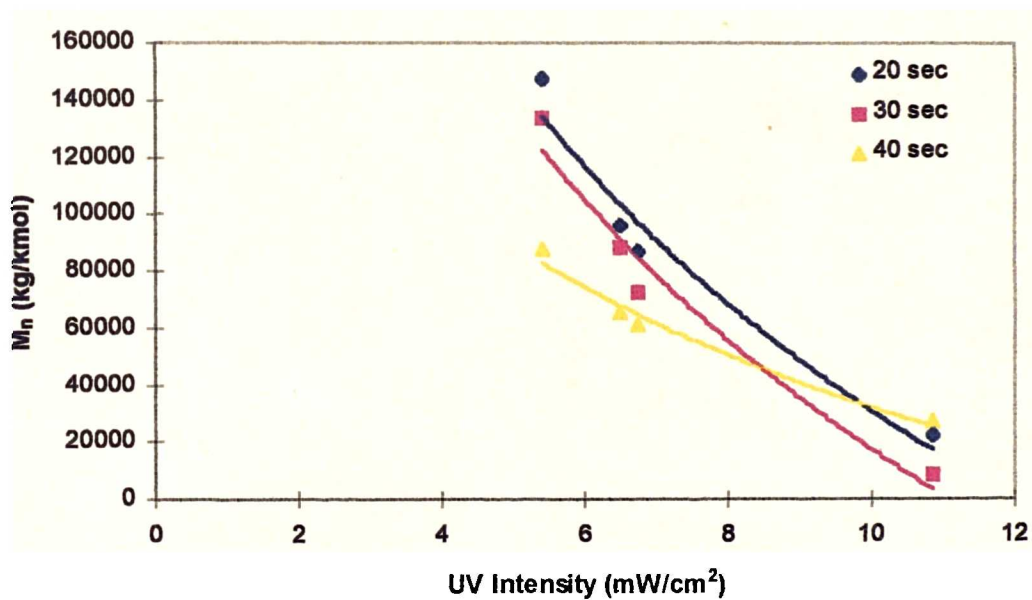


Figure 6.6. Effect of UV Intensity on M_n .

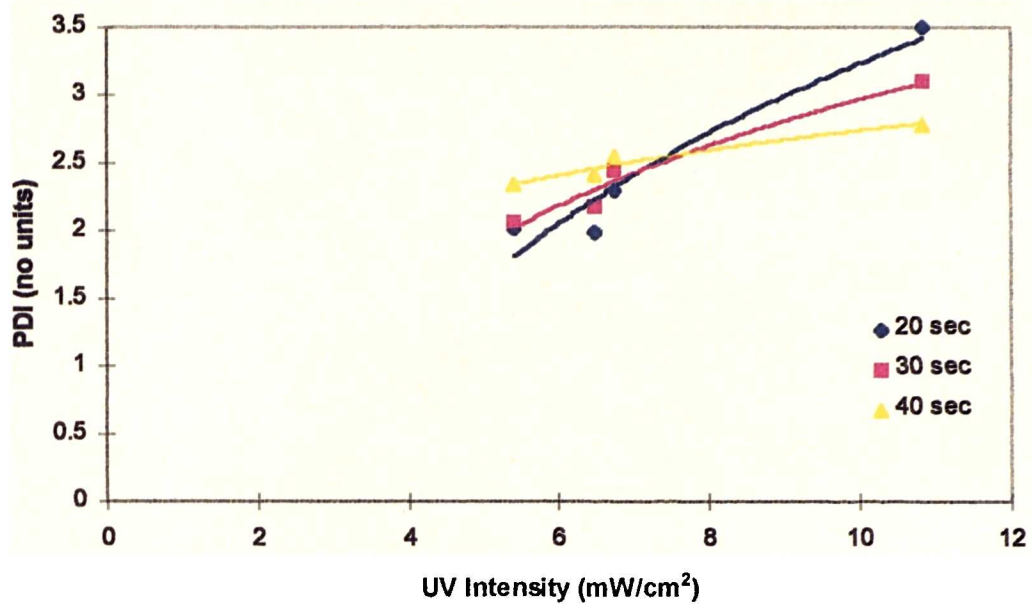


Figure 6.7. Effect of UV Intensity on Polydispersity Index.

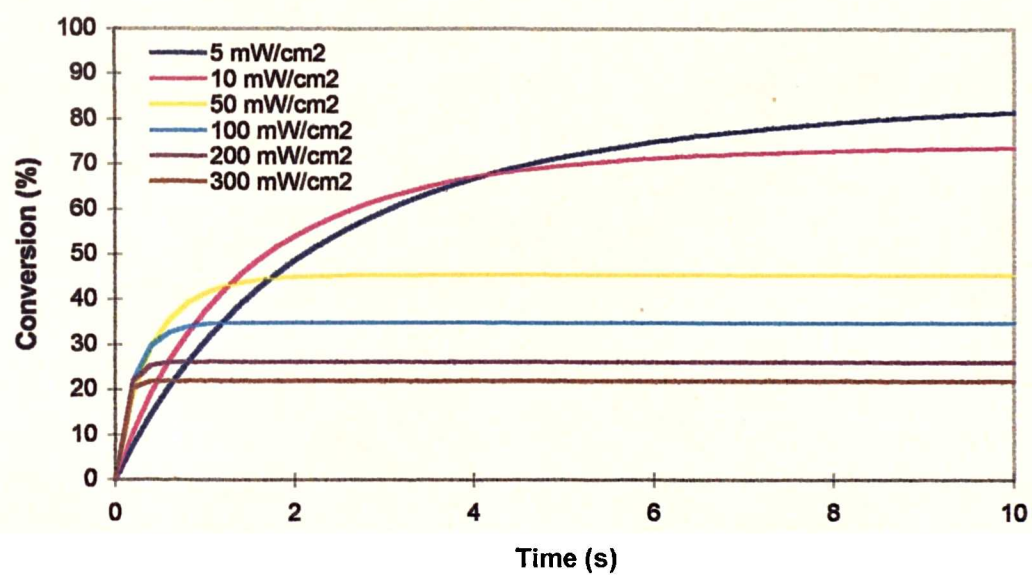


Figure 6.8. Theoretical Effect of UV Intensity over a 10 Second Exposure Time.

6.3 Linear Regression Analysis

Details of the method used for the linear regression and the analysis of the data generated can be found in Chapter 5. Presented here are the resulting equations and an evaluation of the accuracy of the generated model.

Initially, linear regression was performed on all three variables (exposure time, film thickness and UV intensity). Equation (6.1) is the model generated from this regression.

$$y = 10^{-1.313} (t)^{0.934} (d_f)^{-0.099} (I)^{1.339} \quad (6.1)$$

Analysis of the regression data produced shows that film thickness is insignificant in comparison with exposure time and film thickness in this model. A repeat regression was performed on the data including only the two significant variables. Equation (6.2) shows the resulting model.

$$y = 10^{-2.935} (t)^{0.933} (I)^{1.342} \quad (6.2)$$

In order to provide a model of use for comparison with other data if required, the first model was repeated using S.I. units for all the data. Previously UV intensity has been quoted in mW/cm² and film thickness in μm. The model using S.I. units is Equation (6.3) below. Figure 6.9 illustrates the accuracy of this model with respect to the experimental data obtained. The values of conversion are low due to the experimental conversions achieved, and there is some scattering of the data points from the perfect correlation. Generally, the model tends to under-predict slightly at a film thickness of 400 μm, and for the two higher films the model tends to over-predict marginally. Figure 6.9 indicates that the model gives a suitable estimation of conversion expected, allowing for experimental scatter.

$$y = 10^{-3.243} (t)^{0.934} (d_f(m))^{-0.098} (I(W / m^2))^{1.338} \quad (6.3)$$

These models are based upon the following parameters and cannot be guaranteed beyond the experimental range of values tested.

$$0 \leq t \leq 40 \text{ sec onds}$$

$$400 \leq d_f \leq 1000 \mu\text{m}$$

$$5.41 \leq I \leq 10.85 \text{ mW} / \text{cm}^2$$

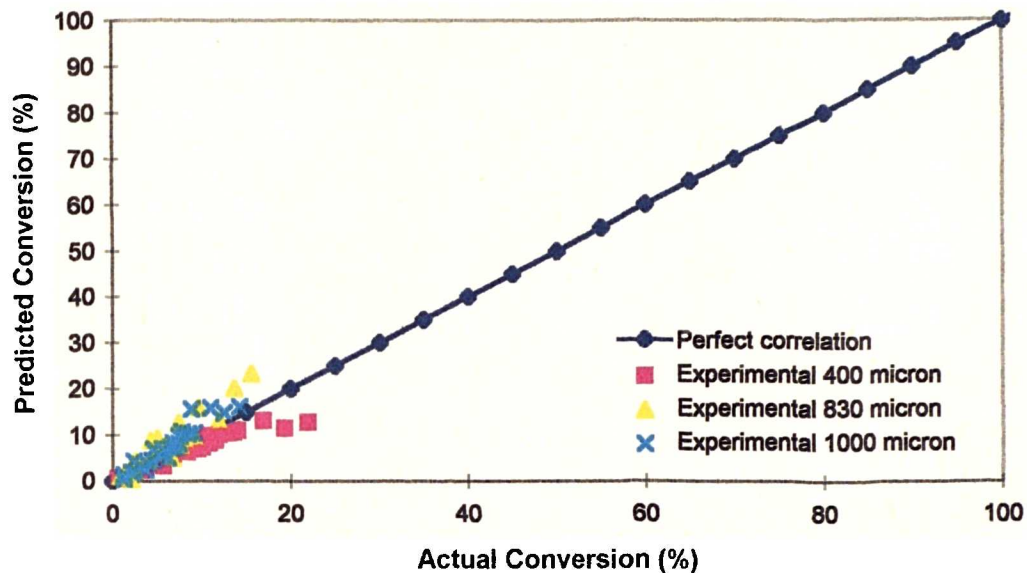


Figure 6.9. Deviation of Model Predictions from Perfect Correlation.

6.4 Discussion

6.4.1 Effect of Exposure Time

As mentioned previously, exposure times of up to 40 seconds only were studied due to the difficulties encountered with the viscosity of product when longer exposures were attempted. Within this range, conversions of up to approximately 25% were achieved. On comparison with the theoretical predictions, this is seen to be much lower than predicted. There are several possible explanations for this, which are partly due to limitations of the theoretical model and are discussed later in this chapter. Other possible reasons for not achieving the conversions predicted include the possibility that in the static system the viscosities generated are such that movement of the growing polymer chains is severely restricted resulting in the cage effect (refer to Chapter 3 for a

more detailed explanation of this phenomenon). This would prevent the conversion of monomer to polymer progressing as assumed in the theoretical model. Alternatively, the polymerisation may be progressing more slowly than anticipated due to inhibition effects. Oxygen inhibition is known to be a problem in free-radical polymerisations, and although the experimental procedure is such that the film is not exposed to atmosphere during the UV irradiation, the presence of dissolved oxygen (which has not been removed during the purging process) in the monomer initially may be sufficient to hinder the polymerisation.

The conclusion that can be drawn from this is that exposure time shows a significant effect on the polymerisation.

6.4.2 Effect of Film Thickness

Results were obtained for three film thickness' of 400, 830 and 1000 μm . Trials were also conducted at 200 μm . However, the small sample size and the high viscosity of the product in these samples resulted in unreliable analysis as a representative sample of the required size could not be collected (the initial volume of monomer held in this test slide is less than 0.7 ml). The results presented earlier in this chapter show little change in conversion with film thickness over the range tested. Data at other film thickness' is required in order to investigate this further. Increasing the film thickness beyond a certain value would however be expected to be detrimental to the polymerisation. As the UV irradiation penetrates the film, a quantity of it (dependent upon the characteristics of the monomer) is absorbed by the monomer mixture and thus the further into the film we proceed, the lower the intensity of the UV irradiation becomes. This results in a range of polymerisation rates throughout the film, the effect being more pronounced with thicker films and / or a highly UV absorbing monomer [62]. In this study, film thickness' of 1 mm or less have been considered and the results indicate that there may not be a significant effect due to film thickness under the range of conditions studied.

If film thickness were demonstrating a pronounced effect on the polymerisation, then we would expect to find that thicker films produced a wider molecular weight

distribution (i.e. higher values of polydispersity index). No trend is detectable in polydispersity index with increasing film thickness however and this would suggest that over the range of film thickness' tested the absorbance of UV by the film is insignificant, and the film is uniformly exposed to the same intensity of UV irradiation. This is supported by the analysis of the linear regression data which concludes that for a 95% confidence interval, the exponent on film thickness was found to be insignificant.

The conclusion drawn from this is that over the range tested (up to 1 mm), the effect of film thickness is insignificant compared to the other variables.

6.4.3 Effect of UV Intensity

For exposure times of 20 seconds and above, the effect of UV intensity on conversion is more significant than for exposure times below this (especially below 10 seconds). A higher intensity generates more initiator radicals and hence more polymer chains are started. However, this also explains the decrease in molecular weight seen with increasing intensity. As more initiator radicals are generated (with continuing exposure to UV) for higher intensities, there becomes more chance of these radicals terminating existing polymer chains if they are not used in starting new chains. This results in lower chain lengths and hence lower molecular weights.

For the longer exposure times, there is an increasing trend in polydispersity index with increasing UV intensity. Again this is explained by the generation of more initiator radicals at higher intensities with increasing exposure time, which are used up both in starting new polymer chains and terminating existing polymer chains. If these radicals are generated more quickly than they can be used in chain initiation then more and more radicals will become involved in chain termination resulting in shorter and shorter chains as exposure time increases, resulting in an increased polydispersity index. This would indicate that there would exist a critical intensity at which the rate of radical production does not exceed the rate of initiator consumption, preventing an increase in the number of radicals available to become involved in chain termination. This would suggest that ideally a very short exposure time to a high intensity UV source would generate a large number of radicals which would all initiate chains, and further

exposure would only result in generating more radicals which would be involved in termination of the growing chains. Termination would then occur by combination only and would be dependent upon local monomer and polymer concentrations and the degree of mixing. This provides another possible explanation for the conversions achieved being lower than those predicted as the model assumes good mixing, and mixing of growing polymer chains with unreacted monomer in the test cells is not promoted.

The conclusion drawn from this is that UV intensity shows a significant effect on the polymerisation.

6.4.4 General Discussion

6.4.4.1 Limitations of Theoretical Model

Induction Period

As was shown previously in this chapter, the presence of an induction period at the beginning of the polymerisations was noted. The theoretical model does not account for the presence of an induction period, and it does not consider the effect of inhibition due to the presence of oxygen. Oxygen inhibition is a well-documented problem in free-radical polymerisations (refer to Chapter 3) due to the scavenging effect of the oxygen on the free radicals. The theoretical model assumes no oxygen presence, and although the monomer is purged with nitrogen before use this cannot absolutely guarantee the removal of all dissolved oxygen from the monomer. The presence of dissolved oxygen will result in an induction period during which very little polymerisation is seen because the oxygen molecules are competing for the free-radicals formed by exposure to the UV. Once the dissolved oxygen has reacted with the radicals, polymerisation of the monomer will proceed.

Mixing

The theoretical model is based upon the assumption of good mixing, i.e. the propagation step is not hindered by the lack of available free radical sites. However, in

the static film trials, as suggested by the nature of this there is no mixing within the test sample. One of the problems associated with this lack of mixing is the onset of the cage effect as mentioned earlier in this chapter. For this reason, the conversions predicted by the model will be higher than was found in the experimental trials.

6.4.4.2 *Characterisation of Polymerisation System*

Unfortunately the viscosity of the monomer / polymer mixture at the conversions achieved presents many problems in the accurate analysis of the sample, limiting the portion of the polymerisation profile that we can define and without data for higher exposure times and at higher conversions it is difficult to conclusively characterise the reaction system. The best that is achieved in this respect is a range of conversions, molecular weights and polydispersity indices for the conditions studied which may be compared with the corresponding data produced from the spinning disc reactor. The comparison of static film and spinning disc data is included in Chapter 8.

6.5 Summary

In summary, various conclusions have been drawn in this chapter regarding the static film polymerisation system, and these are highlighted here. Firstly, increasing the exposure time to UV light was found to have a significant effect on the conversion achieved, with higher exposure times resulting in higher conversions for the range 0 – 40 seconds. Varying the exposure time resulted in no discernible trend in the molecular weight of the polymer produced. Both of these observations are in agreement with expectations for this type of polymerisation, high molecular weight polymer is formed immediately unlike in the step polymerisation process (refer to Table 3.1).

Secondly, increasing the film thickness resulted in no significant effect on either the conversion achieved or the molecular weight of the polymer over the range 400 – 1000 μm . Expectations are that over a larger range of film thickness the effects will be apparent, due to the problems associated with UV penetration into thicker films as discussed previously. The lack of effect over the range studied here however is not

improbable, due to the low absorption coefficient of butyl acrylate (i.e. its relative transparency to UV light).

Thirdly, increasing the UV intensity resulted in increased conversion and a corresponding decrease in molecular weight over the range 5.5 – 11 mW/cm². Again, both of these observations are in agreement with expectations as previously discussed.

For all the conditions studied the actual conversion was found to be lower than that predicted by the theoretical model. This difference can be mostly attributed to limitations in the application of this kinetic scheme to the static film system both in terms of oxygen inhibition and associated induction periods and also the degree of mixing within the system. These are issues that have been discussed in further detail earlier in this chapter.

Finally, although the static film polymerisation has not been fully characterised by this study, the results obtained provide a useful comparison for the spinning disc system.

CHAPTER 7

SPINNING DISC POLYMERISATION

7.1 Introduction

The proposed use of a spinning disc reactor in a photo-initiated polymerisation system and the potential benefits associated with this are discussed in Chapter 1. Briefly, the formation of thin films across the disc surface make this a potential reactor for photo-initiated polymerisations, the reason for this exploratory investigation being to study the suitability of the reactor in the polymerisation of n-butyl acrylate, and highlight the potential for developing this type of reactor.

The variables under study can be divided into three main categories; mechanical, chemical and physical. The mechanical variables are rotational speed and feed flowrate, both of which can be controlled by mechanical means and which affect film thickness and residence time on the disc. The chemical variables are photo-initiator type and concentration, both of which have a direct effect on the chemistry of the polymerisation. The physical variables are temperature, UV intensity and nitrogen purge time and these also have an effect on the polymerisation but are controlled by physical means, e.g. position of the UV lamp.

The effect of all these variables on the conversion, molecular weights and volume of product (i.e. degree of fouling) was studied individually and compared to the theoretical predictions (where relevant).

Linear regression analysis was performed on the experimental data as detailed in Chapter 5, the results of which are discussed later in this chapter.

7.2 Experimental Results

7.2.1 Rotational Speed

Figure 7.1 illustrates the decrease in conversion (from 55% to 20%) observed on the disc as the rotational speed was increased from 200 to 300 rpm. At rotational speeds of 400 rpm and above (maximum tested was 1000 rpm), no polymer was formed. The conversions achieved for all other samples (i.e. collection flask and disc housing) were less than 4% and no trends were observed.

The effect of rotational speed on molecular weights is illustrated in Figure 7.2, which shows an increasing trend in molecular weight with increasing rotational speed over the range which resulted in the production of polymer. The corresponding values of polydispersity index ranged from 1.57 to 2.04, with a marginal decrease seen with increasing rotational speed up to 300 rpm (illustrated by Figure 7.18 in Appendix E).

The volume of polymer collected from the disc was largest for a rotational speed of 200 rpm, with a corresponding decrease observed in the volume of low conversion polymer collected in the flask, i.e. a higher percentage of product remained in the housing, having undergone some degree of polymerisation.

7.2.2 Feed Flowrate

Figure 7.3 shows the observed trend in conversion with increasing feed flowrate. As can be seen there was a definite decreasing trend as flowrate was increased. The decrease was most pronounced at lower flowrates, where an increase from 0.5 ml/s to 2 ml/s resulted in a decrease in conversion from 66% to 26%. Increasing the flowrate beyond this resulted in a less dramatic decrease in conversion.

When considering the effect of feed flowrate on molecular weight, an observed maximum in both M_n and M_w was found as seen in Figure 7.4. This maximum occurred at a feed flowrate of 1.5 ml/s. This corresponded with a minimum value of polydispersity index at this flowrate. Figure 7.19 in Appendix E illustrates the trend in polydispersity index with feed flowrate, and this trend can be clearly seen to be the inverse of the trend in molecular weight. The values of molecular weight and

polydispersity index for feed flowrates of 3 and 4 ml/s are not actually zero, however the sample size was small and this led to difficulties in analysing molecular weights.

The volumes of polymer collected from the disc and housing were highest for the two lowest flowrates studied, with a decrease corresponding to the decrease in conversion seen.

7.2.3 Photoinitiator Concentration

Figure 7.5 shows the conversions achieved with increasing photo-initiator concentration. At very low concentrations (less than 0.25% by weight) no conversion was achieved, however increasing the concentration to 0.5wt% resulted in a rapid increase in conversion (up to 55%). Increasing the concentration to 2wt% resulted in a marginal increase (to 57%) and increasing the concentration beyond this resulted in a decrease in conversion achieved. However, increases in concentration beyond 3wt% (and up to 6wt%) resulted in very little further decrease in conversion and maintained a conversion of 38%. These results indicated that an optimum value of photo-initiator concentration exists between 0.5wt% and 2wt%.

The observed trend in molecular weight with photo-initiator concentration is shown in Figure 7.6. A decrease in molecular weight was observed with increasing concentration up to 3wt%, beyond which both M_n and M_w remain approximately constant. No corresponding trend in polydispersity index was observed, and values ranged from 1.73 to 2.09 (with one exception at 2.74) as illustrated in Figure 7.20 in Appendix E.

No observable trend in volume of polymer collected with photo-initiator concentration was found.

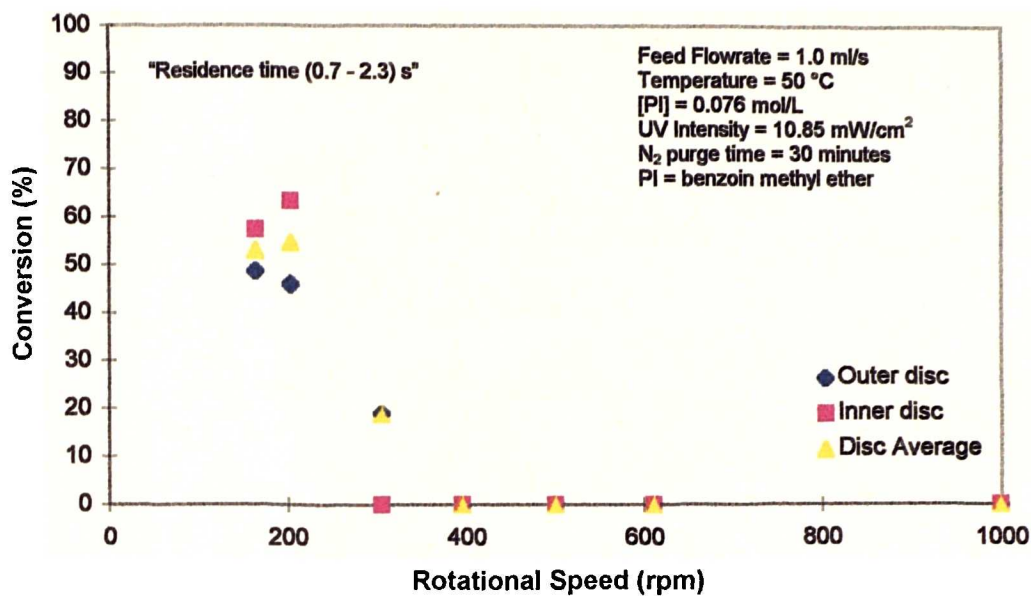


Figure 7.1. Effect of Rotational Speed on Conversion.

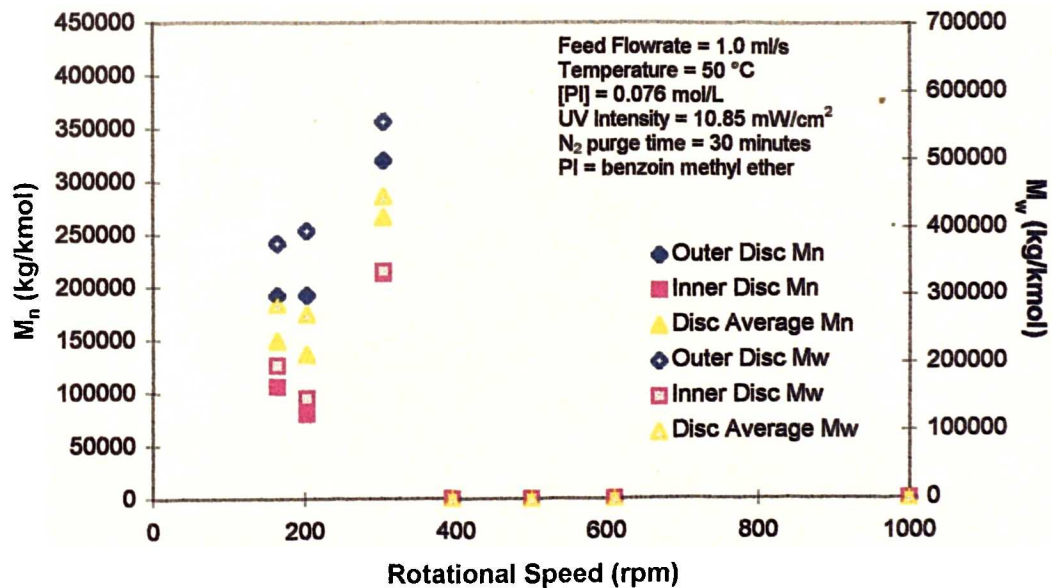


Figure 7.2. Effect of Rotational Speed on Molecular Weight.

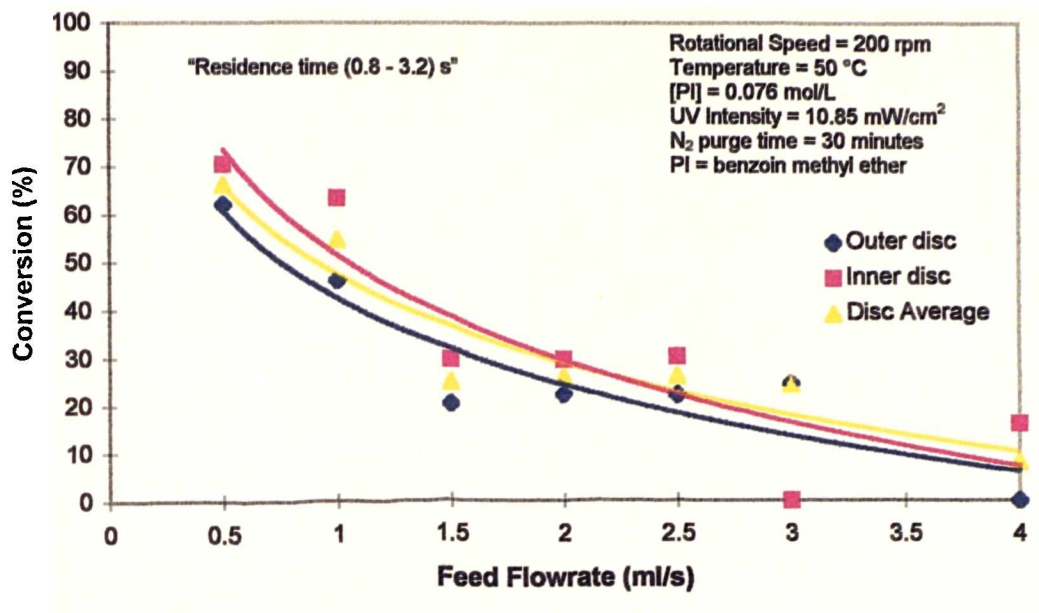


Figure 7.3. Effect of Feed Flowrate on Conversion.

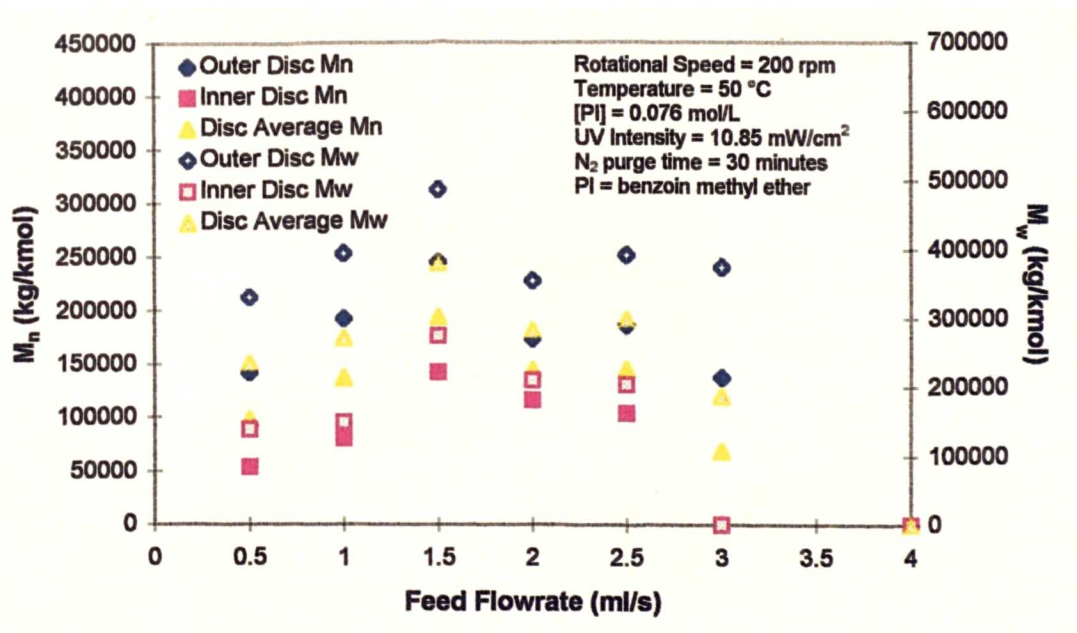


Figure 7.4. Effect of Feed Flowrate on Molecular Weight.

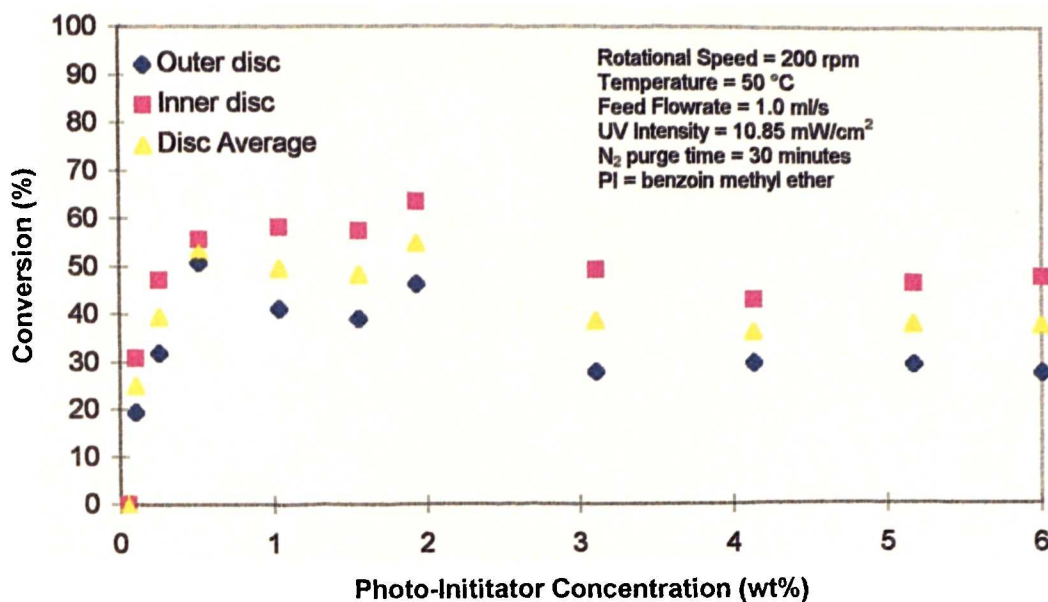


Figure 7.5. Effect of Photo-Initiator Concentration on Conversion.

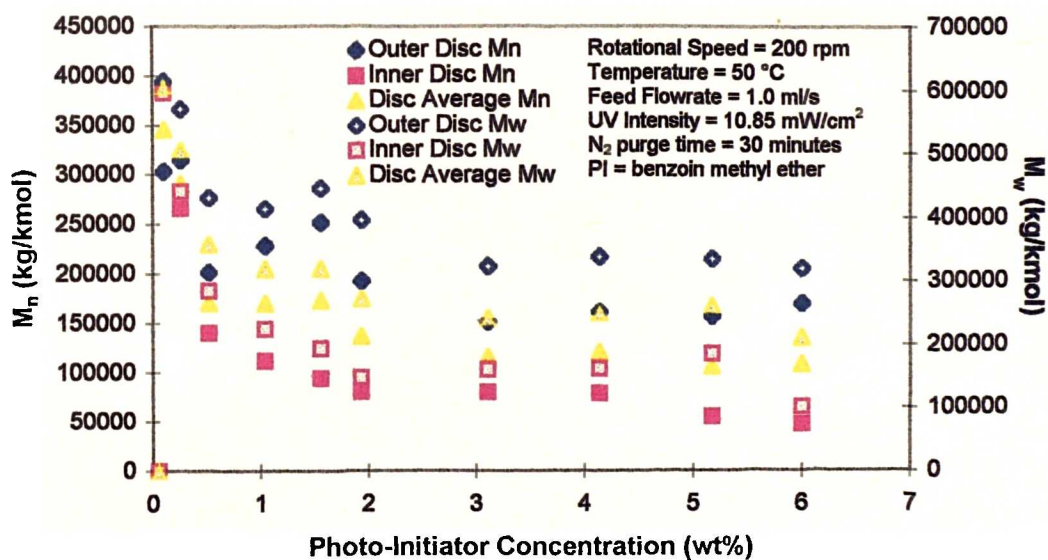


Figure 7.6. Effect of Photo-Initiator Concentration on Molecular Weight.

7.2.4 Temperature

Over the range of temperatures tested (17°C to 60°C) no distinct trend in conversion with temperature was observed. The conversion achieved shows a minimum around 30°C and increases with increasing temperature beyond this with the highest conversion (63%) achieved at the highest temperature tested (60°C). Figure 7.7 presents the experimental results, and as can be seen, the minimum observed is not necessarily a true minimum as the results at 35°C and 40°C are higher than the conversion for 45°C. The results did indicate that generally higher temperatures result in higher conversions.

The molecular weight results are presented in Figures 7.21 and 7.22 in Appendix E, no trends in molecular weight or polydispersity index with temperature were observed.

Temperature was not observed to show a significant effect on the volume of polymer collected from the disc.

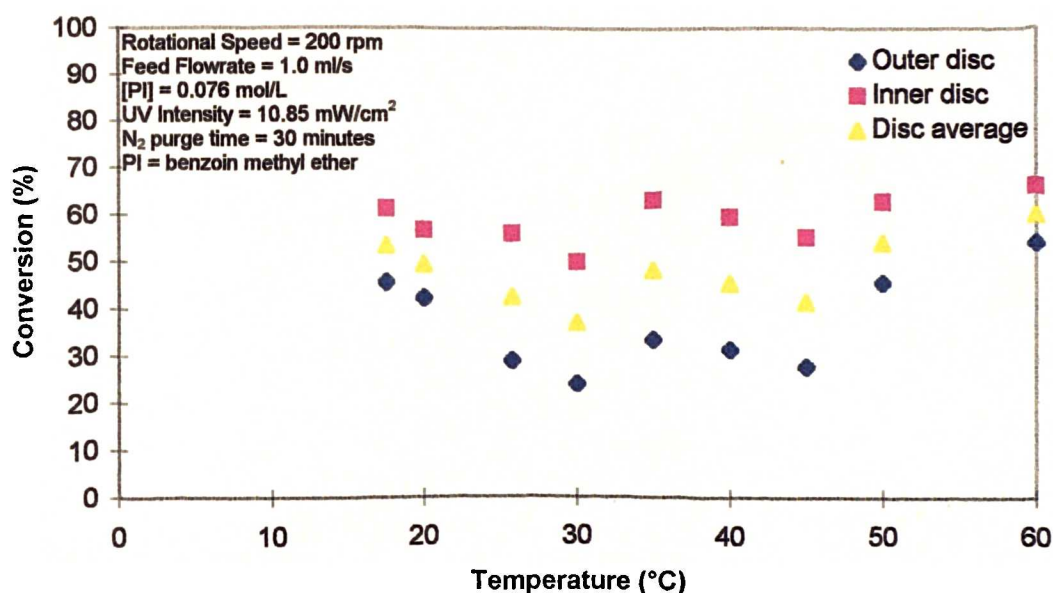


Figure 7.7. Effect of Temperature on Conversion.

7.2.5 Photoinitiator Type

Figure 7.8 shows a comparison of the conversions achieved at an initiator concentration of 2wt% for four different photo-initiators. Benzophenone (under identical conditions) produced no conversion, while the remaining three initiators all produced some high

conversion product. Irgacure 651 resulted in the highest conversion (57%) with benzoin methyl ether producing only marginally lower conversion (55%). The use of benzoin resulted in a conversion of 23% although it was noted during the experiments that benzoin did not readily dissolve in n-butyl acrylate, unlike the remaining initiators. A comparison of the conversions in the samples taken from the reactor housing and collection flask showed consistently higher results when using Irgacure 651 than when using benzoin methyl ether.

A similar comparison was made for all initiators except benzoin at a concentration of 0.076 mol/L and is represented in Figure 7.23 in Appendix E. These results show that for identical concentrations, benzoin methyl ether produced higher conversion on the disc (54%) than Irgacure 651 (45%). The samples from the housing and flask however show negligible conversion for benzoin methyl ether but 10% and 5% respectively for Irgacure 651.

The molecular weight was found to vary with initiator type, benzoin producing an M_n of 196777 with benzoin methyl ether producing an M_n of 161394 and Irgacure 651 producing an M_n of 136621. No obvious difference in polydispersity index was found.

The volume of product collected from the various sample points was found to differ according to photo-initiator type. Irgacure 651 produced the largest volume of polymer on the disc and in the reactor housing, with very little low conversion product collected in the flask (7% of feed at 5% conversion). Benzoin produced noticeably less polymer on the disc and in the reactor housing with more low conversion product collected in the flask. Benzoin methyl ether was found to be somewhere between the two, with 48% of the feed collected in the flask at negligible conversion.

7.2.6 UV Intensity

The range of UV intensities tested was limited by the positioning of the UV lamp, however values between 6.5 mW/cm² and 13.5 mW/cm² were tested. Over this range, very little difference in conversion was observed as shown in Figure 7.9 and increasing intensity within the range available appears insignificant.

No significant trend in molecular weight or polydispersity index with UV intensity was observed over the range tested.

No difference in the volume of product collected from the disc or the flask was observed with increasing UV intensity.

7.2.7 Purge Time

Figure 7.10 shows the effect of varying the nitrogen purge time on the conversion. As can be seen, no nitrogen purge resulted in no conversion. Increasing the purge time to 30 minutes resulted in an increase in conversion (to 55%) and increasing further (120 minutes was the maximum tested) resulted in no additional increase in conversion, in fact a slight decrease was seen.

No real trends in molecular weight and polydispersity index were observed with nitrogen purge time.

The volume of polymer collected from the disc showed an increase with increasing purge time up to 30 minutes but showed no real change when purge time was increased beyond this.

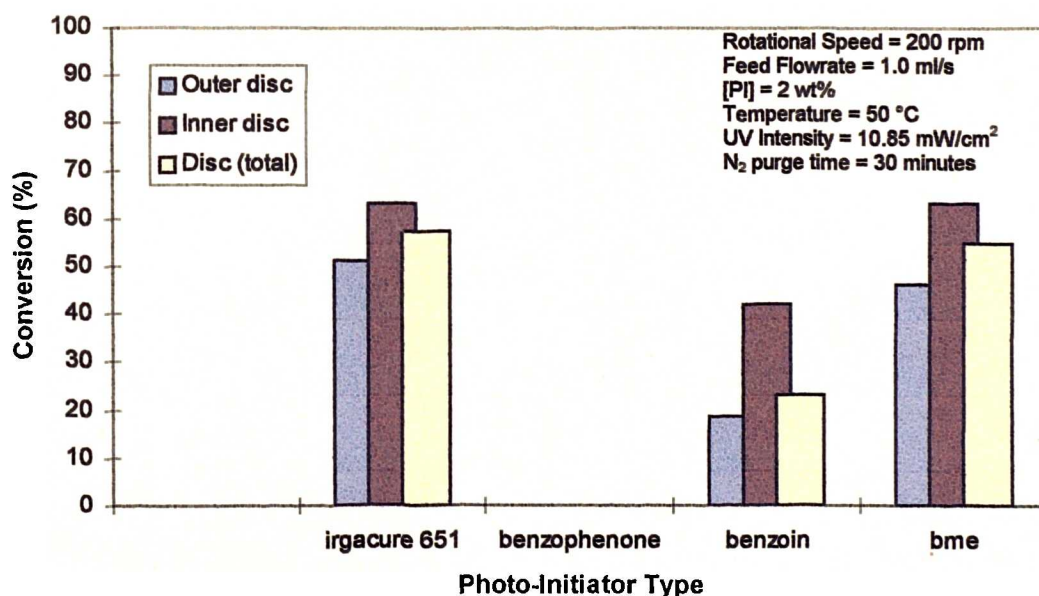


Figure 7.8. Effect of Photo-Initiator Type on Conversion .

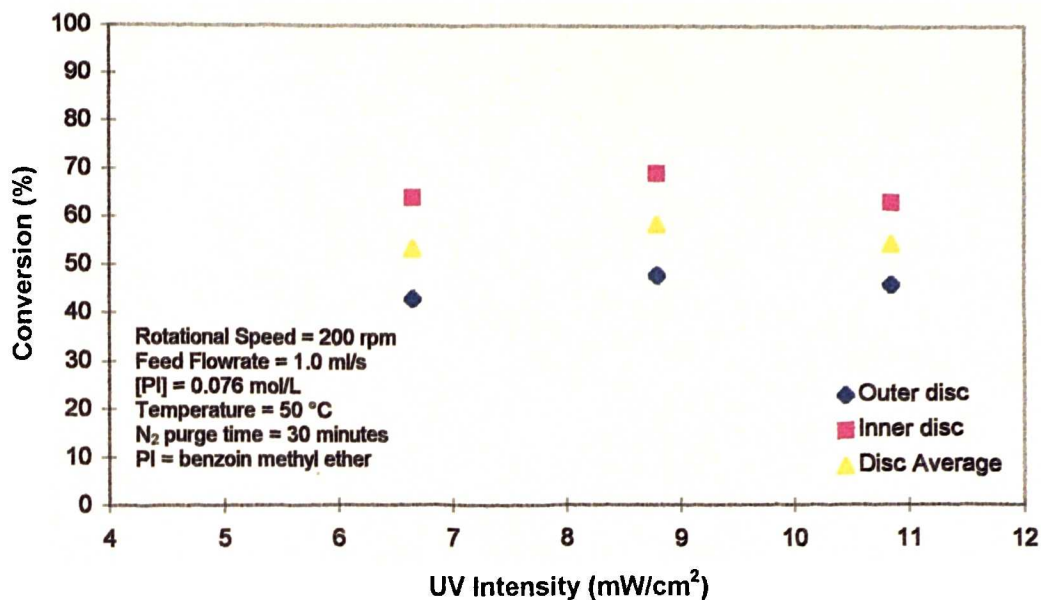


Figure 7.9. Effect of UV Intensity on Conversion.

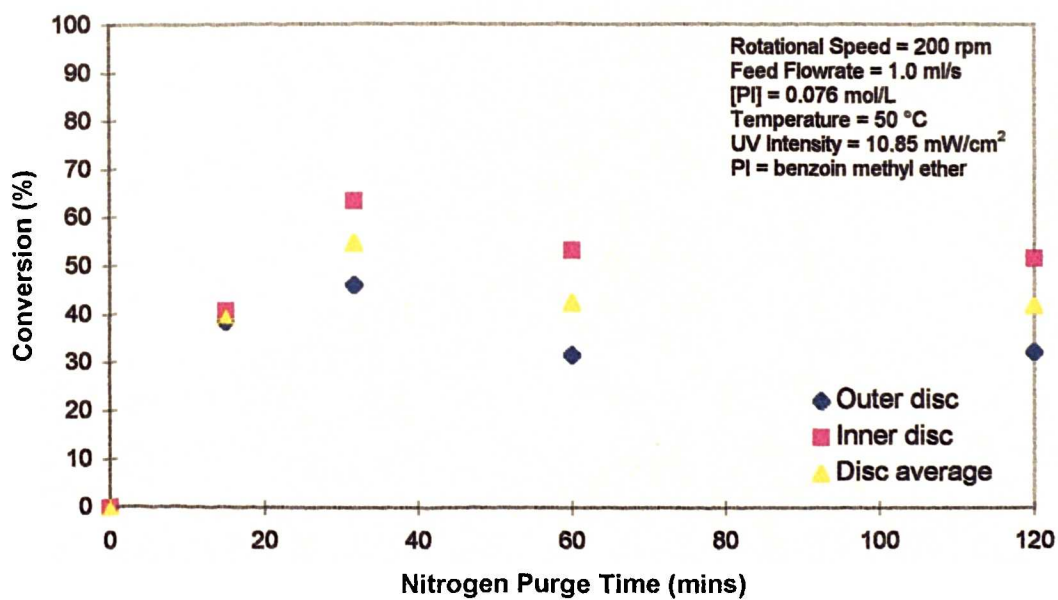


Figure 7.10. Effect of Nitrogen Purge Time on Conversion.

7.3 Linear Regression Analysis

Full details of the linear regression performed and the consequent analysis of the data are detailed in Chapter 5. Presented here are the results of this analysis and the models produced.

Initially, linear regression was performed using all of the variables previously discussed in this chapter, with the exception of nitrogen purge time and photo-initiator type. Nitrogen purge time was excluded from the model as it has no direct relevance on the theoretical model which assumes no oxygen inhibition. As we do not have a correlation between nitrogen purge time and dissolved oxygen levels there is no benefit in including it in the model. The type of photo-initiator used will affect some values within the theoretical model as quantities such as quantum yield are specific to each initiator type, and the effect of these is already accounted for by this model and there is no quantitative value to use in the linear regression. The model resulting from this initial regression is shown as Equation (7.1).

However, analysis of the regression data showed that two of the five variables were insignificant in comparison with the rest. The insignificant variables were temperature and UV intensity and therefore a second regression was performed, omitting these two variables. The resulting model is shown as Equation (7.2). Analysis of this data showed that all three variables were significant in the regression, and the regression itself was significant ($R^2 = 0.759$).

$$y = \frac{1.17 \times 10^5 [\text{PI}]^{0.410}}{(\text{rpm})^{3.260} Q^{0.805} I_0^{0.090} T^{0.136}} \quad (7.1)$$

$$y = \frac{5.11 \times 10^4 [\text{PI}]^{0.416}}{(\text{rpm})^{3.279} Q^{0.821}} \quad (7.2)$$

The conditions for which the final model (Equation (7.2)) is valid are:

Chapter 7

$$0 \leq \text{rpm} \leq 1000$$

$$0 \leq Q \leq 4 \times 10^{-6} \text{ m}^3 / \text{s}$$

$$0 \leq [\text{PI}] \leq 0.23 \text{ mol} / \text{L}$$

$$17 \leq T \leq 60 \text{ }^\circ\text{C}$$

$$6 \leq I_0 \leq 13 \text{ mW} / \text{cm}^2$$

Figure 7.11 illustrates the accuracy of this model to the experimental data. As can be clearly seen there is a reasonable amount of scatter in the points, which indicates that the relationships between the variables in the spinning disc system are more complicated than those in the static film system and the empirical relationships correlated here will give merely an estimate of the conversion expected.

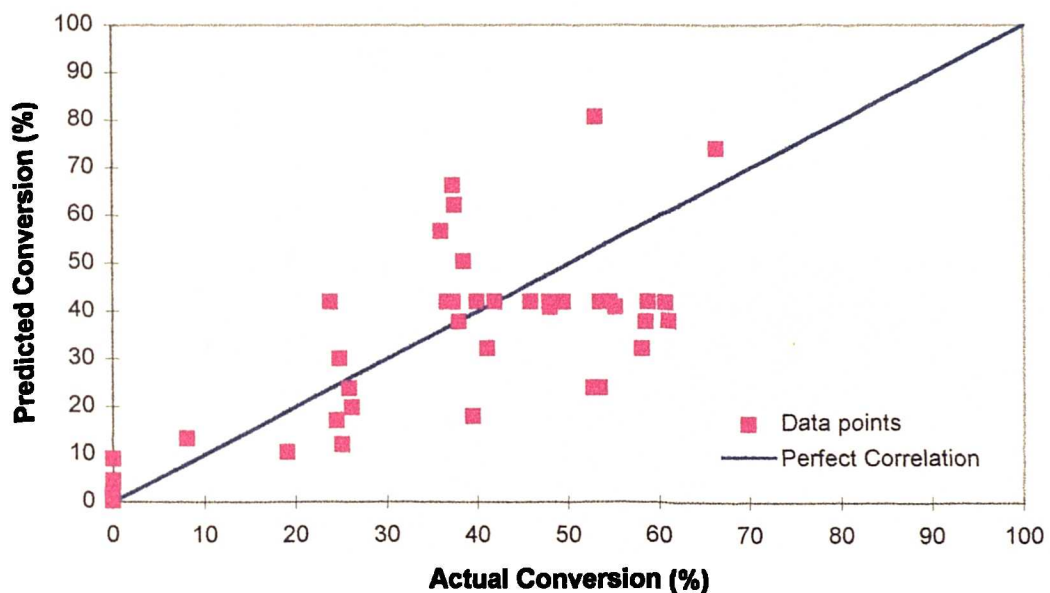


Figure 7.11. Deviation of Model Predictions from Perfect Correlation.

7.4 Discussion

This section contains detailed discussions on the effect each variable has shown on monomer conversion, molecular weight, polydispersity index and volume of polymer formed with reference to the theoretical expectations of each variable. Table 7.1 contains a brief summary of the observed results and is included as a reference for the reader as the results are discussed in detail.

Table 7.1. Summary of Observed Results.

Variable	Range and Units	Observed Effect	Significance in Linear Regression	Exponent from Linear Regression
Rotational speed	150-1000 rpm	Increasing trend in conversion, decreasing trend in molecular weight, no effect on polydispersity index.	Significant	-3.279
Feed flow	1-4 ml/s	Decreasing trend in conversion, definite trends in molecular weight and polydispersity index.	Significant	-0.821
Photo-initiator conc.	0-6 wt%	Definite trends in conversion and molecular weight, no trend in polydispersity index.	Significant	0.416
Temperature	17-60 °C	No distinct trends in conversion, molecular weight or polydispersity index.	Insignificant	(0.136)
Photo-initiator type	N/A	Definite effect on conversion and molecular weight.	N/A	N/A
UV Intensity	6-13 mW/cm ²	No obvious trends in conversion, molecular weight or polydispersity index.	Insignificant	(0.090)
Nitrogen purge time	0-120 min	Some effect on conversion, no trends in molecular weight or polydispersity index.	N/A	N/A

7.4.1 Rotational Speed

Rotational speed shows a significant effect on the conversion achieved and also on the molecular weight of the polymer produced. The significance is confirmed by the linear regression analysis. If we consider the theoretical model (Equation 3.11 in Chapter 3)

Chapter 7

then we can compare the experimental results with the theoretical model and this will assist in explaining the experimental observations. Figure 7.12 illustrates the theoretical effect of rotational speed on conversion in comparison to the experimental results and the predictions based on the linear regression model.

If we consider the theoretical effect, increasing the rotational speed affects the polymerisation system in two ways. The increase in rotational speed results in a decrease in film thickness and a decrease in residence time (hence decreased exposure time). These changes in film thickness and residence time are illustrated in Figure 7.24 in Appendix E (calculations are based upon n-butyl acrylate at 50°C and neglect increases in viscosity as an example). An increase in rotational speed from 150 rpm to 1000 rpm results in a decrease in film thickness from 49 to 15 μm and a decrease in residence time from 2.3 to 0.7 seconds. In reality these values will be higher but without an accurate model of viscosity increase with conversion across the disc, prediction of exact values is impossible. As can be seen from Figure 7.12, increasing the rotational speed from 50 to 1000 rpm results in a predicted decrease in conversion from 69% to 14%. Increasing rotational speed beyond 1000 rpm results in only marginal decreases in conversion. This would indicate that the decrease in exposure time has a more significant effect than the decrease in film thickness when rotational speed is increased, which would explain the fact that no polymerisation was achieved at higher rotational speeds.

A comparison of the experimental results with the model expectations shows that a similar trend is seen but at rotational speeds above 300 rpm no polymer is formed. This deviation is most probably due to errors in the model due to the unknown change in film thickness and residence time across the disc with increasing conversion, and also the model assumption of no inhibition (by oxygen or other).

It is difficult to draw definite conclusions about trends in molecular weight as the range over which values were obtained is small. There does appear to be a decreasing trend in molecular weight with rotational speed and further studies using a higher intensity UV source would be beneficial in terms of extending the range of rotational speeds at which polymerisation occurs.

The conclusions drawn here are that rotational speed is a significant factor in the polymerisation and that further work over a wider range of rotational speeds would be beneficial.

7.4.2 Feed Flowrate

Feed flowrate also shows a significant effect on the conversion achieved and also on the molecular weight of the polymer produced. The significance is confirmed by the linear regression analysis. Figure 7.13 illustrates the theoretical effect of feed flow on conversion in comparison to the experimental results and the predictions based on the linear regression model.

Again the feed flowrate will affect both the film thickness and residence time. Increasing feed flowrate will result in increased film thickness (from 34 to 66 μm over the range studied) and decreased residence time (from 3.2 to 0.8 seconds) as illustrated in Figure 7.25 (Appendix E). The combined effect of these is a predicted decrease in conversion achieved from 70% at a flow of 0.25 ml/s to 27% at 5 ml/s. From Figure 7.13 it can be seen that the general trend followed by the experimental results is very similar to the predicted trend, however at flowrates of 1 ml/s and less the experimental value is higher than that predicted but at flowrates above this, the predicted values are higher. This indicates that the lower the flowrate the better, but in terms of efficiency and throughput this is not necessarily the case. For a given combination of rotational speed and flowrate there are operational limits outside which the disc is not being fully utilised. These limits are illustrated in Figure 7.26 (Appendix E). If the flowrate is too low, full wetting of the disc does not occur and therefore the full capacity of the disc is not being utilised. On the other hand, if the flowrate is too high splashing of liquid from the weir occurs, which means that some of the reactants have different residence times which may result in product with a wider molecular weight distribution.

If we consider the trends in molecular weight and polydispersity, it is interesting to note that we have a maximum in terms of molecular weight which corresponds to a minimum polydispersity index. There is no corresponding maximum in terms of conversion, but this may be an important factor in product quality. This indicates that

for a given rotational speed there may exist an optimum feed flowrate in terms of high quality product (i.e. tight molecular weight distribution).

It was also noted that the volume of polymer produced was higher for the lower flowrates, which fits with the theory that as exposure time is increasing there is an increase in the amount of polymerisation occurring.

The conclusions drawn here are that feed flowrate is a significant factor in the polymerisation, and that for a given rotational speed there exist upper and lower flowrates beyond which the disc is not being efficiently used.

7.4.3 Photo-Initiator Concentration

Photo-initiator concentration shows a significant effect on both conversion and molecular weight which is confirmed by the regression analysis. Figure 7.14 shows the comparison between the experimental results obtained and those predicted by both the theoretical model and the linear regression model. Both the theoretical and regression models predict an increasing trend, which is more marked at lower concentrations. The experimental results however, indicate that there is an optimum value of concentration in terms of conversion achieved, and this lies between 0.5 wt% and 2 wt%. There are two reasons for this, both involving the photo-chemistry of the reaction. For a given UV intensity there will be a maximum number of photo-initiator molecules which will be excited and are therefore available to initiate chains. If more photo-initiator molecules are present than this maximum imposed by the UV intensity then the additional molecules will not be utilised and no further conversion will be seen with the increased concentration. This does not explain the existence of an optimum value however. Any excited initiator molecules which do not initiate chains are likely to be used in terminating growing chains, hence if the UV intensity is such that all the molecules present will be excited, the more radicals present (i.e. higher concentration of initiator) the higher proportion of radicals which are likely to be involved in termination. If the same number of polymer chains are initiated, this results in shorter chains and hence lower conversions than if the chains were allowed to grow further i.e. higher concentrations result in product of lower molecular weight. This explains the

decreasing trend seen in molecular weight. It does not however affect the polydispersity index which shows no change with concentration.

The conclusions drawn here are that photo-initiator concentration is a significant factor in the polymerisation and that an optimum concentration exists for the given conditions. This optimum concentration will vary according to the values of other variables.

7.4.4 Temperature

Temperature does not show as large an effect on conversion as the previous variables, and is found to be statistically insignificant in the linear regression analysis. Figure 7.15 shows a comparison of the experimental data with the predictions based upon both the theoretical and regression models. As the regression considers this an insignificant variable, the regression model predicts no change with temperature. It can be seen however that the theoretical model does predict an increase in conversion from 32% at 10°C to 47% at 50°C. This increase arises because of the changes in density and viscosity with temperature, and the change in k_p . These changes in kinematic viscosity affect the film thickness and exposure time (Figure 7.27 in Appendix E) and hence the model will predict changed conversions. The lower viscosity (at higher temperatures) will allow easier mixing and therefore a higher rate of polymerisation. This is illustrated by the values of k_p given in Table 7.2 [73]. Very little reliable kinetic data has been published for n-butyl acrylate [71,72] which limits the range of temperatures over which the model can be used reliably as it requires a knowledge of k_p at each temperature.

Table 7.2. Values of k_p for Butyl Acrylate.

Temp (°C)	k_p (L/mol.s)
10	12500
30	16300
50	20700

Chapter 7

Considering the experimental data however, there appears to be a minimum in conversion with temperature at around 30°C, which is not predicted. The highest value of conversion achieved was observed at the highest temperature tested (60°C). Further studies on temperature, and more kinetic data at various temperatures for this system are required before any reliable conclusions can be made about the effects of temperature.

No trend in the volume of polymer collected from the disc was observed with temperature. This suggests that an increase in temperature alone would not be sufficient to overcome the problem of polymer fouling on the disc. The problem of fouling is discussed further in Chapter 9.

The conclusions drawn here are that over the range tested the temperature has little effect on the polymerisation and increasing temperature alone is not sufficient to overcome the problem of fouling.

7.4.5 Photo-Initiator Type

The effect of different photo-initiators is more difficult to quantify and predict, but differences in conversions achieved would be expected due to differences in the properties of each photo-initiator. The four initiators tested were; Irgacure 651 (DMPA), benzoin methyl ether, benzoin and benzophenone. The latter of these is classed as a PI₂ type, whereas the remaining three are all classed as PI₁ type photo-initiators. More detailed information on these classifications can be found in Chapter 3, the difference being the method of formation of radicals. PI₁ type photo-initiators form radicals by intramolecular bond-cleavage whereas PI₂ type form radicals by intermolecular hydrogen abstraction. This explains the observation that benzophenone produced no polymerisation, as no additional hydrogen donor was added to the monomer / initiator solution. The three remaining initiators all showed varying degrees of polymerisation. The majority of the studies were conducted using benzoin methyl ether, as data is readily available for this initiator. The results indicate that on an equal mol/L basis, benzoin methyl ether produces higher conversion polymer on the disc (54%) when compared with Irgacure 651 (45%) but much of the feed is still collected as low conversion product in the flask (48% of the feed at negligible conversion).

When using Irgacure 651 only 7% of the feed was collected in the flask at a conversion of 5% and the product collected in the housing showed a conversion of 10% compared to 2% with benzoin methyl ether. The observations, both from the volumes collected and their conversions, and from visual inspection indicate that when using Irgacure 651 a much higher percentage of the feed is undergoing polymerisation to a degree where the change in viscosity is obvious.

The conclusions drawn here are that photo-initiator type can have a dramatic effect on the polymerisation and that for this system Irgacure 651 initiated polymerisation in a higher percentage of the feed than the other photo-initiators tested.

7.4.6 UV Intensity

The range of UV intensities studied was limited by the distance between the UV source and the disc. At the closest position, the intensity seen by the disc was 13 mW/cm^2 and this was reduced to 6 mW/cm^2 by moving the lamp further away from the disc. Figure 7.16 shows a comparison of the experimental and predicted conversions over the range studied. The linear regression analysis found the variations in UV intensity over this range to be insignificant, and the theoretical predictions over this range show only a small expected increase in conversion with increasing UV intensity. If we consider the theoretical effect of intensity on conversion over a larger range however, we can see the effect of significant increases in intensity (Figure 7.17). It can be seen that initially as UV intensity increases, the predicted conversion also increases. However, a point is reached where the conversion predicted reaches a maximum and increasing the UV intensity beyond this results in a decrease in the conversion predicted. Figure 7.17 also illustrates the effect of UV intensity on the maximum conversion achievable (based on Equation 3.11 in Chapter 3). As intensity increases, the maximum achievable conversion decreases. This is due to the higher concentration of radicals at higher intensities. If the rate of consumption of initiator radicals in chain initiation is less than the rate of production of radicals (as expected at higher intensities) then the 'excess' radicals (i.e. those not used in chain initiation) will terminate growing polymer chains. The higher the concentration of 'excess' radicals, the more likely termination is to occur which results in lower molecular weights and lower conversions. Figure 7.17 also illustrates the effect of changing the photo-initiator concentration on this phenomenon.

Chapter 7

As can be seen if the concentration of photo-initiator is increased, the predicted conversions and maximum achievable conversions are higher than for lower initiator concentrations.

The range of intensities studied is not large enough for a trend in molecular weight to be detected but this would be expected to decrease with increasing UV intensity.

The conclusions drawn here are that over the range of UV intensities tested there was no discernible effect on the polymerisation and that studies at higher intensities are required as theoretically, the effect of UV intensity on the polymerisation is significant.

7.4.7 Nitrogen Purge Time

It is a well documented fact that the presence of oxygen inhibits the polymerisation process in the case of free-radical polymerisation and this has been discussed in more detail in Chapter 3. The presence of dissolved oxygen in the liquid monomer and also atmospheric oxygen which can diffuse into the film is a potential problem. To overcome this, a nitrogen purge was used for both the feed solution and the reactor itself. The length of this purge before the start of an experiment was varied to investigate the effect of the nitrogen purging. As presented previously, the experimental results showed no additional increase in conversion for purge times beyond 30 minutes, although for purge times lower than this less conversion was achieved.

The conclusions drawn here are that the 30 minute purge used in the majority of tests was sufficient to reduce the levels of dissolved oxygen and promote a nitrogen atmosphere within the reactor. However, this does not conclusively indicate that all dissolved oxygen has been removed, and the use of other methods of nitrogen purging should be considered.

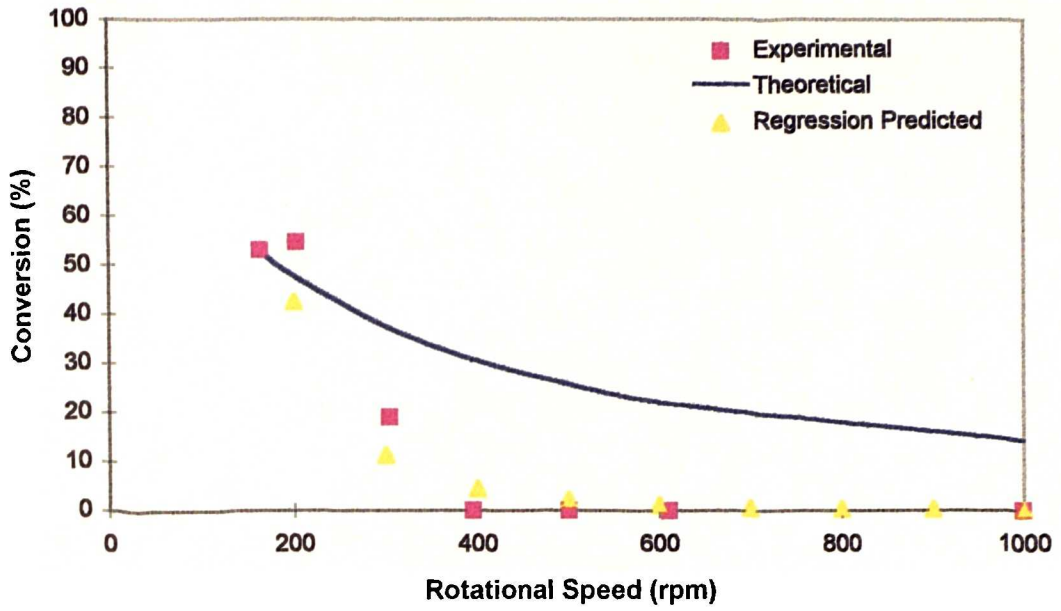


Figure 7.12. Comparison of Experimental and Predicted Conversions with Rotational Speed.

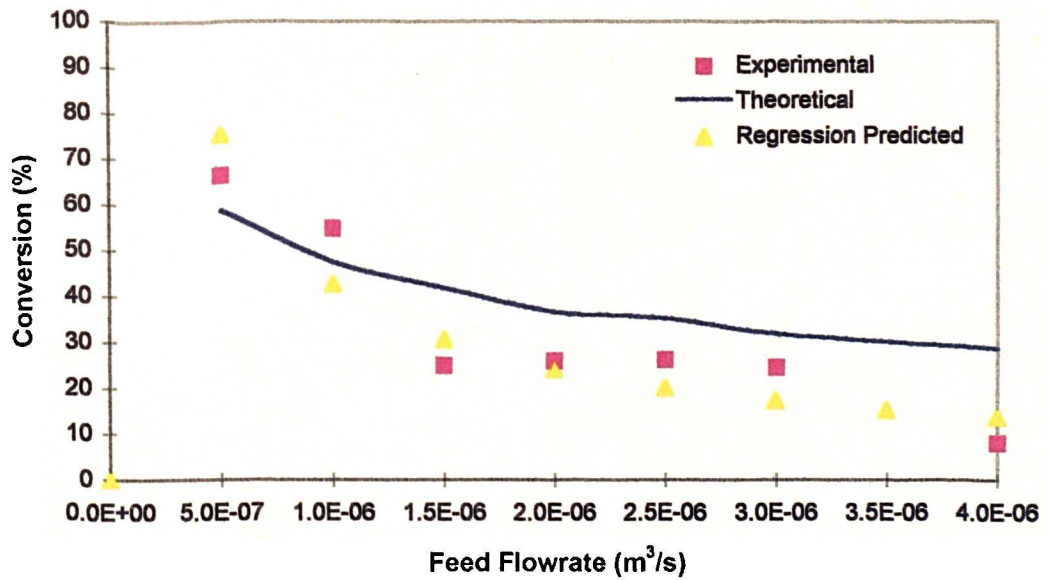


Figure 7.13. Comparison of Experimental and Predicted Conversions with Feed Flowrate.

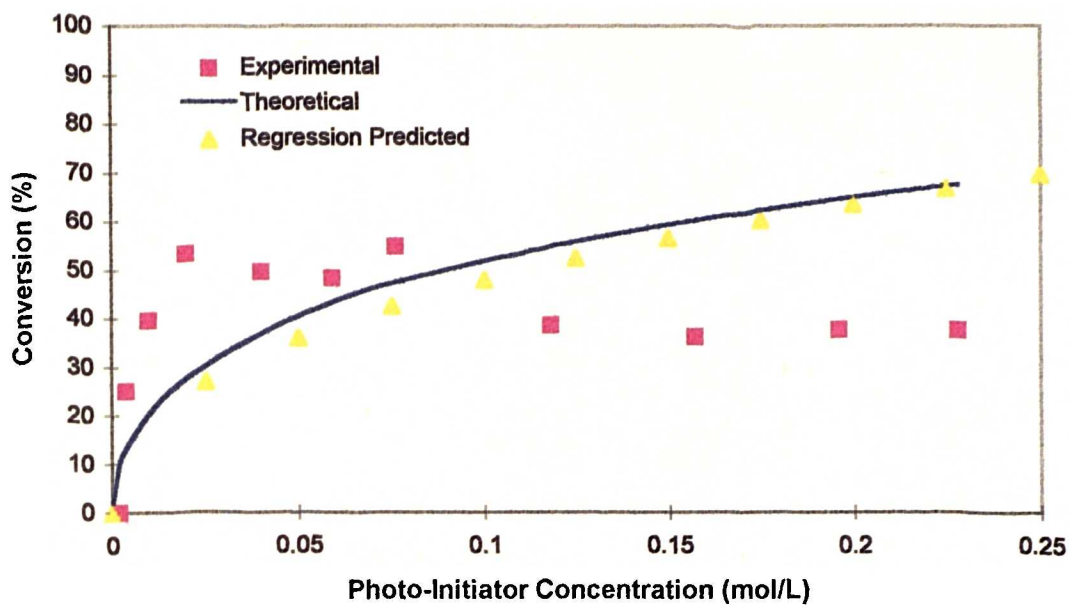


Figure 7.14. Comparison of Experimental and Predicted Conversions with Photo-Initiator Concentration.

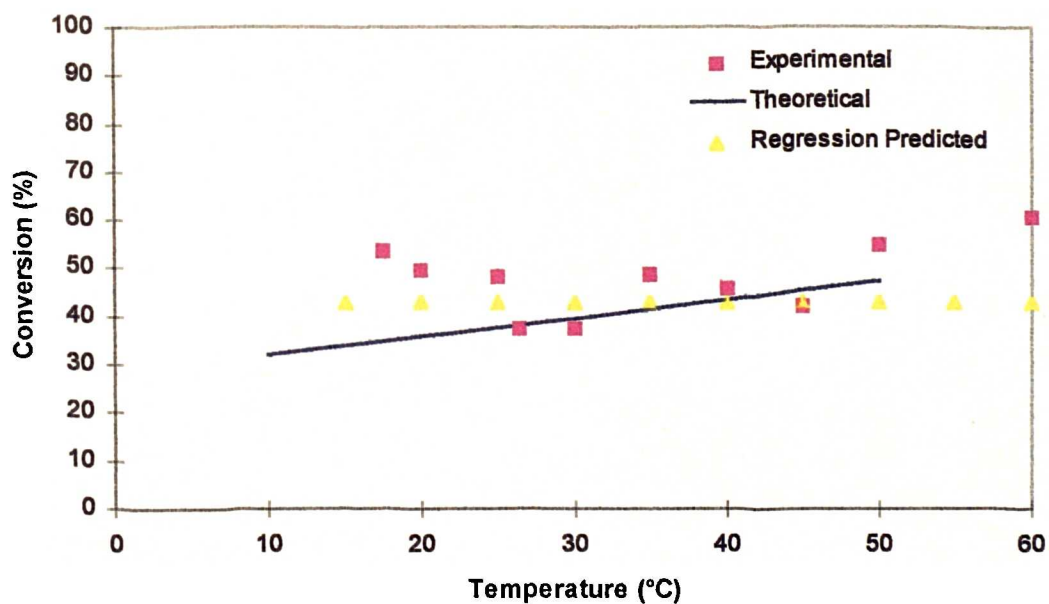


Figure 7.15. Comparison of Experimental and Predicted Conversions with Temperature.

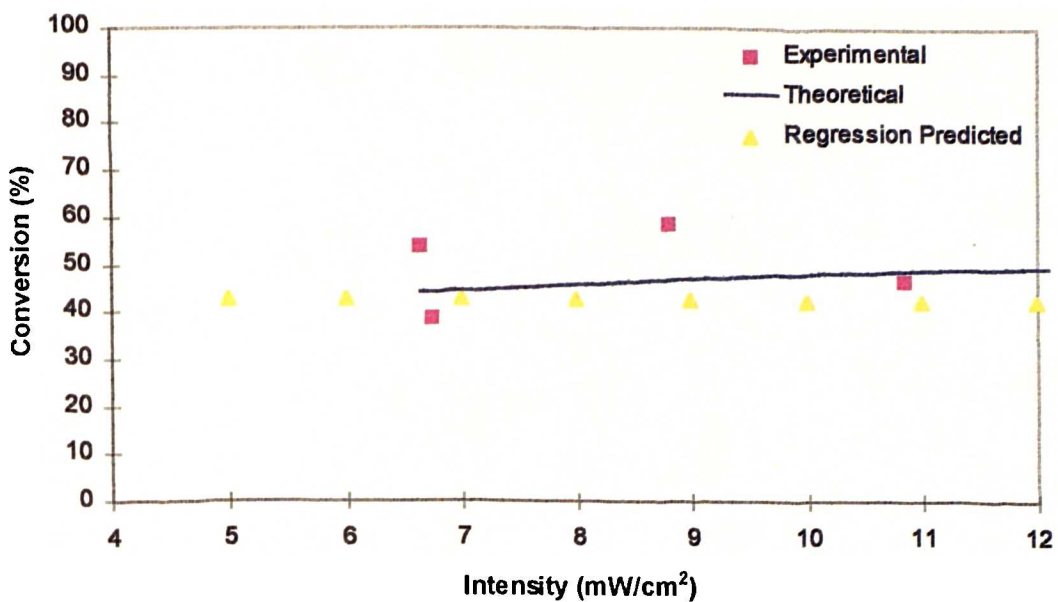


Figure 7.16. Comparison of Experimental and Predicted Conversions with UV Intensity.

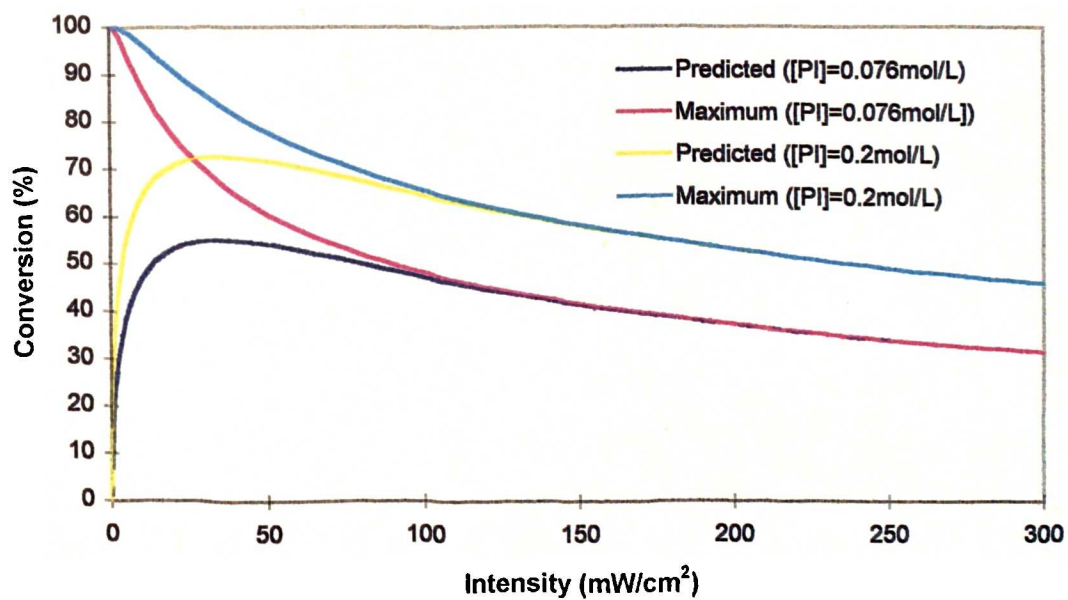


Figure 7.17. Theoretical Effect of UV Intensity on Conversion.

7.4.8 General Discussion

In cases where a higher conversion was achieved, a layer of polymer was found to remain on the disc itself. This can be considered to be fouling, as ideally the polymer should be formed whilst the reactants are flowing across the disc and then collected in the reactor housing and not on the disc. This is in part due to the increased viscosities associated with higher conversions but also appears to be an effect of the 'stickiness' of the polymer / monomer mixture. Even for reasonably low conversions (around 20%) this mixture tends to have adhesive properties, and this causes the layer to form on the disc. Possible methods of overcoming fouling are discussed in Chapter 9.

The conclusion drawn here is that for this system as it stands fouling is a problem which must be overcome.

The design of the disc is detailed in Chapter 4, and this includes the modification to the disc to attain more even flow distribution. A possible concern of having this weir in the centre of the disc was that material in this well would be exposed to UV irradiation prior to flowing across the disc. The set-up was such that the well was shrouded from the UV lamp by a rubber bung which held the feed pipe in place above the weir. Samples from the weir were taken (where there was liquid remaining) and analysed in the same way as all other samples. Results of the analysis of these samples showed negligible, if any, conversion. This indicates that the shrouding of the well is effective and that polymerisation does not occur until the feed is flowing across the disc.

Where there was a layer of polymer remaining on the disc, samples were taken from both the inner and outer sections of the disc. The inner section was that part of the disc irradiated with UV and the outer section was that part of the disc outside the beam of the UV lamp. Samples taken from the inner section of the disc showed generally higher conversions but lower molecular weights than the samples from the outer section. Comparisons in conversion and molecular weight have been made using an average value for each trial but it is interesting to note this difference between the two sections. This indicates that under these conditions fouling is occurring, which leads to the build up of polymer on the disc, but also that there appears to be good mixing across the disc. This is indicated by the increase in molecular weight of the polymer across the disc. If the mixing was poor then we would not expect to see much change in the molecular

weight as the chances of fresh monomer reacting with the radical sites would be reduced. However, if mixing is good, a constant supply of monomer will be available to add on to the growing polymer chains resulting in higher molecular weight polymer. Good mixing should also result in a tighter molecular weight distribution and better product quality.

7.4.9 Limitations of Experimental Set-Up

As detailed in the design of the rig (Chapter 4) a flat glass top was constructed for the reactor to allow the UV lamp to be brought as close to the disc as possible, thereby increasing the UV intensity at the disc. A limitation of this however is that although the intensity is higher, the closer the lamp is brought to the disc, the smaller the exposed area becomes so the exposure time is reduced. Ideally the disc should be fully illuminated by a constant intensity of UV light. The other limitation relating to this is the actual range of UV intensities available for study. A second UV source of higher intensity would be very useful in investigating the effect of UV on the polymerisation.

The collection system was initially designed for low viscosity products and this causes a limitation when investigating polymerisations. The high viscosity product formed does not flow through the product outlets and into the collection flask but instead collects in the reactor housing. Low conversion product or unconverted feed does still collect in the flask however. The limitation imposed by this is that each run must be limited to a volume of 200 ml. If a larger volume is used there is a danger of overflow between the reactor baseplate and drive shaft. This prevents us from running a continuous polymerisation with the current set-up of the reactor.

7.5 Summary

In summary, the study of the photo-initiated polymerisation of n-butyl acrylate on a spinning disc reactor considered the effects of seven variables on the molecular weights of the polymer produced and on the conversion of monomer to polymer. Of these seven variables, four showed significant effects on the polymerisation (rotational speed, flowrate, photo-initiator concentration and photo-initiator type) and three showed little or no effect (temperature, nitrogen purge time and UV intensity).

Chapter 7

It is perhaps not surprising that neither temperature nor nitrogen purge time showed significant trends in terms of molecular weight or conversion. Temperature has considerably less effect in a photo-initiated polymerisation than in a thermally initiated system. Considering the nitrogen purge, if the oxygen levels are sufficiently depleted then the polymerisation will not be subject to its inhibiting effects and therefore the effect of increasing the purge time beyond the minimum required would not be expected to show an effect. From the theory however, it is known that the UV intensity will have an effect on the polymerisation, as discussed previously. If we consider the range of intensities achievable using a single UV source (as in this study) then any variation in intensity is only achievable by repositioning the Source at various distances from the reaction surface. With a single UV source of the type used, the range is severely limited and without the use of differing intensity sources it is difficult to investigate the effect of UV intensity accurately.

Four of the seven variables did show significant effects on the polymerisation system. Changing the type of photo-initiator used affects the chemistry of the system and it was found that of the four initiators tested, Irgacure 651 (DMPA) produced the best results, while the use of benzophenone resulted in no polymerisation. The remaining two initiators both produced results but neither were found to be as effective as DMPA. This highlights the importance of careful choice of photo-initiators for a given polymerisation system. The photo-initiator concentration was also found to affect the conversion achieved and an optimal concentration was found to exist, which is due to the mechanism by which photo-initiated polymerisation proceeds and has been discussed previously.

Both rotational speed and flowrate of reactants affect the film thickness of the polymerising media and the residence time across the reaction surface (which controls the exposure time to UV light). Increasing rotational speed resulted in significant decreases in conversion, which can be accounted for by the reduced exposure time to the UV source. Increasing the reactants flowrate also resulted in decreased conversion, again due to the lower exposure times but also partly due increased film thickness.

The conclusions drawn from this study are presented in Chapter 8, and recommendations for further work in Chapter 9.

CHAPTER 8

CONCLUSIONS

8.1 Introduction

The aim of this chapter is firstly to gather the conclusions drawn previously regarding the static film polymerisation (Chapter 6), spinning disc reactor polymerisation (Chapter 7) and heat transfer study (Appendix A). Secondly, a comparison between the static film and spinning disc polymerisation is considered and the conclusions that can be drawn from this comparison are included here.

8.2 Static Film Polymerisation

Within the range of parameters studied (exposure times of up to 40 s, film thickness of up to 1 mm and UV intensity of 5.41 to 10.85 mW/cm²) it was concluded that both the exposure time and UV intensity showed a significant effect on the static film polymerisation. It was also concluded that over this range, film thickness showed no statistically significant effect on the static film polymerisation.

Full characterisation of the polymerisation system was not achieved from the static film studies and further work that will more fully characterise the polymerisation is highlighted in Chapter 9.

The results of these static film studies are useful for comparison with the spinning disc reactor results and the conclusions drawn from this comparison are discussed later in this chapter. Conversions of up to 23% were achieved with values of M_n up to 147184, M_w up to 296115 and polydispersity indices between 1.98 and 4.43 attained.

8.3 Spinning Disc Polymerisation

The ranges of parameters studied were: rotational speeds of up to 1000 rpm; feed flowrates of up to 4 ml/s; photo-initiator concentrations of up to 0.23 mol/L;

temperatures from 17°C to 60°C; UV intensity up to 13 mW/cm²; nitrogen purge times of up to 120 minutes; and four different photo-initiators (benzoin methyl ether, benzoin, Irgacure 651 and benzophenone). The conclusions drawn are valid only within these parameters.

It was concluded that rotational speed, feed flowrate, photo-initiator concentration and nitrogen purge time all showed a statistically significant effect on the spinning disc polymerisation. It was also concluded that temperature and UV intensity showed no significant effect on the polymerisation.

There exists an optimum photo-initiator concentration for a given set of conditions and the value of this optimum under varying conditions would be of interest for future studies.

The largest problem encountered, which needs to be overcome, is that of polymer fouling on the disc. This is discussed further, with some possible solutions in Chapter 9.

The 30 minute nitrogen purge was sufficient (i.e. increasing beyond 30 minutes resulted in no further conversion) using the set-up detailed in Chapter 4, although no conclusive tests were conducted to determine the dissolved oxygen level present after purging. Tests did conclude that the nitrogen purge to the reactor was sufficient to reduce the atmospheric oxygen levels to less than 0.5%.

The results of these spinning disc studies can be compared with the static film results and the conclusions drawn from this comparison are discussed later in this chapter. Conversions of up to 66% were achieved with values of M_n up to 345444, M_w up to 604518 and polydispersity indices between 1.36 and 2.74 attained.

The spinning disc reactor shows definite potential for photo-initiated polymerisations but further studies are necessary if it is to be developed industrially and to overcome the problem of fouling of the reaction surface and recommendations for this are made in Chapter 9. A patent application has been made concerning the use of UV initiation for polymerisations conducted in a spinning disc reactor.

8.4 Spinning Disc Versus Static Film Polymerisation

The spinning disc reactor shows that higher conversions are achieved than in the static film case, with conversions of up to 66%, almost three times greater than the highest achieved from the static film (23%).

The use of the spinning disc reactor also results in higher molecular weights than the static film polymerisation, with M_n of 345444 c.f. 147184 and M_w of 604518 c.f. 296115, which shows an increase of over 100% in the highest values achieved when comparing both sets of data.

Finally, the range of polydispersity indices attained is much lower with the spinning disc than for the static film. The values range from 1.30 to 2.74 for the spinning disc results compared with 1.98 to 4.43 for the static film results. This reduction in polydispersity index indicates that good mixing is achieved in the spinning disc reactor whereas there is no mixing occurring in the static film studies.

From the comparison of the results for both the spinning disc and static film polymerisations, it is concluded that the polymer produced on the spinning disc has a higher conversion and narrower molecular weight distribution than that produced by the static film method. This indicates that the product quality will be improved by the use of the spinning disc reactor.

8.5 Heat Transfer

The range of parameters studied were; rotational speeds of up to 1400 rpm, feed flowrates of up to 2.7 L/min, cooling water flowrates of up to 10 L/min, temperatures between 30°C and 40°C and channel widths of 0.75 mm, 1.75 mm and 2.75mm. The conclusions drawn are valid only within these parameters.

It was concluded that feed flowrate and cooling water flowrate showed the most significant effect on the heat transfer characteristics of the reactor, and channel width and disc thickness were both shown to be significant by analysis of the regression data although not as significant as the previous two variables. It was also concluded that

Chapter 8

temperature and rotational speed showed no significant effect on the heat transfer characteristics of the reactor.

It was concluded that for a water-like viscosity, and dependent upon the conditions, overall heat transfer coefficients of up to $10 \text{ kW/m}^2\text{K}$ are achievable. The spinning disc reactor shows good heat transfer characteristics and is potentially suitable for exothermic reactions that are currently difficult to control, although full characterisation of the reactor in terms of heat transfer has not yet been conducted.

CHAPTER 9

RECOMMENDATIONS FOR FUTURE WORK

9.1 Introduction

The aim of this chapter is to make recommendations for further research based upon the conclusions made in the previous chapter and from experience gained throughout the investigation.

9.2 Further Polymerisation Work

9.2.1 Static Film

Studies are required over a wider range of film thickness to investigate further the effect of this variable on the static film polymerisation. Data for film thickness' between those already studied would be beneficial in helping to determine trends as there are insufficient data points, with only the three films tested, to conclusively determine the effect on the polymerisation.

The range of UV intensity studied was limited as only one UV lamp was used. Higher intensities from a second UV source would also help to more fully characterise the polymerisation.

Throughout the static film studies, the photo-initiator used was Irgacure 651 at a concentration of 2 wt% (on monomer) and studies at other concentrations and with other photo-initiators would give a better understanding of the polymerisation system.

9.2.2 Spinning Disc Reactor

Over the range of UV intensities studied, it was concluded that in the spinning disc reactor this variable showed no significant effect on the polymerisation. The range of intensity was limited as for the static film work and comparisons with a higher UV

intensity are required to investigate the effect of this further. Interestingly from the theory (explained and illustrated in Chapter 7), increasing intensity up to a certain value is expected to show an increase in conversion, however increasing beyond this is expected (from the kinetic model (Equation (2.13)) to lead to a decrease in the maximum conversion achievable and hence lower overall conversion. There is however published work on UV curing using lasers which indicates that increasing the UV intensity from 10 mW/cm² to 80 mW/cm² resulted in an increase in final conversion from 80% to 95% [39]. This needs to be investigated experimentally for the spinning disc system.

The predictions made in terms of conversion are based upon the literature model, with the values of film thickness and exposure time calculated from the film thickness and residence time on the spinning disc under the varying conditions. This has limitations however, in that the residence time and film thickness will change with viscosity as the polymerisation occurs across the disc. A model of how this viscosity changes with conversion and how this affects the film thickness and residence time would be an essential tool in producing an accurate model for the polymerisation and this would therefore be a very useful piece of work, which was beyond the scope and timescale of this investigation.

Throughout the spinning disc reactor work, fouling of the reaction surface by high viscosity polymer was found to be a problem. Increasing the disc temperature was not found to significantly decrease the amount of fouling, and the effect of increasing rotational speed on the fouling was inconclusive as the decreased exposure time at higher rotational speeds resulted in little or no polymerisation occurring. At higher UV intensities, it is expected that polymer would be produced over a larger range of rotational speeds as the additional energy available will partly balance the reduced exposure times. This would be a useful study. Other potential methods of overcoming fouling on the disc are the possibility of coating the reaction surface with some 'non-stick' material that would inhibit fouling even at higher viscosities, or alternatively manufacturing a reaction disc from such a material. The problem may however have been exaggerated in this study by the use of butyl acrylate because poly (butyl acrylate) is known to be softer and much tackier than either poly (ethyl acrylate) or poly (methyl

acrylate) even at room temperature [21]. The impact of changing the disc material, or coating it, on the heat transfer characteristics must be considered.

In this spinning disc reactor, the disc radius is 0.1m, which is considerably smaller than many of the spinning discs previously built and studied within the Chemical and Process Engineering Department at Newcastle University. Based upon the model discussed previously, Figure 9.1 illustrates the predicted effect of changing the disc size on the conversions achieved for a constant feed flowrate, cooling water flowrate, UV intensity and photo-initiator concentration. From these predictions it can be seen that a larger disc would be expected to produce higher conversions (due to the increased residence time) and that there may exist an optimum rotational speed. Figure 9.2 also shows the effect of increasing the disc radius but for a constant rotational speed. It can be seen that a radius will be reached beyond which the increase in conversion achieved will be negligible. There will also be a physical limitation on the size of the disc. In order to investigate this experimentally however, a new test facility would be required, which has the capacity to use discs of varying size, i.e. an interchangeable disc assembly would be required. A drawback of increasing the disc size for this polymerisation however, is the need for constant UV irradiation across the disc. An arrangement which allows irradiation of the whole disc from a UV source would be required, and the larger the disc the more difficult this would be.

9.3 Other Applications

Based upon the heat transfer characteristics of this reactor presented in Appendix A, the suitability for other strongly exothermic reactions is a possible area for future research, and it is recommended that a full heat transfer characterisation of the reactor is conducted. A potential exothermic reaction suitable for study in this system is sulphonation [105]. Industrially the sulphonation of linear alkyl benzene (LAB) is conducted using gaseous SO_3 diluted in oxygen in order to control the exotherm. The potential for the use of liquid SO_3 directly in this case is just one reaction that can be considered. This reactor may be suitable for the study of any fast exothermic reaction and a preliminary study on this has been completed [106].

A preliminary study on the use of the spinning disc reactor for neutralisation reactions, an industrially important example of mass transfer limited reactions, has also been completed [107]. The study concluded that the spinning disc reactor is suitable for this type of reaction, due to the promotion of micromixing on the disc.

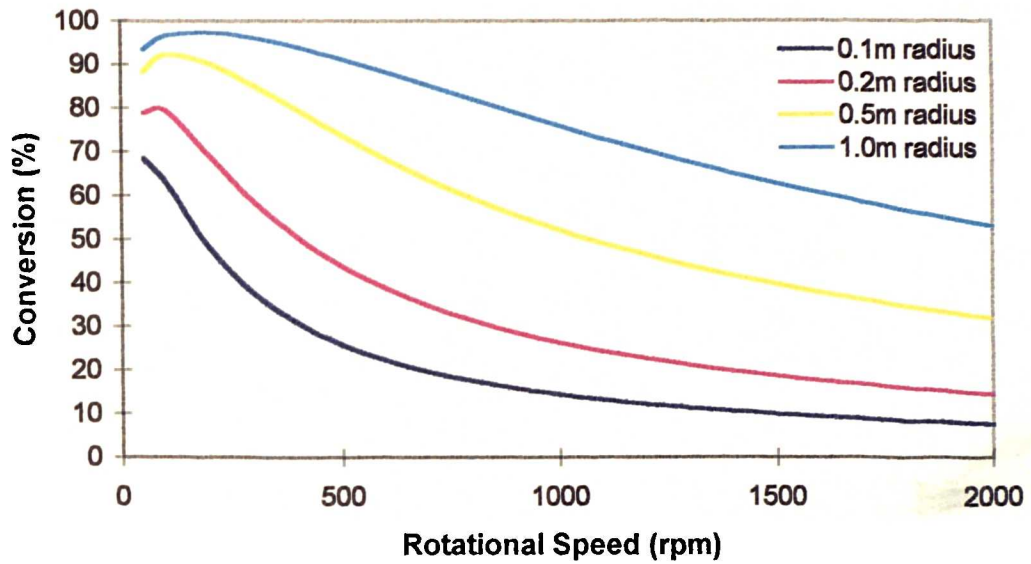


Figure 9.1. Predicted Effect of Increasing Disc Size on Conversion With Varying Rotational Speed.

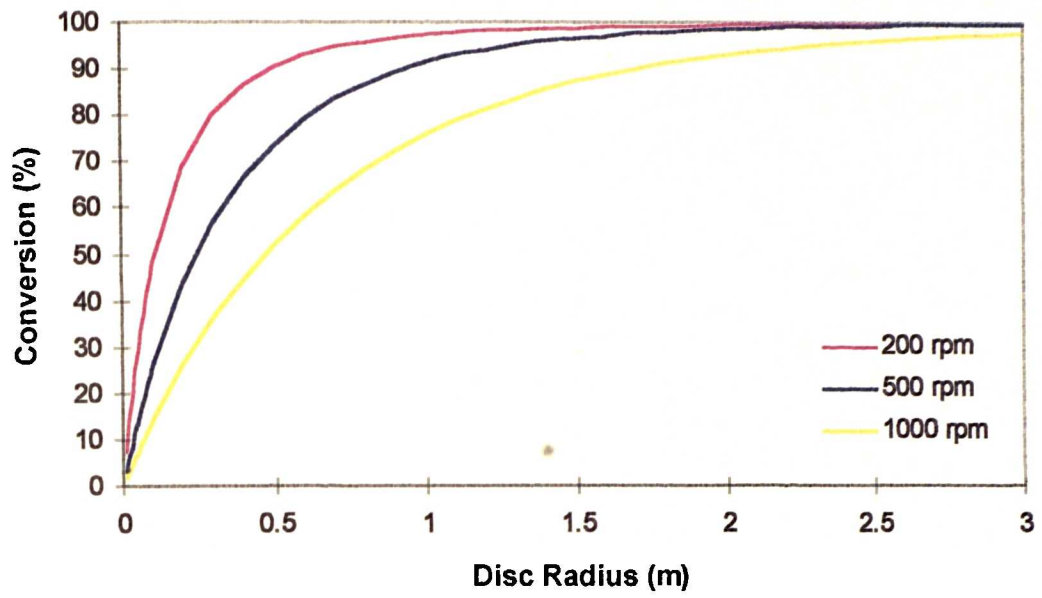


Figure 9.2. Predicted Effect of Increasing Rotational Speed on Conversion (With Disc Radius).

NOMENCLATURE

	Description	Units
ΔH	heat of reaction	kJ/mol
ΔT	temperature difference	$^{\circ}\text{C}$
[M]	monomer concentration	mol/L
[PI]	photo-initiator concentration	mol/L
A	heat transfer area	m^2
	or absorbance	(no units)
C	value used within calculation	(none)
c	speed of light	m/s
C_p	specific heat capacity	kJ/kgK
d	diameter	m
d_f	film thickness	m
d_h	hydraulic diameter	m
E_A	activation energy	kJ/mol
h	Planck's constant	erg.s
h_i	internal heat transfer coefficient	$\text{kW}/\text{m}^2\text{K}$
h_o	topside heat transfer coefficient	$\text{kW}/\text{m}^2\text{K}$
I	UV intensity	mW/cm^2
I	or initiator molecule	n/a
I_0	incident UV intensity	mW/cm^2
I_a	absorbed UV intensity	mW/cm^2
k	thermal conductivity	kW/mK

Nomenclature

k_i	initiation rate constant	L/mol.s
k_p	propagation rate constant	L/mol.s
k_t	termination rate constant	L/mol.s
L	$=\sqrt{(v/\omega)}$	None
m	mass flowrate	kg/s
M	denotes either monomer or molecule	(n/a)
M_n	number average molecular weight	kg/kmol
M_R	molecular mass	kg/kmol
M_w	weight average molecular weight	kg/kmol
Q	volumetric flowrate	m ³ /s
q	heat flux	kW
R•	radical species	(n/a)
R_p	rate of polymerisation	mol/Ls
S	sensitiser molecule	(n/a)
t	time	s
T	temperature	°C
U	overall heat transfer coefficient	KW/m ² K
V	velocity	m/s
x	radial distance	m

Greek Symbols

δ	thickness	m
ϵ	molar absorption coefficient	L/mol.cm
μ	dynamic viscosity	Ns/m ²

Nomenclature

ν	kinematic viscosity (μ/ρ)	m^2/s
ρ	density	kg/m^3
ω	radial acceleration	rad/s
λ	wavelength	m
ν	frequency	$/\text{s}$
δ_c	channel width	m
ν_i	rate of initiation	mol/Ls
ν_p	rate of propagation	mol/Ls
ν_R	rate of radical production	mol/Ls
ν_t	rate of termination	mol/Ls

Dimensionless Groups

Nu	Nusselt number
Pr	Prandtl number
Re	Reynolds number
Ta	Taylor number

Subscripts

act	actual
c	cold
h	hot
I	inlet
max	maximum
min	minimum

Nomenclature

o	outlet
pol	polymerisation
prop	propagation
1	thermocouple position: cooling water prior to inlet
2	thermocouple position: cooling water inlet
3	thermocouple position: cooling water outlet
4	thermocouple position: feed inlet
5	thermocouple position: feed outlet
6	thermocouple position: reactor atmosphere

Abbreviations

DMPA	dimethoxy phenol acetate
GPC	gel permeation chromatography
IR	infra-red
MEHQ	methyl ether hydroquinone
NTU	number of transfer units
THF	tetrahydrofuran
UV	ultra-violet

Definitions

(Unless indicated otherwise, all definitions are those given in The New Shorter Oxford English Dictionary [108].)

atactic	“having or designating a polymeric structure in which the repeating units have no regular configuration”
disproportionation	“a transfer of atoms or valency electrons between identical

Nomenclature

	atoms or ions so as to give dissimilar products”
homogeneity	“the quality or condition of being homogeneous, i.e. consisting of, or involving a single phase”
inhomogeneity	(also heterogeneity) “the property of being inhomogeneous, i.e. not uniform throughout; consisting of, or involving more than one phase”
isotactic	“having or designating a polymeric structure in which all the repeating units have the same stereochemical configuration”
photolysis	“decomposition or dissociation of molecules by the action of light; an instance of this”
photopolymerisation	“polymerisation brought about by the action of light”
quantum efficiency/yield	“the proportion of incident photons that are effective in causing photo-decomposition, photo-emission or similar photo-effect”
saturated	“(of an organic compound, molecule, group etc) having a structure containing the greatest number of hydrogen atoms, and hence having no multiple bonds between carbon atoms”
stereochemical	“pertaining to the branch of chemistry that deals with theoretical differences in the relative position in space of atoms in a molecule, in relation to differences in the optical and chemical properties of the substances”
syndiotactic	“having or designating a polymeric structure in which the repeating units have alternating stereochemical configurations”
unsaturated	“(of an organic compound, molecule, group etc) not saturated; having one or more multiple bonds”

REFERENCES

1. Ramshaw, C., (1993), The Opportunities for Exploiting Centrifugal Fields, *Heat Recovery Systems & CHP*, 13 (6), 493-513.
2. Mallinson, R. & Ramshaw, C., (1979), European Patent No. 2568B
3. Ramshaw, C. & Winnington, T., (1997), Rotex: an Intensified Absorption Heat Pump, 2nd Intl. Conference on Process Intensification in Practice, Antwerp, 63-68.
4. Ramshaw, C. & Winnington, T., (1986), European Patent No. 327230.
5. Zheng, C., Guo, K., Song, Y., Zhou, X., Ai, D., Xin, Z. & Gardner, N.C., (1997), Industrial Practice of HIGRAVITEC in Water Dearth, 2nd Intl. Conference on Process Intensification in Practice, Antwerp, 273-288.
6. Green, Andrew, (1998), Process Intensification: The Key to Survival in Global Markets?, *Chem. & Ind.*, 2 March 1998, 168-172.
7. Mercier, P. & Kouidri, F., (1997), Turbulent Flows Loaded with Particles in Compact Heat Exchangers - Application to Particulate Fouling, 2nd Intl. Conference on Process Intensification in Practice, Antwerp, 235-244.
8. Reay, D.A., (1994), Compact Heat Exchangers: A Review of Current Equipment and R&D in the Field, *Heat Recovery Systems & CHP*, 14 (5), 459-474.
9. Stonestreet, P., & Mackley, M.R., (1997), Evaluation of Oscillatory Flow Mixing in Tubular Reactors for Continuous Processing, 2nd Intl. Conference on Process Intensification in Practice, Antwerp, 245-264.
10. Edge, A.M., Pearce, I. & Phillips, C.H., (1997), Compact Heat Exchangers as Chemical Reactors for Process Intensification (PI), 2nd Intl. Conference on Process Intensification in Practice, Antwerp, 175-190.
11. Charlesworth, R.J., (1996), The Steam Reforming and Combustion of Methane on Micro-Thin Catalysts for use in a Catalytic Plate Reactor, PhD Thesis, University of Newcastle-upon-Tyne.

References

12. Boodhoo, K.V.K., Jachuck, R.J. & Ramshaw, C., (1997), Spinning Disc Reactor for the Intensification of Styrene Polymerisation, 2nd Intl. Conference on Process Intensification in Practice, Antwerp
13. Boodhoo, K., Dalgleish, J.C., Jachuck, R.J. & Ramshaw, C., (1997), Process Intensification: The Opportunity Presented by Spinning Disc Reactor Technology, 417-424.
14. Jachuck, R.J.J. & Ramshaw, C., (1995), Process Intensification: Spinning Disc Polymeriser, IChemE Research Event / First European Conference, Edinburgh.
15. Jachuck, R.J.J. & Ramshaw, C., (1994), Process Intensification: Heat Transfer Characteristics of Tailored Rotating Surfaces, Heat Recovery Systems & CHP, 14 (5), 475-491.
16. Jazayeri, A. (1981), The Hydrodynamics of Newtonian and Non-Newtonian Liquid Films Flowing Across a Rotating Disc, PhD Thesis, University of Newcastle-upon-Tyne.
17. Woods, W.P., (1995), The Hydrodynamics of Thin Liquid Films Flowing over a Rotating Disc, PhD Thesis, University of Newcastle-upon-Tyne.
18. Bell, C., (1975), The Hydrodynamics and Heat Transfer Characteristics of Liquid Films on a Rotating Disc, PhD Thesis, University of Newcastle-upon-Tyne.
19. Lim, S.T., (1980), Hydrodynamics and Mass Transfer Processes Associated with the Absorption of Oxygen in Liquid Films Flowing Across a Rotating Disc, PhD Thesis, University of Newcastle-upon-Tyne.
20. Boodhoo, K.V.K., (1999), Process Intensification: Spinning Disc Reactor for the Polymerisation of Styrene, PhD Thesis, University of Newcastle-upon-Tyne.
21. Kroschwitz, J.I. (Ed.), (1990), Acrylic & Methacrylic Ester Polymers, Concise Encyclopedia of Polymer Science & Engineering, Wiley-Interscience, 16-20.
22. Nicholson, J.W., (1991), The Chemistry of Polymers, The Royal Society of Chemistry, UK.
23. Odian, G., (1991), Principles of Polymerization, 3rd Edn, Wiley-Interscience, NY.

References

24. Saunders, K.J., (1988), *Organic Polymer Chemistry*, 2nd Edn, Chapman & Hall, NY.
25. Billmeyer, F.W. Jnr, (1984), *Textbook of Polymer Science*, 3rd Edn, Wiley-Interscience, NY.
26. Moad, G. & Solomon, D.H., (1995), *The Chemistry of Free-Radical Polymerization*, Elsevier Science Ltd, Oxford.
27. Dunk, W.A.E., (Feb. 14, 1997), *Application of a Novel Reactor for the Bulk Polymerisation of Reactive Monomers*, Confidential Report, Courtaulds Coatings.
28. Rudin, Alfred, (1982), *The Elements of Polymer Science & Engineering. An Introductory Text for Engineers & Chemists*, Academic Press Inc., USA.
29. Engler, D.A. and Maistrovich, A.R., (Sep. 22, 1987), *Continuous Process for Making Polymers having Pendant Azlactone or Macromolecular Moieties*, U.S. Patent No. 4,695,608.
30. Jacob, J., Chia, L.H.L. and Boey, F.Y.C., (1995), *Microwave Polymerization of Poly (Methyl Acrylate): Conversion Studies at Variable Power*, *J. Appl. Polym. Sci.*, 63 (6), 787-797.
31. Allen, G. (Ed), (1989), *Comprehensive Polymer Science Vol. 3 (1): Chain Polymerisation I*, Chapter 6, Pergamon Press, UK.
32. Allen, G. (Ed), (1989), *Comprehensive Polymer Science Vol. 3 (1): Chain Polymerisation I*, Chapter 1, Pergamon Press, UK.
33. Roffey, C.G., (1985), *Photopolymerization of Surface Coatings*, Chapter 1, John Wiley & Sons, Chichester.
34. Turro, N., (1978), *Modern Molecular Photochemistry*, Cummings Pu. Co.
35. Moore, W.J., (1972), *Physical Chemistry*, 5th Edn, Prentice Hall.
36. Atkins, P.W., (1995), *Physical Chemistry*, 5th Edn, Oxford University Press.
37. Decker, C., (1992), *Photo-Induced Polymerization - Kinetic Study of Ultrafast Processes Induced by UV Radiation or Lasers*, *Photochemistry and Polymeric Systems: Proceedings of Intl. Symposium*, Sept. 1992, Dublin, 32-46.

References

38. Decker, C. and Moussa, K., (1989), Real-Time Kinetic Study of Laser-Induced Polymerization, *Macromolecules*, 22, 4455-4462.
39. Decker, C., Bendaikha, T., Decker, D. & Zahouily, K., (1997), High Speed Polymerisation of Acrylate Monomers by UV Irradiation, *Polymer Preprints, Division of Polym. Chem, ACS*, 38 (1), 487-488.
40. Decker, C., (1984), UV Curing of Acrylate Coatings by Laser Beams, *J. Coatings Tech.*, 56 (713), 29-34.
41. Horie, K., Mita, I. And Kambe, H., (1968), Calorimetric Investigation of Polymerization Reactions I. Diffusion-Controlled Polymerization of Methyl Methacrylate and Styrene, *J. Polym. Sci. (Part A1)*, 6, 2663-2676.
42. Paul, S., (1996), *Surface Coatings Science & Technology*, 2nd Edn, John Wiley & Sons, Chichester.
43. Roffey, C.G., (1985), *Photopolymerization of Surface Coatings*, Chapter 3, John Wiley & Sons, Chichester.
44. Chinmayanandam, B.R. and Melville, H.W., (1954), Photosensitization of Polymerisation Reactions, *Trans. Farad. Soc.*, 50, 73-82.
45. Mahadevan, V. and Santappa, M., (1961), Vinyl Polymerization Photosensitisation by Uranyl Ions, *J. Polym. Sci.* 50, 361-377.
46. Pappas, S.P., (1981), Photoinitiators for Radical, Cationic and Concurrent Radical-Cationic Polymerization. A Personal Account, *Radiation Curing*, 8 (3), 28-35.
47. Mark, Herman, F., (1988), *Encyclopedia of Polymer Science & Engineering*, 2nd Edn, Vol. 11, John Wiley & Sons.
48. Ledwith, A., (1977), Photoinitiation of Polymerisation, *Pure & Appl. Chem.*, 49, 431-441.
49. Timpe, H-J., Ulrich, S., Decker, C. & Fuossier, J.P., (1993), Photoinitiated Polymerization of Acrylates and Methacrylates with Decahydroacridine-1,8-dione / Onium Salt Initiator Systems, *Macromolecules*, 26, 4560-4566.

References

50. Lissi, E.A., (1983), Photoinitiated Polymerisation: Effect of Initiator Absorbance, *J. Polym. Sci., Polym. Chem. Ed.*, 21, 2197-2202.
51. Lissi, E.A. and Zanocco, A., (1984), Photopolymerisation of Methyl Methacrylate by Benzoin Methyl Ether Irradiated as 366 nm: Effect of the Initiator Absorbance upon the Polymerisation Rate, *J. Polym. Sci., Polym. Letters Ed.*, 22, 391-393.
52. Hutchinson, J., & Ledwith, A., (1973), Mechanisms and Relative Efficiencies in Radical Polymerization Photoinitiated by Benzoin, Benzoin Methyl Ether and Benzil, *Polymer*, 14, 405-408.
53. Carlblom, L.H. & Pappas, S.P., (1977), Photoinitiated Polymerisation of Methyl Methacrylate and Methyl Acrylate with ¹⁴C-Labelled Benzoin Methyl Ethers, *J. Polym. Sci., Polym. Chem. Ed.*, 15, 1381-1391.
54. Meier, K., Rembold, M., Rutsch, W. & Sitek, F., (1986), New Results on Photoinitiators on Printing Inks and Clear Coatings, Radiation Curing of Polymers: Proceedings of Symposium of the NW Region of the Industrial Division of Roy. Soc. Chem., 196-208.
55. Oster, G. and Yang, N-L., (1968), Photopolymerization of Vinyl Monomers, *Chem. Rev.*, 68 (2), 125-151.
56. Roffey, C.G., (1985), Photopolymerization of Surface Coatings, John Wiley & Sons, Chichester.
57. Decker, C., (1983), Laser-Induced Polymerisation of Multifunctional Acrylate Systems, *Polym. Photochem.*, 3, 131-142.
58. Decker, C. and Jenkins, A.D., (1985), Kinetic Approach of O₂ Inhibition in Ultraviolet and Laser-Induced Polymerizations, *Macromolecules*, 18, 1241-1244.
59. Bolon, D.A. & Webb, K.K., (1978), Barrier Coats Versus Inert Atmospheres. The Elimination of Oxygen Inhibition in Free-Radical Polymerisations, *J. Appl. Polym. Sci.*, 22, 2543-2551.
60. Decker, C. and Moussa, K., (1987), Photopolymerization of Multifunctional Monomers in Condensed Phase, *J. Applied Polymer Sci.*, 34, 1603-1618.

References

61. Melville, H.W., (1938), The PhotoChemical Polymerisation of MethylAcrylate Vapour, Proc. Roy. Soc. (London), A167, 99-121.
62. Schultz, A.R. & Joshi, M.G., (1984), Kinetics of Photoinitiated Free-Radical Polymerisation, J. Polym. Sci., Phys. Ed., 22, 1753-1771.
63. Salim, M.S., (1990), Overview of UV Curable Coatings, Radiation Curing of Polymers II: Proceedings of 3rd Intl. Symposium of North West Region of the Industrial Division of the Royal Society of Chemistry, 3-21.
64. Knight, R.E., (1986), Areas of Application of UV Curing, Radiation Curing of Polymers: Proceedings of a Symposium of North West Region of the Industrial Division of the Royal Society of Chemistry, 1-11.
65. Martens, J.A., Clemens, L.M. and Zigman, A.R., (Jan. 1, 1980), Acrylic-Type Pressure Sensitive Adhesives by Means of Ultraviolet Radiation Curing, U.S. Patent No. 4,181,752.
66. Decker, C., (1984), Laser-Induced Polymerisation, ACS Symposium Series, 266, 207-223.
67. Decker, C., (1986), Laser Curing of Acrylic Coatings, Radiation Curing of Polymers: Proceedings of a Symposium of North West Region of the Industrial Division of the Royal Society of Chemistry, 16-31.
68. Holman, R. & Oldring, P., (1988), UV & EB Curing Formulation for Printing Inks, Coatings and Paints, SITA Technology, London.
69. Dunk, W.A.E., (Feb. 14, 1997), Photo-Initiation of Polymerisation by Free-Radical Mechanisms, Confidential Report, Courtaulds Coatings.
70. Hutchinson, R.A., Paquet, D.A. et al., (1995), The Application of Pulsed-Laser Methods for the Determination of Free-Radical Polymerisation Rate Coefficients, DECHEMA Monographs (5th Int. Workshop on Polymer Reaction Engng), 131, 467-492.
71. Lyons, R.A., Hutovic, J., Piton, D.I. et al., (1996), Pulsed-Laser Polymerization Measurements of the Propagation Rate Coefficient for Butyl Acrylate, Macromol., 29, 1918-1927.

References

72. Maeder, S. & Gilbert, R.G., (1998), Measurement of Transfer Constant for Butyl Acrylate Free-Radical Polymerisation, *Macromol.*, 31, 4410-4418.
73. Beuermann, S., Paquet, D.A.(Jr), McMinn, J.H. & Hutchinson, R.A., (1996), Determination of Free-Radical Propagation Rate Coefficients of Butyl, 2-Ethylhexyl and Dodecyl Acrylates by Pulsed-Laser Polymerisation, *Macromol.*, 29, 4206-4215.
74. Burnett, G.M. & Melville, H.W., (1947), Determination of the Velocity Coefficients for Polymerisation Processes. I. The Direct Photopolymerisation of Vinyl Acetate, *Proc. Roy. Soc. (London)*, A189, 457-480.
75. Melville, H.W. and Valentine, L., (1950), Rate Coefficients in the Polymerization of Styrene, *Trans. Farad. Soc.*, 46, 210-227.
76. Burrell, C.M., Majury, T.G. & Melville, H.W., (1951), A Dielectric Constant Method of Following the Non-Stationary State in Polymerisation. I. The Theory of the Method, *Proc. Roy. Soc. (London)*, A205, 309-322.
77. Majury, T.G. & Melville, H.W., (1951), A Dielectric Constant Method of Following the Non-Stationary State in Polymerisation. II. The Operation and Performance of the Instrument, *Proc. Roy. Soc. (London)*, A205, 323-335.
78. Majury, T.G. & Melville, H.W., (1951), A Dielectric Constant Method of Following the Non-Stationary State in Polymerisation. III. The Determination of Rates of Polymerisation and of Radical Lifetimes, *Proc. Roy. Soc. (London)*, A205, 496-516.
79. Olaj, O.F., Bitai, I. & Hinkelmann, F., (1987), The Laser-Flash-Initiated Polymerisation as a Tool of Evaluating (Individual) Kinetic Constants of Free-Radical Polymerisation. 2^a). The Direct Determination of the Rate Constant of Chain Propagation, *Makromol. Chem.*, 188, 1689-1702.
80. Davis, T.P. O'Driscoll, K.F., Piton, M.C. & Winnik, M.A., (1989), Determination of Propagation Rate Constants Using a Pulsed Laser Technique, *Macromol.*, 22, 2785-2788.

References

81. Olaj, O.F. & Schnöll-Bitai, I., (1989), Laser-Flash-Initiated Polymerisation as a Tool for Evaluating (Individual) Kinetic Constants of Free-Radical Polymerisation. 5. Complete Analysis by Means of a Single Experiment, *Eur. Polym. J.*, 25 (7/8), 635-641.
82. Hoyle, C.E., Chang, C.H. & Trapp, M.A., (1989), Laser-Initiated Polymerisation of Methyl Methacrylate: Effect of Pulse Repetition Rate and Photoinitiator Concentration on Polymerisation Efficiency, *Macromol.*, 22, 3607-3611.
83. Buback, M, Gilbert, R.G. et al., (1995), Critically Evaluated Rate Coefficients for Free-Radical Polymerisation. I: Propagation Rate Coefficient for Styrene, *Macromol. Chem. & Phys.*, 196, 3267-3280.
84. Material Safety Data Sheet: n-butyl acrylate, Sigma-Aldrich Chemicals.
85. Perry, Robert H., (1984), *Perry's Chemical Engineers Handbook*, 6th Edn, McGraw-Hill Chemical Engineering Series.
86. Ryan, C.F. and Gormly, J.J., (1963), Photopolymerisation Practical Details: Syndiotactic Poly (isopropyl acrylate), *Macromolecular Synthesis*, 1, 30-37.
87. Boutin, J. & Neill, J., (1977). German Patent, Gr. Offen. No. DE2716606.
88. Boutin, J., (1980), European Patent No. EP8246.
89. Kricheldorf, Hans R. (Ed), (1992), *Handbook of Polymer Synthesis Part A*, Marcel Dekker Inc., USA, 223-249.
90. Bizari, S., Schellenberg, T. & Ishikawa, Y., (Feb. 1998), Acrylic Acid & Esters, Marketing Report, *Chemical Economics Handbook*, (<http://www.cbrd.sriconsulting.com/CEH/>).
91. Allen, G. (Ed), (1989), *Comprehensive Polymer Science Vol. 3 (1): Chain Polymerisation I*, Chapter 5, Pergamon Press, UK.
92. Elliott, David J., (1995), *Ultraviolet Laser Technology and Applications*, Academic Press Inc., USA.
93. Muncaster, Roger, (1989), *A-Level Physics*, 3rd Edn, Stanley Thornes (Publishers) Ltd, UK, 487.

References

94. Lucas, H.J. and Pressman, D., (1938), Determination of Unsaturation in Organic Compounds, *Ind. Eng. Chem., Anal. Ed.*, 10 (3), 140-142.
95. Siggia, S., (1963), *Quantitative Organic Analysis via Functional Groups*, 3rd Ed., J. Wiley & Sons, 301-306.
96. Critchfield, F.E., (1959), Determination of Alpha, Beta-Unsaturated Acids and Esters by Bromination, *Anal. Chem.*, 31 (8), 1406-1408.
97. Leonard, E.C., (1970), *High Polymers Series*, 24: Vinyl and Diene Monomers Part 1, Wiley-Interscience, New York.
98. Brandrup, J., Immergut, E.H. & Grulke, E.A (Ed) (1998), *Polymer Handbook*, 4th Edn, John Wiley & Sons.
99. Wiley, R.H. and Brauer, G.M., (1948), Refractometric Determination of Second-Order Transition Temperatures in Polymers III. Acrylates and Methacrylates, *J. Polym. Sci.*, 3 (5), 647-651.
100. Mitchell, John Jnr, (1987), *Applied Polymer Analysis & Characterization: Recent Developments in Techniques, Instrumentation, Problem Solving*, Hanser, NY.
101. Pitts, D.R. & Sissom, L.E., *Schaum's Outline Series: Theory and Problems of Heat Transfer*, McGraw-Hill Book Co.
102. Montgomery, Douglas & Peck, Elizabeth, *Wiley Series in Probability & Mathematical Statistics: Introduction to Linear Regression Analysis*, John Wiley & Sons, Chichester.
103. Lindley, D.V. & Scott, W.F., (1984), *New Cambridge Elementary Statistical Tables*, Cambridge University Press, UK.
104. Kern, Donald Q., (1965), *Process Heat Transfer*, McGraw-Hill Chemical Engineering Series (International Editions).
105. Herman de Groot, W., (1991), *Sulphonation Technology in the Detergent Industry*, Kluwer Academic Publishers, Netherlands.
106. O'Brien, John, (1997), *Fast Exothermic Reactions on a Spinning Disc Reactor*, MEng Dissertation, Dept. of Chemical & Process Engineering, University of Newcastle-upon-Tyne.

References

107. Louche, Christophe, (1998), Dynamics of Spinning Disc Neutralisation Reactors, Erasmus Student Report, Dept. of Chemical & Process Engineering, University of Newcastle-upon-Tyne.
108. Brown, Lesley (Ed.), (1993), The New Shorter Oxford English Dictionary, Volumes 1 & 2, Clarendon Press, Oxford.
109. Coulson, J.M & Richardson, J.F., (1990), Chemical Engineering Volume 1: Fluid Flow, Heat Transfer and Mass Transfer, 4th Edn, Pergamon Press, UK.

APPENDIX A

PRELIMINARY HEAT TRANSFER STUDY

A.1 Introduction

This appendix contains the results of the preliminary heat transfer study conducted on the spinning disc reactor. Previous work conducted on spinning discs (refer to Chapter 1) presents a correlation for the heat transfer coefficient achieved from the top surface of a spinning disc. This reactor, however, is the first spinning disc with an internal cooling system built at Newcastle University and the heat transfer coefficient of this disc assembly was unknown. This study investigates the effect of five variables on the heat transfer performance of the reactor, quantified by the overall heat transfer coefficient (U value). The U value is an essential characteristic for any piece of heat transfer equipment when considering the viability of an exothermic reaction and the results of this study provide a useful indication of the suitability of this SDR for these types of reaction.

The variables considered were; rotational speed, cooling water flowrate, feed flowrate, feed temperature, and channel width. Both rotational speed and feed flowrate affect the flow characteristics across the reaction surface of the disc whereas cooling water flowrate and channel width affect the internal flow characteristics of the disc assembly. Temperature was not expected to affect the U value and several temperatures were tested to investigate this. Rotational speed was easily controlled using the variable speed motor, and both cooling water and feed flowrates were easily adjusted via the respective rotameters. Feed temperature was maintained, and adjusted, by means of a temperature controlled water bath. The channel width for cooling water flow was varied by means of purpose made spacers, providing three different widths, and was adjusted by a relatively simple procedure involving the removal of the top disc.

A.2 Treatment of Results

The raw data files produced by the data logging software were imported into MSExcel and the temperature profile of the trial was checked to ensure that conditions were as

close to steady-state as possible. An example profile is shown in Figure A.1. Average values of the temperatures over this steady state period were taken, and the relevant temperature differences calculated. The six temperatures measured were: T_1 - cooling water prior to inlet; T_2 - cooling water inlet, T_3 - cooling water exit, T_4 - feed inlet, T_5 - feed exit and T_6 - atmosphere. The two required temperature differences were calculated from Equations (A1) and (A2), where ΔT_e is the external temperature difference (feed) and ΔT_i is the internal temperature difference (cooling water).

$$\Delta T_e = T_4 - T_5 \quad (\text{A1})$$

$$\Delta T_i = (T_3 + (T_2 - T_1)) - T_2 = T_3 - T_1 \quad (\text{A2})$$

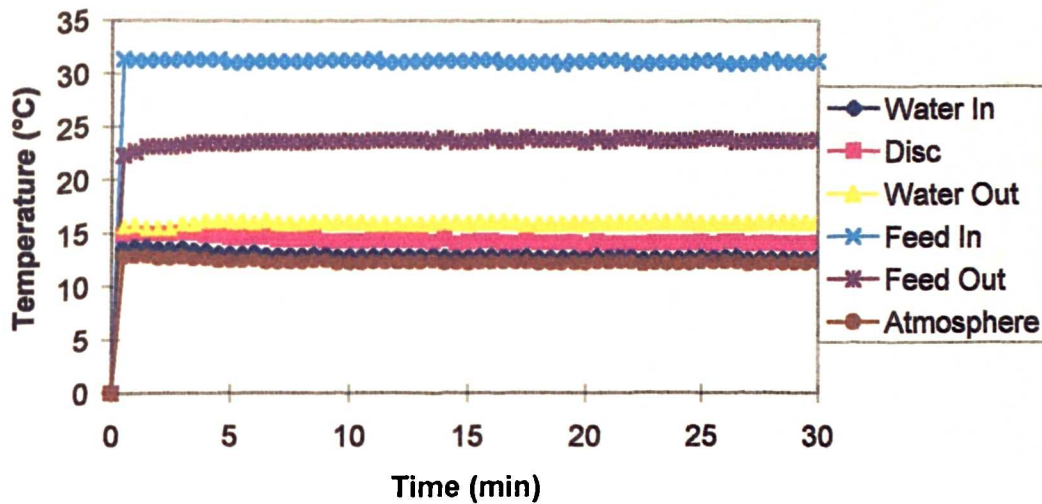


Figure A.1. Example Temperature Profile for Heat Transfer Study.

A.2.1 Heat Balance

Figure A.2 shows a schematic representation of the system under study. A heat balance on this system considers that the heat removed from the feed stream must be equal to the heat gained by the system, which although mainly by the cooling water system, could also be by the atmosphere inside the reactor housing. A thermocouple was positioned to monitor this ambient temperature. Under conditions of steady-state, the

ambient temperature in the reactor housing was always found to be constant and very close to the ambient temperature outside the reactor, effectively eliminating the consideration of heat transfer to atmosphere from the heat balance. Therefore, in an ideal system, the heat gained by the cooling water must be equal to the heat lost by the feed stream (Equation A3). Allowing for experimental errors, and the difficulty in achieving an ideal system, a 10 % error in the heat balance was deemed acceptable. Any results outside this acceptable margin of error were excluded from the following calculations and analysis.

$$\dot{m}_h C_{ph} \Delta T_e = \dot{m}_c C_{pc} \Delta T_i \quad (\text{A3})$$

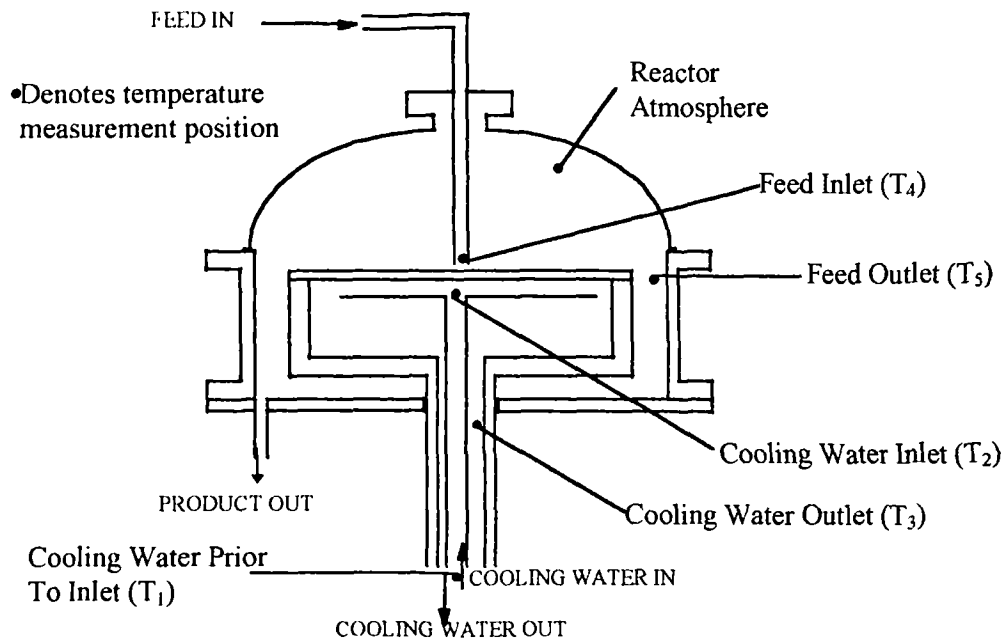


Figure A.2. Schematic Representation of System for Heat Balance Purposes.

A.2.2 Calculation of Overall Heat Transfer Coefficient (U Value)

The overall heat transfer coefficient was calculated using a correlation for heat exchanger effectiveness for a parallel flow single pass heat exchanger [101]. The effectiveness is calculated from Equation (A4) using Equations (A5) and (A6) to calculate the actual and maximum possible heat transfer (q_{act} and q_{max}) respectively.

$$\varepsilon = \frac{\text{actual heat transfer}}{\text{maximum possible heat transfer}} = \frac{q_{\text{act}}}{q_{\text{max}}} \quad (\text{A4})$$

$$q_{\text{act}} = \dot{m}_h C_{ph} \Delta T_o \quad (\text{A5})$$

$$q_{\text{max}} = \dot{m}_h C_{ph} \Delta T_{\text{max}} \quad \text{where} \quad \Delta T_{\text{max}} = \text{feed inlet } (T_4) - \text{cooling water inlet } (T_2) \quad (\text{A6})$$

The number of transfer units (NTU) was then calculated from Equation (A7) using Equation (A8) to calculate C.

$$\varepsilon = \frac{1 - \exp[-NTU(1 + C)]}{1 + C} \quad (\text{A7})$$

$$C = \frac{C_{\text{min}}}{C_{\text{max}}} = \frac{\dot{m}_h C_{ph}}{\dot{m}_c C_{pc}} \quad (\text{A8})$$

From this value of NTU and Equation (A9) the overall heat transfer coefficient, U can be calculated.

$$NTU = \frac{UA}{C_{\text{min}}} \quad (\text{A9})$$

The correlation adopted here refers to a parallel flow single pass heat exchanger, which does not fully describe the flow in this system. The section of flow of interest (along the underside of the disc) is close to parallel flow, although the flow area is constantly changing with radial distance (see Figures A3 and A4), and ideally the cooling water temperature would be measured at the outer edge of the disc. Physically, this was not possible due to the nature of the rotating hollow disc assembly, and therefore the flow from here to the outlet (located some distance down the drive shaft) cannot be described as parallel flow. This is recognised as a limitation of this approach and should be taken into consideration in further heat transfer characterisation of this reactor system.

A.2.3 Calculation of Reynolds Number

When considering heat transfer involving fluid flow, the characteristics of the flow are very influential in determining the heat transfer coefficient. Reynolds number is an essential indication of fluid flow characteristics and the heat transfer coefficient is dependent upon this. Therefore, a study of the Reynolds numbers under the various flow conditions tested is included in order to develop an understanding of the fluid flow characteristics.

Figure A.3 illustrates the flow inside the disc assembly. More detailed engineering drawings can be found in Appendix B and a detailed description of the test facility is contained in Chapter 4. The flow can be considered to be flow in a closed channel and as is illustrated in Figure A.4, the flow area is constantly changing with the increasing radial distance from the inlet, although the volumetric flowrate is constant. There will be a corresponding decrease in the velocity of the fluid as it flows towards the outer edge of the disc and hence the Reynolds number will also be greatest towards the centre, decreasing towards the outer edge. An average value of Reynolds number for each set of conditions has therefore been calculated and used to illustrate changes in Reynolds number with changing conditions.

Figure A.6 shows the variation in internal Reynolds number across the disc with varying cooling water flowrate. The radial distances range from 0.02 m to 0.09 m (and not 0 to 0.1 m) to account for the area at the centre of the disc where the fluid enters and the flow is established. This also accounts for the exit of the water internally being less than the disc radius due to the thickness of the dish assembly. The full range of cooling water flowrates used in the studies is shown in Figure A6, and it is clear that the Reynolds number is higher at the centre and decreases, as expected, with the decreasing velocity across the disc. The values of Reynolds number calculated range from 50 to 2700, dependent upon the volumetric flowrate and radial distance across the disc. The estimation of Reynolds number is based upon flow in a closed rectangular channel (at any radial point) and the corresponding laminar-turbulent-flow transition values vary from 1900-2800 [85]. From this, it would appear that the flow inside the disc is mainly in the laminar region.

Re_e , i.e. external Reynolds number (for the reaction surface of the disc) was calculated from Equation (A10) [18] for all feed flowrates tested.

$$Re_e = \frac{Q}{xv} \quad (A10)$$

Changes in individual film heat transfer coefficients for the disc surface under varying conditions of flow and rotational speed were estimated using the correlation for Nusselt number given in Equation (A11).

$$Nu = 10^{-2} \left(\frac{Re^2}{Ta} \right)^{1/3} R^{3/2} Pr^2 \quad (A11)$$

where $Nu = \frac{hL}{k}$ and $L = \sqrt{\frac{v}{\omega}}$

Again, values were calculated at intervals across the disc and an average value taken.

Re_i , i.e. internal Reynolds number for the disc, was calculated from Equation (A12).

$$Re_i = \frac{\rho v d}{\mu} = \frac{v d_h}{\nu} \quad (A12)$$

The assumption was made that at any radial point inside the disc, the flow was similar to flow in a closed rectangular channel. The hydraulic diameter (d_h) was calculated from Equation (A13) [85] and velocity calculated from Equation (A14).

$$d_h = 4r_h = 4 * \left(\frac{\text{cross - sectional area of flow}}{\text{wetted perimeter}} \right) \quad \text{where:}$$

cross - sectional area of flow = circumference of circle of radius x * channel width
Wetted perimeter = 2 * (circumference of circle of radius x + channel width) (A13)

i.e.

$$d_h = 4 * \left(\frac{2\pi x \delta_c}{2(2\pi x + \delta_c)} \right) = 4 * \left(\frac{\pi x \delta_c}{2\pi x + \delta_c} \right)$$

$$v = \frac{Q}{A} = \frac{Q}{2\pi r \delta_c} \quad (\text{A14})$$

The internal heat transfer coefficient was estimated from the correlation for Nu with laminar flow [109] given in Equation (A15).

$$\text{Nu} = 1.66 \left(\text{Re} \text{Pr} \frac{d}{l} \right)^{1/3} \quad (\text{A15})$$

where $\text{Re} \text{Pr} \frac{d}{l} > 12$

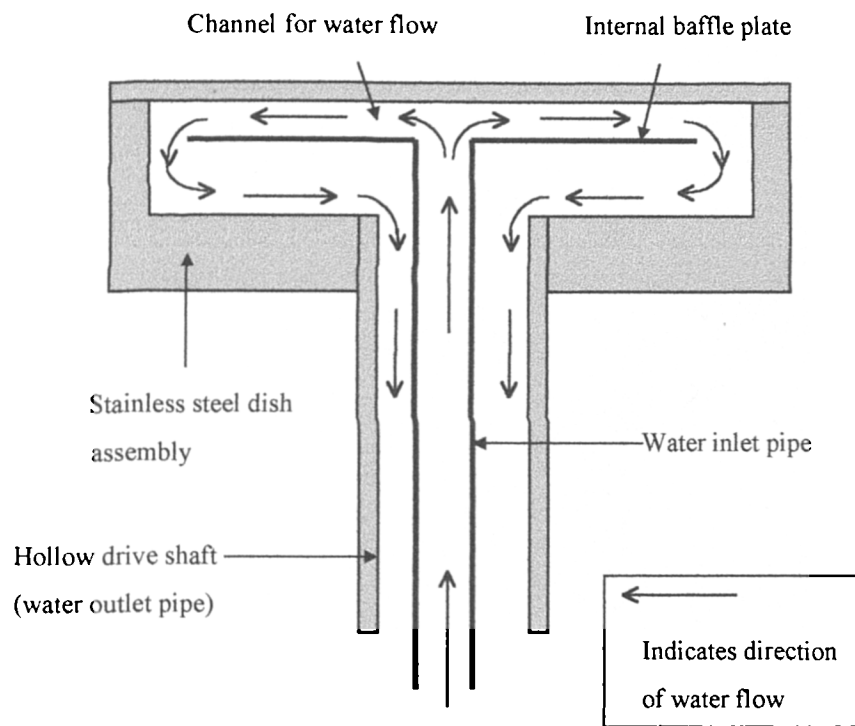


Figure A.3. Schematic Diagram to Show Flow Inside the Disc (Cross Section).

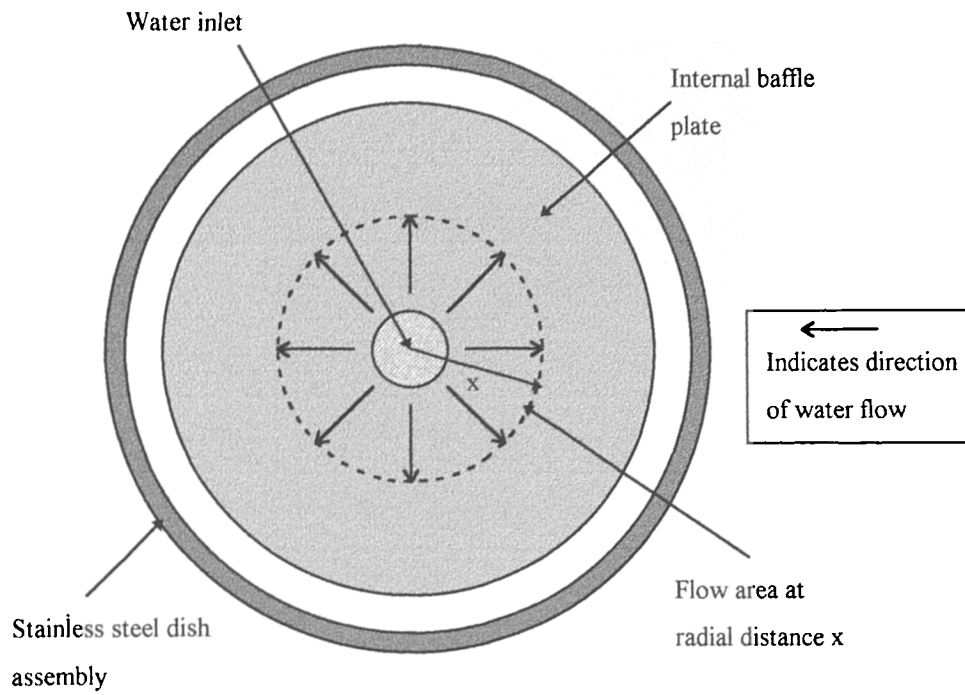


Figure A.4. Schematic to Show Flow Inside the Disc (Top View with Reaction Disc Removed).

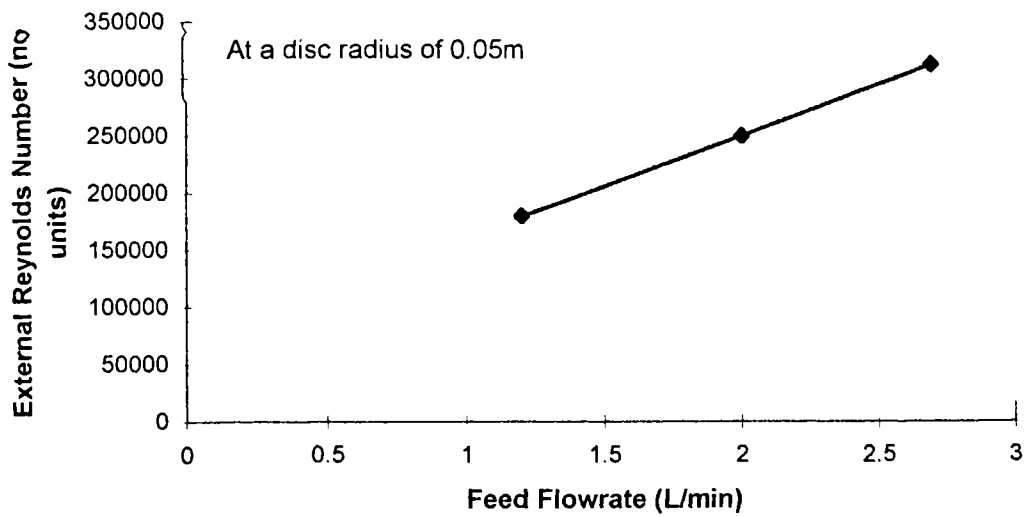


Figure A.5. Variation in External Reynolds Number with Feed Flowrate

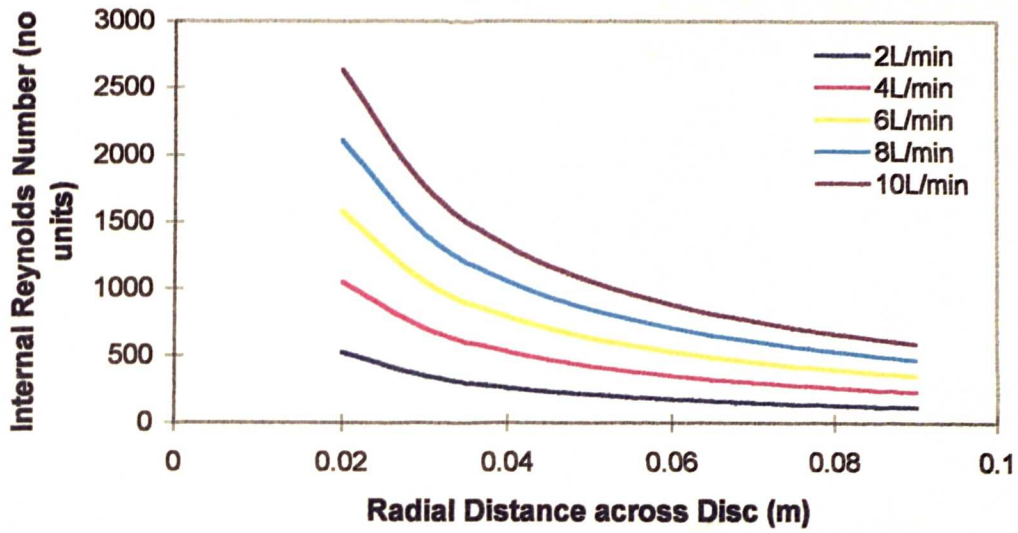


Figure A.6. Variation in Internal Reynolds Number with Cooling Water Flow.

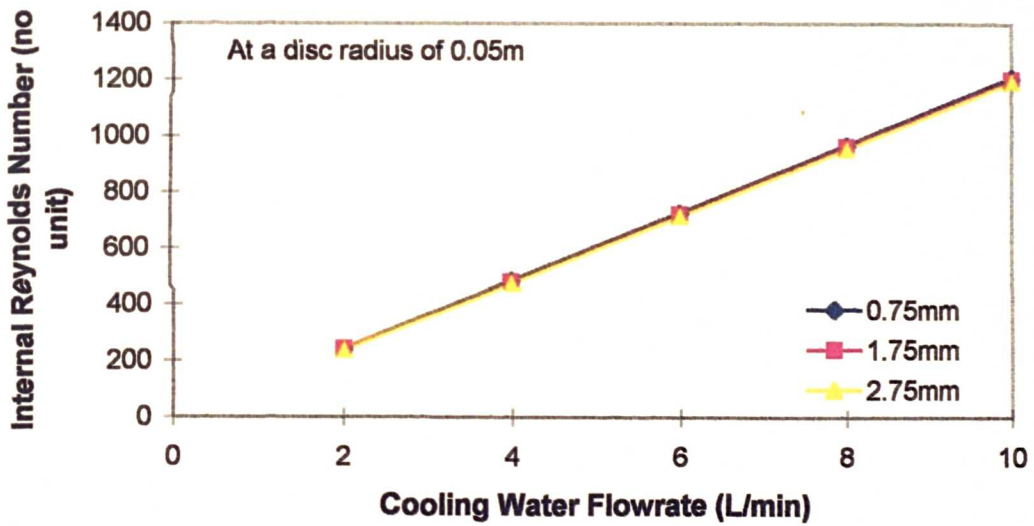


Figure A.7. Effect of Channel Width on Internal Reynolds Number.

A.3 Results and Discussion

A.3.1 Rotational Speed

Figure A.8 shows the effect of rotational speed on the experimental U value. No change in U value with increasing rotational speed is apparent. The calculation of internal Reynolds number does not account for rotational speed, but is determined mainly by the velocity of the cooling water flow inside the disc. If we consider the individual heat transfer coefficients then we find that the internal coefficient is the limiting value in the determination of the U value. This can be illustrated by considering the flow characteristics inside the disc, the associated Reynolds number indicating that the flow is in the laminar regime. Using the laminar flow correlation for Nu given in Equation (A15), h_i is estimated to be 1.6 kW/m²K for a cooling water flowrate of 2 L/min, increasing to 2.7 kW m²K for a cooling water flowrate of 10 L/min. Therefore we would expect h_i to be the limiting film coefficient and hence changes in rotational speed, which affect h_o only, would not show a significant influence on the *overall heat transfer coefficient*. Further consideration of the effect of rotational speed at higher cooling water flowrates, where h_i may be less of a limiting value would be of interest in a full heat transfer characterisation of the SDR.

The conclusion drawn from this is that over the range tested, rotational speed shows no obvious effect on the heat transfer characteristics. It may however play a larger part at higher cooling water flowrates where the flow inside the disc is in the turbulent regime.

A.3.2 Feed Flowrate

Figure A.9 shows the effect of the feed flowrate on the experimental U value. The U value calculated can be seen to increase with increasing feed flowrate, the increase being more significant at a higher cooling water flowrate. Although the feed flowrate does not affect the conditions inside the disc assembly, it controls the flow conditions across the disc, which therefore affects the overall heat transfer coefficient of the disc assembly. Although it has been discussed previously that the internal heat transfer coefficient will be the limiting value, the increase in feed flowrate shows significant

changes in h_o while h_i remains constant for a given cooling water flowrate. This change in h_o with feed flowrate is closely related to the corresponding change in Re across the disc which is illustrated by Figure A.5. The change in U value is noticeably higher at higher cooling water flowrate, and this indicates that as the internal Reynolds number is increased, then h_i becomes less of a limiting value and changes in the flow characteristics across the disc (e.g. feed flowrate), which affect h_o , will show more influence on the U value as h_i increases.

The conclusion drawn from this is that feed flowrate has a significant effect on the U value, which can be explained by changes in the external Reynolds number.

A.3.3 Cooling Water Flowrate

Figure A.10 shows the effect of the cooling water flowrate on the experimental U value. An increasing trend in U value with flowrate can clearly be seen. If we consider the associated change in internal Reynolds number (Figure A.6) then it can be seen that this trend is similar to the change in Reynolds number with increasing flowrate. These results are as expected, increasing the flowrate increases the capacity for heat transfer, resulting in higher U values.

The conclusion drawn from this is that cooling water flowrate shows a significant effect on the heat transfer characteristics, as expected.

A.3.4 Channel Width

Figure A.11 shows the effect of channel width on the experimental U value. A very gradual (but not significant) decrease in U value with increasing channel width can be seen over the range studied. This trend was apparent in all the cooling water flowrates studied (of which two are shown in Figure A.11). If we consider the effect of channel width on the internal Reynolds number we see only a very small, almost unnoticeable change with increasing channel width (Figure A.7). The effect of increasing the channel width is to decrease the velocity, but the magnitude of the width in comparison to the circumference at any given radial distance on the disc is small, which accounts for the very small changes observed.

The conclusion that can be drawn from this is that very little change in U value is observed with increasing channel width.

A.3.5 Feed Temperature

Figure A.12 shows the effect of the feed temperature on the experimental U value. Very little change in U value with increasing temperature over the range tested can be seen. If we consider the effect of temperature on the Reynolds number for a water system such as this we find, $Re \propto \frac{\rho}{\mu} \left(\text{or } \frac{1}{\nu} \right)$. As temperature increases both the density and viscosity (and hence the kinematic viscosity) of the system decrease, which would lead to an increase in Reynolds number. However, under the experimental conditions studied the change in kinematic viscosity is negligible, and the corresponding increase in Reynolds number can also be considered negligible. We would not therefore expect to see a change in U value with temperature in this case. For larger temperature ranges and/or other systems the changes in Reynolds number may not be negligible and each system must be considered according to its conditions.

The conclusion drawn from this is that over the temperature range studied, and for a water system, no change in U value with temperature was identified.

A.4 Conclusions

The preliminary study of the heat transfer capability of this SDR shows that U values of up to 9 kW m²K can be achieved, dependent upon operational conditions.

In the case of all the variables studied, the trend (or lack of one) in U value closely resembles the trend in Reynolds number, confirming that the heat transfer capacity is closely related to the flow characteristics (as quantified by Reynolds number).

Over the variable ranges studied, cooling water flowrate and feed flowrate were found to have marked effects on the U value achieved, whereas rotational speed, channel width and feed temperature showed very little or no effect.

This study gives an indication of the suitability of this SDR for applications involving exothermic reactions, and highlights areas of possible interest for a full heat transfer characterisation, using different heat transfer media and conditions.

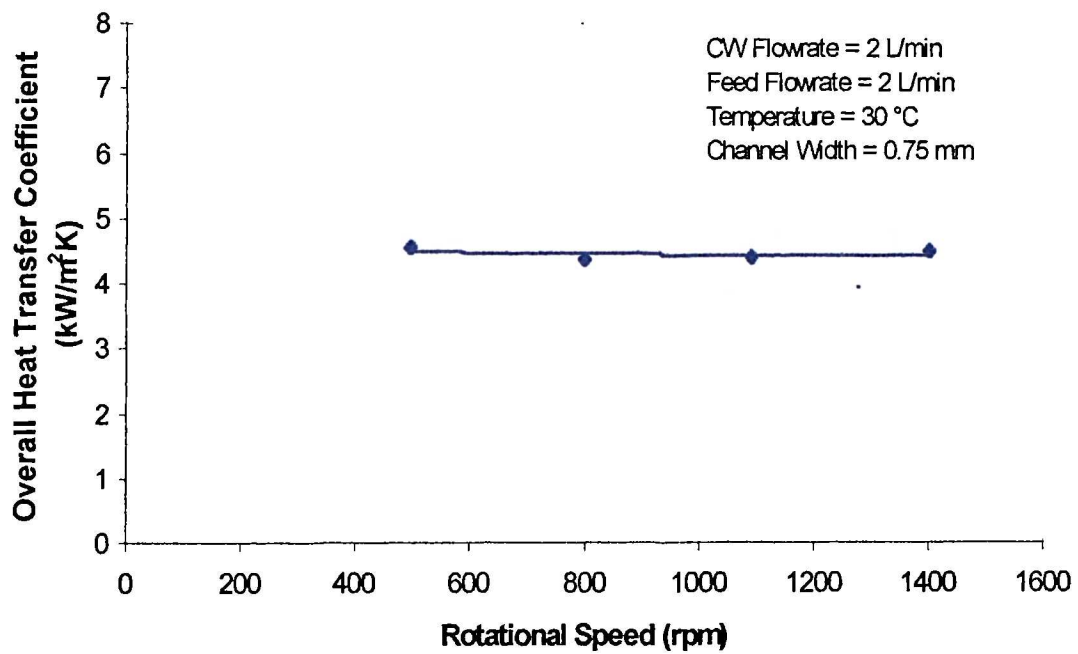


Figure A.8. Effect of Rotational Speed on the U Value.

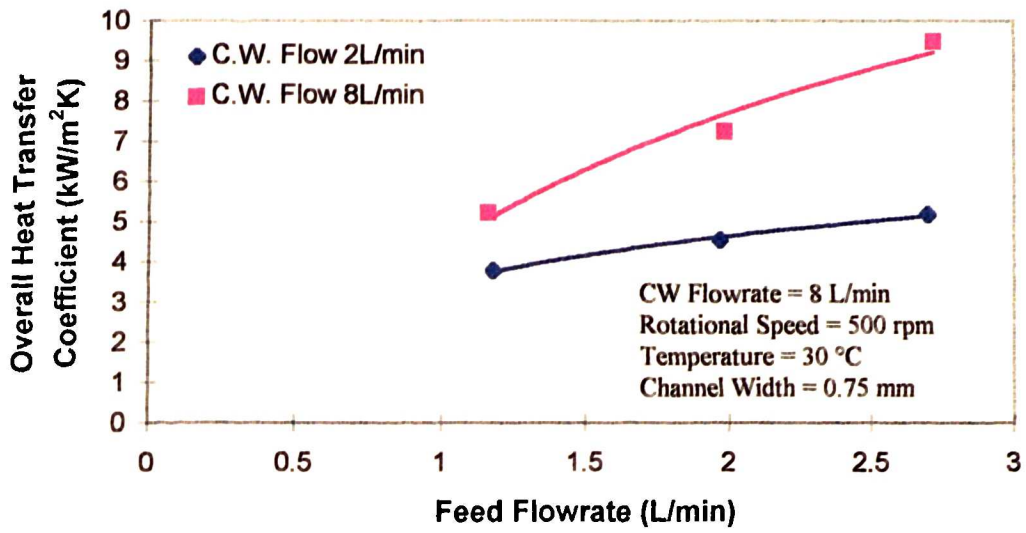


Figure A.9. Effect of Feed Flowrate on the U Value.

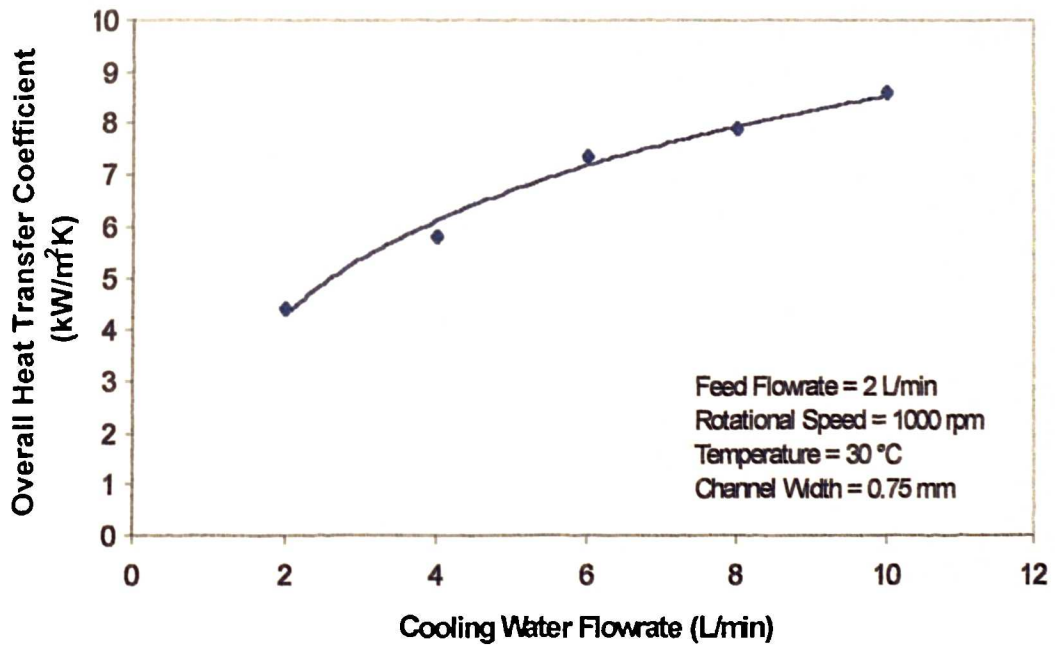


Figure A.10. Effect of Cooling Water Flowrate on the U Value.

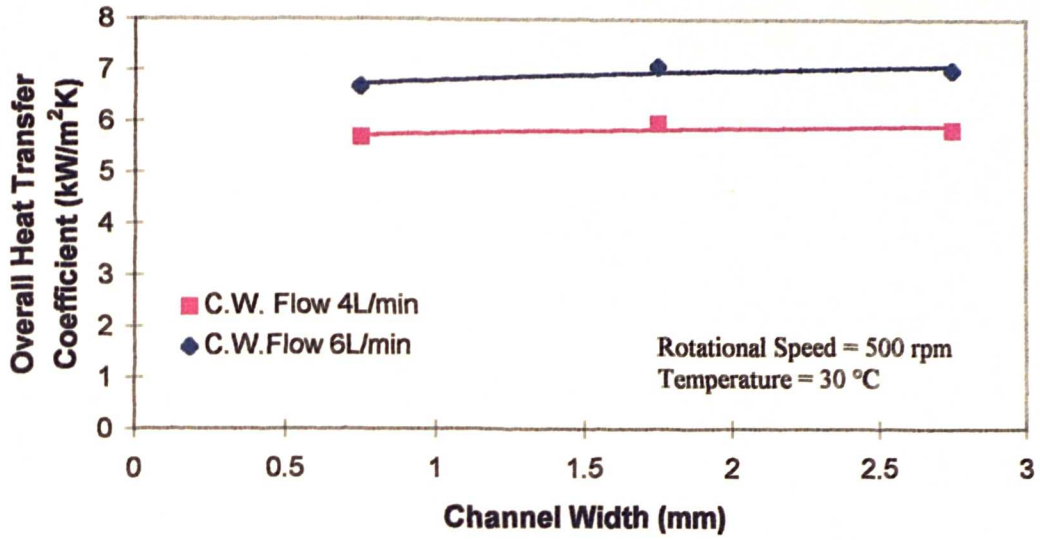


Figure A.11. Effect of Channel Width on the U Value.

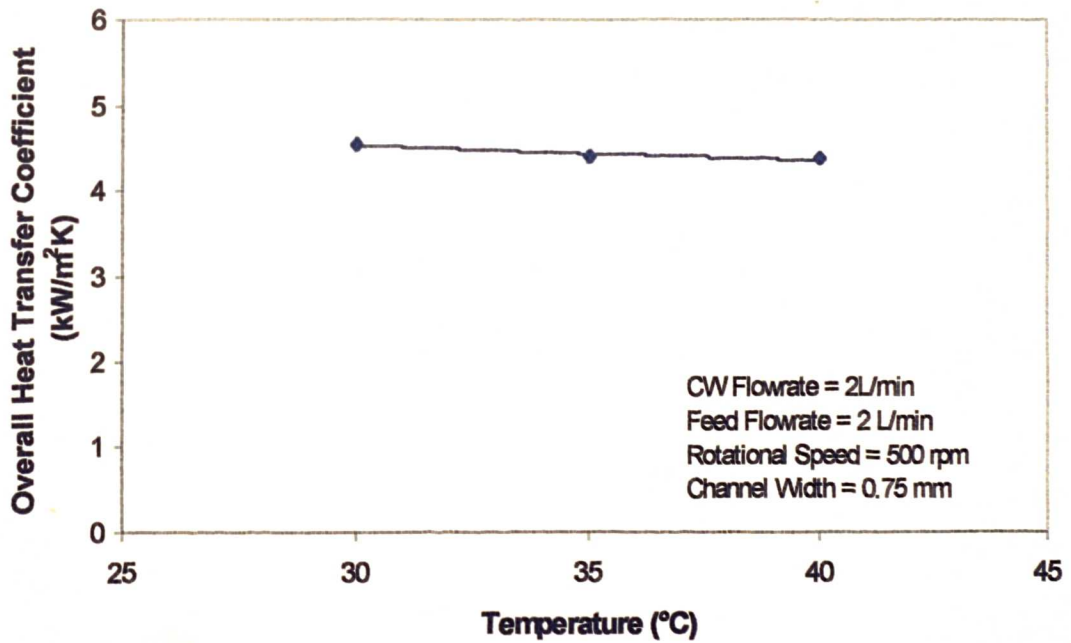
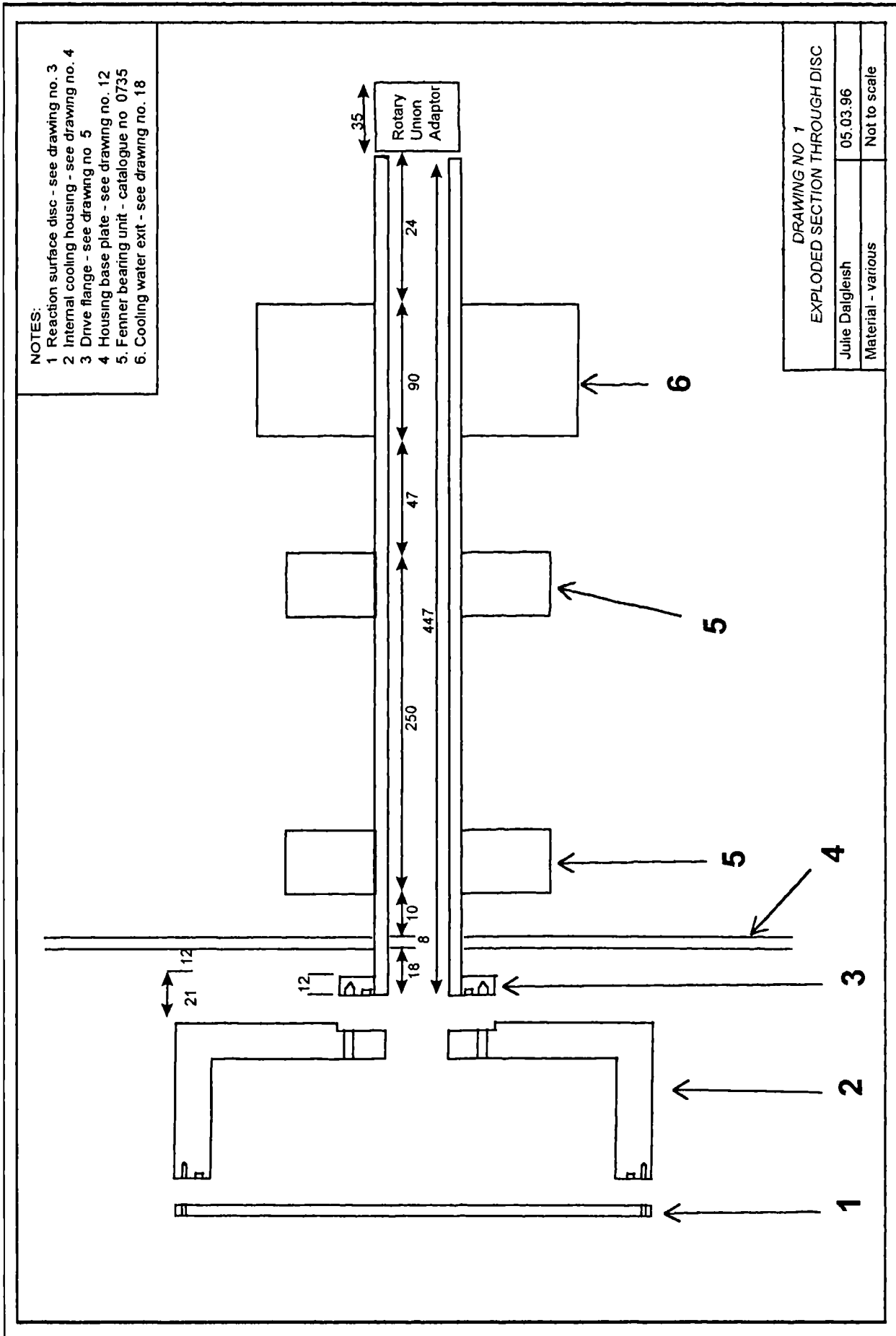


Figure A.12. Effect of Temperature on the U Value.

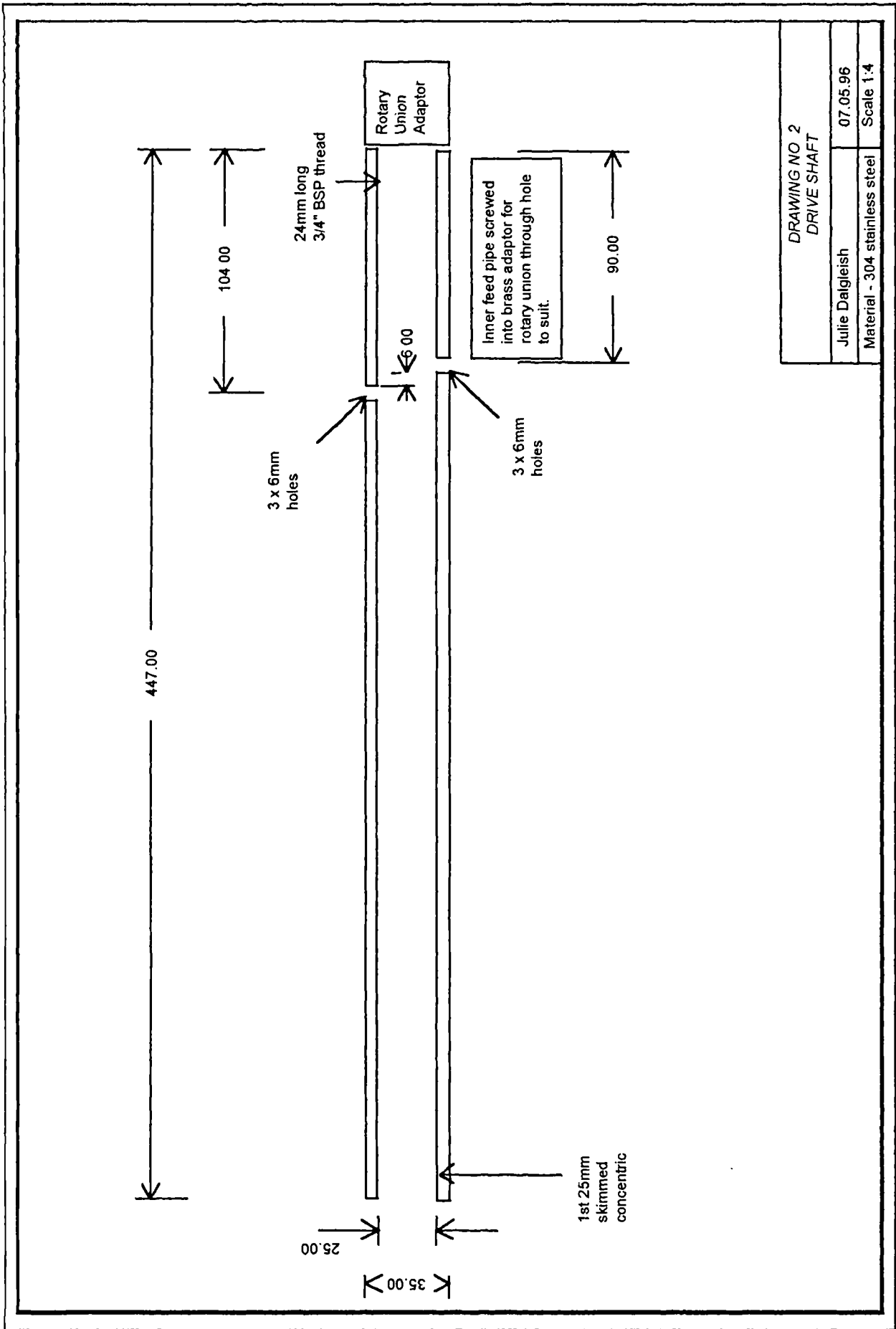
Appendix B

ENGINEERING DRAWINGS

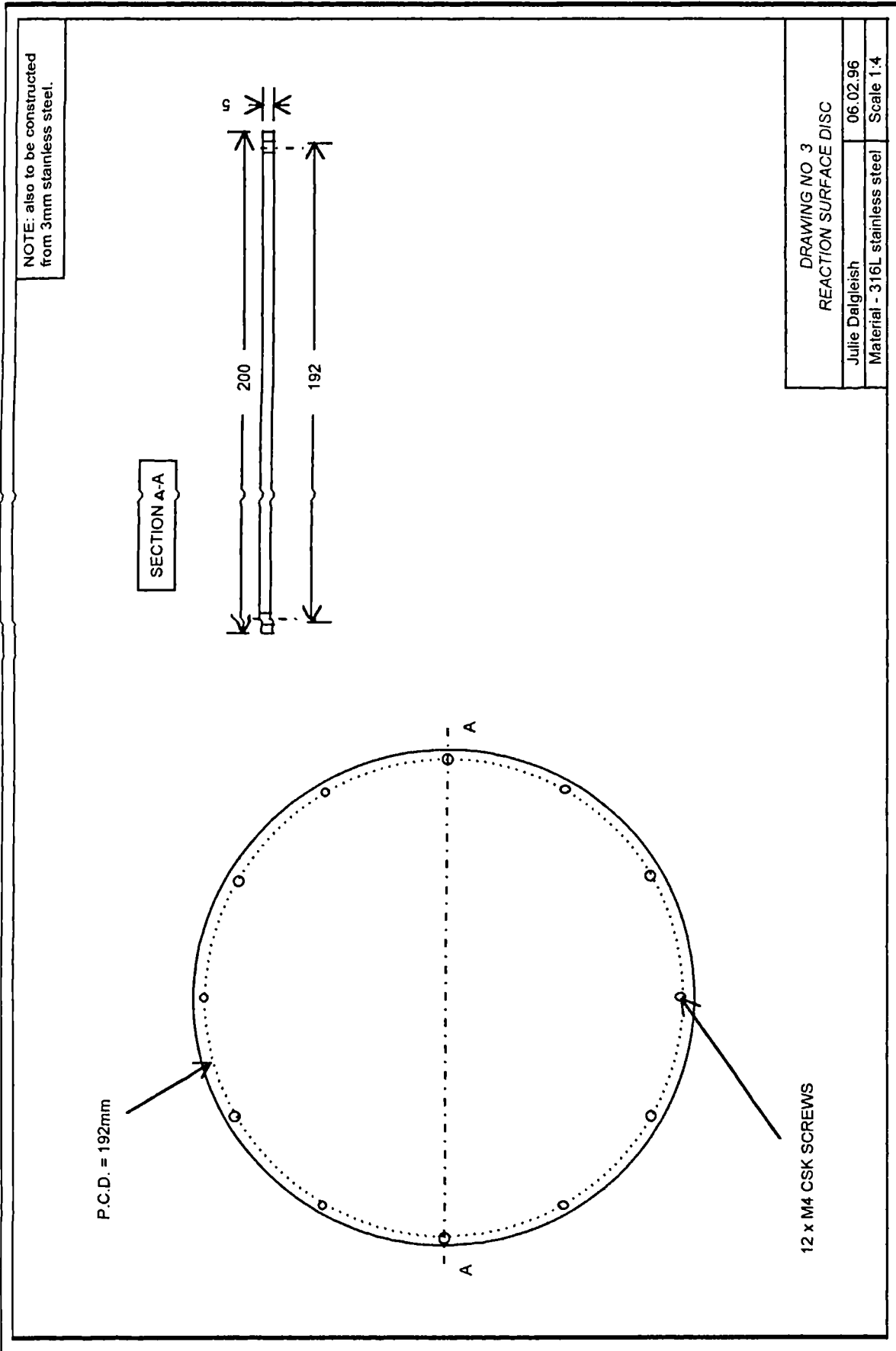
Drawing No.	Description	Page No
1	Exploded section through disc	149
2	Drive shaft	150
3	Reaction surface disc	151
4	Internal cooling housing	152
5	Drive flange	153
6	Exploded section of housing	154
7	External exchanger top flange	155
8	External exchanger base flange	156
9	External exchanger base flange (2)	157
10	External exchanger wall	158
11	External exchanger wall (no coils)	159
12	Housing base plate	160
13	External exchanger (no coils)	161
14	Feed system	162
15	Feed system (2)	163
16	Cooling water entry	164
17	Water entry - weir and collar	165
18	Cooling water exit	166
19	Framework for rig	167
20	Framework for rig (2)	168
Figure 4.7	Calibration Curve for Intensity with Lamp Distance	169

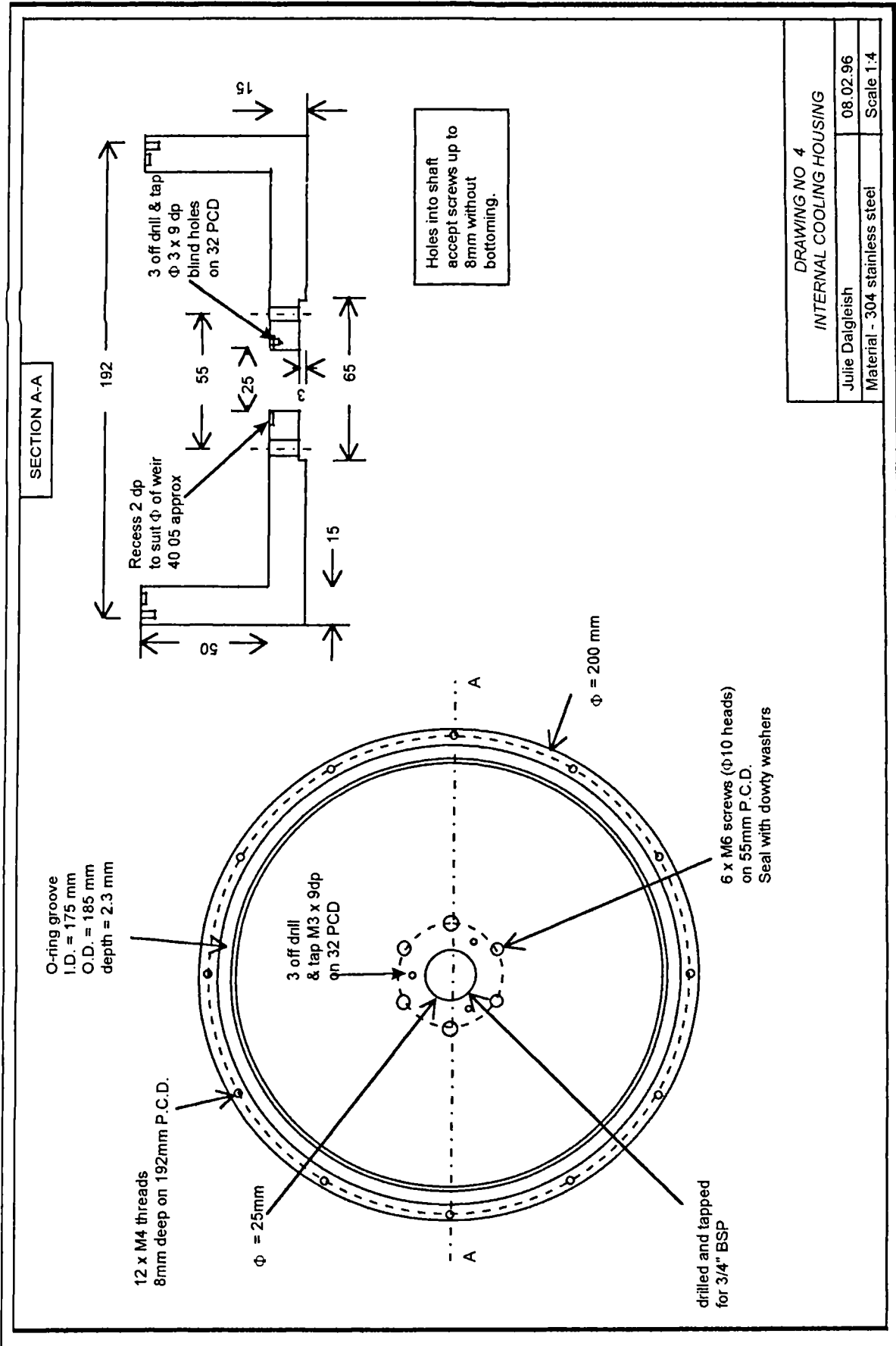


Appendix B

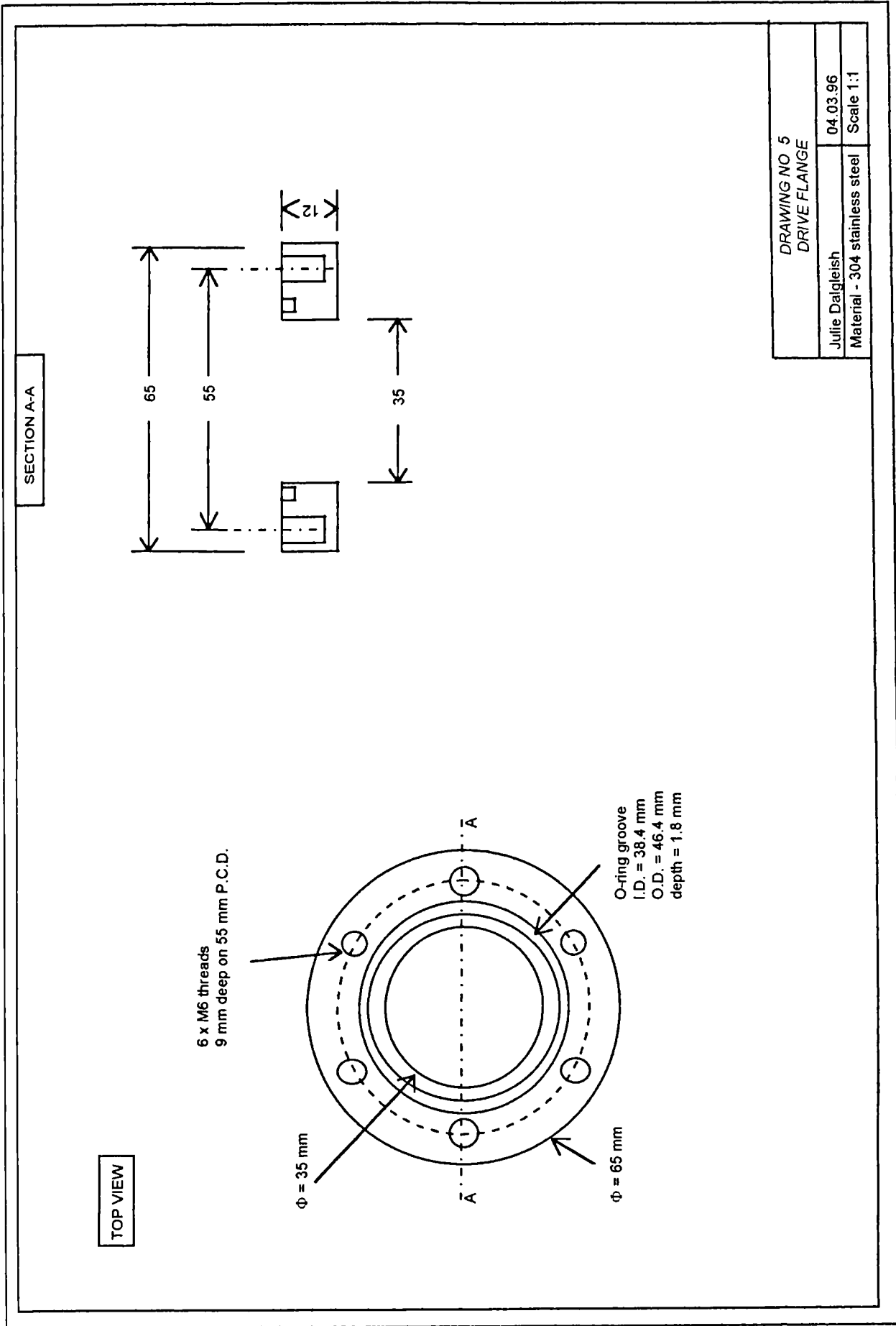


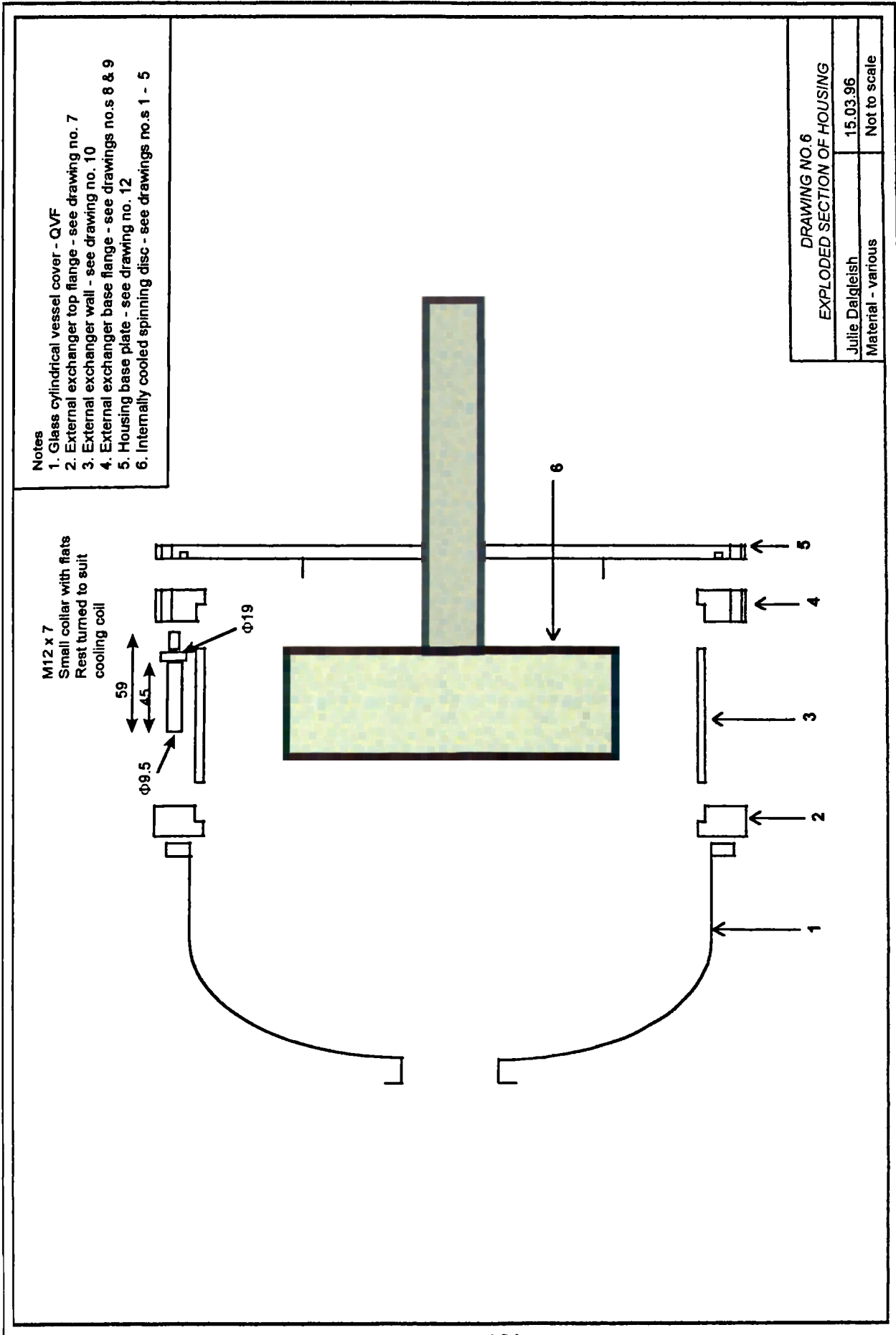
DRAWING NO 2	
DRIVE SHAFT	
Julie Dalgleish	07.05.96
Material - 304 stainless steel	Scale 1:4

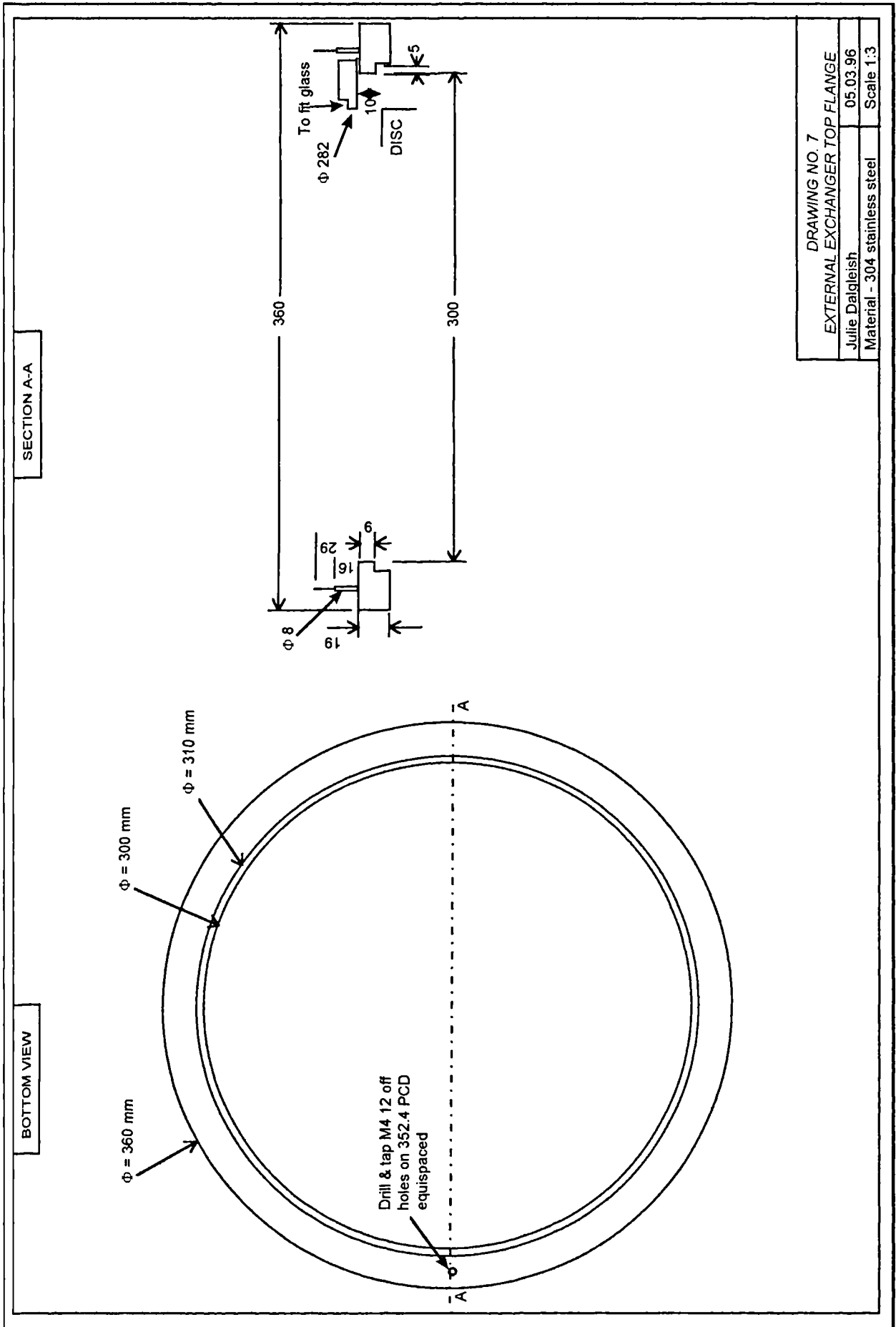


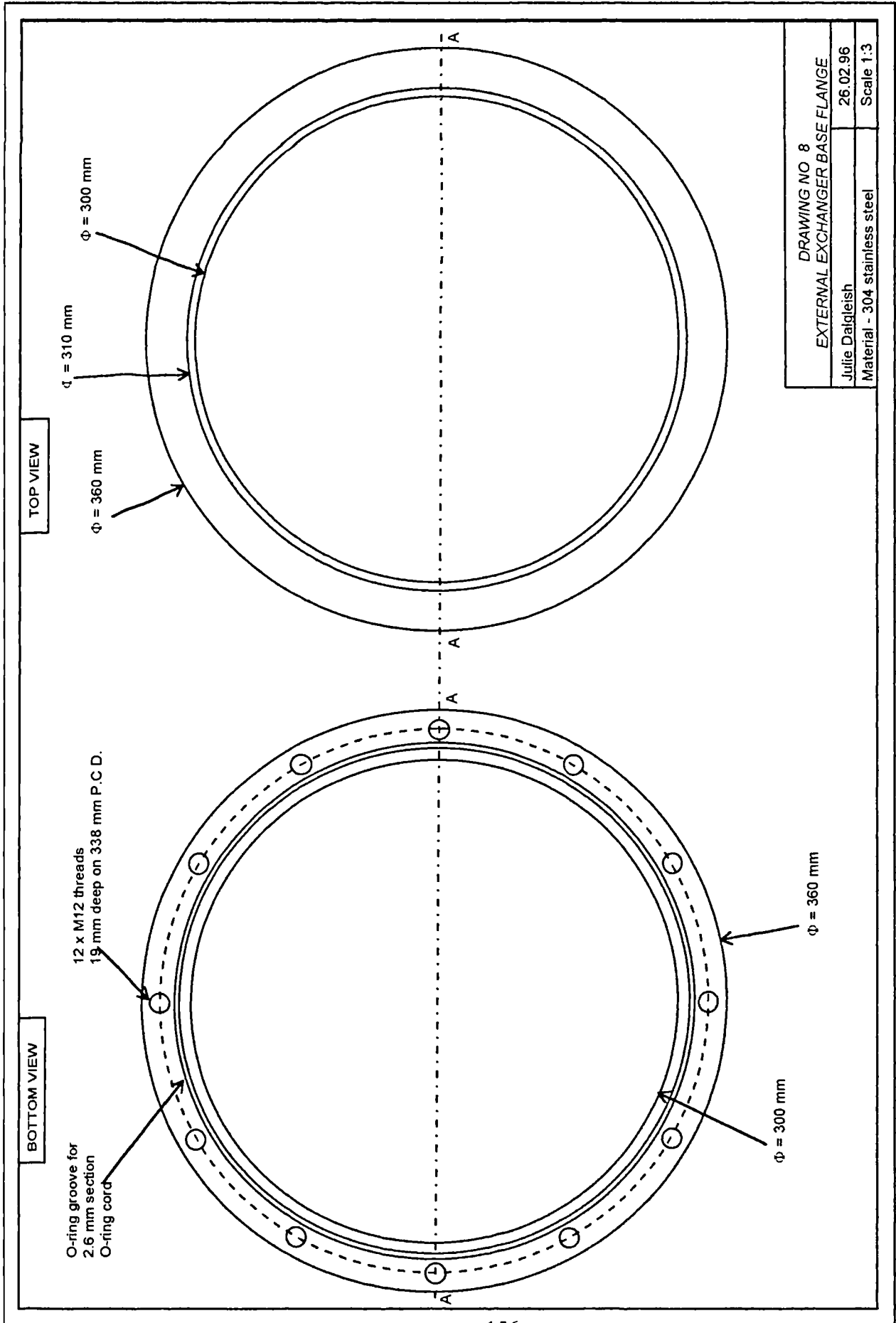


DRAWING NO 4	
INTERNAL COOLING HOUSING	
Julie Dalgleish	08.02.96
Material - 304 stainless steel	Scale 1:4

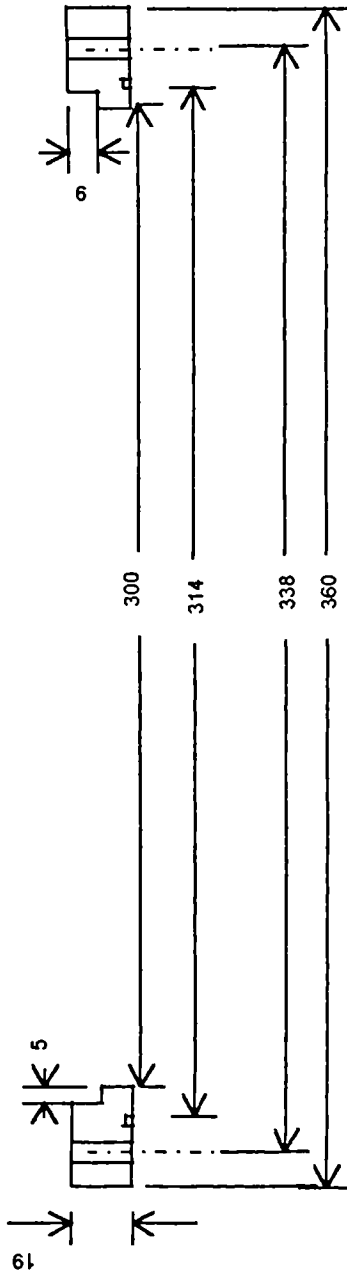




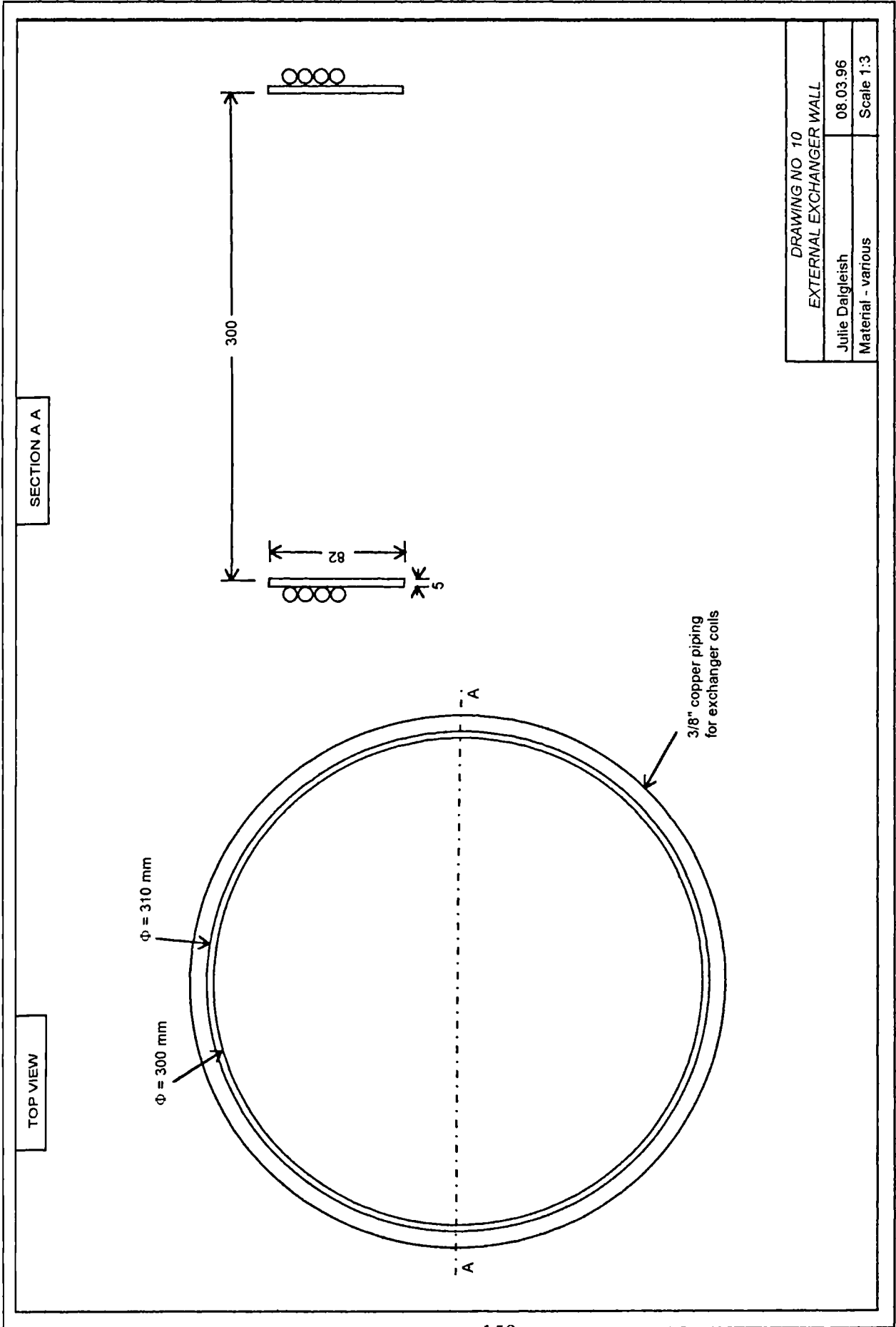


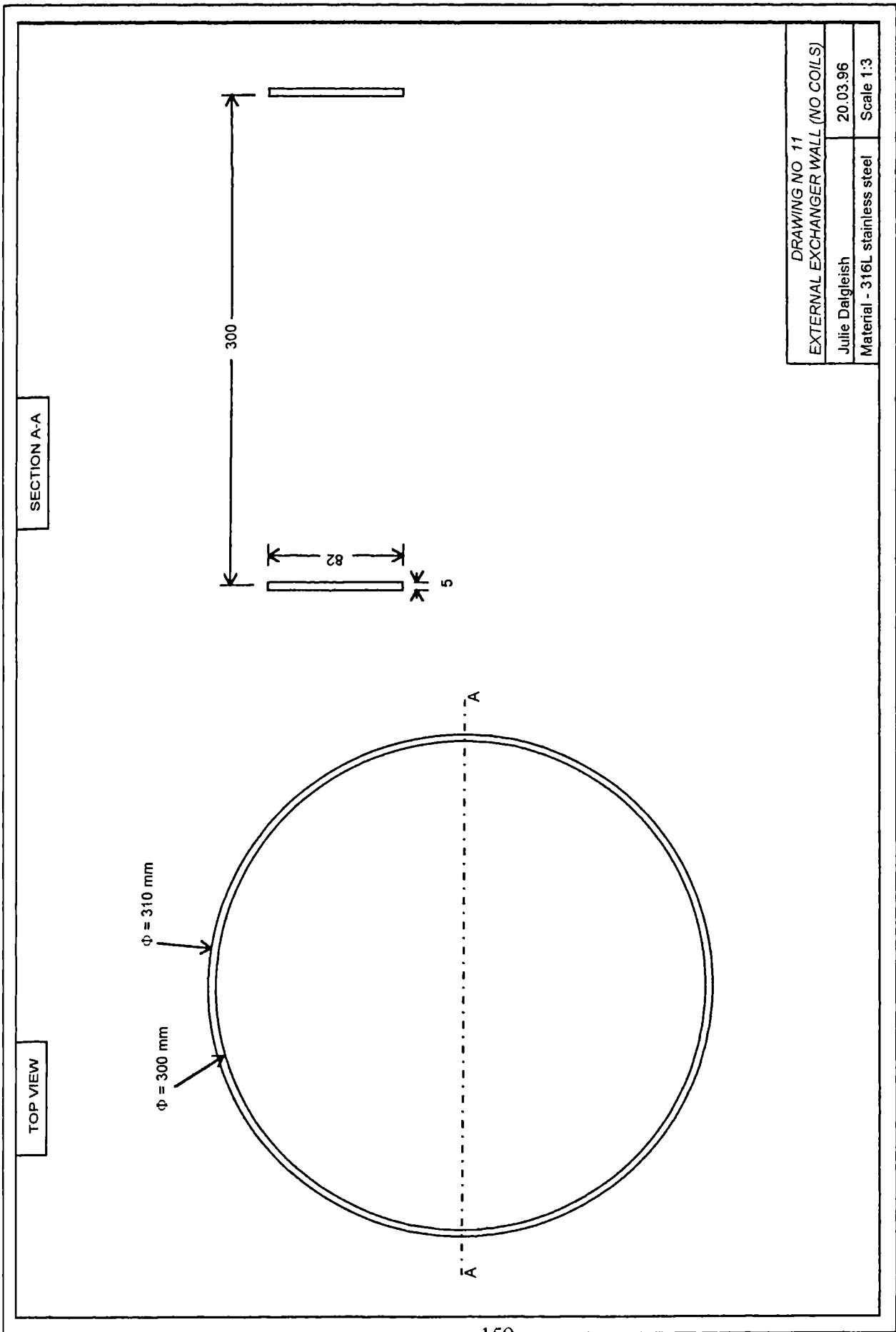


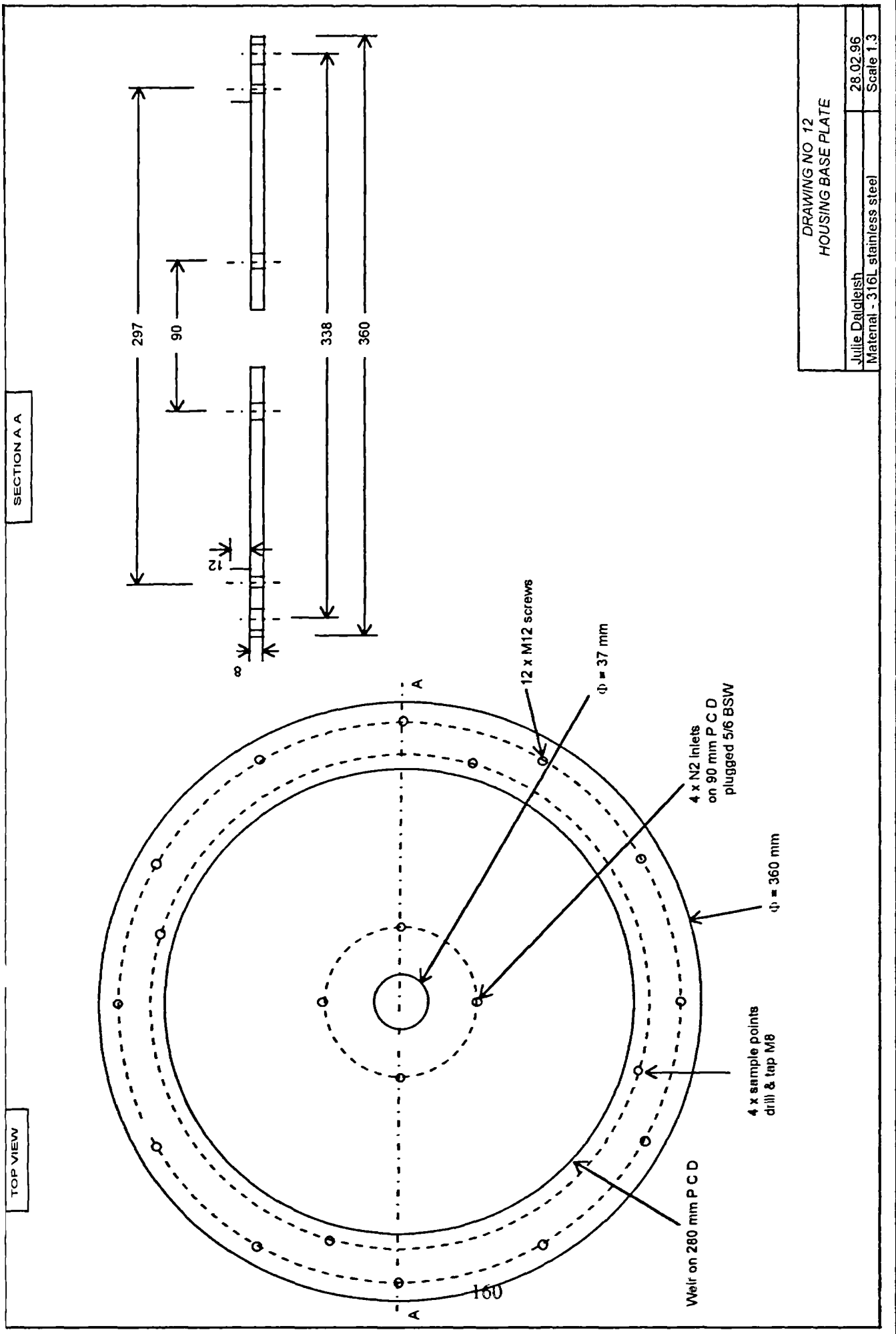
SECTION A A FROM DRAWING NO 8



DRAWING NO 9	
EXTERNAL EXCHANGER BASE FLANGE (2)	
Julie Dalgleish	26.02.96
Material - 304 stainless steel	Scale 1:2





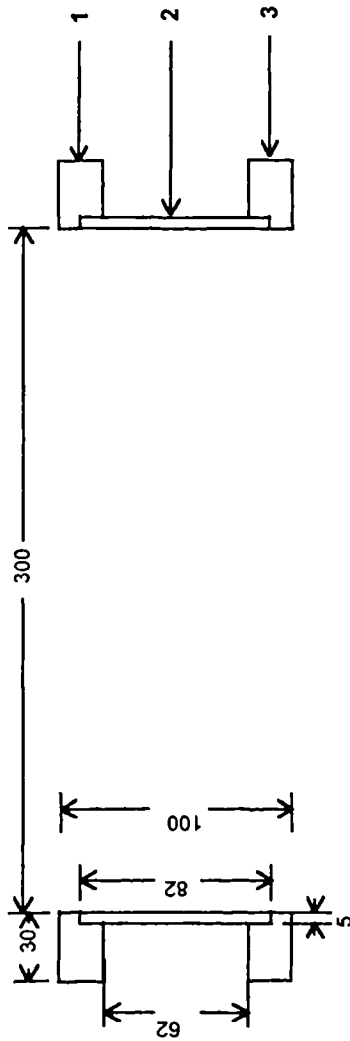


DRAWING NO 12	
HOUSING BASE PLATE	
Julie Daldalish	28.02.96
Material - 316L stainless steel	Scale 1:3

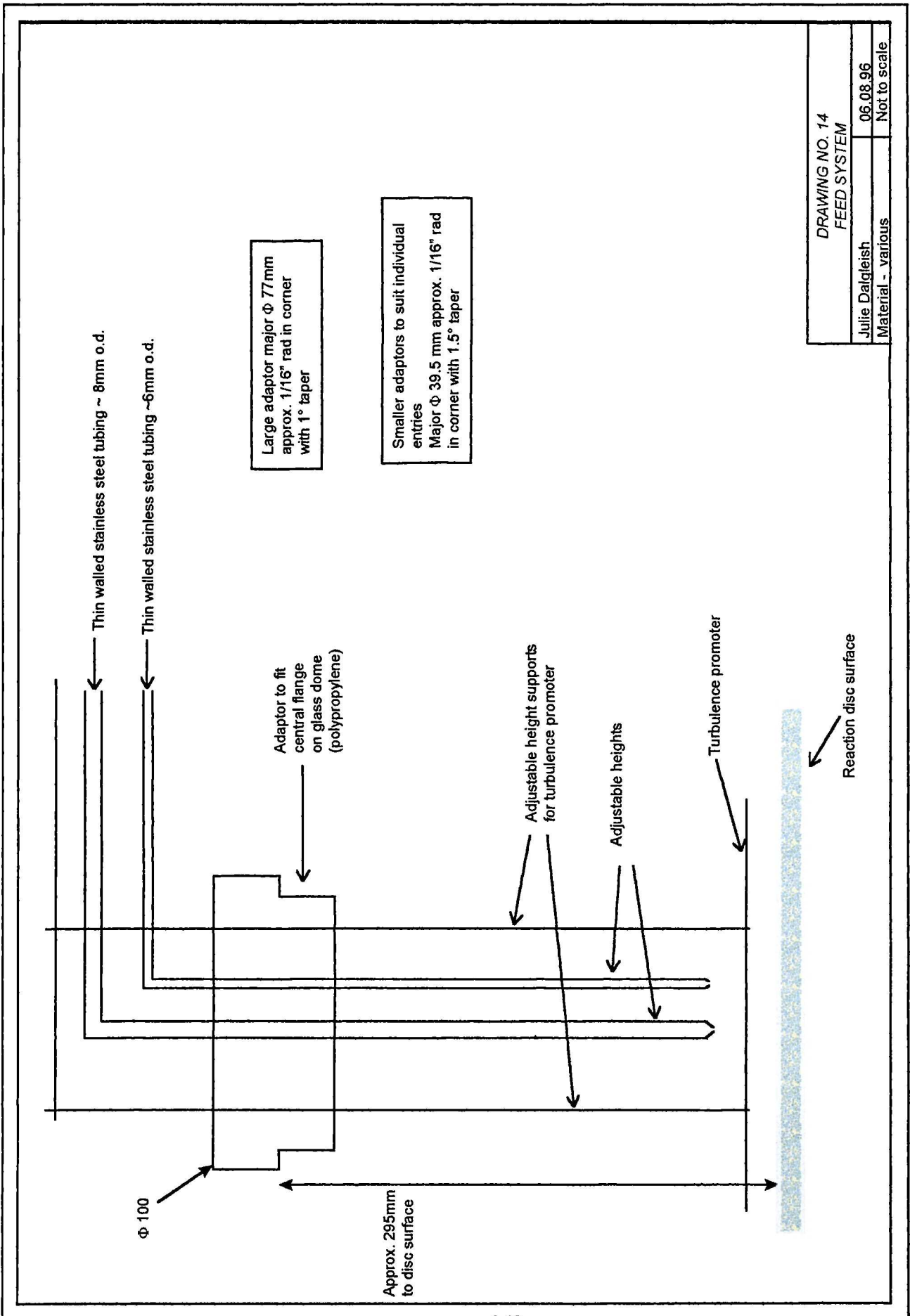
Appendix B

NOTES:

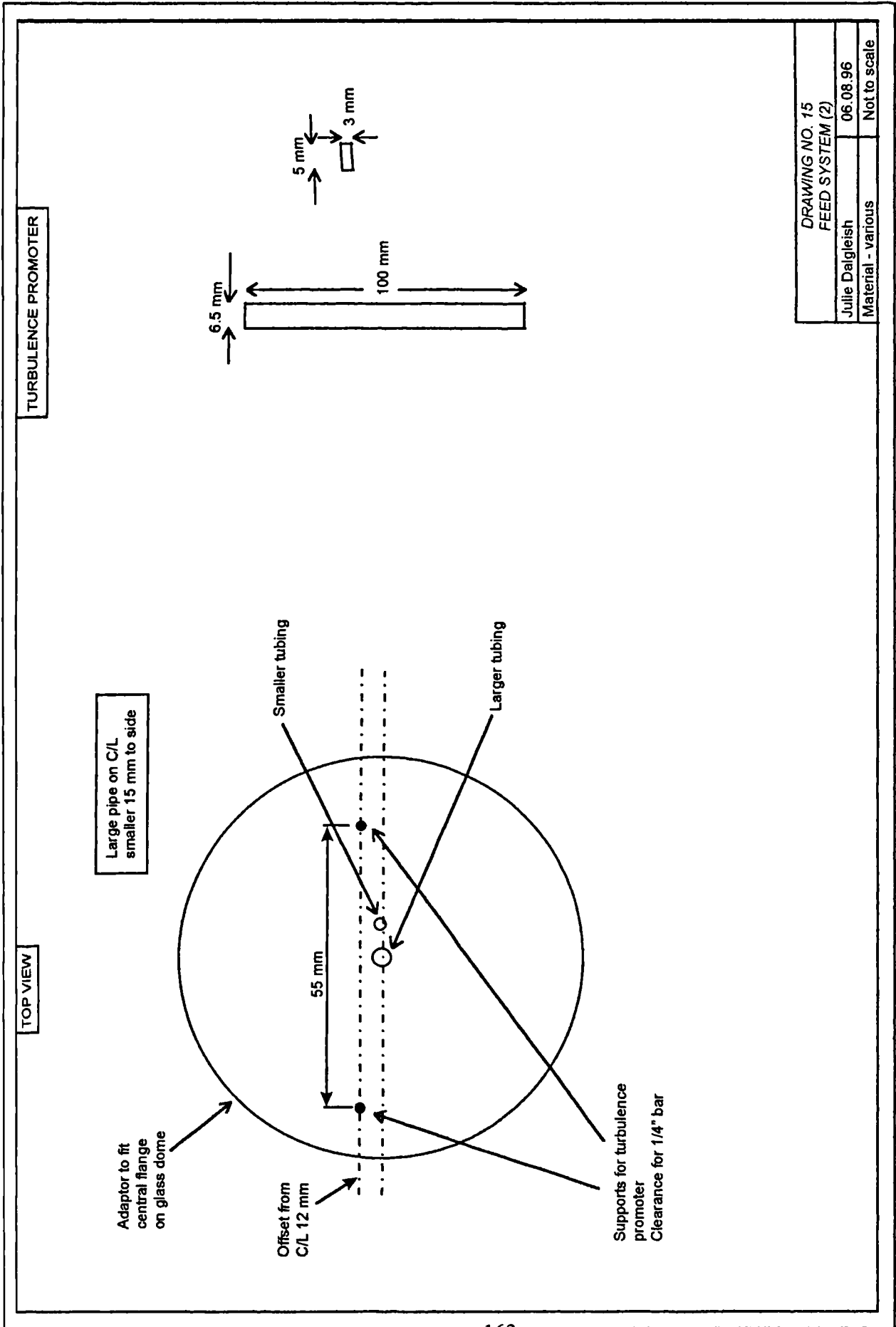
- 1 External exchanger top flange - see drawing no. 7
- 2 External exchanger wall - see drawing no. 10
- 3 External exchanger base flange - see drawing no.s 8 & 9

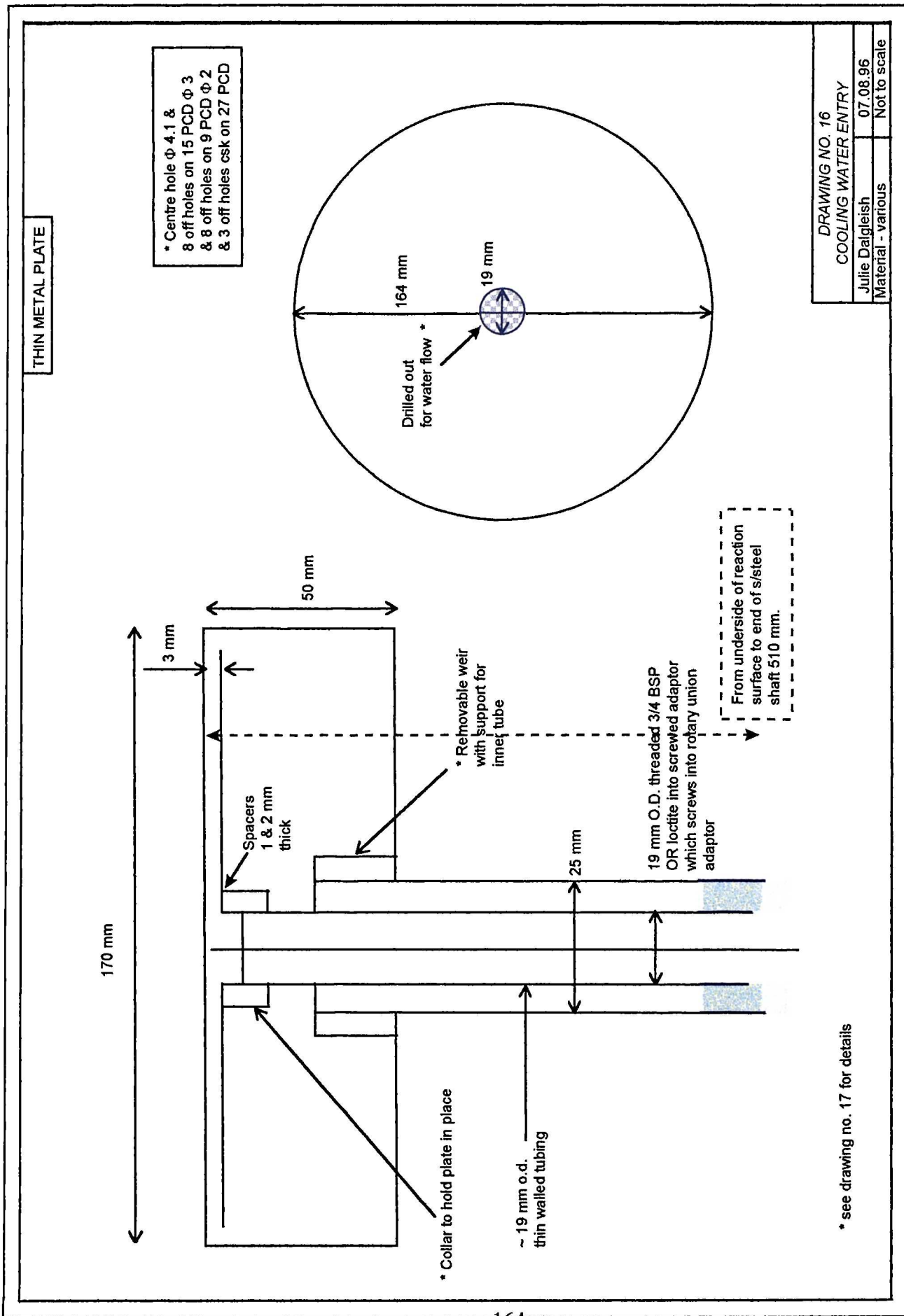


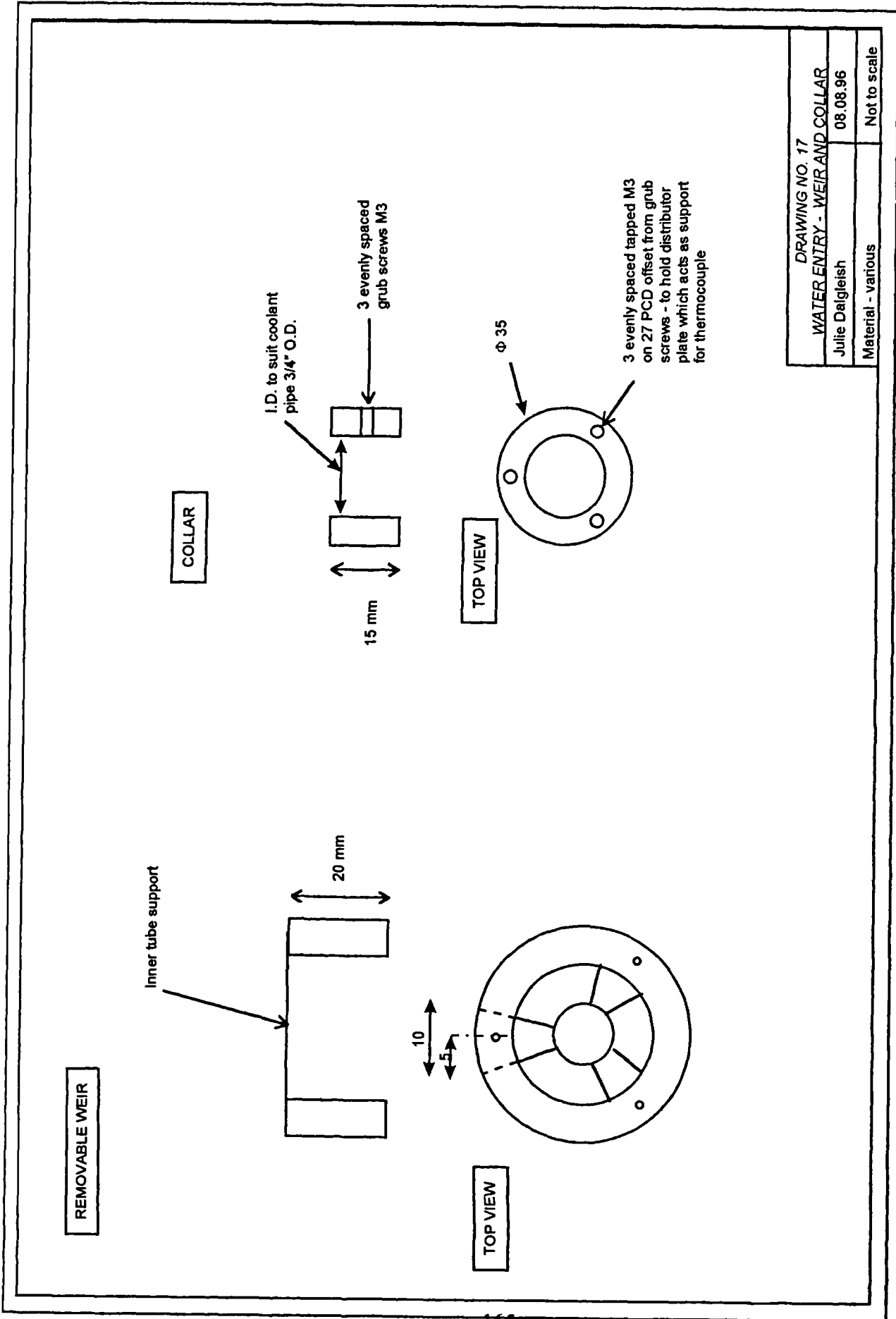
DRAWING NO 13	
EXTERNAL EXCHANGER (NO COILS)	
Julie Dalgleish	27.03.96
Material - stainless steel	Scale 1:2



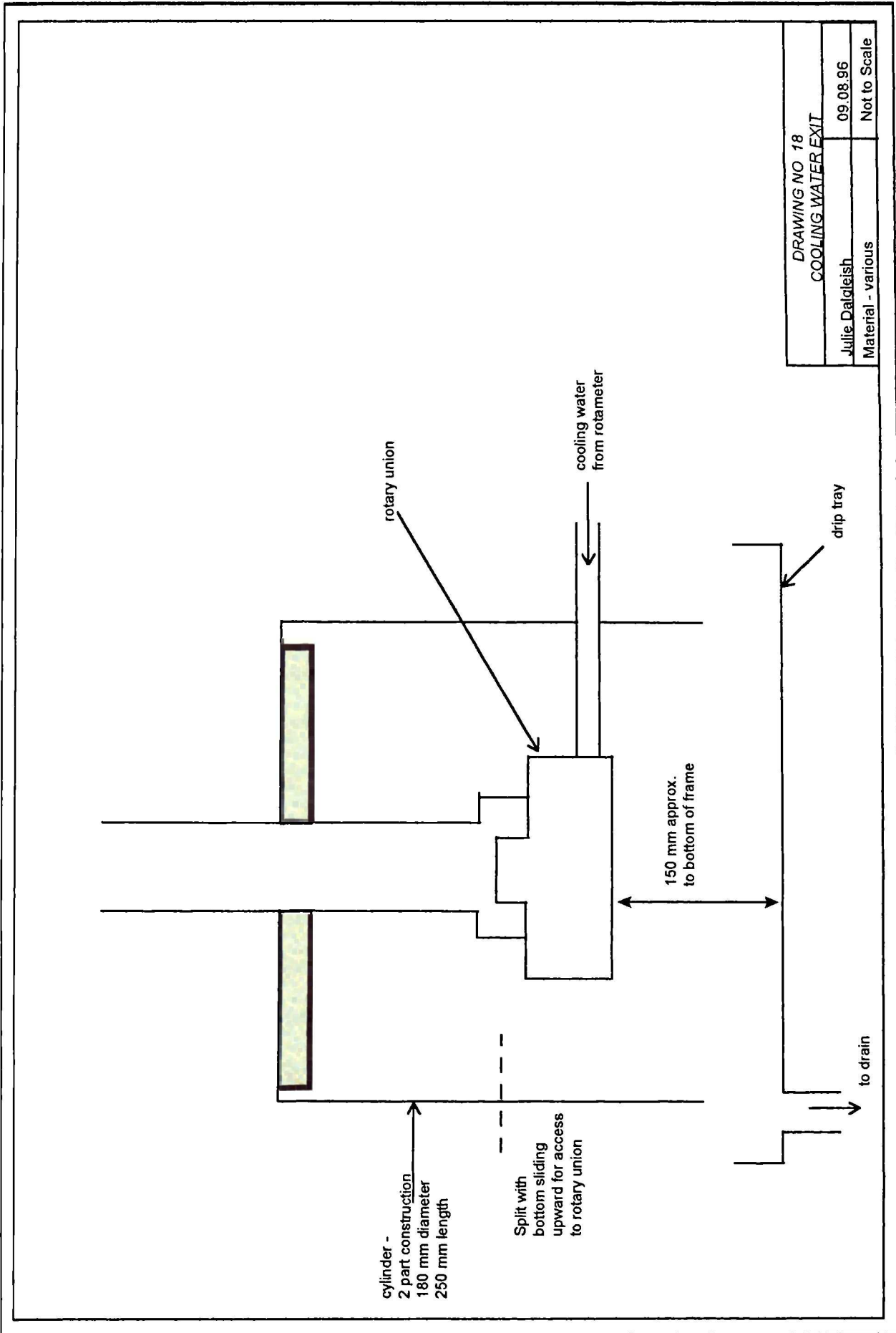
DRAWING NO. 14	
FEED SYSTEM	
Julie Dalgleish	06.08.96
Material - various	Not to scale



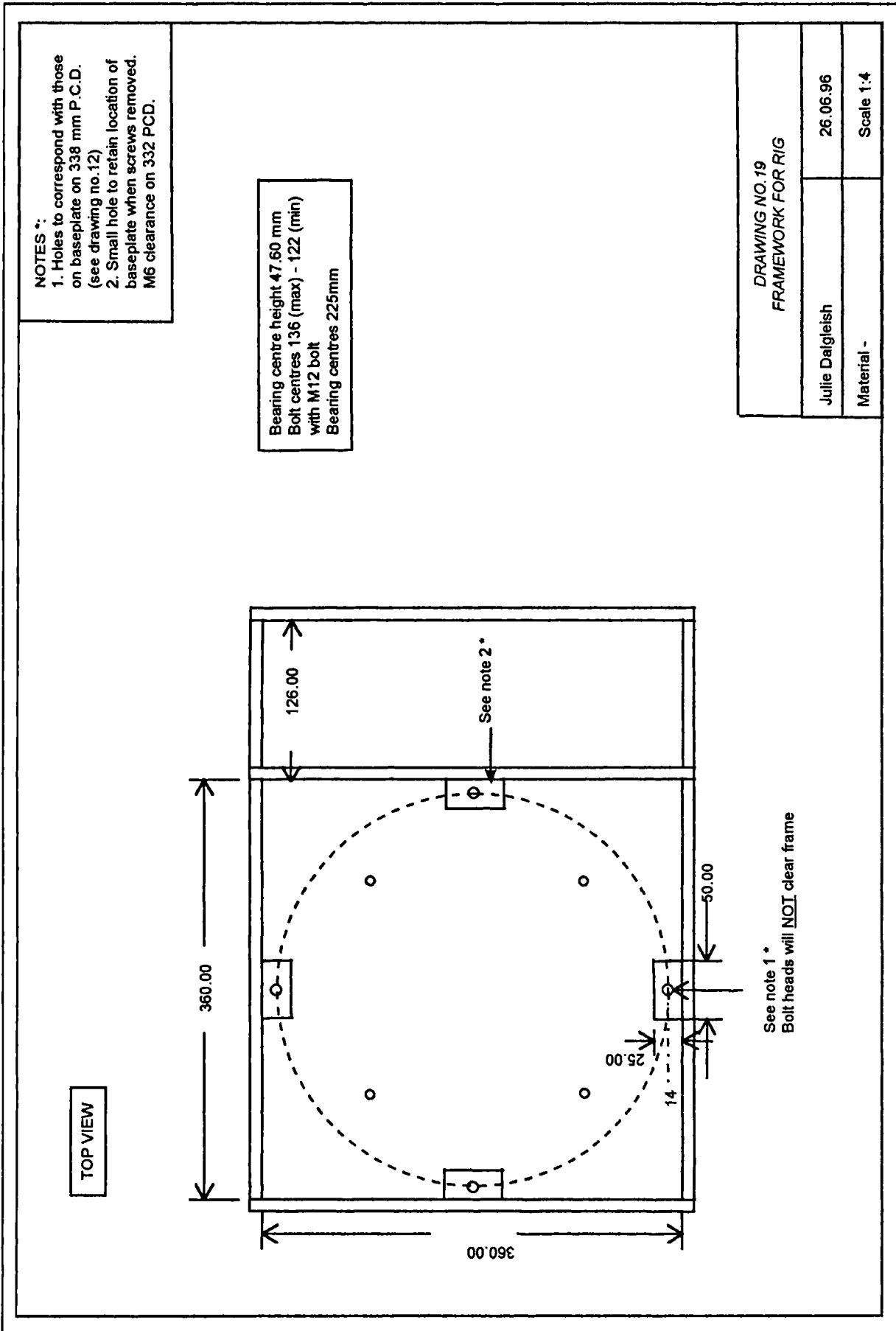




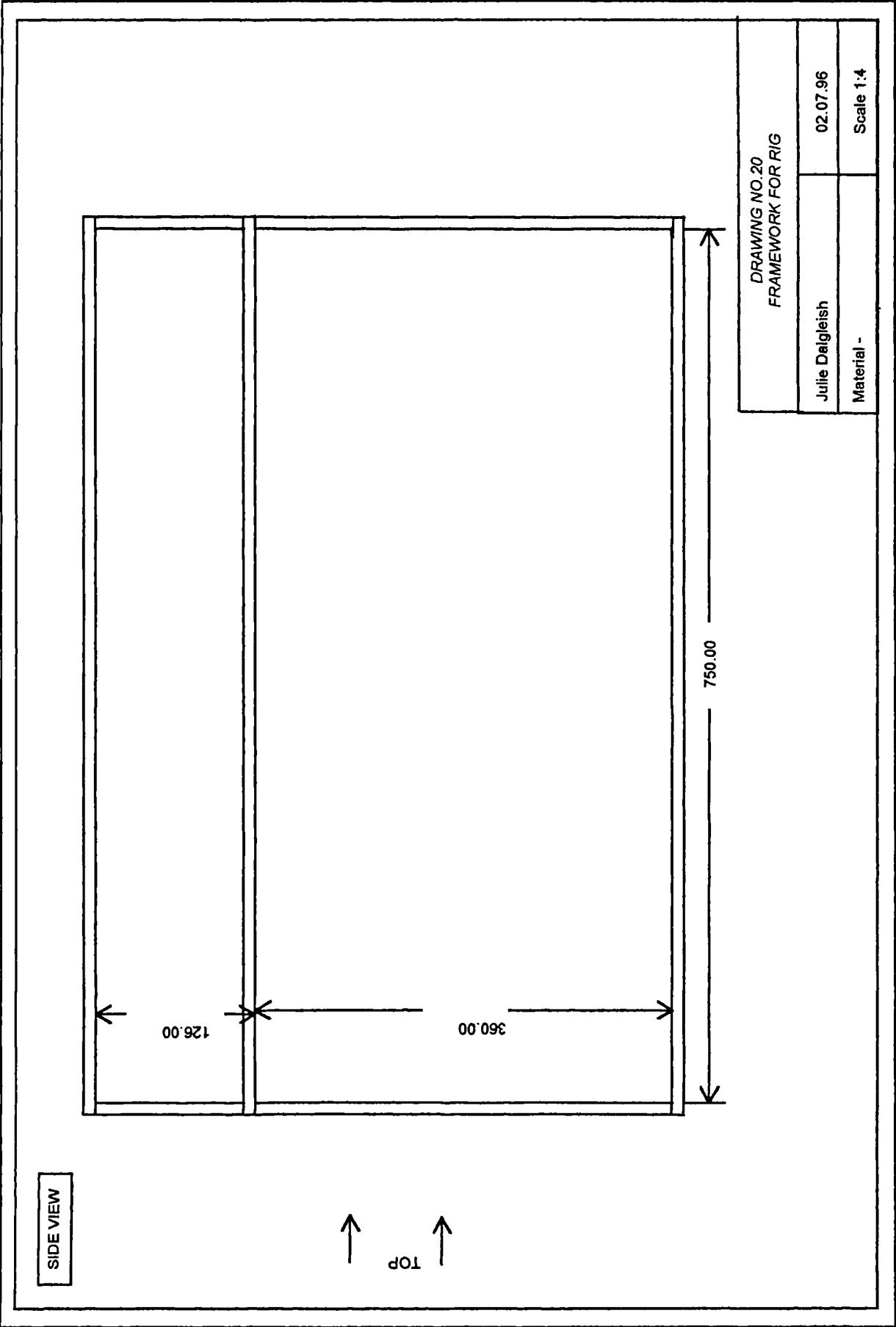
DRAWING NO. 17	
WATER ENTRY - WEIR AND COLLAR	
Julie Dalgleish	08.08.96
Material - various	Not to scale



Appendix B



Appendix B



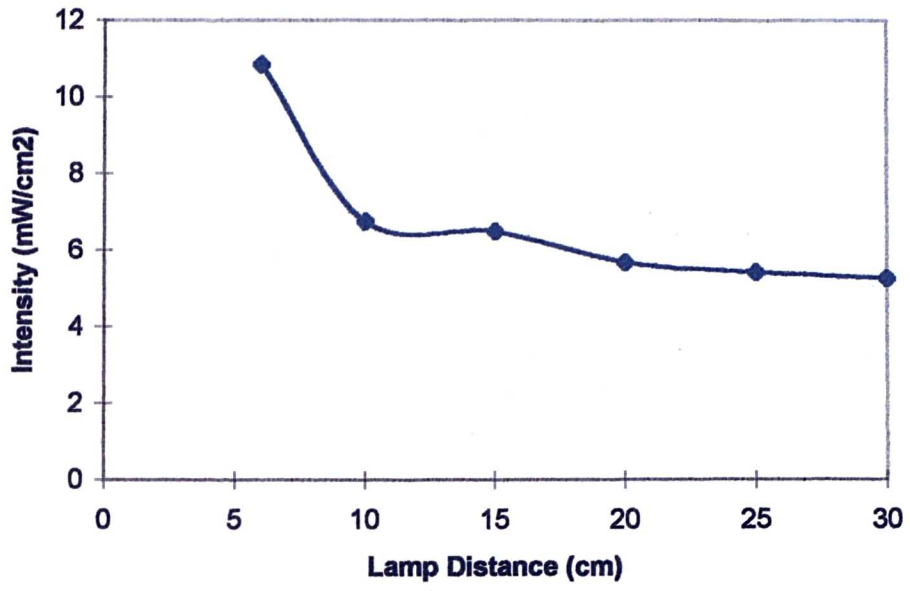


Figure 4.7. Calibration Curve for Intensity with Lamp Distance.

Appendix C

EXPERIMENTAL PROCEDURES AND TREATMENT OF RESULTS

Table 5.1. Significance of Linear Regression Models.

Study	Model (Eqn. No.)	R ²	Multiple R	F ₀	Conclusion
Static Film	6.1	0.859	0.927	138.30	significant
	6.2	0.857	0.926	206.97	significant
	6.3	0.859	0.927	138.30	significant
Spinning Disc	7.1	0.760	0.872	24.07	significant
	7.2	0.759	0.871	42.08	significant

Table 5.2. Significance of Individual Variables in Each Regression

Study	Model (Eqn. No.)	Variable	t ₀	Conclusion
Static Film	6.1	intercept	4.048	significant
		exposure time	19.964	significant
		film thickness	0.996	insignificant
		UV intensity	8.633	significant
	6.2	intercept	9.46	significant
		exposure time	19.943	significant
		UV intensity	8.567	significant
	6.3	intercept	7.405	significant

Appendix C

		exposure time	19.964	significant
		film thickness	0.996	insignificant
		UV intensity	8.633	significant
Spinning Disc	7.1	intercept	2.142	significant
		PI concentration	3.260	significant
		rotational speed	10.366	significant
		feed flowrate	2.477	significant
		UV intensity	0.109	insignificant
		temperature	0.322	insignificant
	7.2	intercept	2.437	significant
		PI concentration	3.435	significant
		rotational speed	10.898	significant
		feed flowrate	2.621	significant



Corporate Analytical Report

To : D. Arnold
Report Number : A1/4178/1
Customer Reference : 2680/98

Date: 23/10/97

Methyl Hydroquinone in Butyl Acrylate

Author(s): Q. English

INTRODUCTION

Two samples of butyl acrylate monomer were supplied. One was thought to contain 50 - 150 ppm methyl hydroquinone (MeHQ) as inhibitor, the other had been treated to remove it. The samples were examined to confirm that the MeHQ had been removed.

CONCLUSIONS

1. Methyl hydroquinone is easily detectable in the untreated sample.
2. No methyl hydroquinone could be detected in the treated sample.
3. Accurate quantitation has not been attempted at this stage

RESULTS

GCMS

The samples were examined by GCMS, after silanisation to improve the chromatography of the phenolic compound. Selected Ion Monitoring was used to improve sensitivity.

The untreated sample gave a significant peak assigned to the MeHQ TMS derivative, which showed the expected major ions of 181, 196 amu.

In the treated sample this peak could barely be detected and it is estimated that the concentration is less than 1/20 of that in the untreated sample.

Accurate quantitation would require provision of a sample of MeHQ and use of an internal standard. This has not been attempted.

Signed:

A handwritten signature in black ink, appearing to be 'Q. English'.

Date:

23/10/97

03:35 Sun Jun 21 1998

Run Number : 2

Run Type : Unknown

Name
 C:\LC-GC\SYSTEM\JULIEC2.STR
 C:\LC-GC\METHODS\JDMON
 C:\LC-GC\METHODS\JDMON
 C:\GPC\RAWDATA\GPC\IES225.002
 C:\LC-GC\RESULTS\RES225.002

Date
 03:01 Sun Jun 21 1998
 15:31 Sat May 16 1998
 15:34 Wed Feb 11 1998
 00:13 Sun Jun 21 1998
 03:34 Sun Jun 21 1998

Response Factors : Replace

Mode : Manual

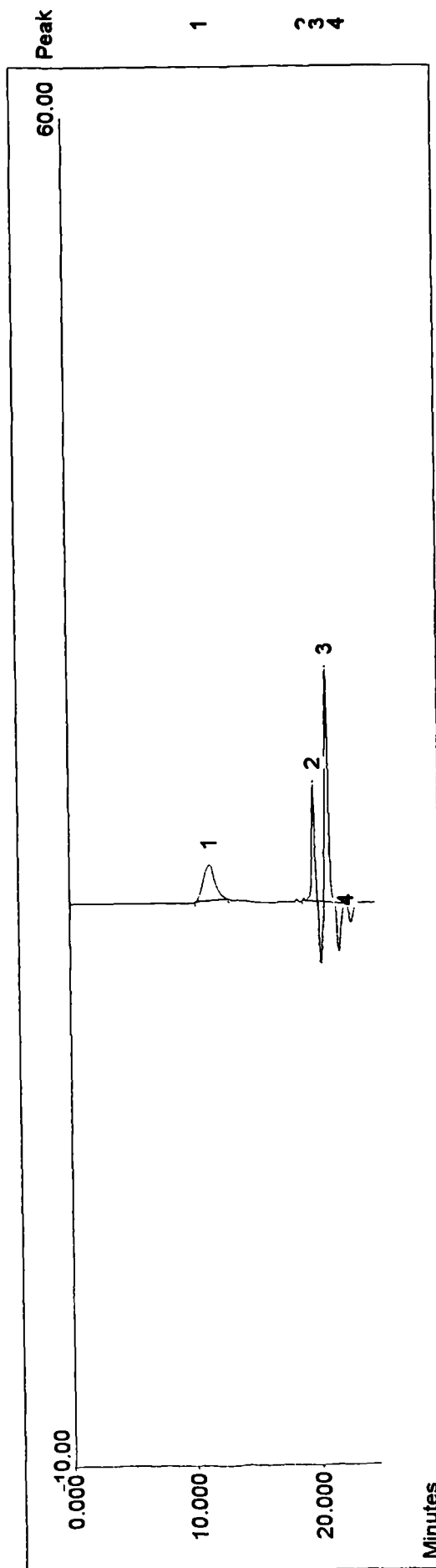
Sample Name :

Sample Amount : 1.0000000

Scale : 1.0000000

Comment:

Analysis method:EXTERNAL STD



Peak Name	Type	RT(Mins)	Area	Height	Base Conc (%g/ml)
1	BBMM	11.367	124.442	1.843	19.447
2	BVMM	19.700	109.163	6.061	19.329
3	VVMM	20.800	177.394	12.073	19.266
4	VBMM	22.300	-50.712	0.050	19.181

Operating Instructions for Spinning Disc Reactor

❶ PRE START-UP PROCEDURES

- 1 Collect UV lamp and experimental procedures file.
- 2 Position UV warning notices and COSHH assessment sheet on enclosure
- 3 Post notice 'experiment in progress: restricted access' on lab. doors
- 4 Reactor assembled and clamps tight
- 5 Connect feed tank to pump and pump to feed pipe
- 6 Connect product collection flask to outlet tubing
- 7 Vent line fully assembled with thermocouple
- 8 Connect flask to condensate outlet
- 9 Switch on extraction
- 10 Measure out required volume of monomer (refer to ERS) and record
- 11 Weigh out required mass of initiator (refer to ERS) and record
- 12 Thoroughly mix initiator into monomer and transfer to feed flask
- 13 Ensure nitrogen control valve is closed (anticlockwise) and open cylinder valve
- 14 Open nitrogen control valve to begin purge for monomer and reactor.
- 15 Leave for 15 minutes.
- 16 Check feed pump and UV lamp are connected to socket
- 17 Place UV lamp in correct position
- 18 Ensure all thermocouples correctly connected
- 19 Open cooling water isolation valve
- 20 Start water flow to condenser
- 21 Set cooling water flow to disc to required value (refer to ERS)
- 22 Set feed pump to required flowrate (refer to ERS) but DO NOT SWITCH ON

Appendix C

- 23 Place blackout screen over window
- 24 Close blackout curtains
- 25 Switch on UV lamp and leave for 10 minutes
- 26 Set up data logger (refer to separate procedure)

② RIG START-UP

- 27 Unlock main control panel
- 28 Check that extraction is running
- 29 Ensure SET SPEED dial is set to zero (anticlockwise)
- 30 Turn on power to control panel
- 31 Press DRIVE START
- 32 Slowly increase rotational speed to the required value (refer to ERS) using SET SPEED dial
- 33 Allow the disc to run for a minute and proceed to section 3

③ EXPERIMENTAL PROCEDURES

- 34 Start data logger by clicking RUN button
- 35 Start reactant pump and allow to run for required time (refer to ERS)
- 36 After the required time, perform ROUTINE STOP procedure

Routine Stop

- a stop reactant pump
- b Switch off UV lamp
- c Stop data logger

Appendix C

④ RIG SHUT DOWN

- 37 Ensure routine stop procedure has been completed and UV lamp is off
- 38 slowly decrease rotational speed to zero using SET SPEED dial
- 39 press DRIVE STOP
- 40 close cooling water flow valve to disc
- 41 Allow 5 minutes from stopping disc and close nitrogen valves
- 42 Stop water flow to condenser
- 43 Close cooling water isolation valve
- 44 Remove product collection pots and label ready for analysis
- 45 Remove condensate collector. If any liquid is present transfer to sample pot and label for analysis
- 46 Switch off extraction

ASSESSMENT OF HEALTH RISK ASSOCIATED WITH PROPOSED EXPERIMENTS OR PROJECTS

Department: CHEMICAL AND
PROCESS ENGINEERING

Personnel involved: JUNE DALGLEISH
(inc. status) (PHD STUDENT)

Title of Experiment/Procedure: PREPARATION OF SAMPLES FOR NMR ANALYSIS.

Aim: TO DISSOLVE SAMPLE IN REQUIRED SOLVENT FOR ANALYSIS.

Substances used:

Hazards identified:

CHLOROFORM - D
(0.5 ml / sample)

TOXIC BY INHALATION, SKIN CONTACT OR INGESTION.
POSSIBLE CARCINOGEN AND MUTAGEN.

N-BUTYL ACRYLATE
(MAX. 0.1 ml / sample)

HARMFUL BY INHALATION OR INGESTION, AVOID SKIN AND
EYE CONTACT. MAY UNDERGO AUTOPOLYMERISATION.
AVOID STRONG HEAT AND LIGHT, STRONG OXIDISING AGENTS,
ACIDS AND BASES.

POLYBUTYL ACRYLATE
(MAX. 0.1 ml / sample)

HIGHLY FLAMMABLE. TOXIC BY INHALATION, INGESTION OR
SKIN CONTACT. AVOID STRONG OXIDISING AGENTS

Question 1: Do quantities/dilutions make normal "Good Chemical Practice" sufficient?
If "yes", no further assessment is necessary.

YES

Information sources:

SIGMA ALDRICH MATERIAL SAFETY DATA SHEETS.

Is there a less hazardous substance?
If so, why not use it?

NO.

Control measures to be adopted: (N.B. Consider cleaners, contractors, maintenance staff and visitors as well as research staff: use a continuation sheet if necessary). Enter Containment level (i.e. open bench, fume cupboard, etc)

USE ONLY IN AN APPROVED FUME CUPBOARD STORED IN A COOL DRY PLACE.
WEAR CHEMICAL RESISTANT GLOVES, SAFETY GOGGLES, LAB COAT.
AVOID ALL CONTACT.

Required checks and their frequency, on the adequacy and maintenance of control measures during the course of the experiment: (N.B. State if any health surveillance is necessary).

Disposal procedures during and at end of experiment:

Estimated cost
of disposal
£

TO BE SENT FOR ANALYSIS

Appendix C

EMERGENCY PROCEDURES

If any of the substances or procedures identified overleaf are likely to pose a special hazard in an emergency, then identify below the action to be taken:

Spillage/uncontrolled release: EVACUATE AREA. WEAR SELF-CONTAINED BREATHING APPARATUS, RUBBER BOOTS AND HEAVY RUBBER GLOVES. ABSORB ON SAND OR VERMICULITE AND PLACE IN CLOSED CONTAINERS FOR DISPOSAL. VENTILATE AREA AND WASH SPILL SITE AFTER MATERIAL PICK-UP IS COMPLETE.

Fire CHLOROFORM IS NON COMBUSTIBLE BUT EMITS TOXIC FUMES UNDER FIRE USE EXTINGUISHING MEDIA APPROPRIATE TO SURROUNDING FIRE CONDITIONS. WEAR SELF-CONTAINED BREATHING APPARATUS AND PROTECTIVE CLOTHING TO PREVENT SKIN AND EYE CONTACT.

If personnel are affected (fume, contamination etc.) treatment to be adopted:
(N.B. Antidotes and special treatments may be obtained through the University Health Service.

CONTACT: FLUSH SKIN WITH WATER FOR AT LEAST 15 MINS. EYES SHOULD BE IRRIGATED IMMEDIATELY WITH COPIOUS AMOUNTS OF WATER.

INHALATION: REMOVE TO FRESH AIR. IF NOT BREATHING, GIVE ARTIFICIAL RESPIRATION. IF BREATHING IS DIFFICULT, GIVE OXYGEN.

INGESTION WASH OUT MOUTH WITH WATER IF CONSCIOUS. CALL A DOCTOR.

Additional Information (where appropriate) e.g. quantities and frequencies:

Name of Assessor: JULIE DALGLEISH

Status of Assessor PHD STUDENT Date 20.01.98 Signed J Dalgleish

Name of Supervisor:
(for students only) DR R.J.J. JARCHUCK Date 21/1/98 Signed R Jarchuck

Head of Dept [Signature] Date 21/1/98 Signed J R BACKHUS

COSHH ASSESSMENT (CONT.)

Hazardous Properties of Substances Involved

- N-butyl acrylate:** Harmful if inhaled or ingested, avoid skin and eye contact. Avoid strong heat and light. Avoid strong oxidising agents, acids and bases. May undergo autopolymerisation.
- Polybutylacrylate:** Highly flammable, produces CO and CO₂ fumes. Toxic by inhalation, ingestion and skin contact. Avoid strong oxidising agents.
- Benzoin methyl ether:** Toxic by inhalation, ingestion and skin contact. Produces CO and CO₂ fumes under fire conditions. Avoid strong oxidising agents and acids.
- Benzophenone:** Harmful if inhaled or ingested. Eye and skin irritant. Produces CO and CO₂ fumes. Avoid strong oxidising and reducing agents.
- Benzoin:** Harmful if inhaled or ingested. Eye and skin irritant. Produces CO and CO₂ fumes. Avoid strong oxidising agents.
- Irgacure 651:** Harmful if inhaled or ingested. Eye and skin irritant. Produces Co_x fumes and other toxic gases. Avoid strong oxidising agents, acids and bases. Protect from light. Very toxic to aquatic organisms, may cause long-term adverse effects in the aquatic environment.

Emergency Procedures - First Aid and Fire Fighting Measures.

FIRST AID MEASURES

N-butyl acrylate:

Eye or skin contact: Flush immediately with copious amounts of water for at least 15 minutes while removing contaminated clothing and shoes. Wash contaminated clothing before reuse.

Inhaled: Remove to fresh air. If not breathing give artificial ventilation. If breathing is difficult give oxygen.

Ingested: Wash out mouth with water if person is conscious. Seek medical attention.

Polybutylacrylate:

Eye contact: Flush immediately with copious amounts of water for at least 15 minutes.

Skin contact: Wash immediately with soap and copious amounts of water. Remove contaminated clothing and wash immediately.

Inhaled: Remove to fresh air. If not breathing give artificial ventilation. If breathing is difficult give oxygen.

Ingested: Wash out mouth with water if person is conscious. Seek medical attention.

Benzoin methyl ether:

Eye or skin contact: Flush immediately with copious amounts of water for at least 15 minutes while removing contaminated clothing and shoes. Wash contaminated clothing before reuse.

Inhaled: Remove to fresh air. If not breathing give artificial ventilation. If breathing is difficult give oxygen.

Ingested: Wash out mouth with water if person is conscious. Seek medical attention.

Appendix C

Benzophenone:

- Eye contact: Flush immediately with copious amounts of water for at least 15 minutes.
- Skin contact: Wash immediately with soap and copious amounts of water.
Wash contaminated clothing before reuse.
- Inhaled: Remove to fresh air. If not breathing give artificial ventilation.
If breathing is difficult give oxygen.
- Ingested: Wash out mouth with water if person is conscious. Seek medical attention.

Benzoin:

- Eye contact: Flush immediately with copious amounts of water for at least 15 minutes.
- Skin contact: Wash immediately with soap and copious amounts of water.
Wash contaminated clothing before reuse.
- Inhaled: Remove to fresh air. If not breathing give artificial ventilation.
If breathing is difficult give oxygen.
- Ingested: Wash out mouth with water if person is conscious. Seek medical attention.

Irgacure 651:

- Eye contact: Flush immediately with copious amounts of water for at least 15 minutes.
- Skin contact: Wash immediately with soap and copious amounts of water.
Do not use organic solvents.
- Inhaled: Remove to fresh air. If not breathing give artificial ventilation.
If breathing is difficult give oxygen.

Appendix C

Ingested: Affected person should drink 500-800 ml water, if possible with suspended activated carbon for medical use. Seek medical attention.

FIRE FIGHTING MEASURES

In all cases:

Extinguishing media: water spray, CO₂, dry chemical powder or foam.

Protective equipment: self-contained breathing apparatus, protective clothing.

Exposure hazards: emits toxic fumes.

Unusual hazards: vapour may travel considerable distance to ignition

N-butyl acrylate & source and flash back.
polybutylacrylate

CONTAINED SPILLAGE / RELEASE MEASURES

In all cases:

1. Evacuate area.
2. Shut off all sources of ignition.
3. Follow steps 4 + below for individual chemicals.

N-butyl acrylate:

4. Wear self-contained breathing apparatus, rubber boots and heavy rubber gloves.

Appendix C

5. Cover with dry lime or soda ash, pick up, keep in a closed container and hold for waste disposal.
6. Ventilate area and wash spill site after material pickup is complete.

Polybutylacrylate:

4. Wear self-contained breathing apparatus, rubber boots and heavy rubber gloves.
5. Cover with dry lime, sand or soda ash.
6. Place in covered containers using non-sparking tools and transport outdoors.
7. Ventilate area and wash spill site after material pickup is complete.

Benzoin methyl ether:

4. Wear self-contained breathing apparatus, rubber boots and heavy rubber gloves.
5. Sweep up, place in a bag and hold for waste disposal. Avoid raising dust.
6. Ventilate area and wash spill site after material pickup is complete.

Benzophenone:

4. Wear respirator, chemical safety goggles, rubber boots and heavy rubber gloves.
5. Sweep up, place in a bag and hold for waste disposal. Avoid raising dust.
6. Ventilate area and wash spill site after material pickup is complete.

Benzoin:

4. Wear respirator, chemical safety goggles, rubber boots and heavy rubber gloves.
5. Sweep up, place in a bag and hold for waste disposal. Avoid raising dust.

Appendix C

6. Ventilate area and wash spill site after material pickup is complete.

Irgacure 651:

4. Wear respirator, chemical safety goggles, rubber boots and heavy rubber gloves.
5. Sweep up, place in a closed container and hold for waste disposal.
6. Avoid raising dust and prevent contamination of drains.

Experimental record sheet - exothermic spinning disc reactor.

SECTION 1: TO BE COMPLETED BEFORE START OF EXPERIMENT.			
Date:		Type of run	
Previous reference no.		Reference no.	
Monomer		Volume (ml)	
Initiator		Mass (g)	
Rotational speed (rpm)		Drive speed (rpm)	
Cooling water flow (l/min)			
Feed flow (ml/s)			
Length of run (min)			
Results filename			
Completed by		Time completed	
SECTION 2: TO BE COMPLETED DURING EXPERIMENT.			
Monomer		Volume (ml)	

Appendix C

Initiator		Mass (g)	
Drive speed readout (rpm)			
Cooling water flow (l/min)			
Feed flowrate (ml/s)			
Data file			
Renamed file			
		✓	Time
All warning notices in position			
Feed system connected			
Vent line connected			
Collection pots in position			
Rig fully assembled and locating clamps tight			
Extraction on			
Nitrogen purge on			
Feed pump and UV lamp ready			
Thermocouples correctly connected			
Cooling water flow through disc started			
All blackout curtains in position			
UV lamp switched on			
Data logger ready			
Disc started			
Data logger started			
Feed pump started			
Feed pump stopped			

Appendix C

UV lamp off			
Data logger stopped			
ROUTINE STOP completed			
Disc stopped			
Cooling water flow through disc stopped			
Nitrogen purge stopped			
Collection pots labelled			
Extraction off			
READY FOR CLEANING			
CLEANED AND REASSEMBLED			
Completed by		Date & time	

Appendix D

STATIC FILM POLYMERISATION RESULTS.

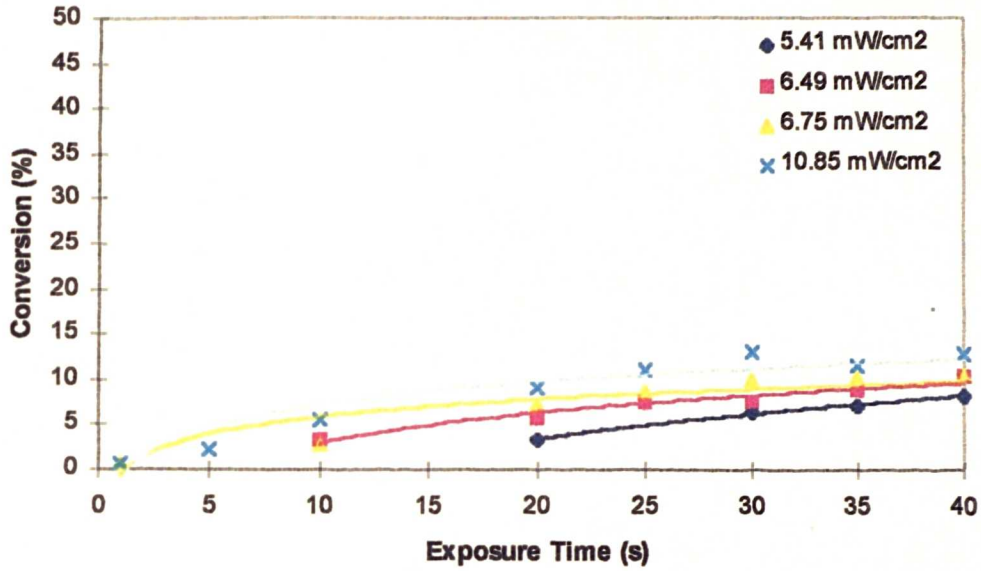


Figure 6.10. Effect of Exposure Time on Conversion (400 μm).

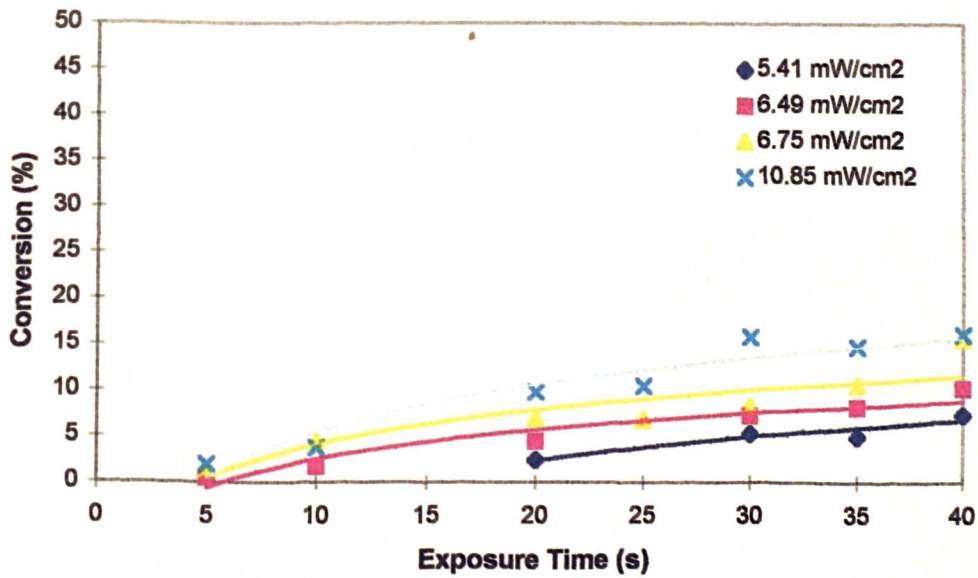


Figure 6.11. Effect of Exposure Time on Conversion (1000 μm).

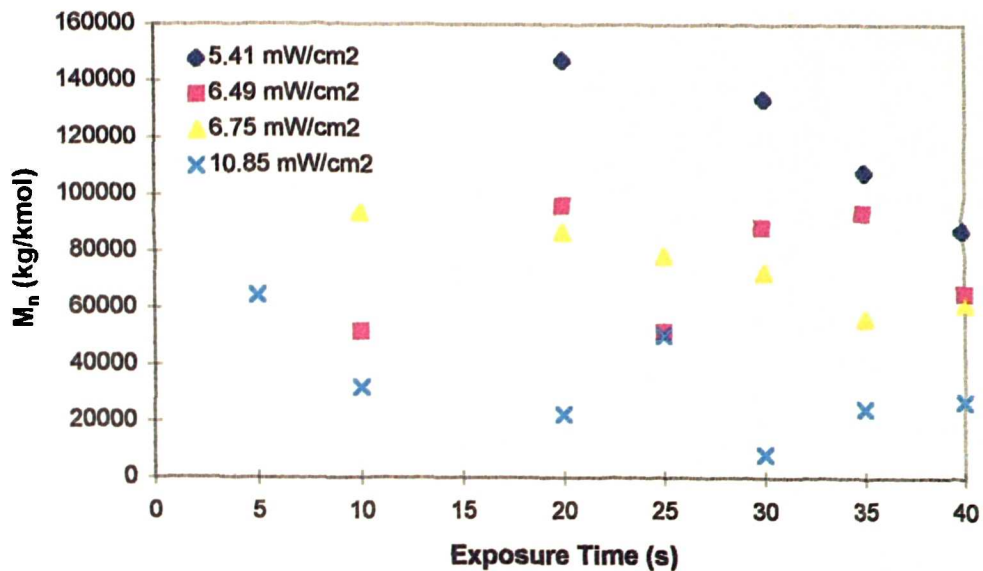


Figure 6.12. Effect of Exposure Time on M_n (400 μm).

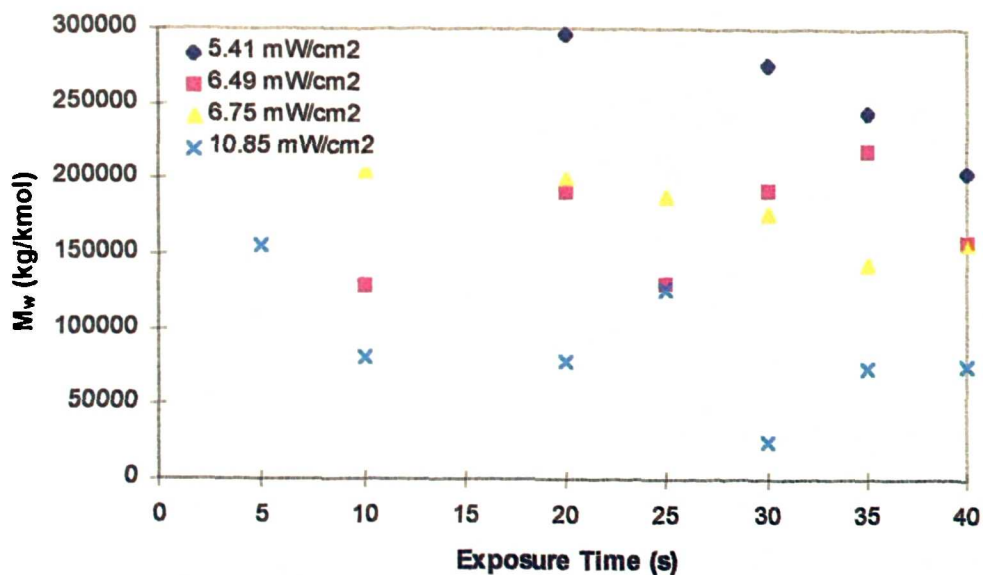


Figure 6.13. Effect of Exposure Time on M_w (400 μm).

Appendix D

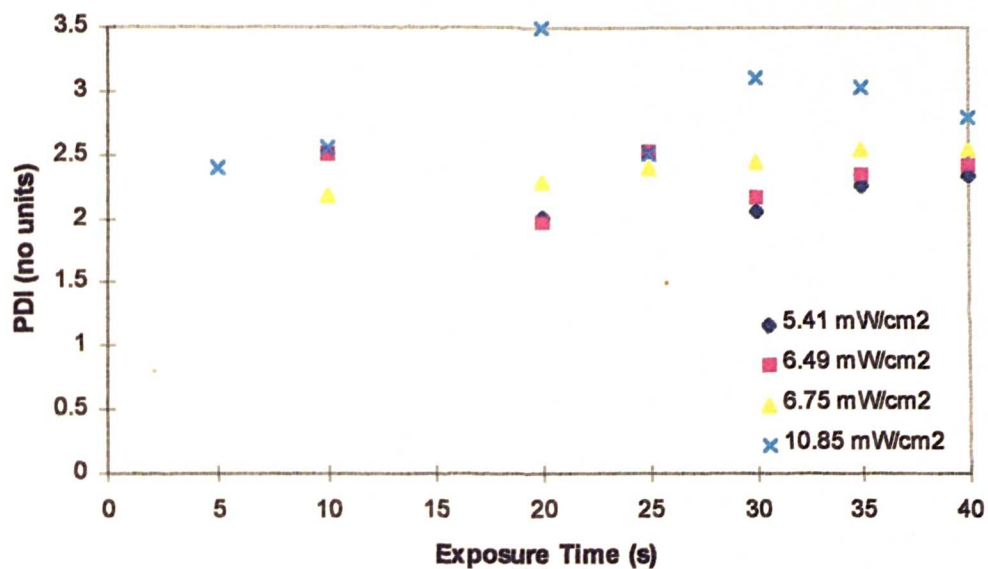


Figure 6.14. Effect of Exposure Time on Polydispersity Index (400 μm).

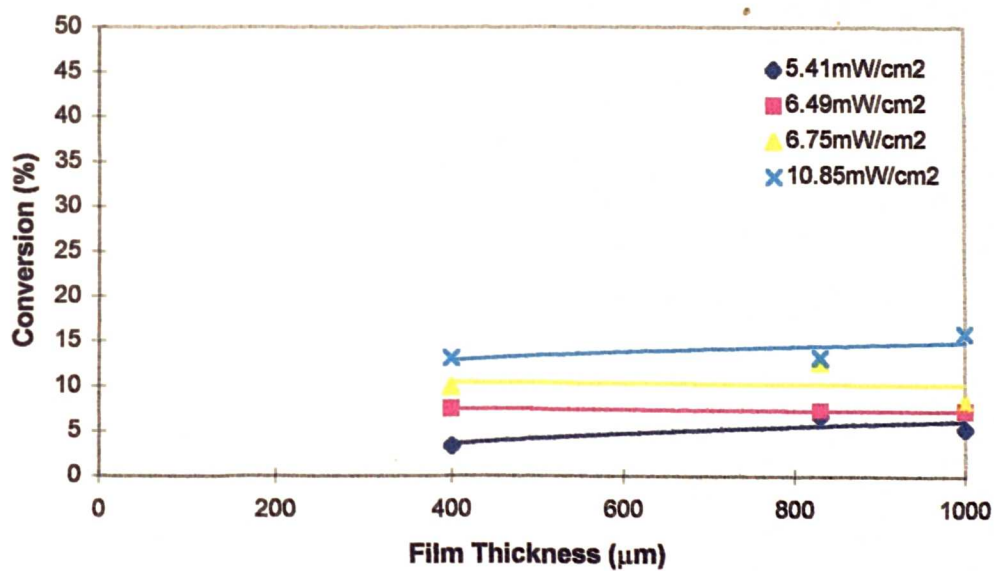


Figure 6.15. Effect of Film Thickness on Conversion (30s Exposure Time).

Appendix D

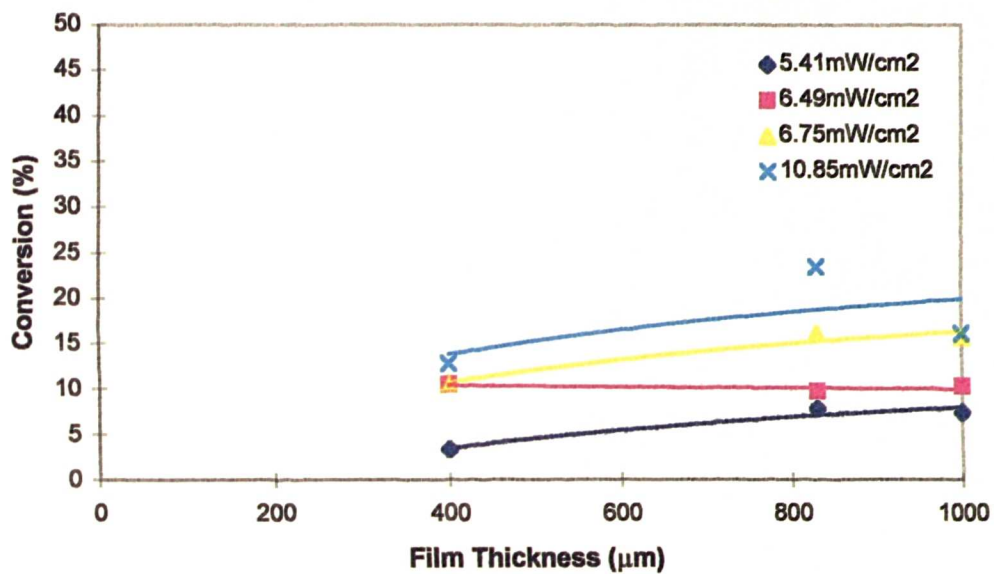


Figure 6.16. Effect of Film Thickness on Conversion (40s Exposure Time).

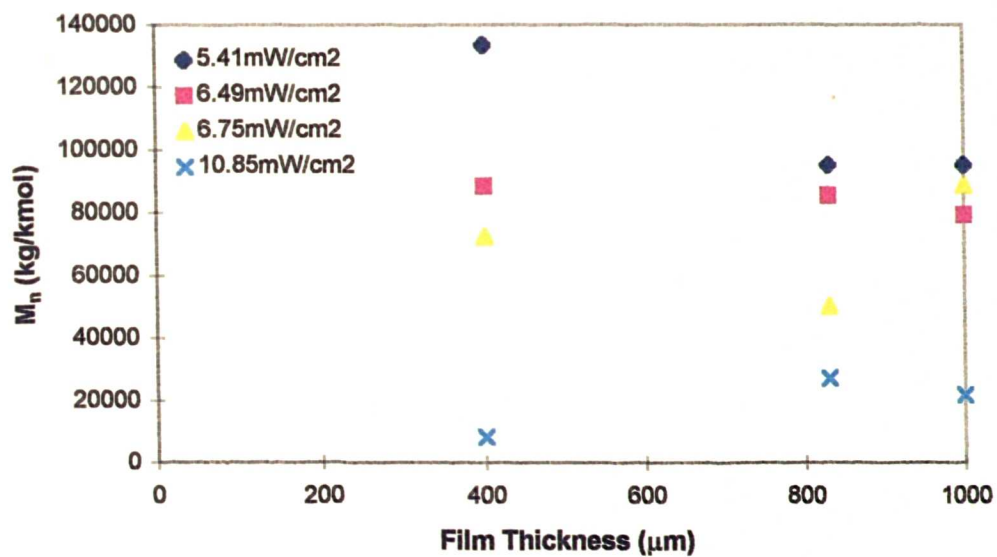


Figure 6.17. Effect of Film Thickness on M_n . (30s Exposure Time).

Appendix D

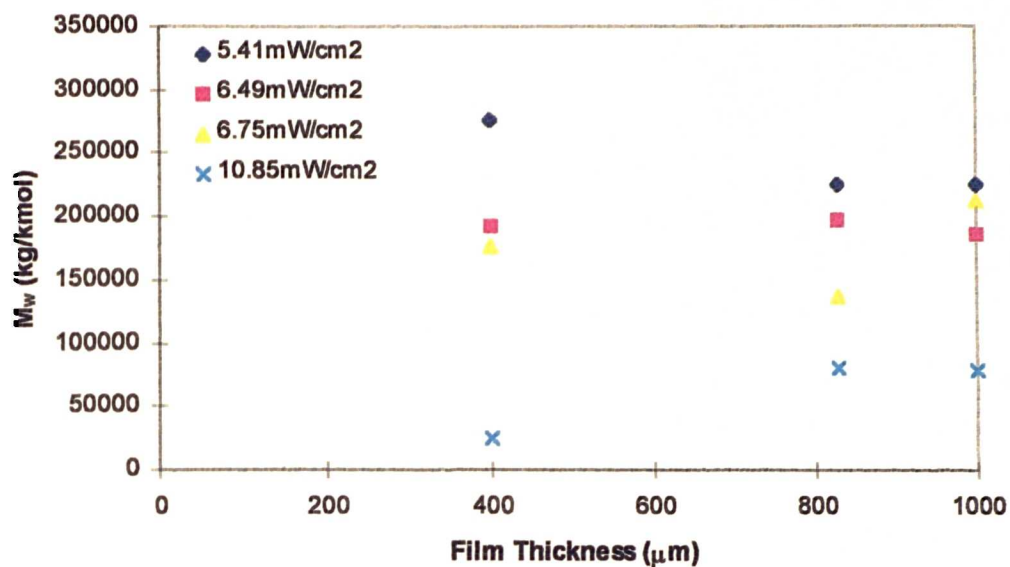


Figure 6.18. Effect of Film Thickness on M_w (30s Exposure Time).

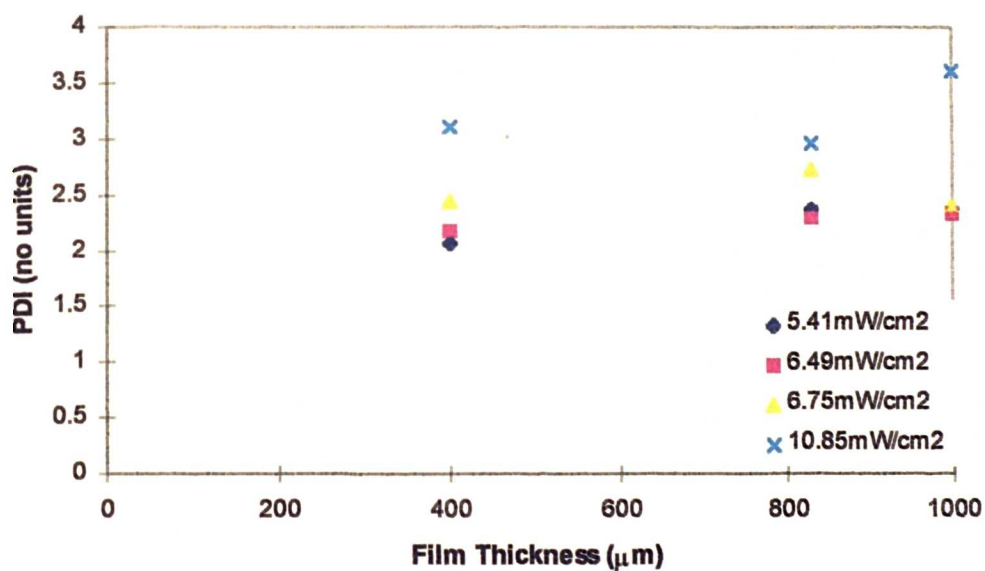


Figure 6.19. Effect of Film Thickness on Polydispersity Index (30s Exposure Time).

Appendix E

SPINNING DISC POLYMERISATION RESULTS

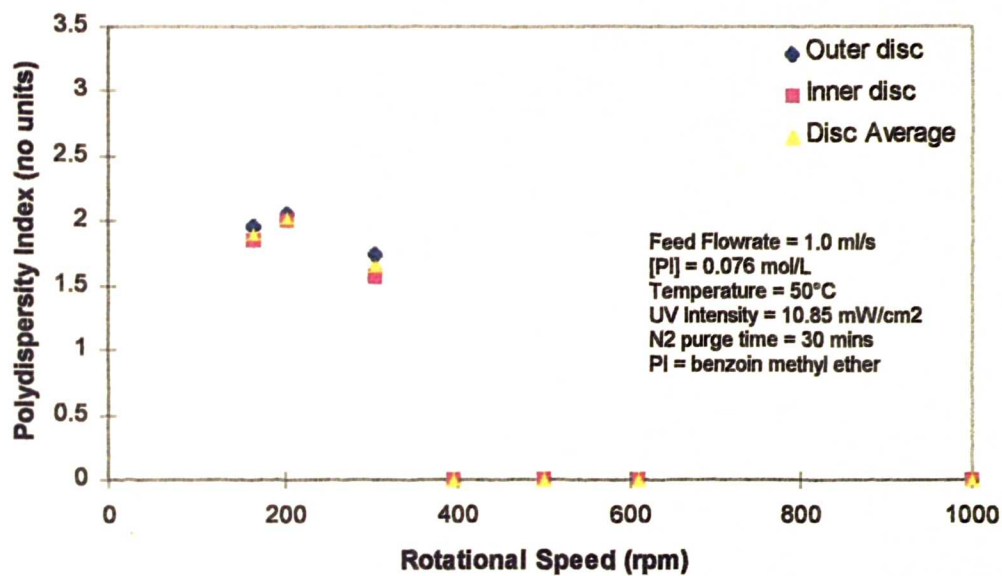


Figure 7.18. Effect of Rotational Speed on Polydispersity Index.

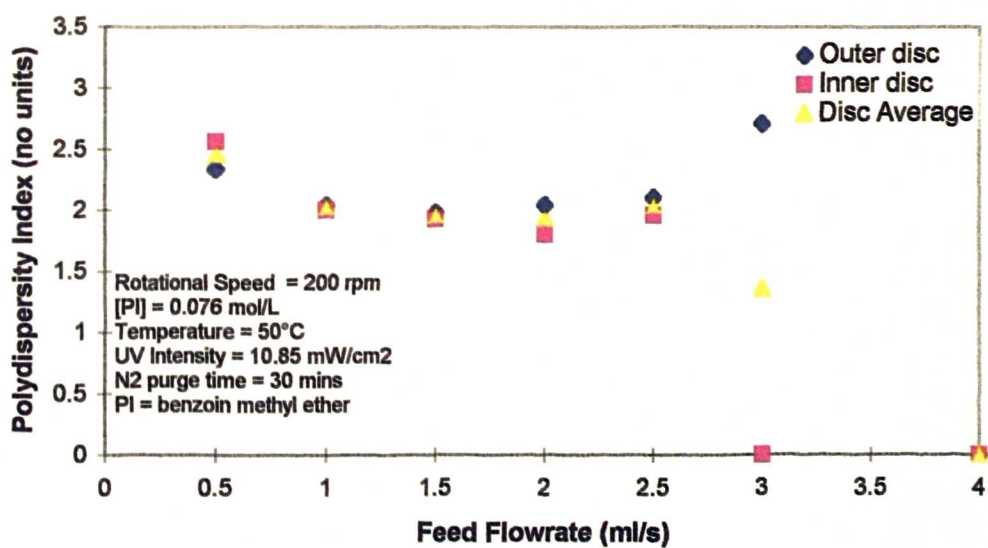


Figure 7.19. Effect of Feed Flowrate on Polydispersity Index.

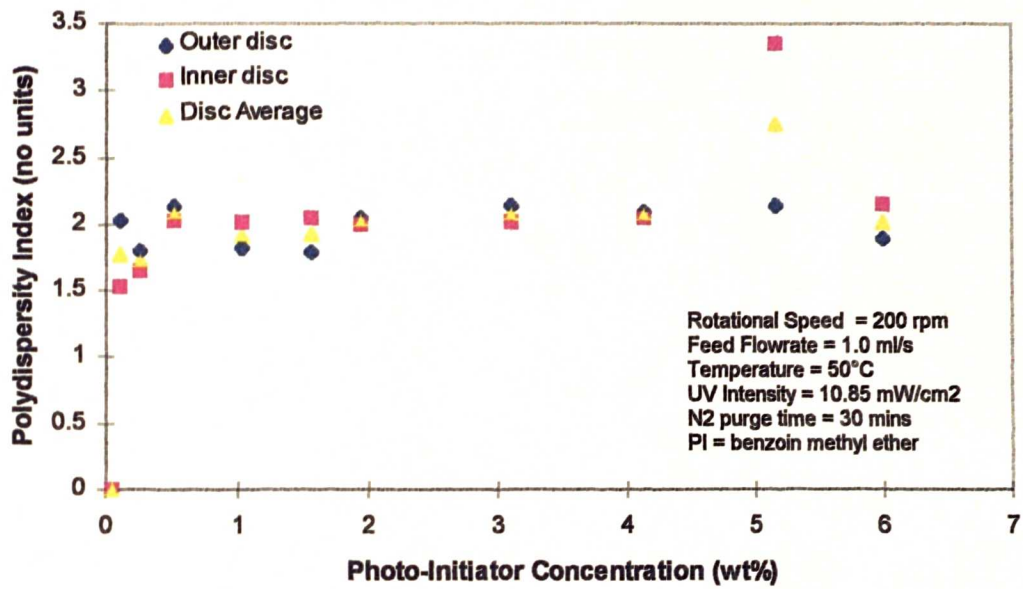


Figure 7.20. Effect of Photo-Initiator Concentration on Polydispersity Index.

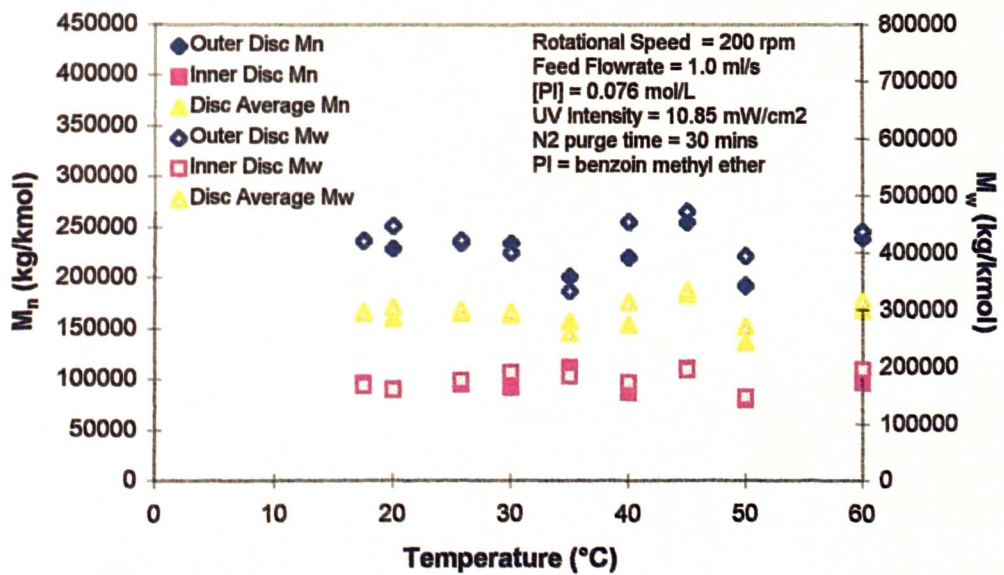


Figure 7.21. Effect of Temperature on Molecular Weight.

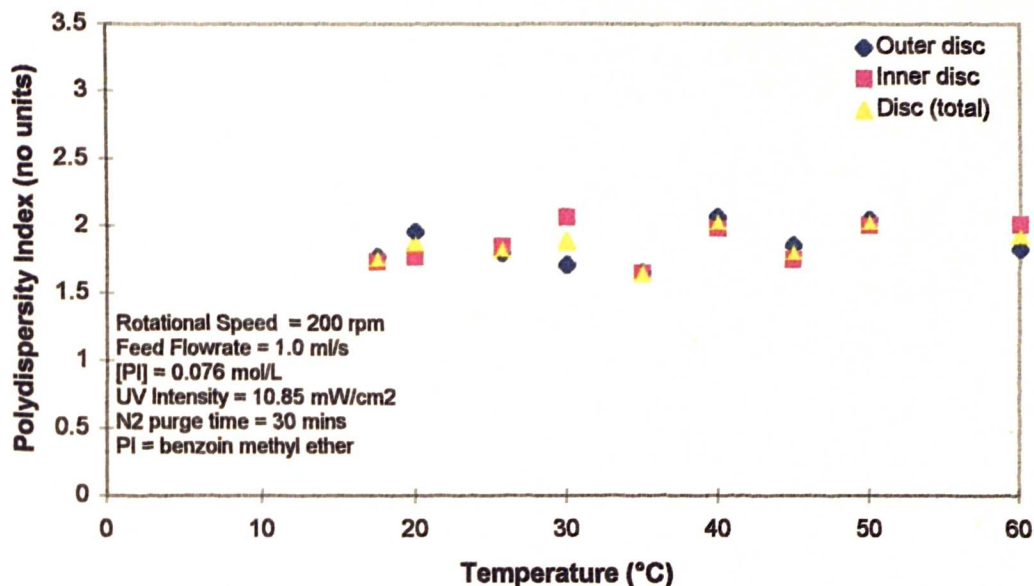


Figure 7.22. Effect of Temperature on Polydispersity Index.

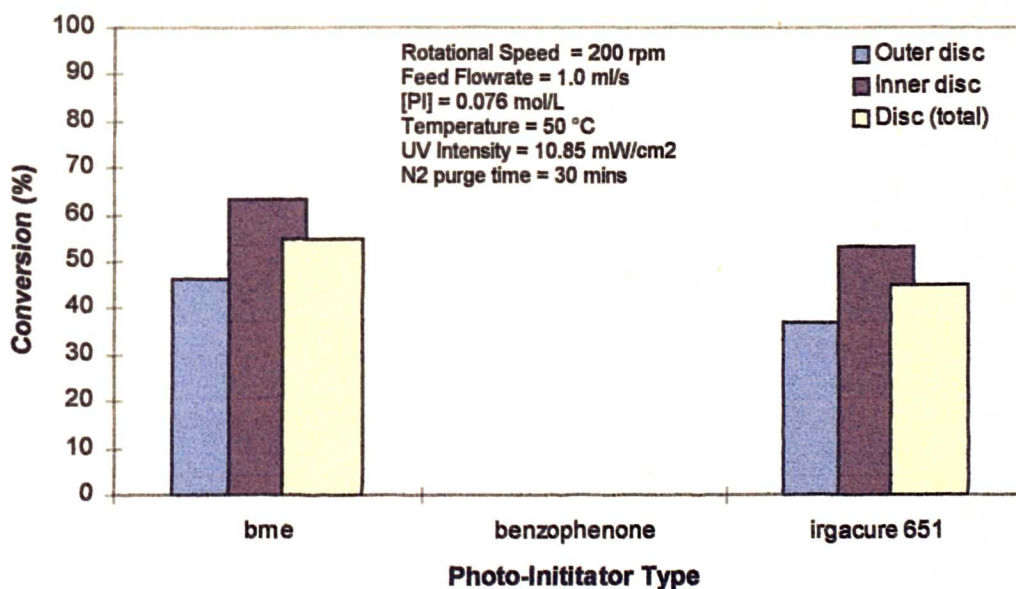


Figure 7.23. Effect of Photo-Initiator Type on Conversion for 0.076 mol/L Concentration.

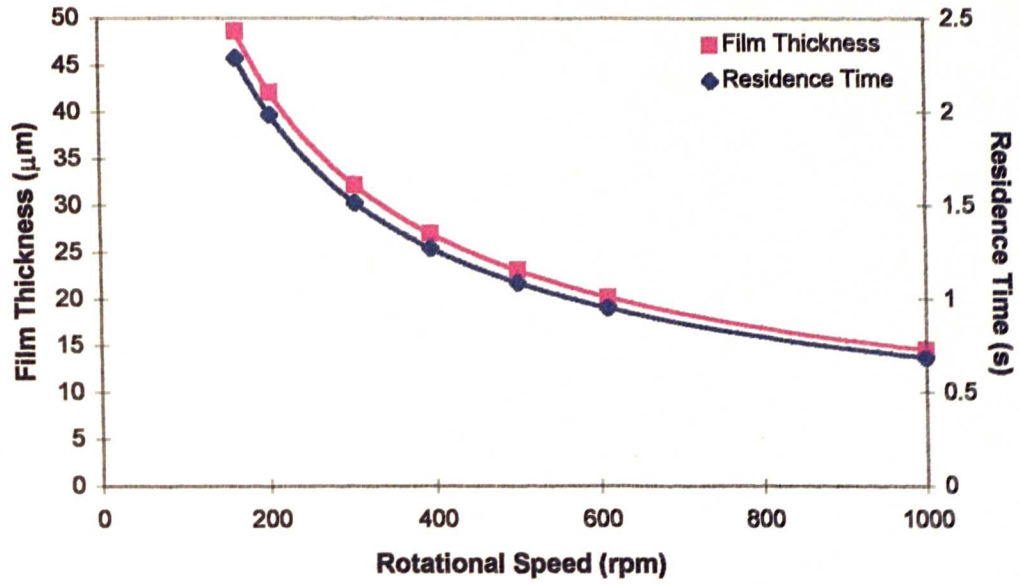


Figure 7.24. Effect of Rotational Speed on Film Thickness and Residence Time.

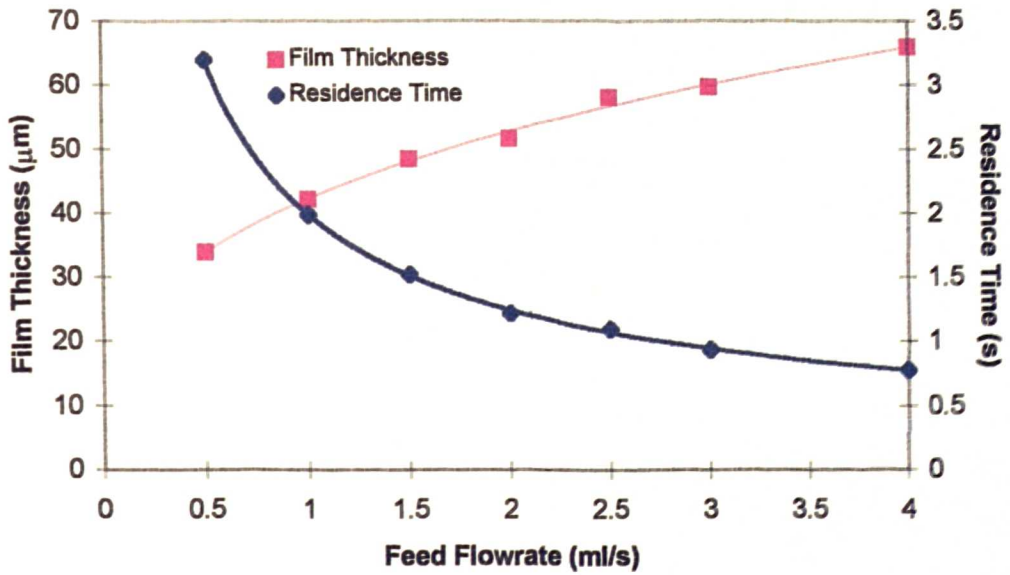


Figure 7.25. Effect of Feed Flowrate on Film Thickness and Residence Time.

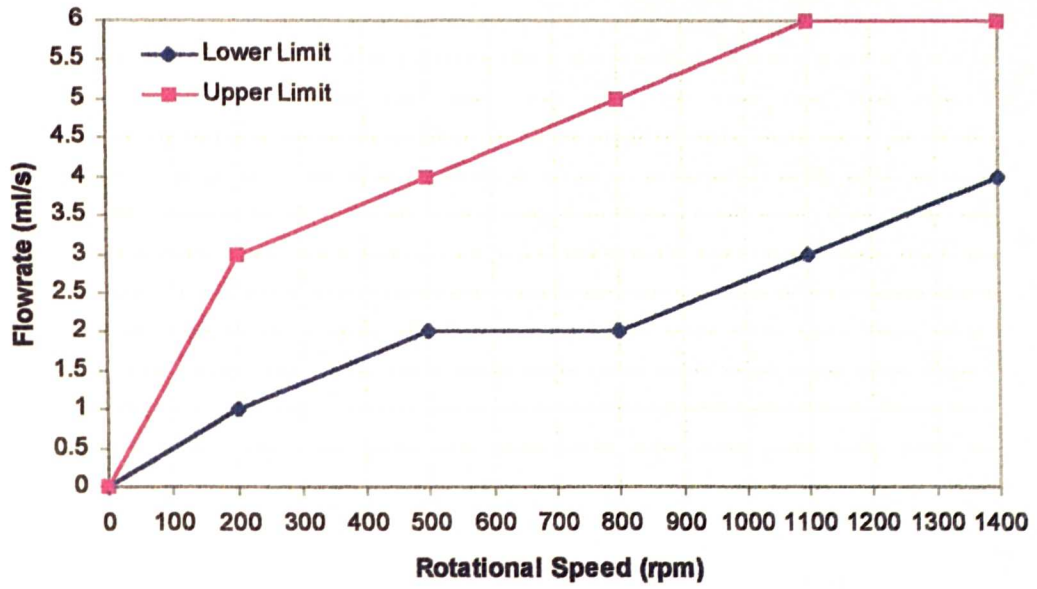


Figure 7.26. Operational Limits for Rotational Speed and Feed Flowrate.

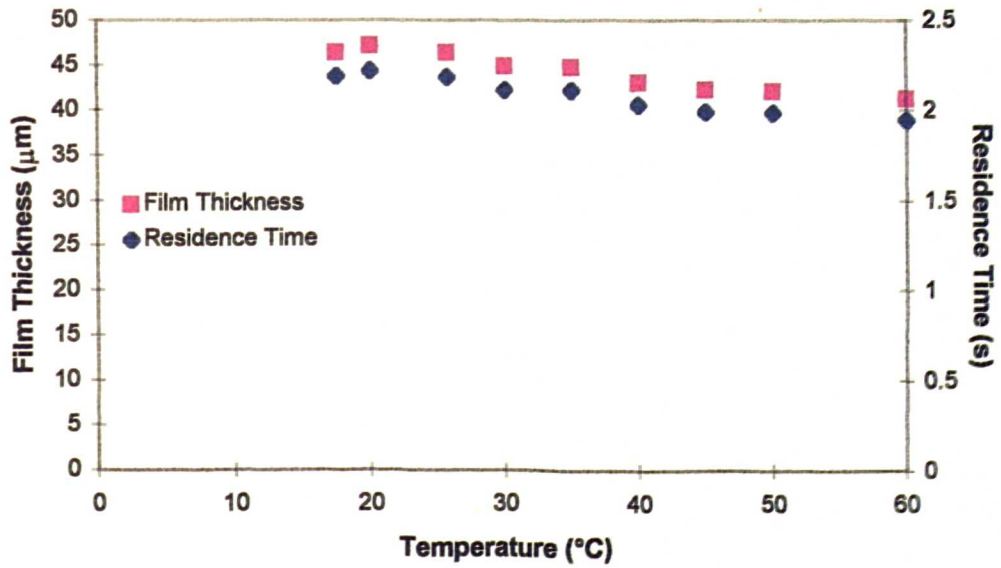


Figure 7.27. Effect of Temperature on Film Thickness and Residence Time.